

Monitoring of the impact of the extraction of marine aggregates, in casu sand, in the zone of the Hinder Banks

Scientific Report 3 – January - December 2015 and
Synthesis for the period 2011-2015

Vera Van Lancker, Matthias Baeye, Giacomo Montereale-Gavazzi, Dries Van den Eynde

MOZ4-ZAGRI/I/VVL/2016/EN/SR01

Prepared for

Flemish Authorities, Agency Maritime Services & Coast, Coast. Contract 211.177 <MOZ4>
ZAGRI



Table of contents

Abbreviations	3
Executive summary	4
Samenvatting	6
Preface	8
1. Introduction	9
2. Monitoring design	12
3. Materials and methods	14
3.1. Measurements and spatial observations	14
3.1.1. Longer-term measurements at a fixed location	14
3.1.2. Short-term spatial observations (<i>RV Belgica</i>)	15
3.1.3. In-situ measurements and sampling	15
3.1.4. Visual observations	16
3.1.5. Water column properties derived from water samples	18
3.1.6. Water column properties derived from optical measurements	18
3.1.7. Water column properties derived from ADCPs	20
3.1.8. Seabed properties derived from acoustical measurements	21
3.1.9. Seabed properties derived from sampling	21
3.1.10. External data	21
3.2. Modelling	22
3.2.1. Model validations	22
3.2.2. CFD Modelling	22
4. Results	24
4.1. Natural variation in sediment processes	24
4.2. Human-induced variation	55
4.2.1. Introduction	55
4.2.2. Near-field impacts	55
4.2.3. Far-field impacts	56
4.3. Modelling of changing hydrographic conditions	56
5. Integrated assessment of the monitoring 2011-2015	59
5.1. Introduction	59
5.2. Integrated monitoring approach	59
5.3. Physical impact assessment	60
5.3.1. Monitoring results	60

5.3.2.	Hypothetical cause-effect relationships _____	64
5.3.3.	Relevance of results <i>w.r.t.</i> to other monitoring _____	67
5.4.	Assessment of impacts <i>w.r.t.</i> the Belgian MSFD environmental targets _____	70
5.4.1.	Evaluation _____	70
5.4.2.	Recommendations on the MSFD indicators, monitoring and evaluation _____	75
5.5.	Lessons learned and recommendations for the continuation of extraction practices _____	77
5.5.1.	Lessons learned _____	77
5.5.2.	Recommendations for the continuation of extraction _____	80
6.	<i>Outreach</i> _____	81
7.	<i>Acknowledgments</i> _____	81
8.	<i>References</i> _____	83
9.	<i>Annexes</i> _____	84
	<i>Annex A. RV Belgica Campaign Reports</i> _____	84
	<i>Annex B. Video footage 2015</i> _____	84
	<i>Annex C. Impact of extraction on the bottom shear stress in zone 4</i> _____	84
	<i>Annex D. Monitoring results HBMC, FPS Economy</i> _____	84
	<i>Annex E. Publications</i> _____	84

Reference to this report

Van Lancker, V., Baeye, M., Montereale-Gavazzi, G. & Van den Eynde, D. (2016). Monitoring of the impact of the extraction of marine aggregates, in casu sand, in the zone of the Hinder Banks. Period 1/1 - 31/12 2015 and Synthesis of results 2011-2015. Brussels, RBINS-OD Nature. Report <MOZ4-ZAGRI/I/VVL/2016/EN/SR01>, 85 pp. (+5 Annexes, 190 p).

Abbreviations

ADCP	Acoustic Doppler Current Profiler
AUMS	Autonomous Underway Measurement System
BM-ADCP	Bottom-mounted Acoustic Doppler Current Profiler
BPNS	Belgian Part of the North Sea
COPCO	Continental Shelf Service of FPS Economy
CTD	Conductivity-Depth-Temperature
DGPS	Differential Global Positioning System
DoY	Day of Year
EMS	Electronic Monitoring System
FPS Economy	Federal Public Service Economy, SMEs, Self-Employed & Energy
FSZ	Flow separation zone
GES	Good Environmental Status
HM-ADCP	Hull-mounted Acoustic Doppler Current Profiler
Hs	Significant wave height
ILVO	Institute for Agricultural and Fisheries Research
LISST	Laser In-Situ Scattering and Transmissometry
Mab:	Depth in Meter above bottom
MFB, MP7	Measuring Network Flemish Banks; measuring pile 7 (Westhinder; Flanders Hydrography)
MSFD	European Marine Strategy Framework Directive
NE	Northeast-directed (flood)
OBS	Optical Back Scatter
ODAS	Oceanographic Data and Acquisition System
OPTOS-BCZ	Hydrodynamic model applied to the Belgian coastal zone
POC	Particulate Organic Carbon
PON	Particulate Organic Nitrogen
PSD	Particle-size distribution
RHIB	Rigid Hull Inflatable Boat
RSSI	Received Signal Strength Indicator
ROV	Remotely operated vehicle
RV	Research Vessel
SPM(C)	Suspended Particulate Matter (Concentration)
SW	Southwest-directed (ebb)
TASS	Turbidity Assessment Software System (www.ecoshape.nl)
TC	Tidal coefficient
Tidal phase (xx)	Spring/Neap/Mid tide, with indication of the tidal coefficient
TKE	Turbulent kinetic energy
TSHD	trailing suction hopper dredgers
UGent-RCMG	Ghent University, Renard Centre of Marine Geology
UTC	Universal Time Coordinates
VLIZ	Flanders Marine Institute

Executive summary

Integrated monitoring of the effects of aggregate extraction is needed to reach Good Environmental Status of the marine environment by 2020 (European Marine Strategy Framework Directive (MSFD); 2008/56/EC). To improve the management of the activity, understanding of the causes of the impact is crucial, as well as insight into natural variability, and therefore increased process and system knowledge is required. Additionally, when exploitation is within or near Habitat Directive areas, appropriate assessments are needed of all stressors (92/43/EEC). In 2012, new extraction activities started in a far offshore sandbank area in the Belgian part of the North Sea (BPNS), just north of a Habitat Directive area. Here, ecologically valuable gravel beds occur adapted to a clear water regime. Therefore, a dedicated monitoring programme was set-up, with focus on assessing changes in seafloor integrity and hydrographic conditions, two descriptors that define Good Environmental Status. Seafloor integrity relates to the functions that the seabed provides to the ecosystem (e.g., structure; oxygen and nutrient supply), whilst hydrographic conditions refer to currents, turbidity and/or other oceanographic parameters of which changes could adversely impact on benthic ecosystems.

The monitoring programme started in 2013, though first dedicated measurements were acquired in 2011. State-of-the-art instrumentation was used, to measure the 3D current structure, turbidity, depth, backscatter and particle size of the material in the water column, both in-situ and whilst sailing transects over the sandbanks. In the most intense extraction sector, seabed sediments were sampled in detail. In the Habitat Directive area, gravel bed integrity (i.e., epifauna; sand/gravel ratio; grain-sizes; patchiness) was measured as well. Additionally, visual observations were made through scientific divers, video frames and a remote operated vehicle.

It needs emphasis that during this first phase of the monitoring, development of monitoring strategies and methodologies was critical, as well as setting-up a baseline. Important new results were obtained; for the period 2011-2015 these relate to: (1) quantification of natural variability; (2) sediment plume formation and deposition, differentiating between small and large trailing suction hopper dredgers; (3) far-field impacts, with focus on the gravel beds within the Habitat Directive area, and (4) bottom shear stress modelling in view of predicting long-term changes in hydrographical conditions.

Regarding seafloor integrity focus was on the assessment of changes in habitat occurrences and distribution. Most striking was the enrichment of fine-grained material in the coarse permeable sands of the gravel area, classifying them as mixed sediments, hitherto not mapped on the BPNS. In the gravel areas, also more sand was observed than expected from previous mapping. Although no direct relationship could yet be made with the intensive extractions a step-wise impact hypothesis is formulated that needs further investigation: (1) excess of fine-grained materi-

al and sand from overflow of the trailing suction hopper dredgers; (2) deposition in the near field and in the gullies along the tidal stream axis; (3) resuspension by beam trawling; and (4) longer lasting deposition of sediments in morphologically complex areas that preferentially trap fine-grained sediments. The mechanism of trapping was studied combining field measurements and modelling. Further monitoring is required since favourable colonization and growth of epifauna on the gravel beds is critical for the maintenance and increase of biodiversity.

Regarding extraction-induced long-term changes in hydrographic conditions, three scenarios were simulated. These showed that the changes of the bottom shear stress in the area, where no impact was allowed ('outside distance'), remained limited to around 6 %, hence less than the maximum allowance of 10 % as specified within the Belgian implementation of MSFD.

For the continuation of the extraction, it is recommended to restrict the activity to the part of the sandbank where the resource is thickest. The lower part of the sandbank slopes are best avoided since the sediments are more heterogeneous, due to near-surface outcropping of older geological layers. Furthermore, most of the initial extraction took place in the southernmost sector, nearest to the Habitat Directive Area. Whenever possible, it is advised to spread the activity over different sectors to reduce the chance of smothering on the ecologically gravel beds.

Samenvatting

Geïntegreerde monitoring van de effecten van aggregaatextractie is nodig om een goede milieutoestand van het mariene milieu te bereiken in 2020 (Europese Kaderrichtlijn Mariene Strategie (KRMS); 2008/56/EG). Om het beheer van de activiteit te optimaliseren, alsook om de oorzaak-gevolg relaties te begrijpen en inzicht te hebben in natuurlijke variabiliteit, is een grotere proces- en systeemkennis nodig. Bovendien, wanneer de exploitatie in, of in de buurt van een Habitatrictlijnengebied valt, is een passende beoordeling nodig van de effecten van alle stressoren (92/43/EEG). In 2012 startten nieuwe extracties op ver zeewaarts gelegen zandbanken in het Belgische deel van de Noordzee, net ten noorden van een Habitatrictlijnengebied. Hier komen ecologisch waardevolle grindbedden voor, aangepast aan helder water. Een gericht monitoringsprogramma werd opgezet, met focus op het beoordelen van veranderingen in de zeebodemintegriteit en hydrografische condities, twee KRMS descriptoren om de mariene milieutoestand te evalueren. Zeebodemintegriteit betreft de functies die de bodem biedt voor het ecosysteem (bv. structuur, zuurstof en toevoer van voedingsstoffen), terwijl hydrografische condities verwijzen naar stromingen, turbiditeit en/of andere oceanografische parameters waarvan veranderingen een negatieve invloed kunnen hebben op bentische ecosystemen.

Het monitoringsprogramma startte in 2013, maar gerichte metingen werden reeds verricht vanaf 2011. State-of-the-art instrumentatie werd ingezet om de 3D-stroomsnelheidsstructuur, troebelheid, diepte, terugverstrooiingswaarden en deeltjesgrootte van het materiaal in de waterkolom te meten. In de meest intensief ontgonnen sectoren werd het zeebodemsubstraat in detail onderzocht. In het Habitatrictlijnengebied werd ook de grindbedintegriteit (o.a. epifauna; zand/grind verhouding; heterogeniteit) gemeten. Aanvullend werden visuele observaties uitgevoerd, gebruikmakende van wetenschappelijke duikers, videoframes, alsook van een computergestuurd onderwatervoertuig.

In deze eerste fase van monitoring lag de nadruk vooral op de ontwikkeling van opvolgingsstrategieën en methodieken, alsook het bepalen van referentiekaders. Belangrijke nieuwe resultaten werden bekomen; voor de periode 2011-2015 hebben deze betrekking op: (1) het kwantificeren van de natuurlijke variabiliteit; (2) de vorming en afzetting van sedimentpluimen, met onderscheid tussen de effecten van kleine tot grote sleephopperzuigers; (3) ver-veld effecten, met de nadruk op de grindbedden binnen het Habitatrictlijnengebied; en (4) de ontwikkeling van bodemschuifspanningsmodellen om lange-termijnsveranderingen in hydrografische condities, n.a.v. grootschalige extractie, te kunnen voorspellen.

In relatie tot zeebodemintegriteit was het onderzoek gericht op het bepalen van veranderingen in het voorkomen en de verspreiding van habitats. Meest opvallend was de aanrijking van fijn materiaal in de permeabele grove zanden in het

grindgebied, wat maakt dat deze sedimenten zich voor het eerst laten classificeren als 'gemengde' sedimenten. Bijkomend werd in de grindgebieden relatief meer zand aangetroffen dan werd verwacht van vroegere kartering. Geen directe relatie kon worden aangetoond tussen de extracties en de verfijning. Weliswaar worden de resultaten samengebracht in een stapsgewijze impacthypothese die verder dient onderzocht te worden: (i) overmaat aan fijnkorrelig materiaal en zand die in het milieu wordt gebracht door overvloed van de sleephopperzuigers; (2) afzetting in het nabije veld en in de omringende geulen in de as van het stroomgebied; (3) resuspensie door bodemberoerende visserij; en, (4) langduriger afzetting van sedimenten in morfologisch complexe gebieden die fijnkorrelig materiaal kunnen invangen. Het invangmechanisme werd onderzocht op basis van nieuwe metingen, in combinatie met modellen. Verdere opvolging is nodig, gezien het belang van een gunstige kolonisatie en groei van epifauna op grindbedden dat van cruciaal belang is voor het behoud en de toename van de biodiversiteit in het Belgische deel van de Noordzee.

Met betrekking tot extractie-geïnduceerde langetermijnsveranderingen in hydrografische condities werden drie scenario's gesimuleerd. Hierbij werd aangetoond dat veranderingen in bodemschuifspanning, in het gebied waar geen veranderingen toegelaten zijn, beperkt bleven tot 6 %, wat binnen de marge van 10 % ligt zoals vooropgesteld binnen de Belgische implementatie van de KRMS.

Voor de verdere ontginningen wordt aanbevolen de extractie vooral te concentreren op het deel van de zandbank waar de zandvoorkomens het dikste zijn. De voet van de zandbankhellingen wordt het beste vermeden gezien de aanwezigheid van meer heterogene sedimenten, te wijten aan het ondiep voorkomen van oudere geologische lagen. Bijkomend werd nu vastgesteld dat de meeste ontginningen plaatsvonden in de meest zuidelijke sector, net ten noorden van het Habitatrictlijnengebied. Wanneer mogelijk, wordt geadviseerd om de activiteit te spreiden over de 4 sectoren om zo de kans te verkleinen dat fijner materiaal wordt afgezet in de ecologisch waardevolle grindgebieden.

Preface

Results presented in this report relate to the monitoring of aggregate extraction in zone 4, Hinder Banks (MOZ4), for the year 2015. It is a follow-up of the reporting *w.r.t.* the monitoring in 2013 (Van Lancker et al., 2014) and in 2014 (Van Lancker et al., 2015), but also provides a summary of the first period of extraction.

Since 2013, the monitoring activities were financially supported by the Flemish Authorities, Agency Maritime Services and Coast, Coast. The monitoring programme ZAGRI, funded by the revenues of the private sector, and covering all concession zones in the Belgian part of the North Sea, provides a continuous support to MOZ4, as well as for the measurements that commenced in 2011, as for the model development. Since 2015, monitoring is also supported by the Belspo INDI67 research project. In this project, the MSFD indicators on the physical properties of the water-column and seabed interface and related to the descriptors of Good Environmental Status (GES) 'Seafloor Integrity' and 'Hydrographic Conditions', are investigated in detail. Particularly, the research on quantifying changes in bottom shear stress and benthic habitats (from multibeam backscatter) benefits from this additional funding.

The synthesis on the first phase of the monitoring integrates the results obtained and puts them in perspective of the results of the morphological and biological monitoring, respectively carried out by the Continental Shelf Service of FPS Economy (COPCO) and the Institute for Agricultural and Fisheries Research (ILVO).

1. Introduction

Over a 10-yr period extraction of marine aggregates (up to 2.9 million m³ over 3 months) is allowed in the region of the offshore Hinder Banks (concession zone 4), with a maximum of 35 million m³ over a period of 10 years. Concessions were granted in four sectors of extraction (4a-b-c-d). Large trailing suction hopper dredgers (TSHD) can be used, extracting up to 12,500 m³ per run. These practices contrast strongly with previous extraction activities: up to 3 million m³ per year, in 2011, and mostly using vessels with a capacity of 1500 m³ only. Since 2012, extraction is allowed in zone 4. Up to now extraction was concentrated in Sector 4c, with a peak extraction of nearly 2.5 10⁶ m³ in 2014 (Van den Branden et al., 2016) (Figure 1). Such intensive extraction is new practice in the BPNS and the environmental impact is yet to be determined. The volumes are mostly needed in response to the needs of the Coastal Safety Plan bringing the level of protection against extreme storm events at a 1:1000 years return period, including a +30 cm sea level rise by 2050 (www.kustveiligheid.be).

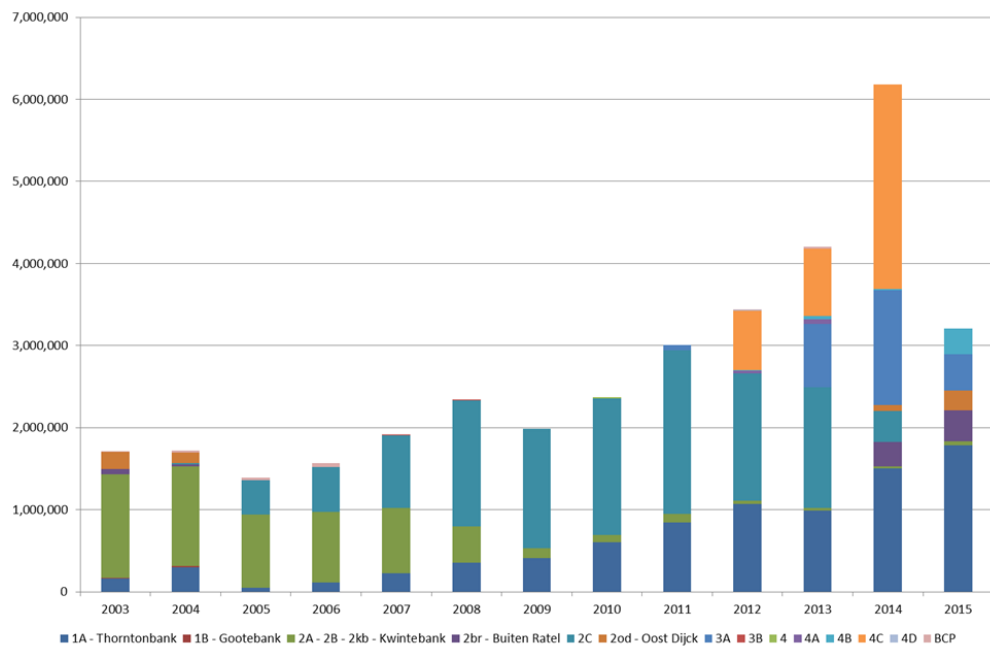


Figure 1. Extracted volumes of marine aggregates (m³) in the period 2003-2015 (Van den Branden et al., 2016). Labels 4, 4a-b-c-d relate to the extraction on the Hinder Banks. Note a peak extraction of nearly 2.5 10⁶ m³ on Sector 4c in 2014.

The Hinder Banks form part of a sandbank complex, located 40 km offshore in the Belgian part of the North Sea (BPNS). On the sandbanks, depths range from -8 m to -30 m (Figure 2); they are superimposed with a hierarchy of dune forms, often more than 6 m in height. The channels in-between the sandbanks reach 40 m of water depth. At present, extraction of aggregates takes place mainly on the Oosthinder sandbank. Sediments are medium- to coarse sands, including shell hash, with

less than 1 % of silt-clay enrichment (Van Lancker, 2009 @SediCURVE database). Tidal currents reach more than 1 ms⁻¹; waves are easily more than 1 m in height (44 % of the time). These offshore sandbanks are the first wave energy dissipaters in the BPNS.

The extraction sectors on the Hinder Banks are near an area protected under the Habitat Directive (92/43/EEC; see box below), called the "Vlaamse Banken". The northern limit of this area was drawn to include ecologically valuable gravel beds (Houziaux et al., 2008) (Figure 2). These beds have the status of "reefs" (Habitat type code 1170). At present, and in contrast to 100 yrs ago (Houziaux et al., 2008, and references therein), the extent of the reefs has become very marginal because of intensive fisheries. With the extraction activities being a new stressor in the area, it is critical to closely monitor the status of these reefs. Particularly, the areas where in 2006 still hotspots of biodiversity were found were targeted, the so-called *refugia*, or protected gravel beds, *sensu* Houziaux et al. (2008). These occur in the troughs of morphologically steep sand dunes ('barchan' dunes), and as such considered more protected from trawling activities.

Habitat Directive

<http://www.health.belgium.be/en/habitats-directive-areas-belgian-part-north-sea>

In implementation of the Habitats Directive (92/43/EEC), the Belgian State designated a Habitat Directive Area "Vlaamse Banken" (Royal Decree of October 16, 2012). The area is 1099.39 km² and located in the southwest of the Belgian part of the North Sea. It borders the French Birds and Habitats area "Bancs de Flandres" and extends to about 45 km offshore. The "Vlaamse Banken" were designated for the protection of the "sandbanks permanently covered with seawater" (Habitat type code 1110) and the "Reefs" (Habitat type code 1170). These sandbanks and reefs are ecologically the most valuable habitats of our North Sea. Two biotopes were characterized as "reefs": (1) reefs formed by the sand mason worms (*Lanice conchilega*), located in shallow water closer to the coast; and (2) the gravel beds occurring more offshore, especially and to a large extent at the level of the Hinder Banks. The gravel beds are a very rare and endangered habitat of gravel and boulders that may or may not be clumped together in the sandy or clayey subsoil and host a unique and rich diversity of species of fauna and flora. They once constituted the biotope of the European oyster which along with the stones were heavily colonised by a very peculiar fauna. Gravel beds fulfil an important function as spawning chamber and nursery of the fish species. Through the use of trawl nets, including the beam trawl their extent has become very marginal (<http://www.health.belgium.be/en/habitat-types-be-protected>).

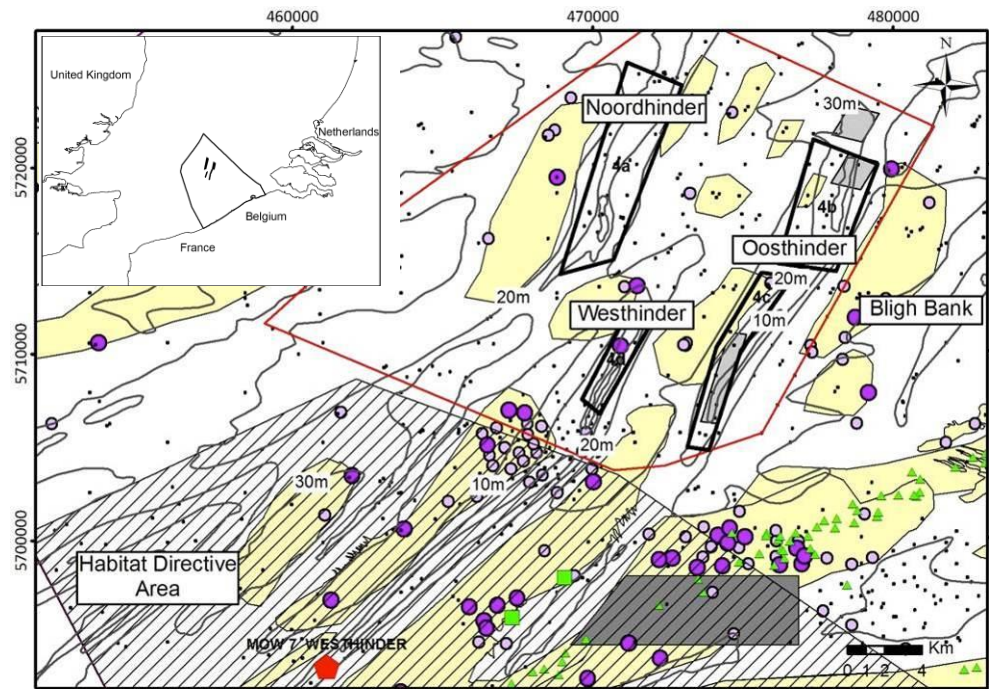


Figure 2. Area of the Hinder Banks, where intensive marine aggregate extraction is allowed in zone 4 (red line) along 4 sectors (black polygons). Within and outside these sectors geomorphological monitoring is carried out by COPCO (light grey polygons). A Habitat Directive area (hatched) is present at a minimum of 2.5 km from the southernmost sectors. Presence of gravel (purple dots) and stones (green triangles) is indicated (size of the dots represents relative amounts of gravel with a minimum of 20 %). In the light yellow areas the probability of finding gravel is high (based on samples, in combination with acoustic imagery). In the gravel refugia (green squares), west of the Oosthinder, ecologically valuable epifauna is present. Indicated also is the position of the Westhinder measuring pole MOW7 (Flanders Hydrography) (red pentagon) where most of the hydro-meteorological data are derived from. Dark grey polygon in the Habitat Directive area is an anchorage zone.

2. Monitoring design

A monitoring programme, with focus on hydrodynamics and sediment transport, has been designed allowing testing hypotheses on the impact of marine aggregate extraction in the far offshore Hinder Banks. Impact hypotheses were based on findings in the Flemish Banks area where 30-yr of extraction practices, and related research on the effects, were available (Van Lancker et al. 2010, for an overview). They have been adapted to incorporate descriptors of good environmental status, as stipulated within the European Marine Strategy Framework Directive (MSFD) (Belgische Staat, 2012). In the context of the present monitoring, main targets are assessing changes in seafloor integrity (descriptor 6) and hydrographic conditions (descriptor 7), two key descriptors of good environmental status, to be reached in 2020.

Summarized, main hypotheses are: (1) Seabed recovery processes are very slow; (2) Large-scale extraction leads to seafloor depressions; these do not impact on the spatial connectedness of habitats (MSFD descriptor 6); (3) Impacts are local, no far field effects are expected; (4) Resuspension, and/or turbidity from overflow during the extraction process, will not lead to an important fining of sediments (e.g., siltation); (5) Marine aggregate extraction has no significant impact on seafloor integrity, nor it will significantly lead to permanent alterations of the hydrographical conditions (MSFD descriptor 7); (6) Cumulative impacts with other sectors (e.g., fisheries) are minimal; and (7) Large-scale extraction does not lead to changes in wave energy dissipation that impact on more coastwards occurring habitats.

The monitoring follows a tiered approach, consisting of in-situ measurements and modelling (Figure 3). Critical is to assess potential changes in hydrographic conditions (MSFD, descriptor 7), as a consequence of multiple seabed perturbations (e.g., depressions in the seabed) and their interactions. This could lead to changes in bottom shear stresses, a MSFD indicator that should remain within defined boundaries¹. Therefore, considerable effort went to current and turbidity measurements along transects crossing the sandbanks, as also on point locations for longer periods. These data serve as a reference and are compared to datasets recorded under the events of intensive aggregate extraction. The extraction gives

¹ For descriptor 7 on hydrographic conditions, the monitoring programme should allow evaluating the following specifications (Belgische Staat, 2012):

- (1) Based upon calculated bottom shear stresses over a 14-days spring-neap tidal cycle, using validated mathematical models, an impact should be evaluated when one of the following conditions is met:
 - (i) There is an increase of more than 10% of the mean bottom shear stress;
 - (ii) The variation of the ratio between the duration of sedimentation and the duration of erosion is beyond the “-5%, +5%” range.
- (2) The impact under consideration should remain within a distance equal to the square root of the area occupied by this activity and calculated from the inherent outermost border.
- (3) All developments need compliance with existing regulations (e.g., EIA, SEA, and Habitat Directive Guidelines) and legislative evaluations are necessary in such a way that an eventual potential impact of permanent changes in hydrographic conditions is accounted for, including cumulative effects. This should be evaluated with relevance to the most suitable spatial scale (ref. OSPAR common language).

rise to sediment plumes and subsequent release of fine material in the water column. As such, dispersion of the fines and the probability of siltation in the nearby Habitat Directive area are studied, since this may cause deterioration of the integrity of gravel beds present in this area. This relates directly to Belgium's commitments within the MSFD stating that the ratio of the hard substrata surface area versus the soft sediment surface area should increase in time (Belgische Staat, 2012). Furthermore, abrasion of the sandbank and/or enrichment of finer material, could lead to habitat changes², another indicator within MSFD (descriptor 6 Seafloor Integrity).

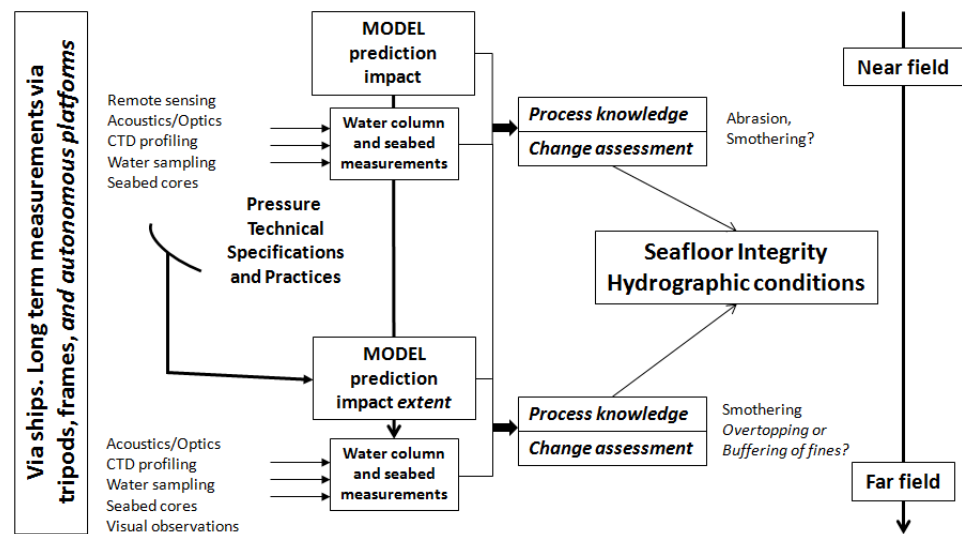


Figure 3. Overview of the research strategy aiming at quantifying both near- and far-field impacts of marine aggregate extraction.

² For descriptor 6 this monitoring programme contributes to the evaluation of the following environmental targets and associated indicators (Belgische Staat, 2012):

- (1) The areal extent and distribution of EUNIS level 3 Habitats (sandy mud to mud; muddy sand to sand and coarse sediments), as well as of the gravel beds, remain within the margin of uncertainty of the sediment distribution, with reference to the Initial Assessment.
- (2) Within the gravel beds (selected test zones), the ratio of the surface of hard substrate (i.e., surface colonized by hard substrata epifauna) against the ratio of soft sediment (i.e., surface on top of the hard substrate that prevents the development of hard substrata fauna), does not show a negative trend.

3. Materials and methods

3.1. Measurements and spatial observations

In 2015, three 1-week campaigns, were organized, all with RV Belgica (ST1507, ST1517, ST1533). Additionally, an opportunity arose to acquire data during ST1502 during which multibeam data and oceanographic data were acquired west of the Westhinder (synergy Belspo INDI67 project). One longer term bottom-mounted ADCP (BM-ADCP) deployment was also conducted. This could be achieved by a demand for extra shiptime during campaign ST1503 (deployment) and ST1505 (recovery). Furthermore, Flanders Marine Institute, VLIZ, provided the opportunity to use a Remote Operated Vehicle for visual observations in the Habitat Directive area, with RV Simon Stevin as the deployment platform. See Table 1, for an overview of the data periods and research areas.

Table 1. Overview of RV Belgica campaigns in 2015. DoY: Day of Year 2015. Numbering of campaigns continues from the period 2011-2014. HD area: Habitat Directive area; T_coeff: maximum Tidal coefficient. If more than 70: spring tidal conditions. Time in UTC.

Nr	Campaign	Area	Time1	Time2	DoY1	DoY2	T_coeff (time max coeff)
17	ST1502	HBBSB ³	2015-02-02	2015-02-04	33	35	75 (4.58 m) 2/2 23:35
18	ST1507	Sector 4b HBBSA ⁴ HD area	2015-03-16	2015-03-20	75	79	75 (4.79 m) 19/3 23:20
19	ST1517	Zone 4 ⁵ Sector 4b HD area	2015-06-22	2015-06-26	173	177	68 (4.45 m) 22/6 03:35
20	SS15-540	HD area	2015-08-10	2015-08-10	222	222	66 (4.36 m) 12/8 23:35
21	ST1533	HD area	2015-12-15	2015-12-18	349	352	77 (4.65 m) 15/12 02:05

3.1.1. Longer-term measurements at a fixed location

Near-bottom processes (currents and turbidity) were further studied using an upward looking bottom-mounted Acoustic Doppler Current Profiler (BM-ADCP; Teledyne/RD Instruments, 1200 kHz Workhorse Sentinel) in the Habitat Directive area, in the trough of a barchan dune where rich gravel beds occur. Aim was to study the relation between the barchan morphology, its fine sediment trapping efficiency and potential deposition in the gravel area (Table 2).

³ HBBSB area is located west of the Westhinder sandbank.

⁴ HBBSA area is located east of the Westhinder sandbank, in the gully with the Oosthinder sandbank. Both areas were defined within the Fisheries exclusion zone where the Belgian Government wants to monitor the effect of fisheries activities. During ST1502; the measurements were conducted in the frame of the Belspo INDI67 project.

⁵ Long tracklines parallel to the axis of the Westhinder-Oosthinder gully.

Table 2. Longer term deployments with a BM-ADCP. Settings of the deployments are given, as also the position. Data were recorded with reference to the bottom; depth in meters above bottom is abbreviated as mab.

Type	Start	End	Bin Size (m)	Remarks
OH-Gravel RDI-BB 1228.8 kHz	2013-07-01 16:45	2013-07-04 07:00* ± 2.5 days	0.25	Fast pinging mode Bins [0.81-15] mab; average ensemble interval 1.5 s Location: 51°24.781'N, 2°31.603'E (± 30 m) Neap tide; tidal amplitude ~3m
OH-Gravel RDI-BB 1228.8 kHz	2015-02-10 20:04 DOY 41 (ST1503)	2015-02-25 07:00 DOY56 (ST1505) ± 15 days	0.50	Fast pinging mode (12) Bins [1.04-13.04] mab; average ensemble interval 2400 s; Time/Ping: 60 s Location: 51°24.781'N, 2°31.603'E (± 30 m) Spring tide at 22/2; T_coeff: 94 (5.38 m)

**This dataset from 2013 was revisited since, due to technical issues, the data only became available in 2015 (see Figure 7, p. 18 and 40-42 in report Year 2). The instrument was placed in Area 2 (main refugium area), in the trough of a barchan dune.*

3.1.2. Short-term spatial observations (RV Belgica)

In 2015, the following observations were made:

- (1) Very-high resolution acoustic measurements were performed with RV Belgica's multibeam system (Kongsberg-Simrad EM3002, 300 kHz): in the gully in-between the Westhinder and Oosthinder (both long track-lines and in-part full-coverage). The system was used also to monitor depth and sediment changes in the Habitat Directive area, south of Sector 4c. Depth and backscatter data were obtained.
- (2) Through-tide (13-hrs cycle) transect measurements of hull-mounted ADCP (HM-ADCP) over the barchans dunes, Habitat Directive Area: currents and turbidity; bin size of 1 m (ST1507).

See Annex A, RV Belgica cruise reports for more details.

3.1.3. In-situ measurements and sampling

Water properties

For calibration of the continuous registrations (HM-ADCP; BM-ADCP) water samples were taken using a Niskin bottle of 10 l, mounted on a Seacat profiler (SBE09 CTD system) (ST1502, ST1507). The latter allowed vertical profiling of oceanographic parameters using CTD for salinity, temperature and depth; and optical backscatter sensor (OBS) for turbidity. Particle-size distribution (PSD) and

volume concentration in the water column was measured using a Sequoia type C 100 X Laser In-Situ Scattering and Transmissometry (LISST). Using an annular ring detector, the instrument derives in-situ particle sizes, in the range 2.5 to 500 μm , from the scattering of particles on 32 rings. PSD are presented as concentration (μll^{-1}) in each of the 32 log-spaced size bins. Date and time, optical transmission, water depth and temperature are recorded as supporting measurements (<http://www.sequoiasci.com>). Water samples were filtered on board for suspended particulate matter (SPM) every 30' for a 13-hrs cycle; sometimes ad hoc if alternating with other measurements. Mostly, 1.5 l of water was filtered. Within a 13-hrs cycle, extra filtrations were done, once per hour, for particulate organic carbon (POC/PON) (0.250 l), and a bottle of water (0.33 l) was kept for calibration of the conductivity sensor for salinity.

During campaigns ST1517, sediment particles in the water column were retrieved when RV Belgica measured consistently in one area (Sector 4b and Habitat Directive Area). A centrifuge purifier was used to filter suspended particulate matter from the continuous seawater pump at 3.2 m below the water surface.

Seabed properties

On selected locations seabed sediment samples were taken:

- (1) To characterize, in detail, sediment composition along Sector 4c and Sector 4b and to evaluate deposition of the overflow deposits in the near and far field. During ST1507, in Sector 4c and 4b, Reineck boxcore sediment samples were taken and were on-board sliced at a 1-cm interval. Reinecks were again taken in Sector 4c during ST1533. In the Habitat Directive area, Hamon grabs were taken along the gravel beds with rich epifauna, hence to assess sediment and biological variability (RV Belgica ST1507; ST1517). Locations were defined on the basis of previous sampling efforts.
- (2) During ST1533, Van Veen grab samples were taken for the validation of the multibeam depth and backscatter data.

3.1.4. Visual observations

In 2015, video observations took place during 3 campaigns on RV Belgica (Table 3). The remote operated vehicle (ROV) GENESIS was used on 10/08/2015. All of the visual equipment was made available through VLIZ. The video frame was equipped with a Bowtech Inspector colour zoom camera (Sony $\frac{1}{4}$ " SuperHAD CCD; 18:1 automatic zoom range) and a lightning element. Imagery was recorded in .AVI format and had a standard definition (SD) of 640x480 pixels. Video footage was exported as snapshots from the video. The resolution of the original data and the fact that most images were shot under varying current speeds, affected strongly the sharpness of the extracted images.

Table 3. Visual observations in the Habitat Directive area and in the area around Sector 4b (ROV: Remote Operated Vehicle).

Period	Equipment	Platform	Modus
2015-03-17 to 2014-03-19	Larger video frame	RV Belgica cruise ST1507	Drift
2015-06-24 to 2015-06-25	Larger video frame	RV Belgica cruise ST1517	Drift
2015-08-10	ROV GENESIS	RV Simon Stevin cruise SS15-540	Drift
2015-12-17	Larger video frame	RV Belgica cruise ST1533	Drift

Visual observations were made along regions of interest. As in 2014, the refugia, as defined by Houziaux et al. (2008), were revisited. In addition, video data were also recorded in the gully in-between the Westhinder and Oosthinder, both in the north, near Sector 4b, and in the south. Recordings were also made in the gully west of the Westhinder. As such, all of the gully areas were inspected.



Figure 4. Overview of regions where sampling and observations were conducted in 2015. Reineck boxcoring (dots) in Oosthinder Sector 4c (south) and Sector 4b (north); Hamon grabs (rectangles) in the gully between Westhinder and Oosthinder, as also Video imaging (triangles). Water sampling (small dots) during 13 hrs in Sector 4b, and along a transect in the southern part of the Oosthinder sandbank. Fisheries management area is indicated, comprising two areas, HBBSA and HBBSB, where multibeam monitoring was conducted during ST1502. For details, see campaign reports.

3.1.5. Water column properties derived from water samples

On board, water samples were filtered, in three replicates, using pre-weighted Whatmann GFC filters. These were analysed at the Marine Chemistry Lab (OD Nature, ECOCHEM). Suspended particulate matter concentration (SPMC) (Unit gl^{-1}) was obtained after drying of the filters for 48 hours, after which weight differences were calculated. A deviation of 12 % between the replicates is acceptable (ECOCHEM Standards). Measuring uncertainty of deriving SPM from filtrations is 17 %. Since 2011, 1643 water filtrations have been made in the Hinder Banks area (some in Kwinte Bank area, for comparison). POC/PON analyses (Unit gl^{-1}) were carried out in the laboratory using an Interscience FlashEA 1112 Series Element Analyser. Measuring uncertainty is 12 % for POC; 18 % for PON (ECOCHEM AK 7.0). For salinity (Unit PSU), a Laboratorium salinometer – Portasal 8410 (Guildline) van Ocean Scientific Int. was used; the measuring uncertainty is 0.15 % (ECOCHEM). It needs emphasis that water samples were taken at different levels in the water column. Normal procedure is to take a sample 2-4 mab, depending on wave action, hence platform motion. The depth of the water sample is derived from the CTD profiles (see below). Still, there are important uncertainties on the exact sampling depth, as the Seacat frame is easily carried away by the currents. This complicates the match-ups with ADCP data, a necessary step for calibration towards mass concentrations of SPM.

3.1.6. Water column properties derived from optical measurements

Conductivity-depth-temperature (CTD) and optical backscatter (OBS)

The Seacat profiler was again used to obtain vertical profiles of oceanographic parameters. In 2015 this was done during two campaigns ST1502 and ST1507. Upon request, a Seapoint OBS sensor was used instead of the OBS3 (2011-2012) and OBS3+ (2013-2014) sensors which were standard available on RV Belgica. Calibration curves of data before 2015 indicated no valid correlation between the voltages measured by the OBS3 and OBS3+ sensors and SPMC. Hence, these sensors proved inadequate to derive correctly the lower SPMC in the offshore. These sensors typically measure in the range of 0-4000 NTU, hence they provide no accurate values in the range 0-50 NTU, which is more likely the range in the offshore waters.

The Seapoint OBS replaced the OBS3+ due to it being more sensitive to the low SPMC in offshore areas, with a range from 0 to 125 NTU. This working range was obtained through the use of a jumper cable that amplified the signal by a factor of x20. As such, the sensitivity was 40 mV/NTU compared to 2 mV/NTU without cable and for the standard range of 0-750 NTU (Sea-Bird Electronics Inc., 2013). Following technical specifications (Sea-bird Electronics Inc., 2013), the following formula was used to convert the voltages into NTU:

$$NTU = \frac{500 * \text{Scale factor} * \text{Voltage}}{\text{Cable gain setting}}$$

The scale factor is nominally 1, hence with the chosen cable gain of x20, hence

$$NTU = 25 * Voltage$$

To calibrate the Seapoint OBS, data from RV Belgica ST1502 and ST1507 campaigns were used, during which measurements took place in sector 4b (Hinder Banken), Westhinder and an area near the Kwinte Bank. For the calibration, the OBS signal (voltage) was converted to NTU according to the previously mentioned formula, and was then compared to the SPMC derived from water samples taken in the vicinity of the OBS sensor (Figure 5). From this, a regression was derived to be applied to each individual OBS profile and convert them into SPMC. Note that for the ST1507 13-hrs cycle near Sector 4b, the Seacat frame was lowered to the seabed where it remained for 30'; after the ascend to the surface a new profile was started. This means that measurements continued near bottom for about 30'. This explains the increased amount of near-bottom measurements with often large peaks. For ST1507 this is seen both for the Seapoint-derived SPMC values, as well as for the LISST.

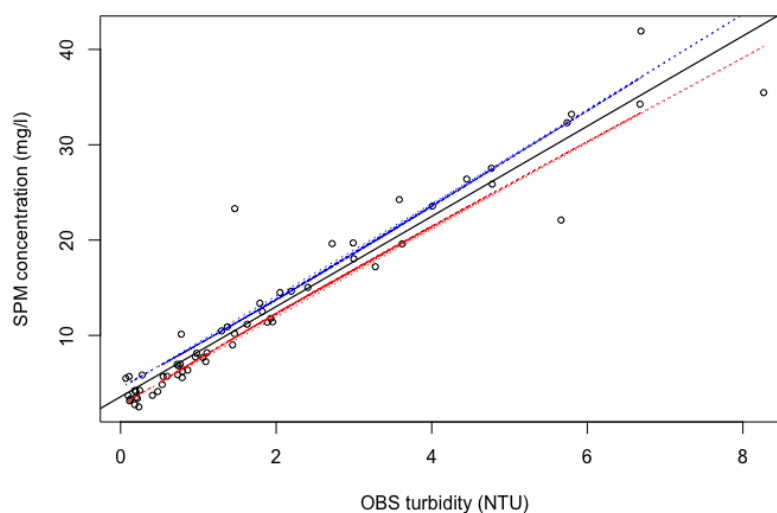


Figure 5. Calibration curve of the Seapoint OBS, using data from RV Belgica campaigns ST1502 and ST1507. A regression was fitted (black line) with the top (blue) and bottom (red) 95 % confidence intervals. Results regression: $SPM = 4.7314 * NTU + 3.5599$; $R^2 = 0.9218$; 61 data points used.

In-situ particle size variation from LISST

Data from the LISST-100X were processed following the guidelines “Processing LISST-100 and LISST-100X data in MATLAB”, posted on the Sequoia Scientific website (Sequoia Sci, 2008). After correction for the background (i.e., instrument and ambient water related) binary data from the rings were converted into volume concentrations (μl^{-1}) per ring. This dataset was further analysed in terms of temporal variability (e.g., throughout a 13-hrs tidal cycle) and over the vertical (i.e., from the surface to 2-3 mab).

3.1.7. Water column properties derived from ADCPs

ADCPs detect the echoes returned from suspended material (i.e. “sound scatterers”) from discrete depths of the water column. Echo intensities, per transmitted pulse, are recorded in counts (also termed the Received Signal Strength Indicator (RSSI), providing indirect information on the currents and density of suspended matter (‘backscatter’) within each ensonified bin. For the backscatter, the values remain relative as the instrument cannot differentiate the echo intensity from various sources (i.e. suspended sediments, debris, plankton, or air bubbles and high levels of turbulence, e.g. due to waves). This bias complicated interpretation of the datasets, as well as quantitative analyses to find correlation with hydro-meteorological datasets.

Currents and turbidity

For recalculation of bin depth of the HM-ADCP to actual depth values below the water surface, a fixed draught of 4 m was added for RV Belgica. With the blanking distance associated to the type of instrument and the bin size (2 bins are lost), the first depth was around 7 m below the water surface for the hull-mounted profiles with RV Belgica (for 1 m bins). Pulses were averaged into ensembles at a time interval of 60 seconds per sample. The average standard deviation (or accuracy) of current estimates was $\pm 0.018 \text{ ms}^{-1}$ for the 300 kHz ADCP, at 1 m bin size; $\pm 0.009 \text{ ms}^{-1}$ for the 1200 kHz for 0.05 m bin size ADCP (RDI software). For the HM-ADCP data of March 2015 (RV Belgica), the average ensemble interval of 1 min (60 pings), together with a ship speed of 1.5 to 3.5 ms^{-1} resulted in a horizontal resolution of 90 to 210 m. This means that differences in vertical velocity profiles over a dune field (e.g., differentiating between stoss slope, crest, lee face) cannot be revealed.

Algorithms were used to convert the measured RSSI counts to acoustic backscatter in decibels (dB) using the echo intensity scale (dB per RSSI count). The echo intensity was multiplied by 0.42 in order to obtain dB values (instead of counts, and accounting for sound absorption, beam spreading and battery decline). These dB values were then converted to mass concentrations of suspended particulate matter (SPM in gl^{-1}), by calibration against SPM values derived from water filtrations during several field campaigns. In the analyses, some portion of the water column under the hull was removed because of disturbances such as air bubbles and ship noise.

For the re-analyses of the BM-ADCP data of 2013, a low-pass filter was used smoothing the data over a 5-min window (200 samples). The deployment was stable over the measurement period as evidenced by the pitch and roll sensor. In the night of 184, a small negligible change of 1 degree in pitch occurred.

3.1.8. Seabed properties derived from acoustical measurements

In 2015, two additional very-high resolution multibeam datasets (RV Belgica Kongsberg EM3002D, 300 kHz) were acquired in the Habitat directive area, more specifically covering the gravel bed refugia: ST1507 (March 2015) and ST1533 (December 2015). Depth and backscatter data were obtained.

These datasets, together with all previously recorded datasets will be treated together to allow intercomparison in the time series. The development of a standardized workflow is in development. In total seven datasets will be available: two before the start of the extraction (2004, Ghent University; 2010); one before the peak of extraction (2013); and four after the peak of extraction (2014-2015).

To allow using MBES backscatter in a monitoring context, a rigorous research is needed on how to classify the data in terms of backscatter variation and subsequently applying change detection algorithms. For the classification process of all datasets it was important to have one time series composed of both multibeam data and seabed samples for validation. This was done in December 2015. This research relates to the Belspo INDI67 project (PhD G. Montereale-Gavazzi). Results are expected by the end of 2016. An important part of the analysis is the investigation of the morphological evolution throughout the time series.

3.1.9. Seabed properties derived from sampling

Sediment samples, from the seabed and the water column, were analysed for grain-size. Most seabed samples were taken with a Hamon grab (VLIZ) retrieving a rectangular volume of sediment from the seafloor, hence capturing all the sediment fractions available. *See Report Year 2 for sediment analyses procedures.*

To validate the multibeam backscatter in terms of seabed substrate classes in the Habitat Directive Area, 30 samples were taken during campaign ST1533, in complement with the acquisition of MBES data. Here, Van Veen grabs were taken since this allowed acquiring a larger number of samples. Sediment types will be categorized in terms of the predominant seabed classes (following EUNIS Level 3 hierarchy) and will be used in the MBES classification process of the seven datasets.

3.1.10. External data

Wave information (significant wave height in m, direction of low and high frequency waves in degrees, low frequency (0.03 Hz to 0.1 Hz) wave energy in cm^2) were obtained, at 30 min interval, from a Wavec buoy (Westhinder location, Flanders Hydrography) at 18 km southwest of the study area (Figure 2). Sea surface elevation and 3D currents (10 min interval) were extracted from the operational 3D hydrodynamical model OPTOS-BCZ (Luyten et al., 2011). Wind velocity and direction (10 min interval) originated from the fixed Westhinder measur-

ing pole (Flanders Hydrography) (for location, Figure 2). A tidal coefficient⁶ was calculated to discriminate easily between spring and neap tide and variability in spring tidal levels. Values of more than 70 were regarded spring; 50 mid tide.

3.2. Modelling

3.2.1. Model validations

Focus of the modelling is to assess changes in hydrographic conditions, as within MSFD, Belgium stipulated that variations in bottom shear stresses should remain restricted in the advent of human activities (see footnote 1) (Belgische Staat, 2012). Before such assessments can be made, it was critical to validate the existing mathematical models, which are at the basis of the calculation of bottom shear stress. Furthermore, sediment plume modelling needed to be developed, to assess the probability of deposition of fine material in the Habitat Directive area, where ecologically valuable gravel beds occur. Reference is made to previous reports:

- Validation of the hydrodynamic model OPTOS-FIN: *report Year 1*
- Validation of the sand transport models MU-SEDIM: *report Year 2, as well as Annex C, for a detailed report on calculations and modelling of bottom shear stresses*
- Validation of advection-diffusion sediment transport models MU-STM: *See report Year 2*

3.2.2. CFD Modelling

An opportunity was taken to obtain results from a modelling exercise carried out by Tomás Fernández Montblanc from the University of Cadiz (CACYTMAR), Faculty of Marine Science. He used OpenFOAM CFD modelling⁷ to simulate flow variation over dune morphologies starting from a non-hydrostatic numerical 2DV (two dimensional vertical plane) flow model. The conventional k-epsilon turbulence model was used to simulate turbulence. In this model k defines turbu-

⁶ For the calculation of the tidal coefficient a methodology was adopted that is commonly used in France, and used by the French Hydrographic Service SHOM (http://fr.wikipedia.org/wiki/Calcul_de_marée). A tidal coefficient represents the amplitude of the tidal level compared to its averaged level and is expressed in hundredths. In France, data is used from tidal levels in Brest where a value of 100 is the maximum astronomical tidal level. For this location, regarded as being representative for the Atlantic coast, the values vary between 20 and 120. Values more than 70 are regarded spring tide; those below neap tide. A coefficient of 95 corresponds to average spring tidal levels; 45 average neap tidal levels. For the calculation of the tidal coefficient for Belgian waters an averaged tidal level (TAW) was taken from a 10-yrns elevation data series (2001-2010) from the tidal gauge at Oostende (Vlaamse Hydrografie, 2011). This value (2.339 m TAW) was subtracted from the high water levels at Oostende (Meetnet Vlaamse Banken, HWO) during each campaign. The outcome was first divided by the averaged value of the most elevated tidal levels (i.e., equinox spring tidal levels; for Oostende this equals to 6/2 m TAW, Vlaamse Hydrografie, 2011) and then multiplied with 100 to obtain the value in hundredths. In short the formula is $[(HWO-2.339)/3*100]$.

⁷ **OpenFOAM** (for "Open source Field Operation And Manipulation", www.openfoam.com) is a toolbox for the development of customized numerical solvers, and pre-/post-processing utilities for the solution of continuum mechanics problems, including computational fluid dynamics (CFD).

lent kinetic energy (TKE⁸). The k-epsilon turbulence model is a high Reynolds number turbulence model, which means the model cannot solve the flow entirely where the Reynolds number is low.

To run the model, a 2D bathymetrical profile of the barchan dune series was provided as input, as well as grain-size and a depth-averaged current of 1 ms⁻¹. Some simple simulations were made.

⁸ The turbulent kinetic energy (TKE) is the energy extracted from the mean flow by the motion of turbulent eddies.

4. Results

4.1. Natural variation in sediment processes

Reference is made to the reports of Yr1 and Yr2 (Van Lancker et al. 2014, 2015) detailing the main natural variations that were current- and wave-induced, based on the 2011-2015 monitoring. Mostly new insights are dealt with here, and are mostly based on new 13-hrs measurements and long-time series obtained with the HM-ADCP and BM-ADCP. New results on SPMC in the water column, as well as in-situ particle sizes were obtained in three areas: (1) in and around Sector 4b; (2) Habitat Directive Area, Oosthinder sandbank south and adjacent gully; and (3) Habitat Directive Area, gully west and east of the Westhinder kink area.

Oosthinder sandbank, Sector 4b

During ST1507, a 13-hrs water sampling and vertical profiling of oceanographic parameters was conducted in Sector 4b (sample location 4, east slope of the sandbank). Figure 6 shows the hydrodynamic conditions during the measurements, as obtained from model results (OPTOS-BCZ) for the Westhinder location (MFB, MP7), ± 30 km southwest of the measurement location. Importantly, the results show an important offset between the timing of HW and LW and the associated maximum current speed. This is important to explain the variation in vertical profiles of SPMC throughout the water column, as displayed in Figure 7. On average SPMC varied around 0.004 gl^{-1} with peaks up to 0.009 gl^{-1} , with highest SPMC under ebb condition (SW-directed), under highest current condition.

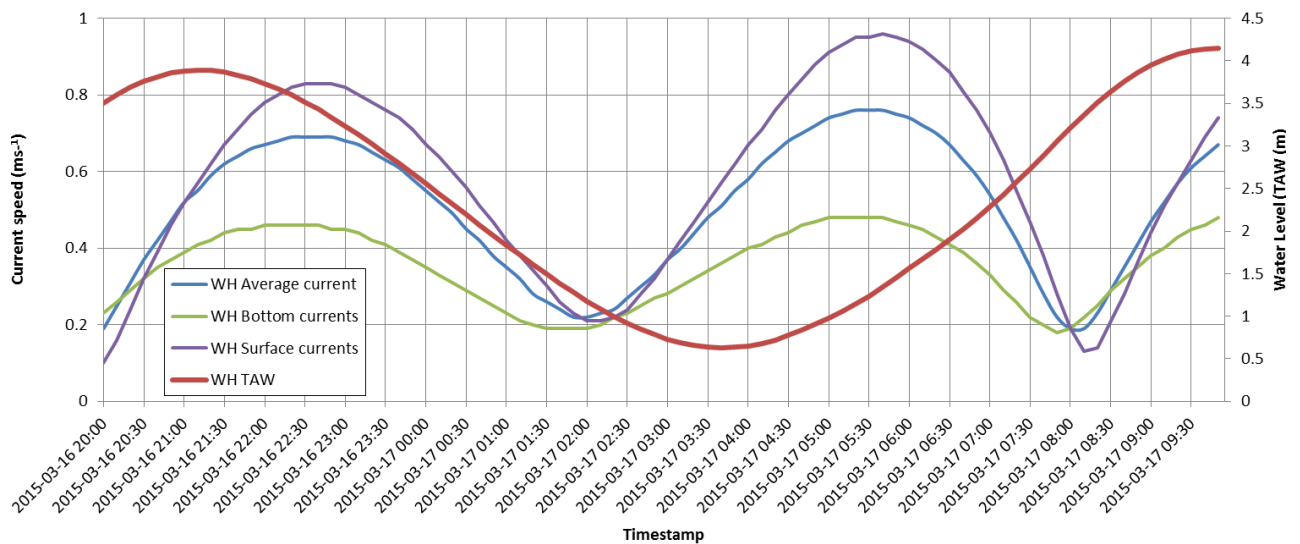


Figure 6. Sector 4b. Water level and current characteristics during the 13-hrs cycle (from OPTOS-BCZ model, MP7 Westhinder location) (grid lines every 30'). Note highest current velocities in: (1) surface waters: HW+1h30 and HW-4h30 (LW+2h); and (2) bottom waters: HW+1h and HW-4h30 (LW+1h30). Slack water: HW-1h30 to -2h00; and HW+4h to 5h. Ebb currents predominated in strength.

The associated LISST profiles (Figure 8) show particle sizes (mean values) from 100-200 μm (Figure 8). Higher than 200 μm mean values were observed at

highest current speeds, after HW and LW (highest SPMC). Still, highest near bottom mean sizes were found at slack tide from HW to LW. The latter is probably corresponding to a flocculation peak, though it is more likely that the maxima at highest current speed correspond to grain sizes. For these profiles there is no clear sequence in smaller and higher particle sizes with smaller sizes at high current speed and bigger sizes at slack tide, which would be the typical floc sequence (breaking up of flocs under high current speeds; aggregation into flocs under low current speeds). More research is needed to understand variation in particle sizes accounting for the nature of the particles and their shape, and this under various hydro-meteo conditions. The present measurements do reveal that highest POC concentrations (and POC:PON ratios up to 7.6) are measured when the current is directed to the NE (up to 0.57 g l^{-1}), with minimum values measured under SSW-directed currents (0.316 g l^{-1} ; POC:PON: 5.14). It should be remarked that the PSD of the water column suspensions also show a mode around $10 \mu\text{m}$, which also occurred in the PSD from seabed samples.

Substrate characteristics

During ST1517, video images were recorded in the gully west of Sector 4b. Aim was to have comparative material within the gullies in the area of the Hinder Banks. A series of selected video footage is shown in Annex B. In short, 4b1 4b4 and 4b7 were located nearest to the gentle western slope of the sandbank where Sector 4b is designated. Small to medium dunes were observed with shell hash sometimes concentrated in patches (especially 4b4), and sometimes fully aligned in the troughs of the dunes. Some brittle stars were observed, as well as organic material deposits. At 4b7 small-sized gravel occurred, with some anemones. Resuspension clouds were evoked when the frame touched the seafloor, pointing to some fine-grained material in the bed. Similar situation for 4b5, located nearer to the axis of the gully, though the wavelength of the dunes was somewhat larger. 4b8 seemed to show more sand abundance, with higher and longer dunes too, but also some small-sized gravel (maybe bigger shells). 4b6 was similar to 4b5 and roughly 4b1. 4b9, closest to the Westhinder sandbank, predominated in sands, again with localized shell hash deposits, as well as organic material. Some video was shot just north of sector 4d, corresponding to the head of the Westhinder sandbank. Here, shell hash deposits were abundantly present, mostly concentrated in the trough of dunes (WHS02 and WHS03) (see also Papili et al., 2015).

Particle-size analyses of the seabed samples showed medium to coarse sands with a mean particle size between 400 and $600 \mu\text{m}$ (Figure 9). 4b1 had around 5 % silt-clay enrichment (finest mode around $10 \mu\text{m}$) and was poorly sorted; 4b4 around 3 % (moderately well sorted). Sample pictures (see cruise report ST1517) showed brown waters. 4b2 and 4b3 had 0 % silt-clay. A centrifuge sample taken in the gully (over a time span of 12h20; Sector 4b sample in Figure 9) showed a polymodal distribution with modes around $330 \mu\text{m}$, $153 \mu\text{m}$, $105 \mu\text{m}$ and $15 \mu\text{m}$.

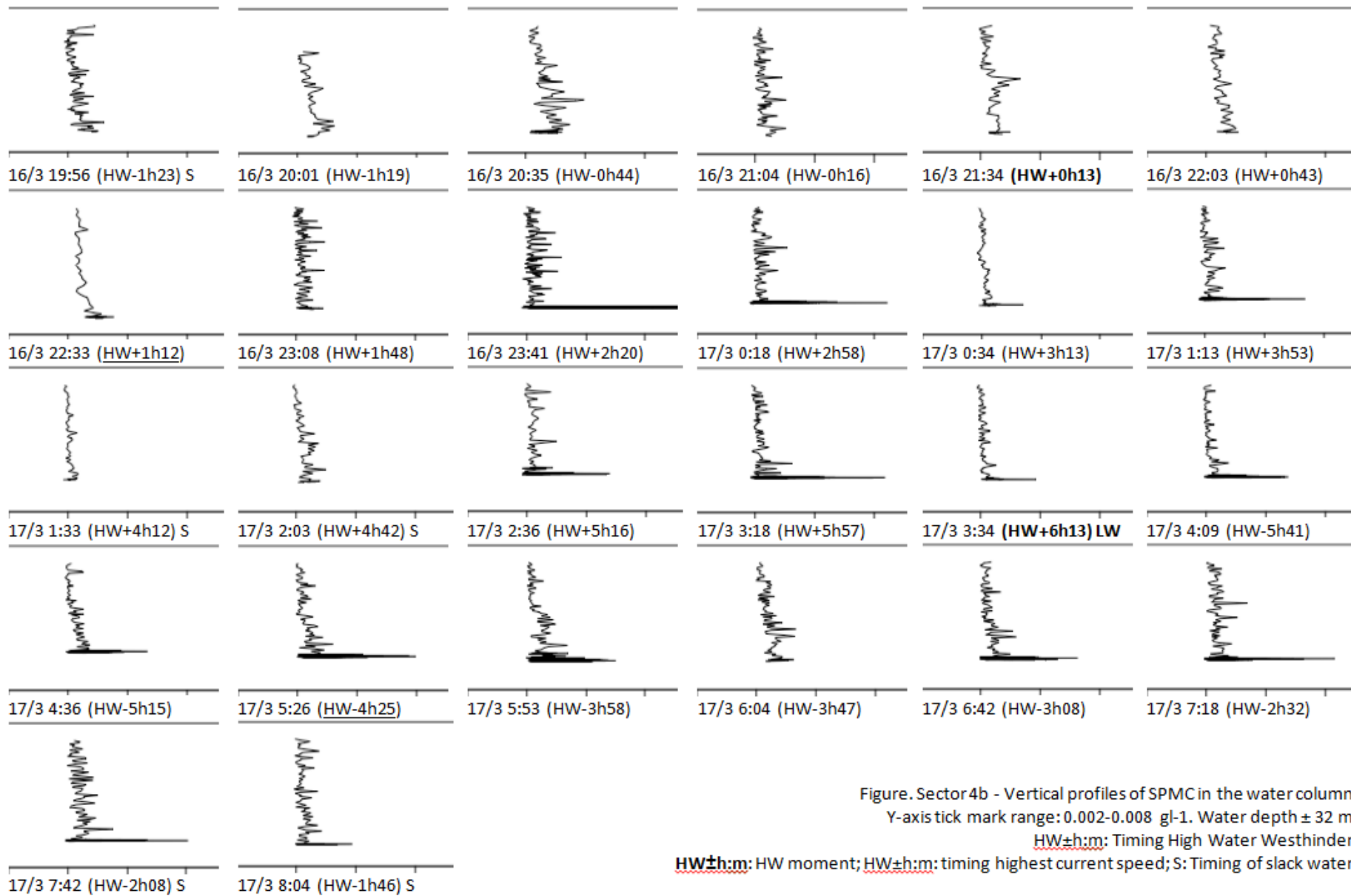
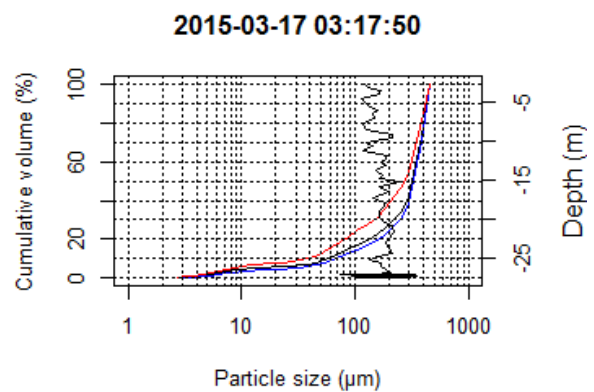
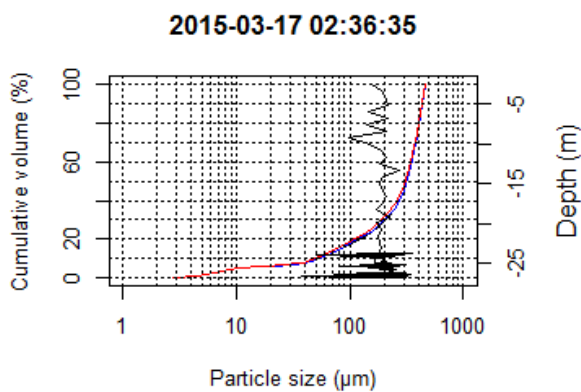
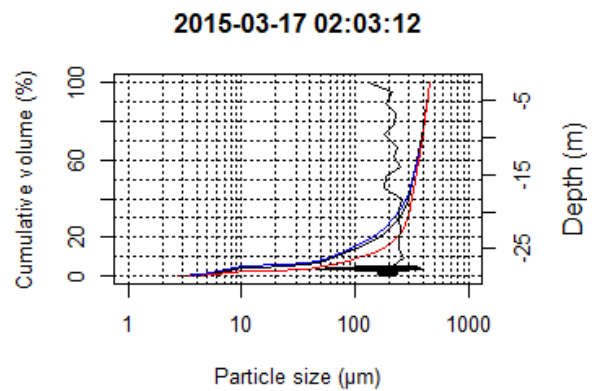
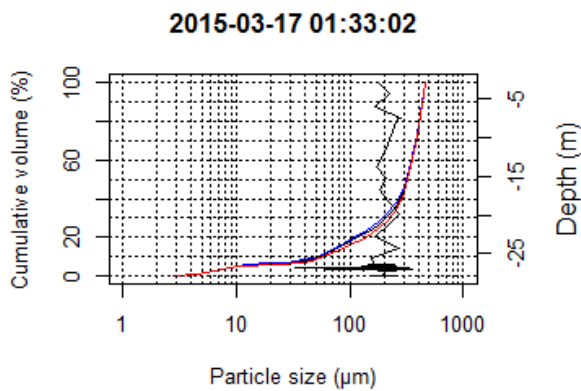
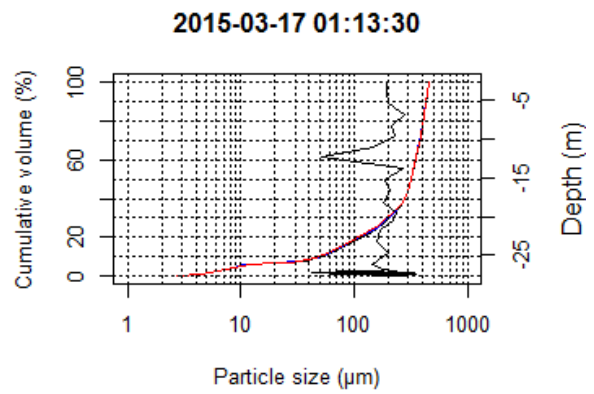
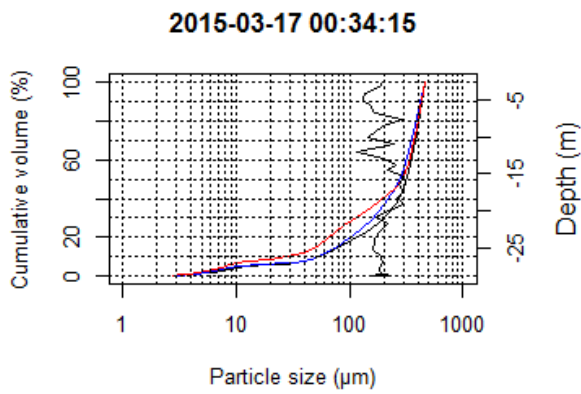
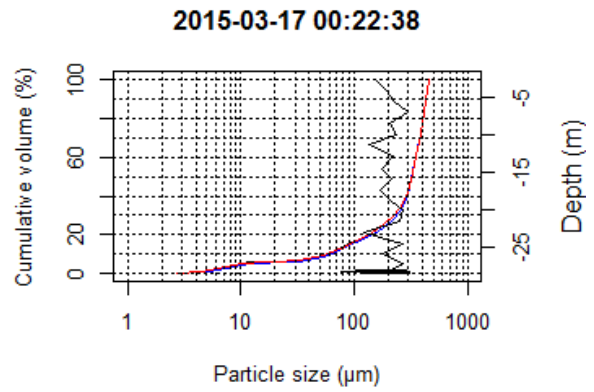
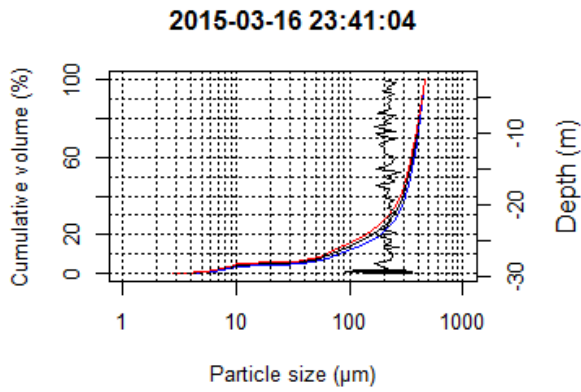
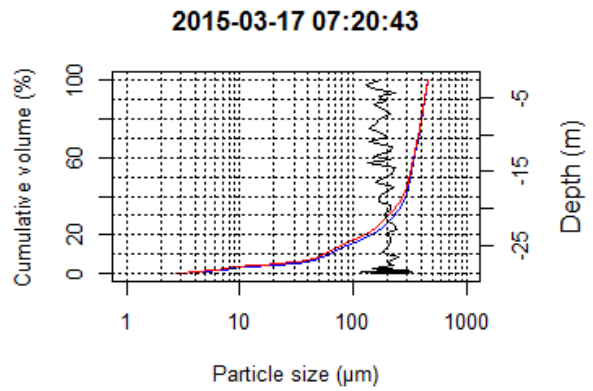
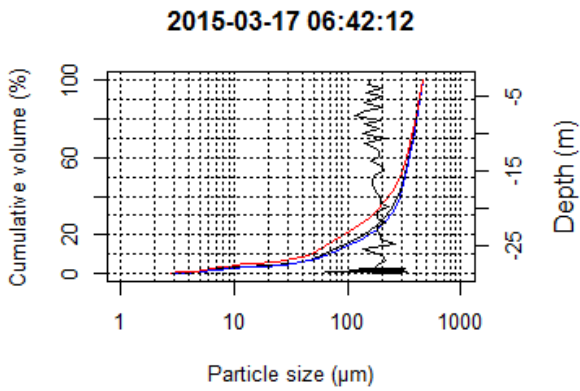
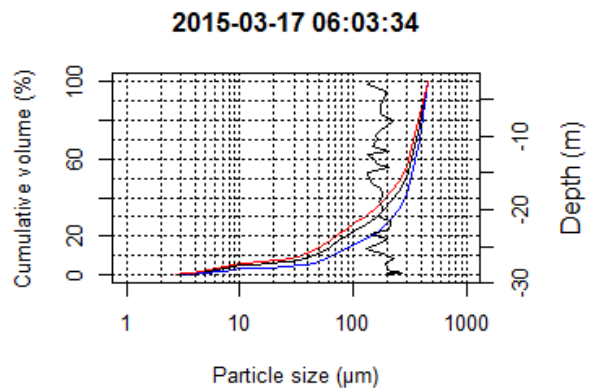
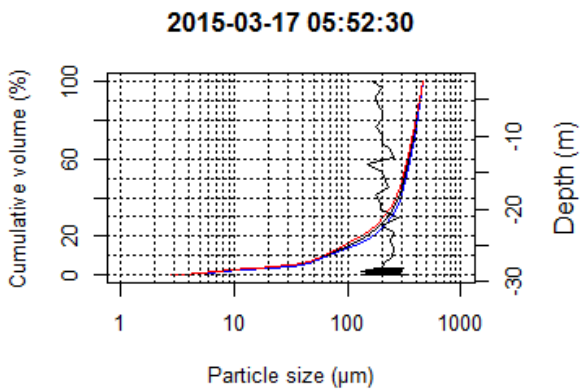
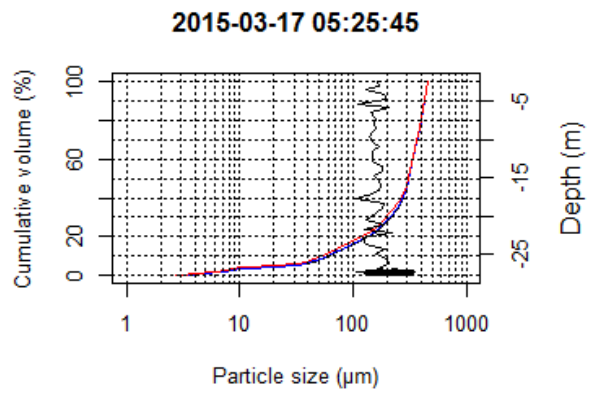
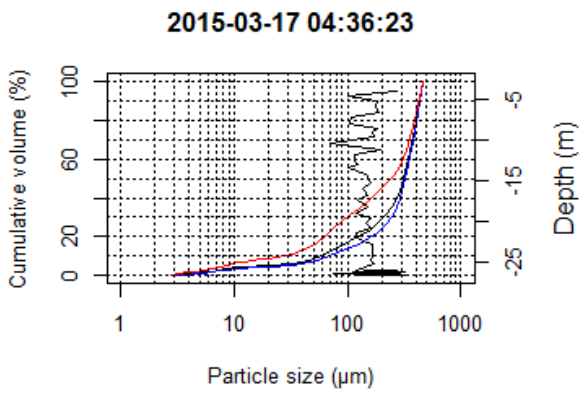
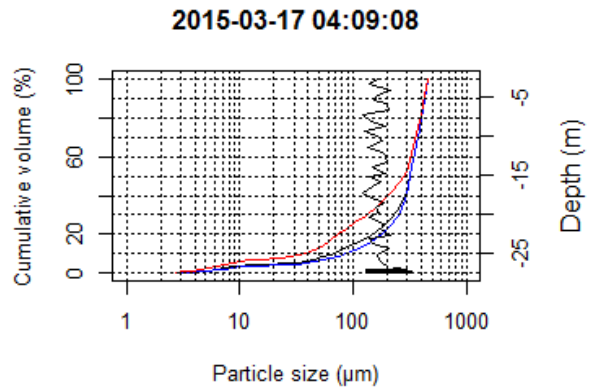
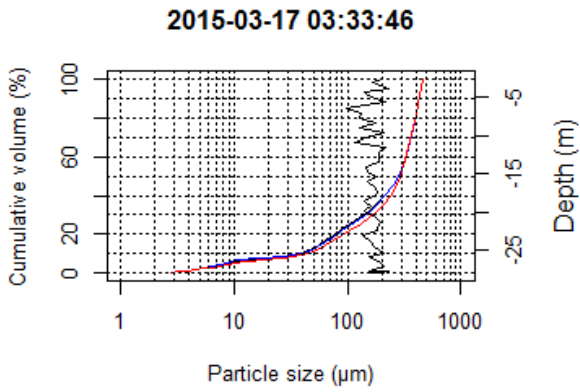


Figure. Sector 4b - Vertical profiles of SPMC in the water column.
 Y-axis tick mark range: 0.002-0.008 g⁻¹. Water depth ± 32 m.
 HW±h:m: Timing High Water Westhinder.
 HW±h:m: HW moment; HW±h:m: timing highest current speed; S: Timing of slack water.

Figure 7. Sector 4b. Vertical profiles of SPMC in the water column.





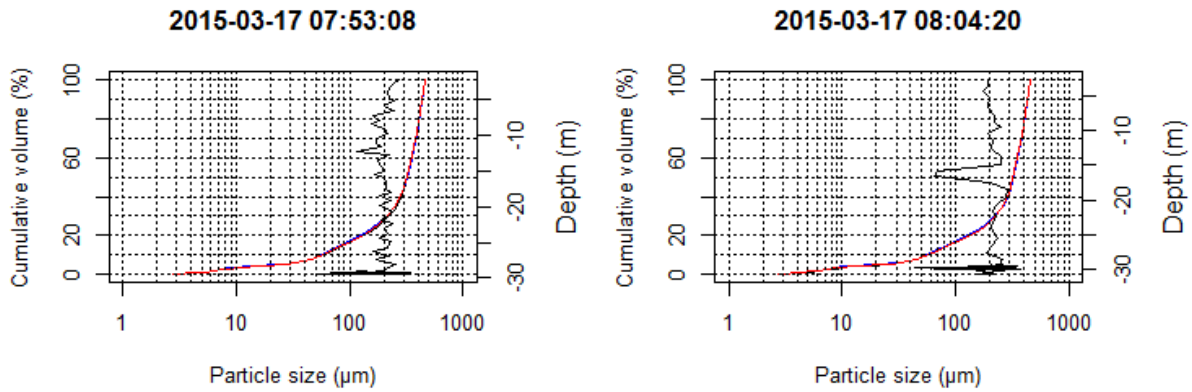


Figure 8. Cumulative particle-size distributions (PSD) in the water column (LISST profiling) (black: average particle size, red: top 10%, blue: bottom 10%) together with mean grain size (grey) of each individual profile taken during the measurement cycle. Timestamp is related to the value that maximum depth was reached. See previous figure for tidal level related data per timestamp.

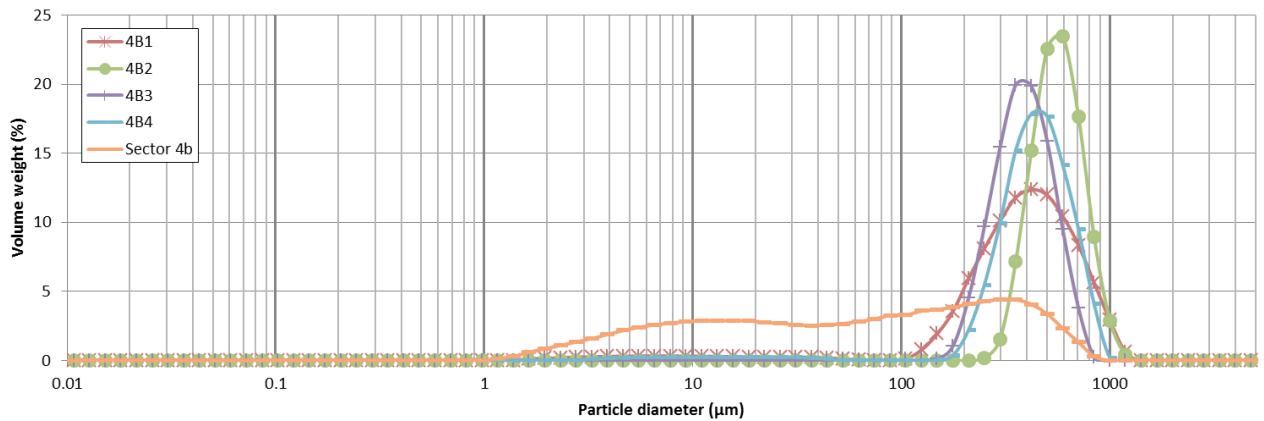


Figure 9. Particle-size distribution (PSD) of samples taken in the gully west of Sector 4b (ST1517), Oosthinder sandbank. 4B1 to 4B4 refer to seabed samples. A Hamon grab was used for the sampling, except for sample Sector 4b which has been collected with a centrifuge, hence representative of particles in the water column. See cruise report ST1517 for more details and pictures of the samples taken.

Habitat Directive Area, Oosthinder sandbank south and adjacent gully

Natural variation in sediment processes was further investigated in the Habitat Directive area, particularly along the barchan dunes, where ecologically valuable gravel beds occur (Figure 10). Variation in currents and turbidity were investigated in detail to assess to what extent the typical morphology of the barchan dunes gives rises to eddy formations which could lead to enhanced trapping of fine material in the water column. Hypothesis was that the more fine material is available in the water column (e.g., by intensive aggregate extraction), the more material is trapped and can ultimately lead to a smothering of the gravel beds in the troughs of the barchan dunes. This is important since the Belgian implementation of MSFD specifically stipulates that in the gravel areas the ratio of hard versus soft substrata should not decrease.

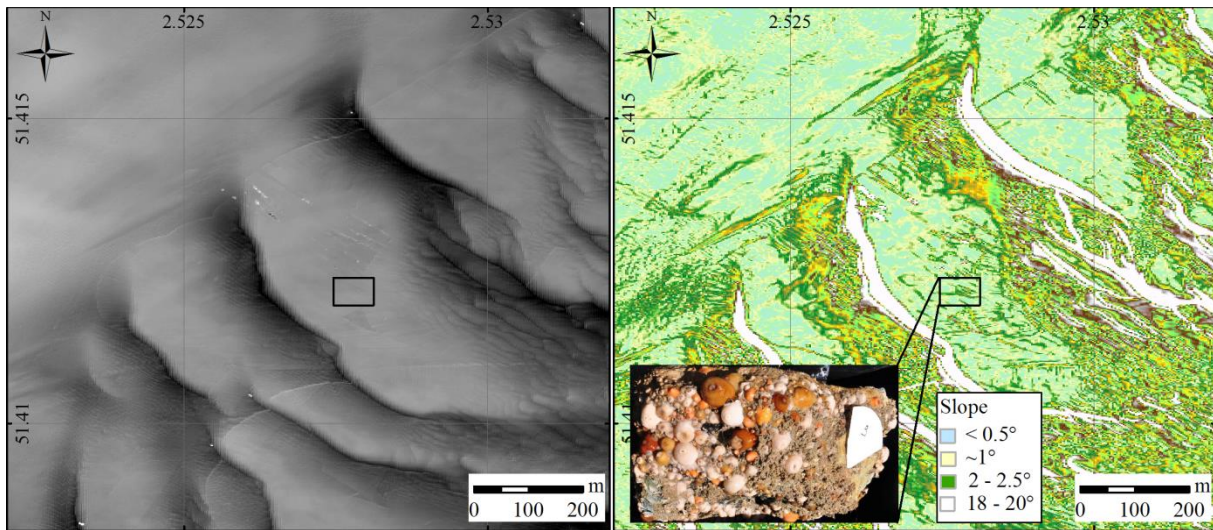


Figure 10. Bathymetry (left) and slope (right) map of barchan dunes, where the dune troughs host gravel beds overgrown with epifauna (-30 m MLLWS) and richer species compositions. The dunes are 6 to 7 m in height with wave lengths of around 200 m. The complex dune morphology protects the fauna from abrasion from fisheries, though it is hypothesized that the nature of biodiversity in the dune troughs is also related to acceleration and deceleration of the current over the steep dunes ($\sim 20^\circ$; locally up to 30°), resulting in trapping of fine-grained sediments near the lee side. The source of the fine-grained material may be natural, or anthropogenically-induced. In the longer term, depending on the nature of the flora and fauna, the addition of the fine-grained material may be beneficial (nutrient input) or adverse (smothering) for biodiversity. The slope variations in the troughs (up to 2° - 2.5°) are indicative of the occurrence of gravel beds. The inset is a sampled gravel block (20 cm) (Van Lancker, 2017).

Following, the BM-ADCP dataset of 2013 is re-discussed, since more data were recovered from this deployment: 5 tidal cycles (5 HWs and 5 LWs) during neap tide (tidal amplitude ~ 3 m) (Area 2; report Yr2, Fig. 7 p. 18) (Figure 11, Figure 12, Figure 13 & Figure 14). From these plots, it can be inferred that during maximum flood currents the variance on the currents is higher than during ebb maximum. During slack tide phases currents have the lowest variance in their magnitude. This could point to a transition from laminar to turbulent flow under stronger tidal conditions, and only during flood, hence in the direction of the steep slope of the dunes. Under these conditions higher SPMC occurred mostly. Figure 17 is a synthesis of the difference in SPMC between flood and ebb. Note that the recordings presented are recorded under neap tidal conditions; higher contrasts are expected under spring tidal conditions.

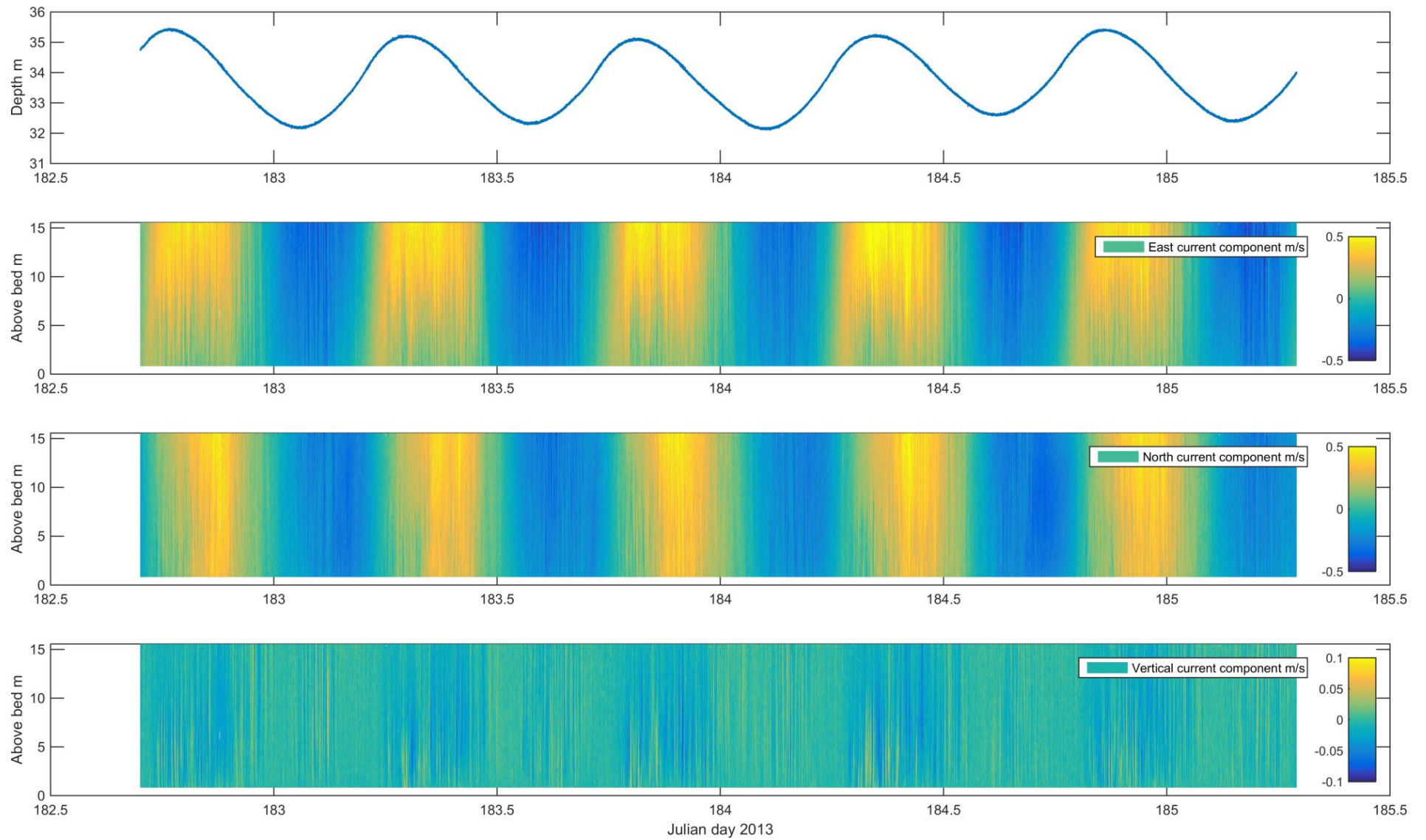


Figure 11. BM-ADCP dataset in the trough of a barchan dune, along southern part of Oosthinder sandbank (2013-07-01 - 2013-07-04; Neap tide, tidal amplitude ~ 3 m): water current components (east, north, vertical), together with the water elevation. Note the temporal fluctuations in the current data.

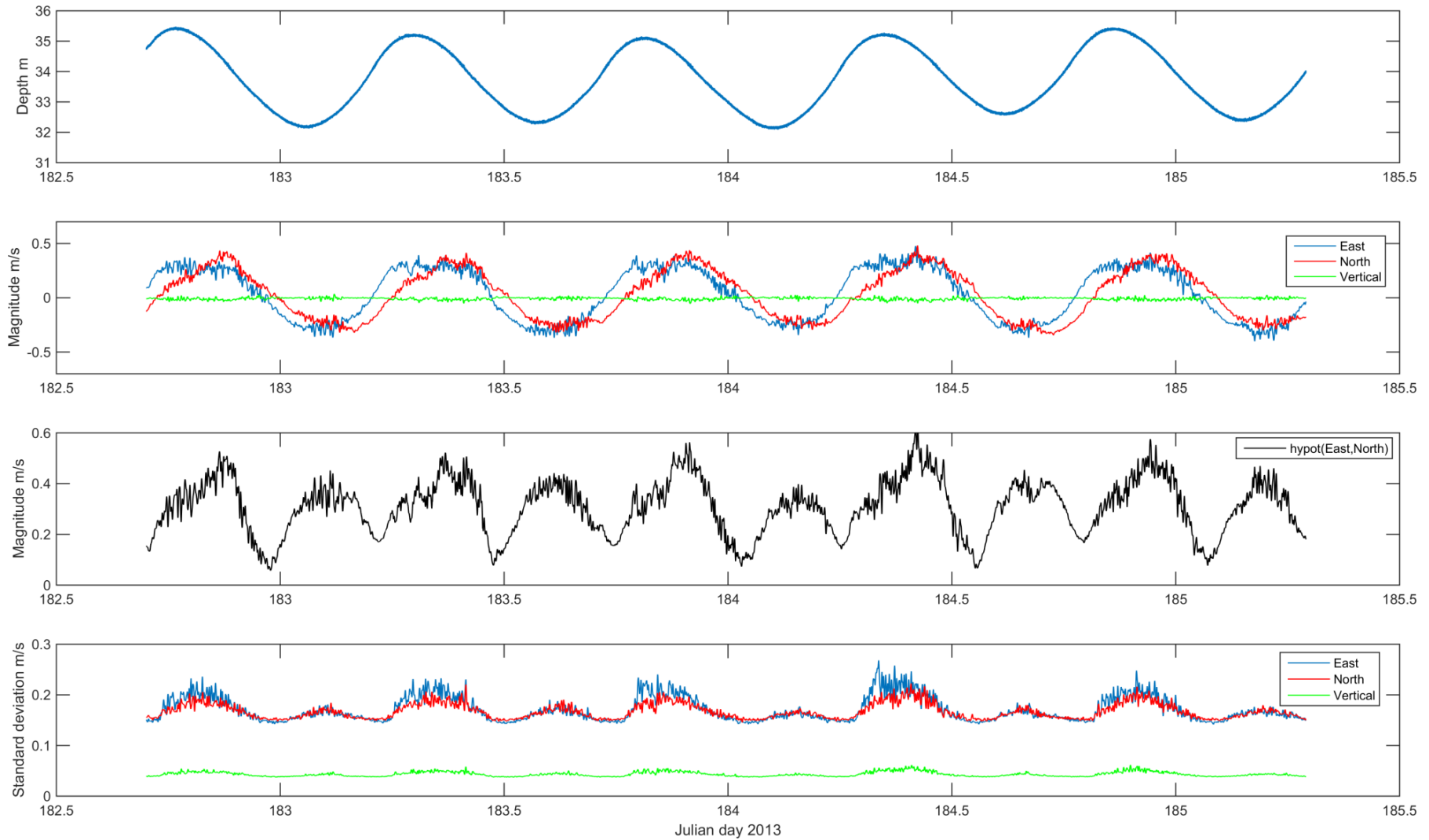


Figure 12. BM-ADCP dataset in the trough of a barchan dune, along southern part of Oosthinder sandbank (2013-07-01 - 2013-07-04; Neap tide, tidal amplitude ~ 3 m): overview of ‘depth-averaged’ (actually the lower half of the water column) hydrodynamics. Subplot 1; tidal water elevation; subplot 2; vertically-averaged currents components. Subplot 3 (black line): total horizontal current magnitude; subplot (4): vertically derived standard deviations. Note the higher variance of the flood current as compared to its ebb counterpart.

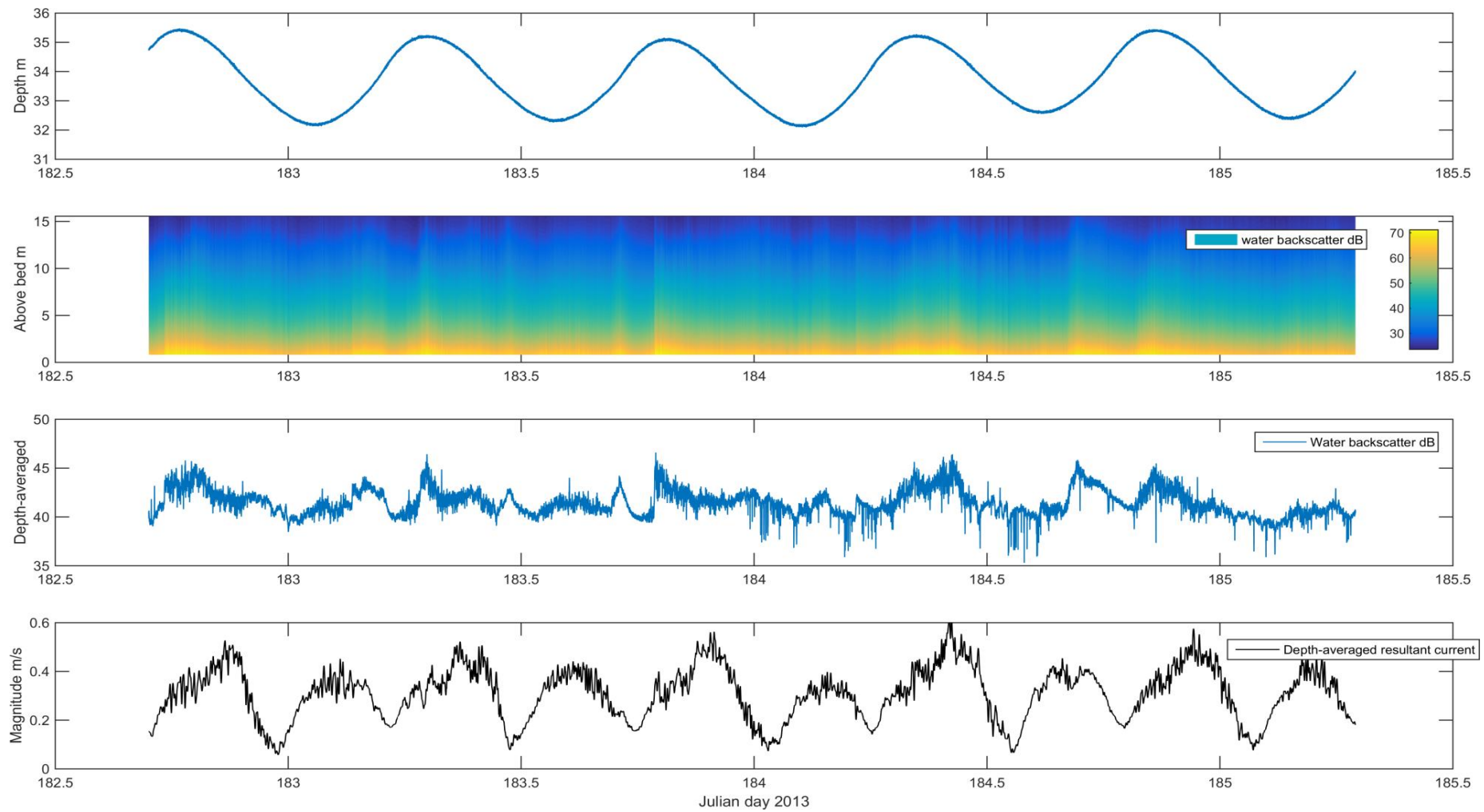


Figure 13. BM-ADCP dataset in the trough of a barchan dune, along southern part of Oosthinder sandbank (2013-07-01 - 2013-07-04; Neap tide, tidal amplitude ~ 3 m): time series of the echo-intensity data (in dB), in combination with depth-averaged resultant current.

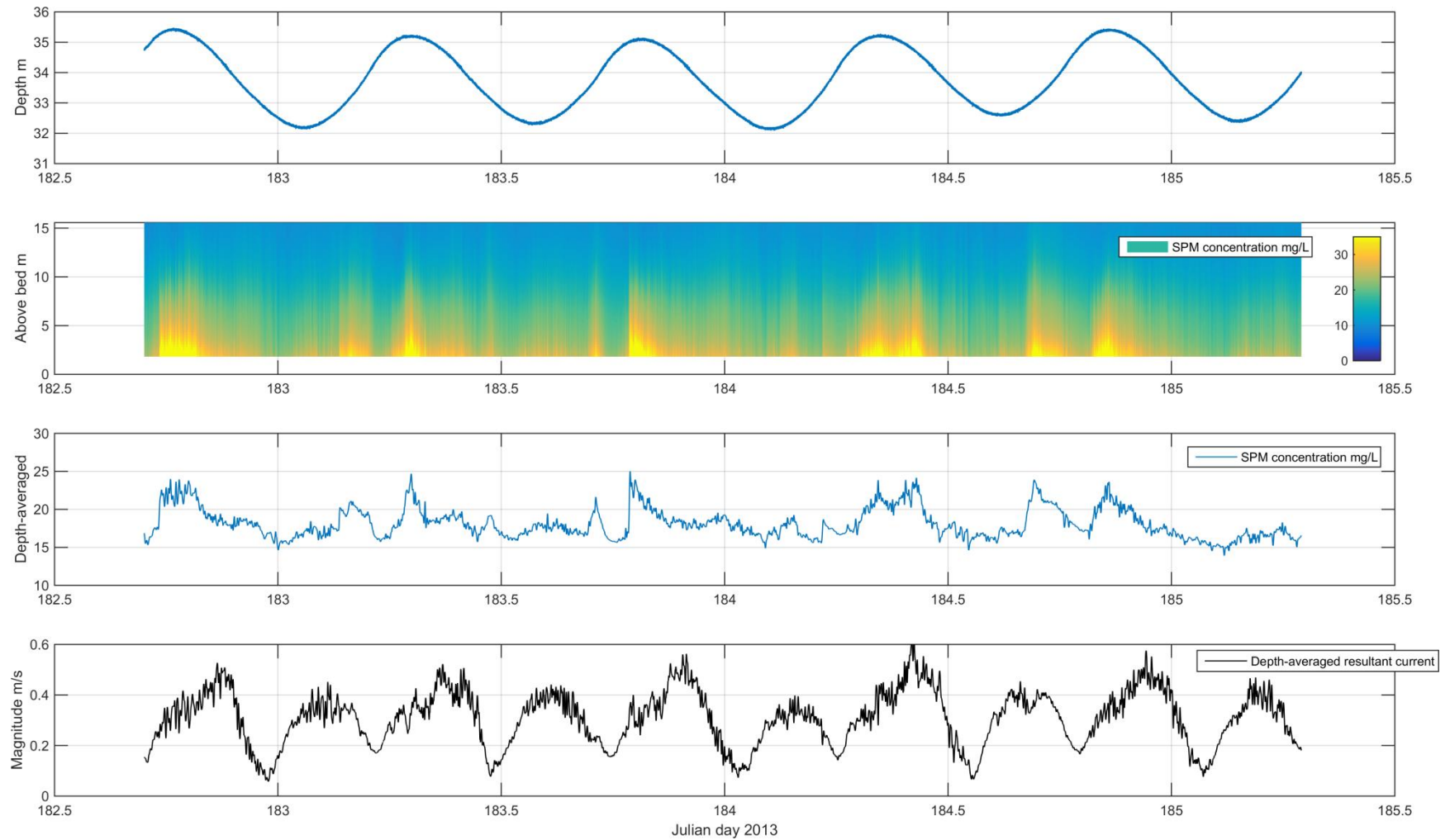


Figure 14. BM-ADCP dataset in the trough of a barchan dune, along southern part of Oosthinder sandbank (2013-07-01 - 2013-07-04; Neap tide, tidal amplitude ~ 3 m): time series of SPMC, as converted from the backscatter data, in combination with depth-averaged resultant current. Note that mostly higher SPMC are observed under flood conditions. There is an overall relationship between current magnitude and SPM concentration; however there are shorter-term relationships (between magnitude and SPMC) that are less good.

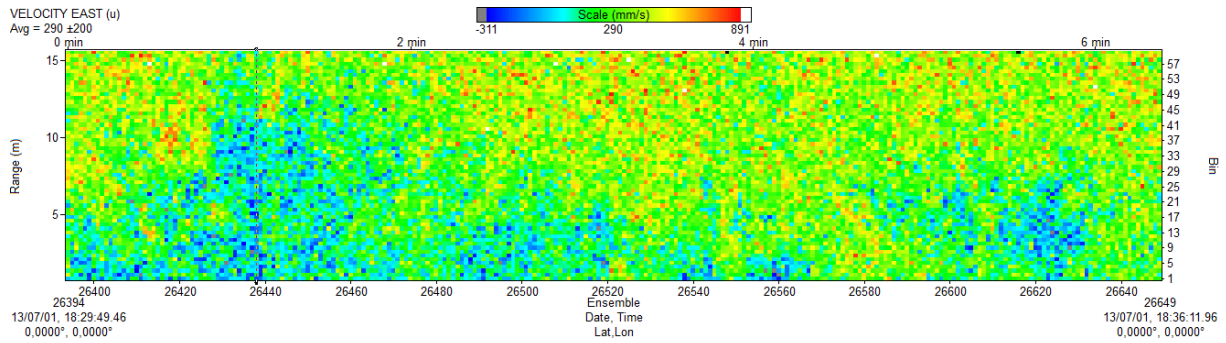


Figure 15. Observations of short-term fluctuations (intermingling of negative (blue) values) in the lower water column (data frame of 7 min), as recorded by the 2013 BM-ADCP deployment (2013-07-01 - 2013-07-04) (screenshot from WinADCP software).

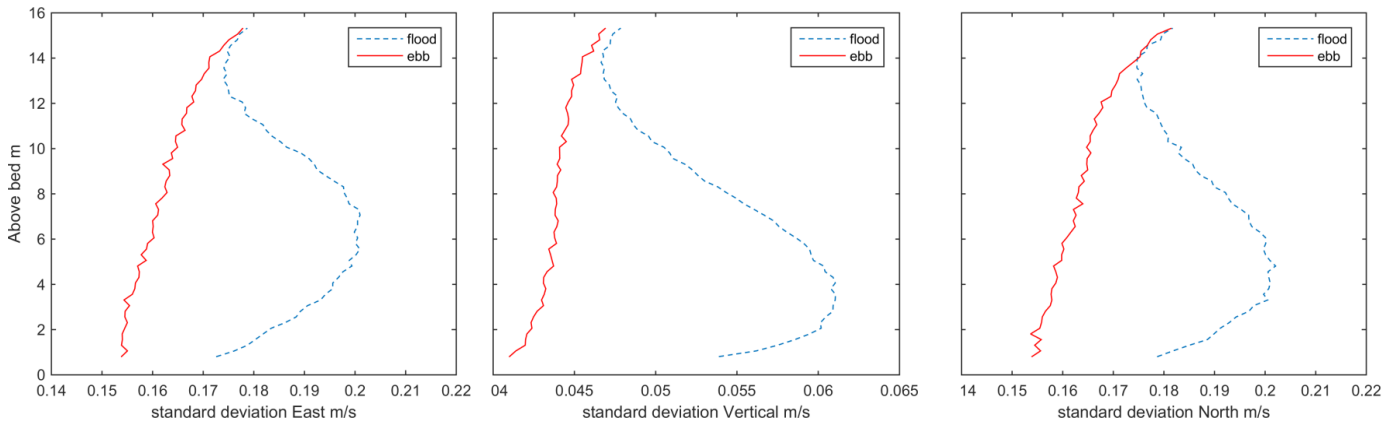


Figure 16. Standard deviation for the three current components near the lee side of a step barchan dune as recorded by a BM-ADCP (2013-07-01 - 2013-07-04). Note clearly the high variance of the currents under flood conditions (overall in the region lower than -13 m; highest below -8 m, as compared to the ebb counterpart).

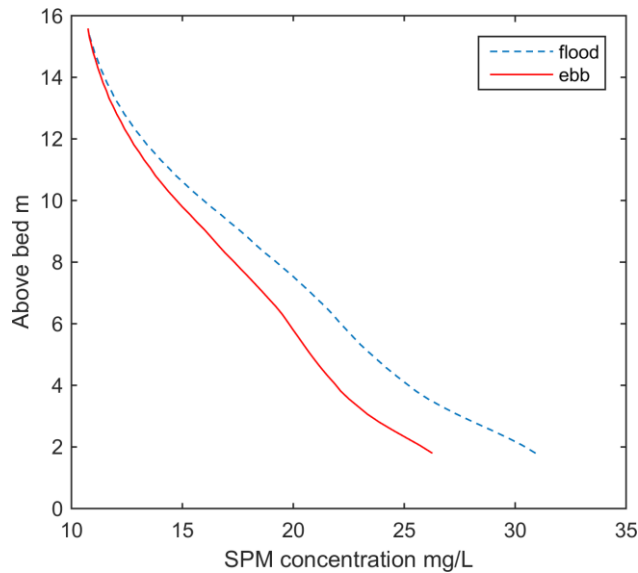


Figure 17. Synthesis of the difference in SPMC under flood and ebb conditions (BM-ADCP; 2013-07-01 - 2013-07-04). Flood SPMC increases more when reaching closer to the seabed compared to ebb SPMC.

The longer term BM-ADCP deployment of February 10-25, 2015 confirmed previous observations on current and turbidity variations in the barchan dune area.

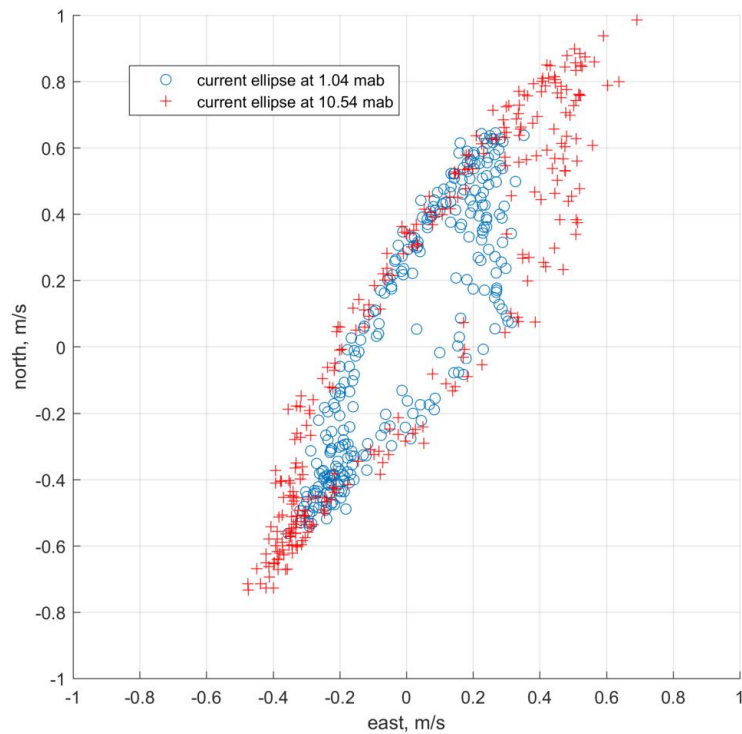


Figure 18. Current ellipse for different heights, at 1 and 10.5 mab. Flood currents are fully developed for heights more than 10.5 mab. Below 10.5 mab the flood current is reduced, likely pointing to flow reversal near the lee side. This result is similar to what was found previously (Van Lancker et al., 2015 Fig. 30 p. 44). Note that spring and neap tide conditions are mixed together in this plot.

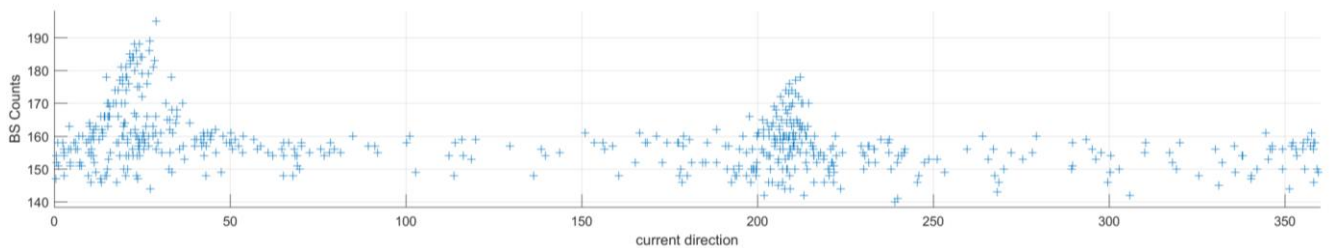


Figure 19. Relationship of current direction and corresponding backscatter (BS counts), as a proxy for water turbidity. Flood current corresponds to somewhat higher turbidity. Note that spring and neap tide conditions are mixed together in this plot.

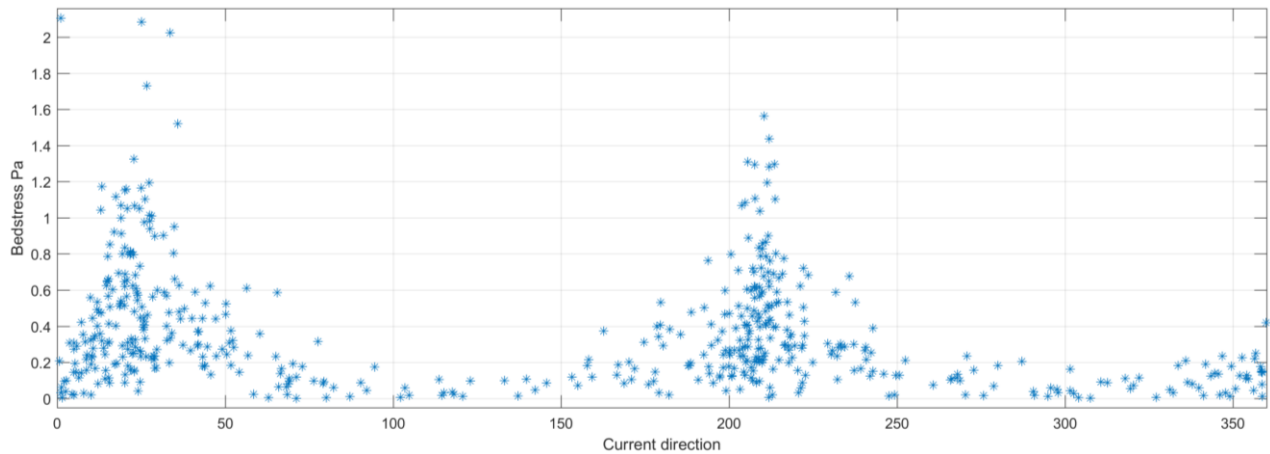


Figure 20. Relationship of current direction and corresponding bed shear stress (Pa). Both ebb and flood currents induce about the same shear stresses at the seabed. Note that spring and neap tide conditions are mixed together in this plot. Bed shear stress is calculated from the logarithmic current profile. Based on the first 5 bins above the bottom (between 1 and 3 mab).

In March 2015 (2015-03-19 21:30:28.06 -2015-03-20 08:27:28.54), a short transect was sailed back-and-forth over a series of barchan dunes for 13-hrs. Currents and turbidity were measured with RV Belgica’s HM-ADCP. Aim was to depict current and turbidity variability over the dune morphology.

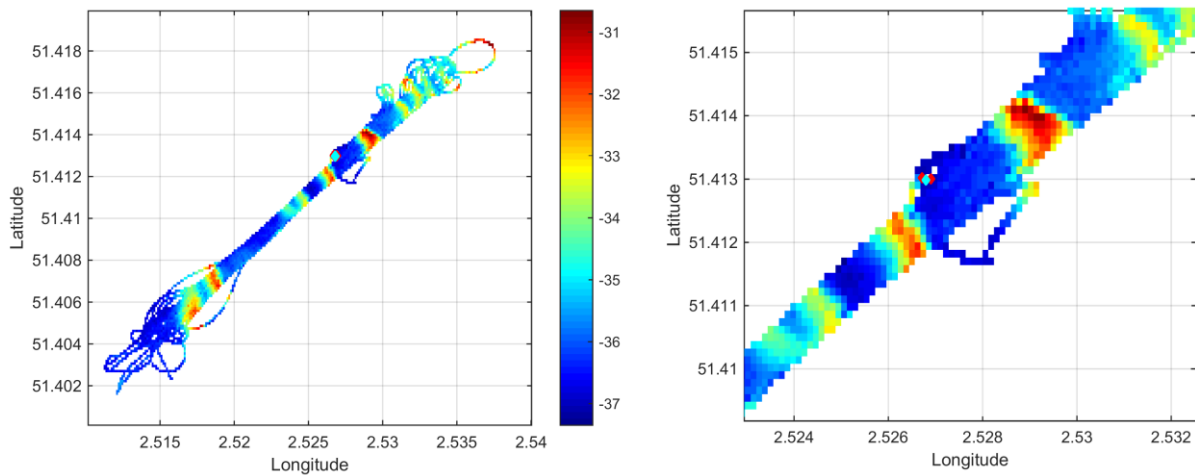


Figure 21. HM-ADCP transect over a series of barchan dunes. RV Belgica ST1507. Left: full transect; Right: zoom on location of BM-ADCP (diamond), at about 90 meters from the barchan dune crest.

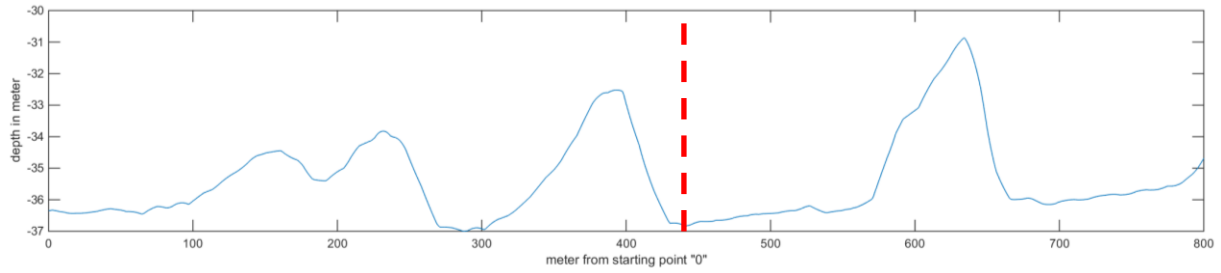


Figure 22. Morphology of the transect with barchan dunes of 5-6 m in height. Dashed line indicates the location of the BM-ADCP (OH-GRAVEL), as discussed previously. Note that the bathymetrical profile shows a little scour mark at the toe of the barchan dune that might be associated with a return flow.

In the following figures, current strength (ms^{-1}) is displayed for the part of the transect (0-250 m section) in the trough of a barchan dune, under SW directed (ebb) and NE directed (flood) currents. Although, the transects alternated (back-and-forth) it is remarkable that higher currents were measured when RV Belgica sailed to the NE. Figure 23 shows that persistent higher currents were measured when sailing in the direction of the steep slope of the dunes.

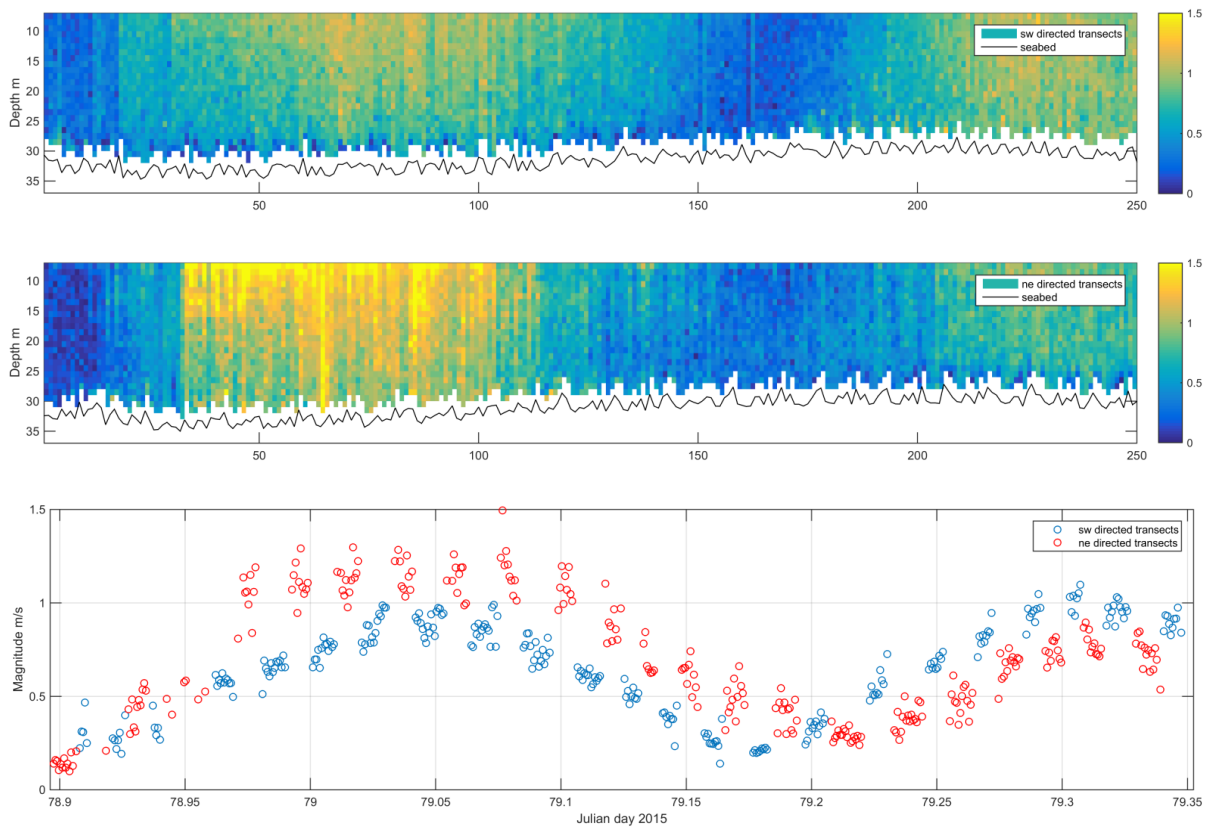


Figure 23. Current velocity field through time as RV Belgica sailed to the SW and to the NE, alternatingly. Upper 2 graphs: current strength over the time period in ensembles; Lower 2 graphs: current strength over the time period in Julian date_Higher currents were measured sailing in a NE direction, in the direction of the steep slope of the dunes. Clearly, the sailing direction impacted on the flow measurement, and depended also on the current direction (see further). Following pers. comm. with experts in the field, the cause for the directional bias when using bottom track would be non-uniform flow. Since this causes having a skewed horizontal velocity distribution, it is very hard to sample the flow for left-to-right transects in the same way that one would for right-to-left transects.

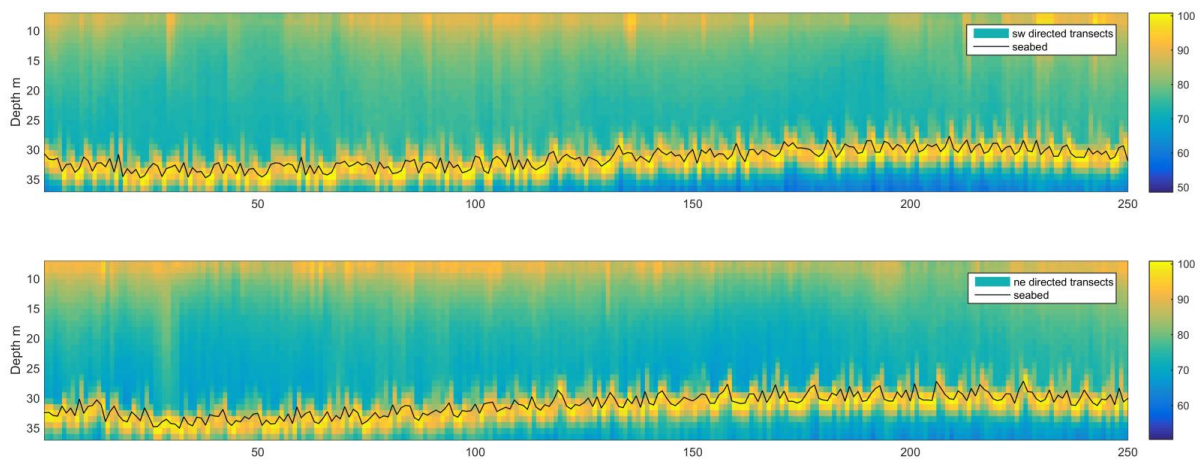


Figure 24. SPMC evolution over the 13-hrs cycle (ensemble 0-250).

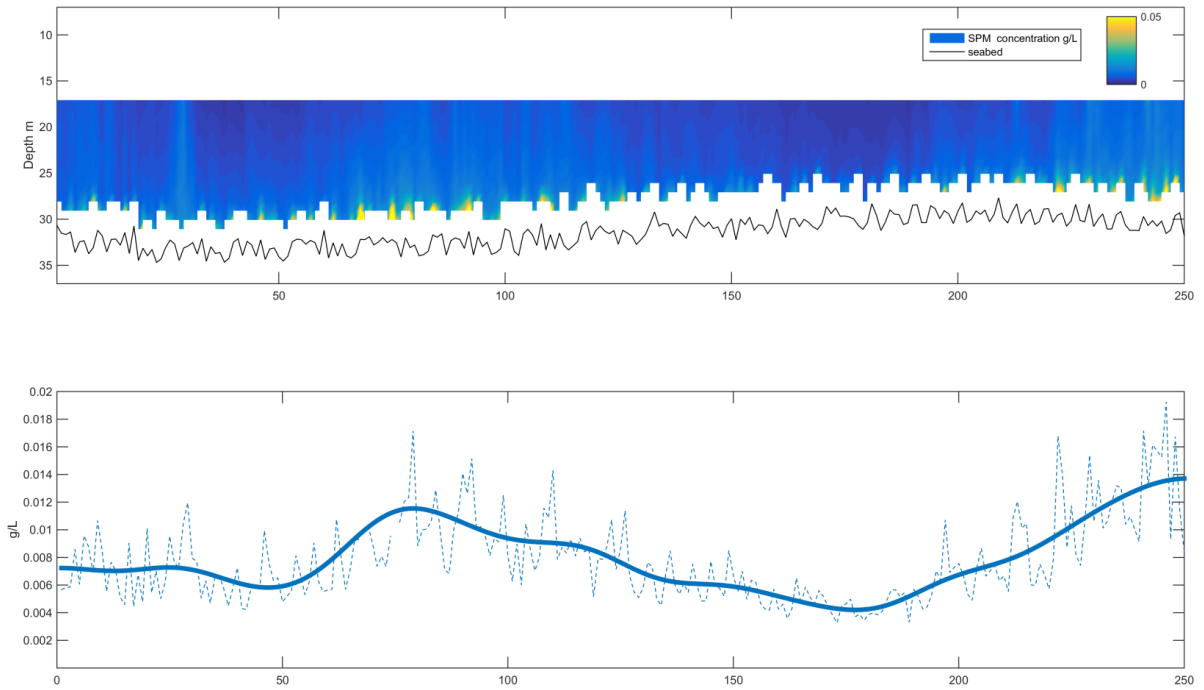


Figure 25. SPM evolution over the 13-hrs cycle (ensemble 0-250) and vertically averaged for the lower half of the water column with flood and ebb maxima of about 0.010 and 0.014 g/L . During this time period, SPM was indeed somewhat higher under ebb conditions. This might be explained by wind waves with H_s of 1.5 m under NNE winds.

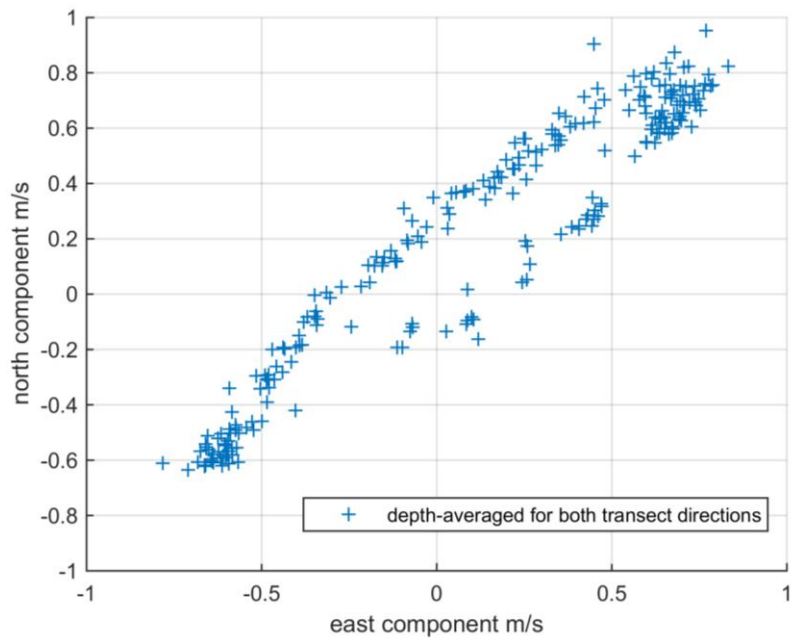


Figure 26. Tidal ellipse (horizontal velocity components), as derived from the HM-ADCP dataset. A flood-dominance can be observed.

Next, the results are discussed in view of testing the hypothesis that gyre or vortex structures are formed in the lee side of the dunes, as put forward by conceptual models (Omidyeganeh et al., 2013; Lefebvre et al., 2014) and by some field data (see Lefebvre et al., 2014 for an overview). When dunes are steep enough ($\sim 30^\circ$), a flow separation zone (FSZ) is formed.

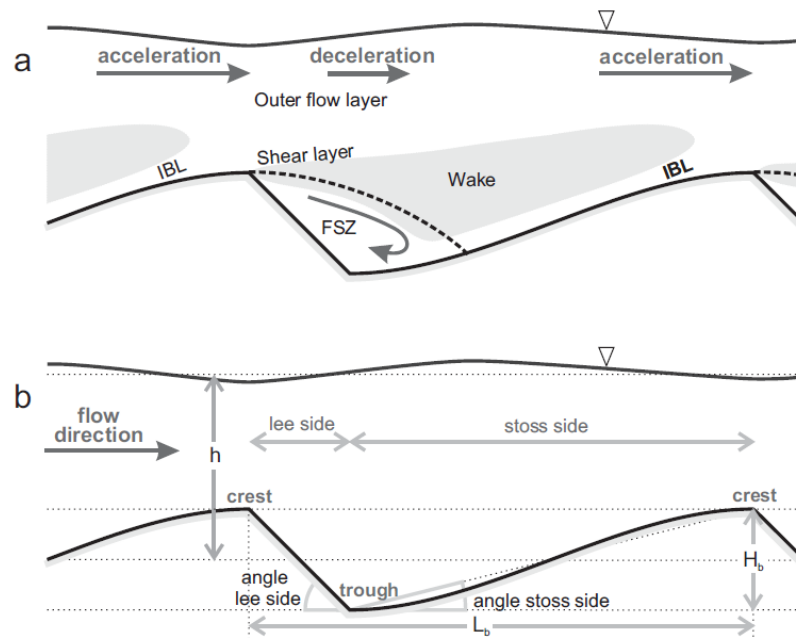


Figure 27. (a) Schematics of flow over two-dimensional asymmetric angle-of-repose dunes; IBL: internal boundary layer; FSZ: flow separation zone; (b) definition of bed form parameters; H_b : bed form height; L_b : bed form length; and h : mean water depth (Lefebvre et al., 2014).

Hitherto, it has not been possible to detect clearly such gyre structures in the field data. This might be due to the HM-ADCP aboard RV Belgica (300 kHz) and the specifications that did not allow depicting small-scale variability in the data. However, from all data recorded so far, it is clear that the flow is non-uniform in the lee side of the barchan dune and this under flood current mainly. Tidal current ellipses in the predicted extent of a potential FSZ have repeatedly shown that the flood current is not fully developed towards the bottom, hence pointing to weaker currents locally.

The CFD modelling of the flow over the dune series provided some extra insight into the flow field. In Figure 28 differences in turbulent kinetic energy (TKE) and current vectors are displayed over the dune(s). No flow reversal or downstream wake vortices were simulated. This might be due to: (1) the model applied (k -epsilon model) works fine in free stream regions, but not in areas with obstructions ('wall' effect); (2) barchan dunes are 3D structures, whilst now simplified 2D profiles were used as input; (3) a parabolic current profile was used with low velocity near the seabed. In any case, the higher TKE near the foot of the lee side likely points to the existence of a return flow. The reduction in current strength at the foot of the lee side (± 30 m wide) may provide a highly suitable niche for biological communities to thrive. It favours deposition of fine-grained material too, though a threshold may exist up to which this remains beneficial.

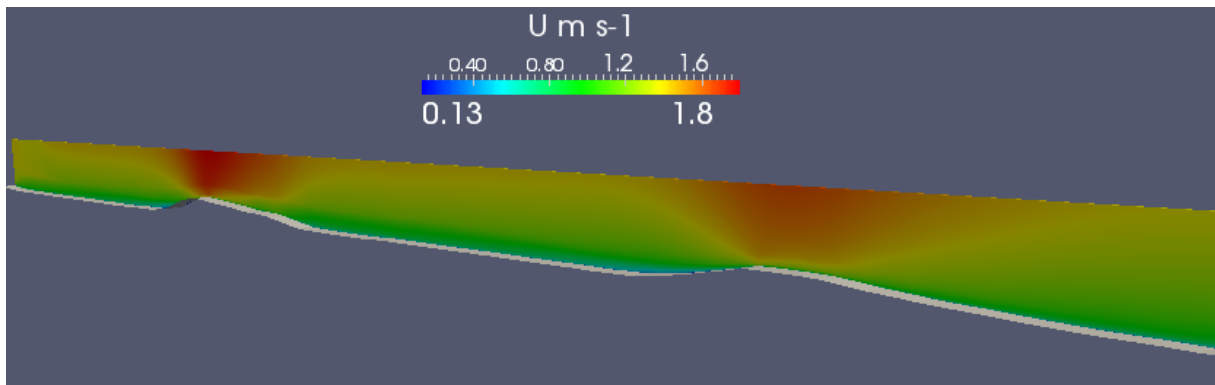
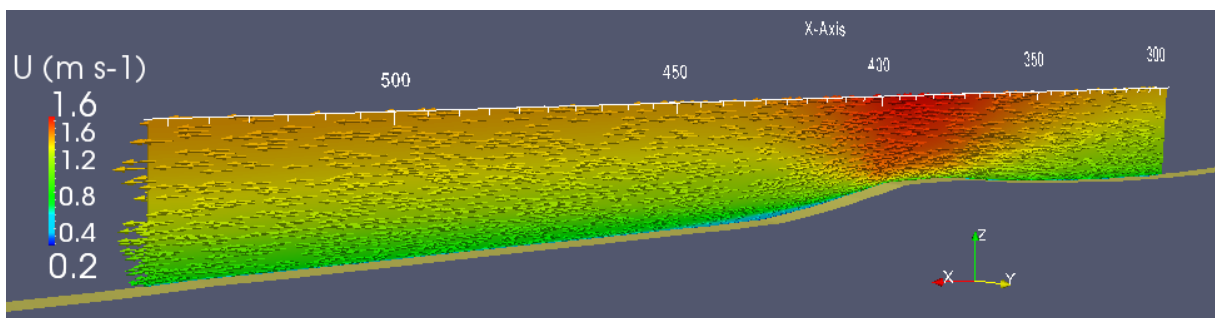
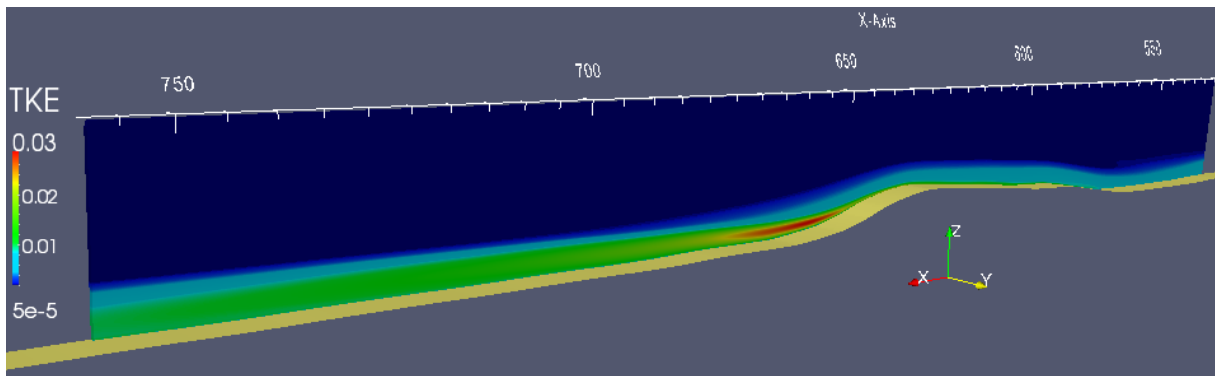


Figure 28. CFD modelling results of TKE and currents over the barchan dune morphology. Field data on bathymetry, grain-size and current strength were provided (Courtesy of Tomás Fernández Montblanc, University of Cadiz (CACYTMAR), Faculty of Marine Science). Note higher TKE values in the wake of the dune. Acceleration of the current was simulated over the dune crest, with subsequent flow deceleration in the wake of it. In the flow separation zone lowest currents were simulated.

Substrate characteristics

During ST1507, video imaging was carried out in Area 2 (main refugium as defined by Houziaux et al., 2008). As previously observed, gravel blocks occurred overgrown with epifauna (Annex B). In the refugium area *s.s.* no small to medium dunes occurred, which is probably linked to its position in the FSZ, as discussed above.

In the ST1517 campaign the wider area around the refugium was video-imaged: BV1, BV2, BV3, BV4, BV5, BV6 and VVR3 (Figure 29). These locations were chosen based on multibeam backscatter (BS) imagery acquired in 2013 (FPS Economy), RV Simon Stevin 30/07/2013). Aim was to validate the variation in BS: the darker the image the lower the backscatter. Interesting were the bands of lower backscatter that showed a continuum from the main gully into the barchan dune area.

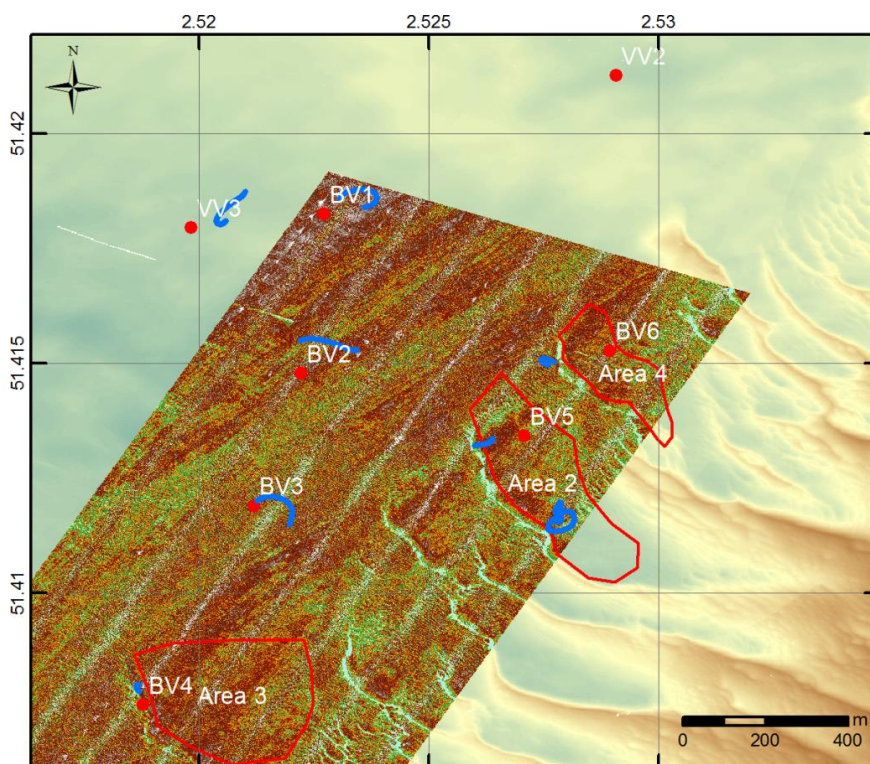


Figure 29. ST1517. Locations of samples (red dots) and video imagery (blue line) around the barchan dune area where rich epifauna generally occurs (red polygons). Background is a multibeam backscatter mosaic acquired in 2013 (FPS Economy, RV Simon Stevin 30/07/2013). Red coloured zones are indicative of gravel occurrences.

At VV3 and BV1 a very coarse substrate was encountered with high densities of small-sized gravel and sporadically some bigger blocks, mostly encrusted with polychaetes. No dunes were observed, likely because of a limited sand cover. Small patches of organic material deposits occurred. BV2 was clearly more sandy; small dunes occurred, interrupted locally by some gravel (with anemones attached to them) and some concentrations of shell hash. Some organic material deposits were observed. Similar situation for BV3, though this location is at the edge of an area with abundant sand deposits, organized into small to medium

dunes. BV4, lying in Area 3 (lee side zone of the southernmost barchan dune area) was positioned on the dune itself and not in the through. Hence, imagery showed the presence of coarse sands, rich in shell hash. Some patches of organic matter were present. BV5, in Area 2, was again in a dune wake zone and showed small-sized gravel *a.o.* overgrown with anemones, sometimes appearing in bands. The video track ran into the dune, hence showing a seabed with coarse sands and shell hash. BV6 (Area 4) was mal-positioned on the topzone of the next dune, hence coarse, shell-rich sands were seen, as well as clean medium to coarse sands organized in to medium to large dunes. Annex B shows some extra images in Area 2 ('Sonia1' images). These are again indicative of a FSZ: patches of gravel overgrown with epifauna, and a surrounding coarse sandy seabed with few dunes, probably because of the limited sand cover.

The ROV dive in august 2015 was executed in Area 4, near the lee side of the southernmost barchan dune. In 2014 (ST1417), divers observed extensive fields of gravel with epifauna (see report Yr2). The new observations did not confirm this and merely showed sandy substrates, although based on the ROV positioning, the ROV remained in the wake zone of the dune (Figure 30 and Figure 31).

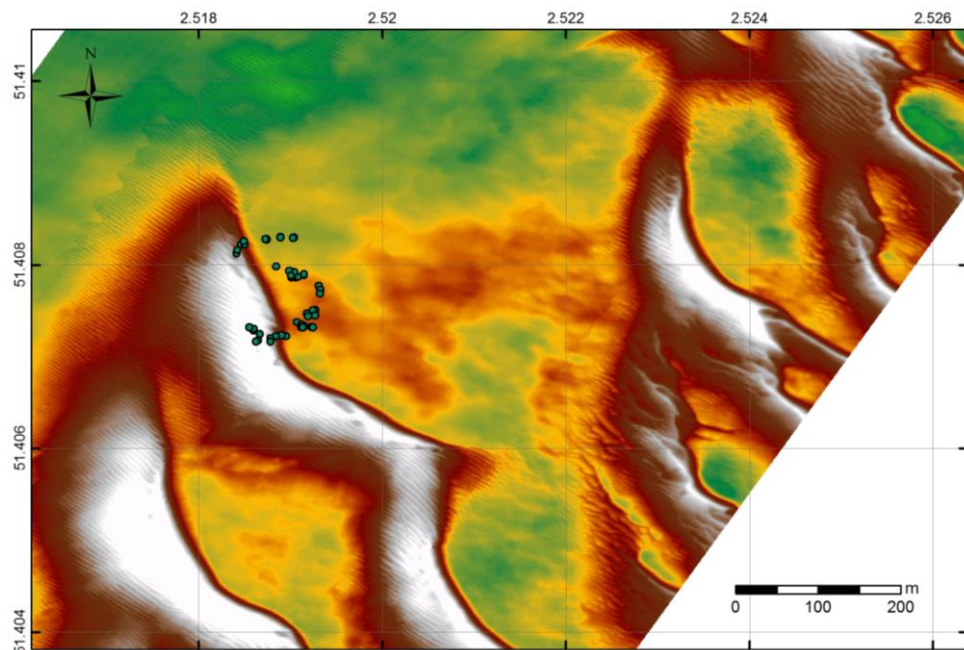


Figure 30. Track of the ROV GENESIS (deployed from RV Simon Stevin on 10/08/2015) in area 4, the southernmost gravel bed area.



Figure 31. Example of video footage in area 4 on 10/08/2015.

Note that in all of the imagery no trawling marks have been observed.

New PSD results of seabed samples in the barchan dune area, and the surrounding gully (ST1507; ST1517), confirmed the presence of medium to coarse sands with a coarse modus ranging from 350 μm to 600 μm (Figure 32). All samples had more than 1 % silt-clay enrichment. Overall, the samples contained brown to very brown waters, except for BV3 (see pictures in campaign report ST1517). In Area 4 (ST1507) percentages were 11 to 19 %. In the deeper parts of the gully the sandy part of BV1 and BV2 had 4.3 % and 5.9 % silt-clay and VV3 12.4 %. A near bottom water sample taken at BV4, in Area 3, showed a polymodal distribution with modes around 330 μm , 15 μm , 6 μm and 0.94 μm . A centrifuge sample taken in the barchan dune area (over a time span of 11h33; OH Barchan dune in Figure 32) showed a polymodal distribution with modes around 256 μm , 154 μm , 105 μm and 15 μm .

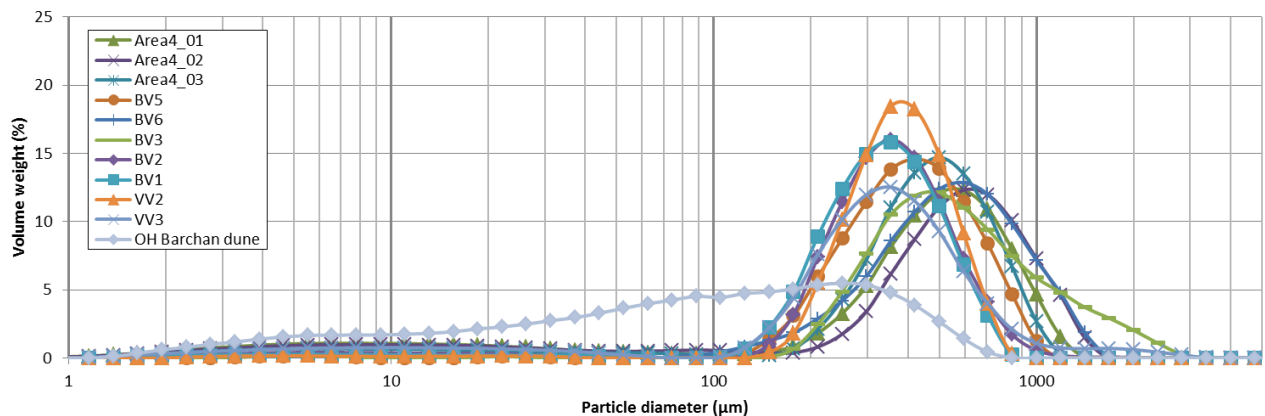


Figure 32. Particle-size distribution of samples taken in the gully in-between Westhinder and Oosthinder, as well as in the barchan dune area. A Hamon grab was used for the sampling, except for sample OH Barchan dune which has been collected with a centrifuge, hence representative of particles in the water column. See cruise reports ST1507 and ST1517 for pictures of the samples taken; locations are presented in Figure 9 of report ST1517.

Synthesis sediment processes in the Habitat Directive area

Based on field measurements and modelling results, the following characteristics in the barchan dune field can be confirmed:

- Dominance of the flood current (NE directed).
- No direct evidence of flow reversal near the lee side though this would be common for dunes with steep slopes (20-30°) as is the case here. Measurements did show: (1) mid-column and near-bed deceleration of the flood current; (2) higher variance of the flood current as compared to its ebb counterpart; (3) evidence of a transition of laminar to turbulent flow after HW to LW slack.
- Sediment resuspension under both flood and ebb peak velocities. Generally more SPMC under flood conditions, though this depends on hydro-meteo conditions. More SPMC under turbulent flow conditions, which only occur under flood conditions.
- In the flow separation zone a higher TKE and weaker currents were modelled; this enhances trapping of fine-grained sediments.
- Both ebb and flood currents induce about the same shear stresses at the seabed.
- Rectilinear currents, with a strong directionality of the peak currents, but low currents during slack water. In water depths of around 30 m, deposition of fine-grained material during slack water is likely.
- From bathymetric measurements some scour is perceived near the lee side which likely correspond to the extent of the flow separation zone.
- No to few ripples in the FSZ, pointing to weaker currents and/or less sand available.
- Seabed substrate is coarsest in the FSZ with normally minimal sand thicknesses.
- All seabed samples had more than 1 % silt-clay enrichment, with percentages up to more than 10 %. Overall, water-sediment interface samples were characterized by brown to very brown waters.
- Regardless the depth, the seabed must be reworked sporadically. In the period 2011-2015 no trawling traces from fisheries have been observed in and around the barchan dune area, whilst fisheries are active in the area.

Habitat Directive Area, gully west and east of Westhinder kink area

Measurements were taken in the gully west (HBBSA) and east (HBBSB) of the Westhinder kink area (ST1502; Spring T_{coeff.} 75) (Figure 33). Multibeam data were recorded along transects and vertical profiling of oceanographic parameters were taken in an alternating scheme. Aim was to study the influence of water column dynamics on multibeam backscatter variations (Belspo INDI67). The timing of the vertical profiling was dependent on the time needed to sail the multibeam lines, hence was not fixed to a ± 0.5 h time interval. In total more than a full 13-hrs cycle was sampled.

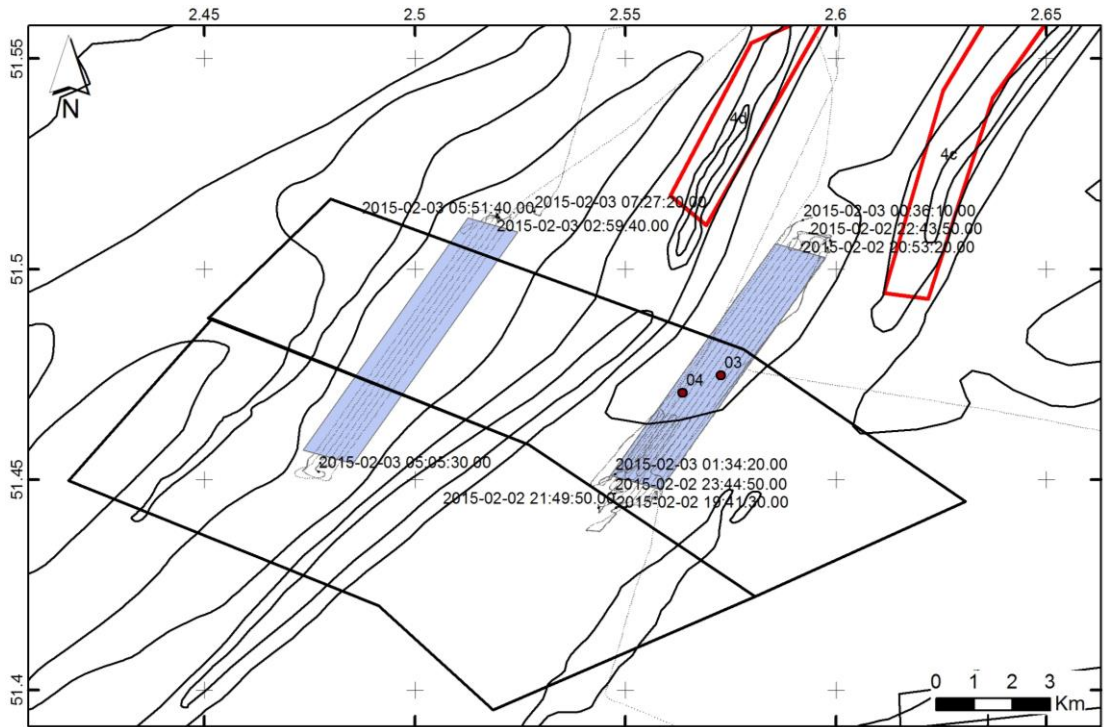


Figure 33. Timing and location of vertical profiling of oceanographic parameters, east of the Westhinder kink area (HBBSB) and subsequently west of the kink (HBBSA) (purple areas) (ST1502). The MBES transects are indicated in light grey. Thick polygons represent the fisheries management zones. In the northern zone fisheries will be prohibited in the future; in the southern part alternative fishing gear will be mandatory. Red polygons are the marine aggregate sectors. (3) and (4) are the locations of the 2 seabed samples represented in Figure 40. (ST1507).

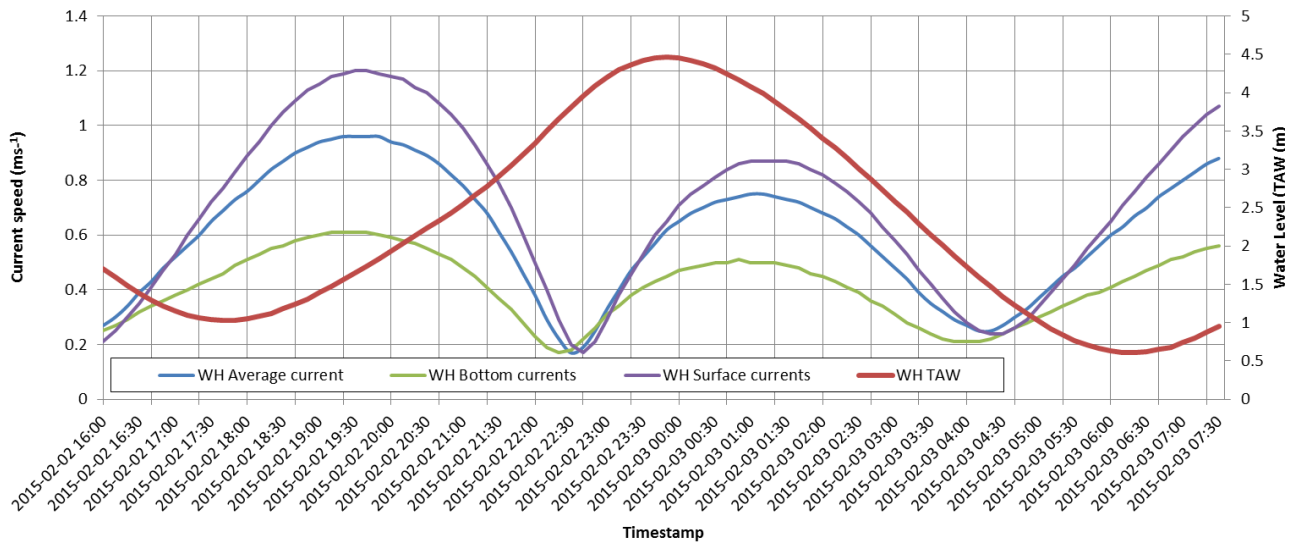


Figure 34. ST1502 - Water level and current characteristics (from OPTOS-BCZ model, MP7 Westhinder location) (grid lines every 30'). Note highest current velocities in: (1) surface waters: HW+1h30 and HW-3h (LW+1h30); and (2) bottom waters: HW+1h and HW-3h (LW+1h). Slack water: HW-1h; and HW+3h to 4h. Ebb currents predominated in strength.

Vertical profiling of SPMC over the water column showed concentrations around 0.006-0.007 gl^{-1} , with a maximum around 0.016 gl^{-1} under the ebb highest current velocities ($\pm 1\text{h}30$ after ebb). With increasing current velocities, there is clear gradient of higher concentrations above the bed. LISST profiles show particle sizes (mean values) from 100-200 μm . A clear vertical gradient is observed at highest current speeds (after LW). Averaged over the water column the mean is highest just after slack tide before HW.

In comparison, subsequent 13-hrs water profiling in a gully near the Kwinte Bank showed concentrations around 0.01-0.015 gl^{-1} with increases to over 0.060 gl^{-1} around flood peak tidal currents. Much stronger vertical gradients were observed here. As a comparison Figure 35 shows both 13-hrs cycles in one plot. Particle size variations in the water column (from LISST profiling) are shown in Figure 38 and Figure 39. Sizes vary between 100-200 μm , with the maximum particle size around HW.

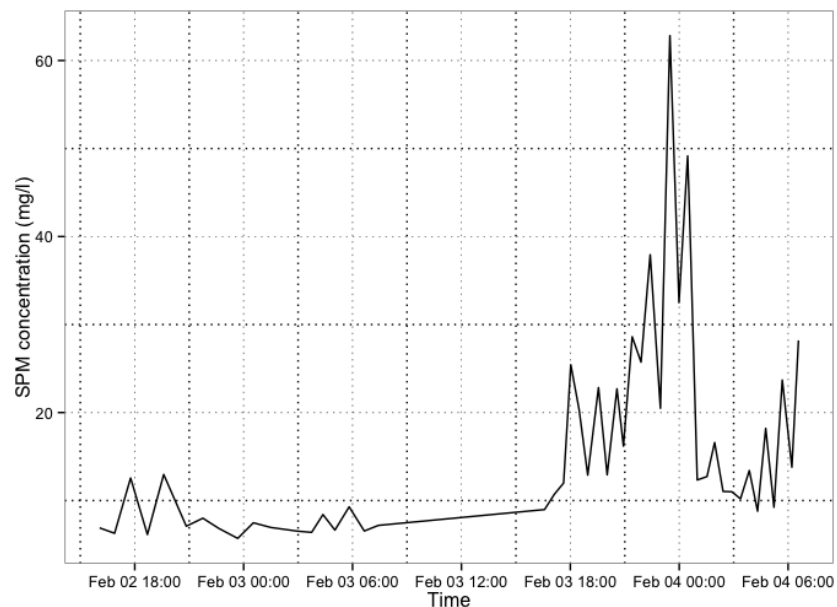


Figure 35. Evolution of bottom SPMC based on OBS measurements throughout two 13h-cycles along the gullies west and east of the Westhinder and Kwinte Bank, KWGS area (ST1502). Westhinder gully measurements: 2015/02/02 17:15 – 2015/02/03 07:20; KWGS measurements: 2015/02/03 17:30 – 2015/02/04 08:30. For 2/2: LW: 17h45; HW: 23h45. 3/2: LW: 6h20; HW: 12h14; LW: 18h46. 4/2: HW: 00h30; LW: 7h06. Note the strong contrast in turbidity between the 2 off-shore areas.

Substrate characteristics

During ST1507, video imaging was carried out also in the gullies west and east of the Westhinder sandbank. Aim was to characterize the gravel areas and the surrounding soft substratum. A selection of video footage is shown in Annex B:

- Western gully: HB06, HB07, HB08, HB10 and HB12: Small to larger sized gravel blocks occurred, though the soft sandy substratum was predominant.

Gravel blocks generally did not host rich epifauna. Shell hash was present in the troughs of the dunes and was concentrated locally. Small to medium-sized dunes occurred with often deposition of organic matter at the lee side of the dunes (e.g., HB11). Resuspension clouds were evoked when the video frame touched the bottom.

- Eastern gully: HB14, HB15, HB16: Compared to the western samples, gravel abundance seemed higher in this gully and sand thickness less. At location 15 and 16, small gravel was present abundantly. Again organic material deposits were observed.

Two particle-size distributions are shown for seabed samples (Hamon grab) taken in subarea HBBSB (ST1507). Medium sands predominated with a mean grain-size around 350 μm .

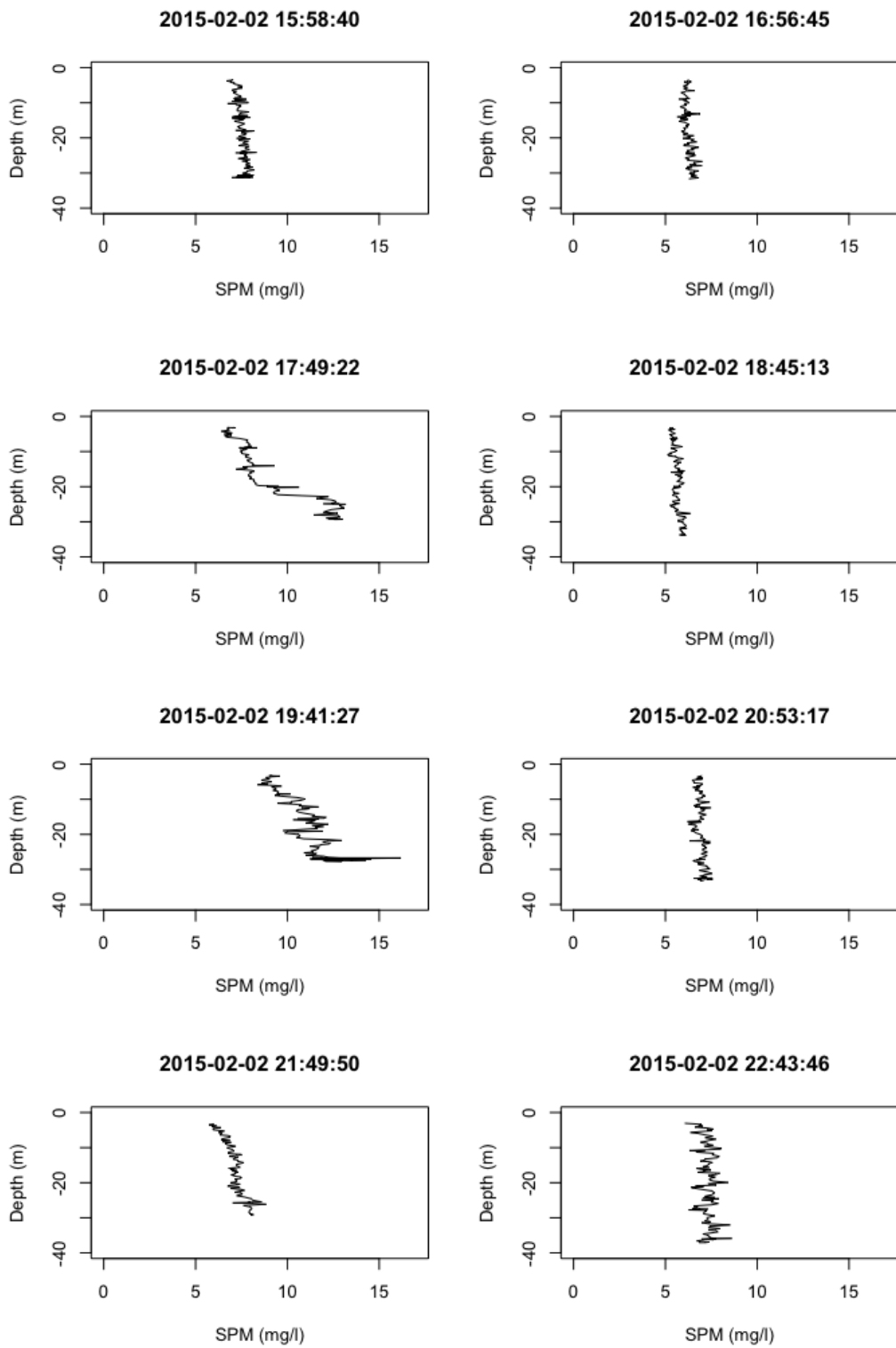


Figure 36. SPMC along vertical profiles taken in the gullies east and west of the Westhinder sandbank (ST1502, 2015-02-02 17:15 – 2015-02-03 07:20). Timestamp is related to the closest valid value to the seabed.

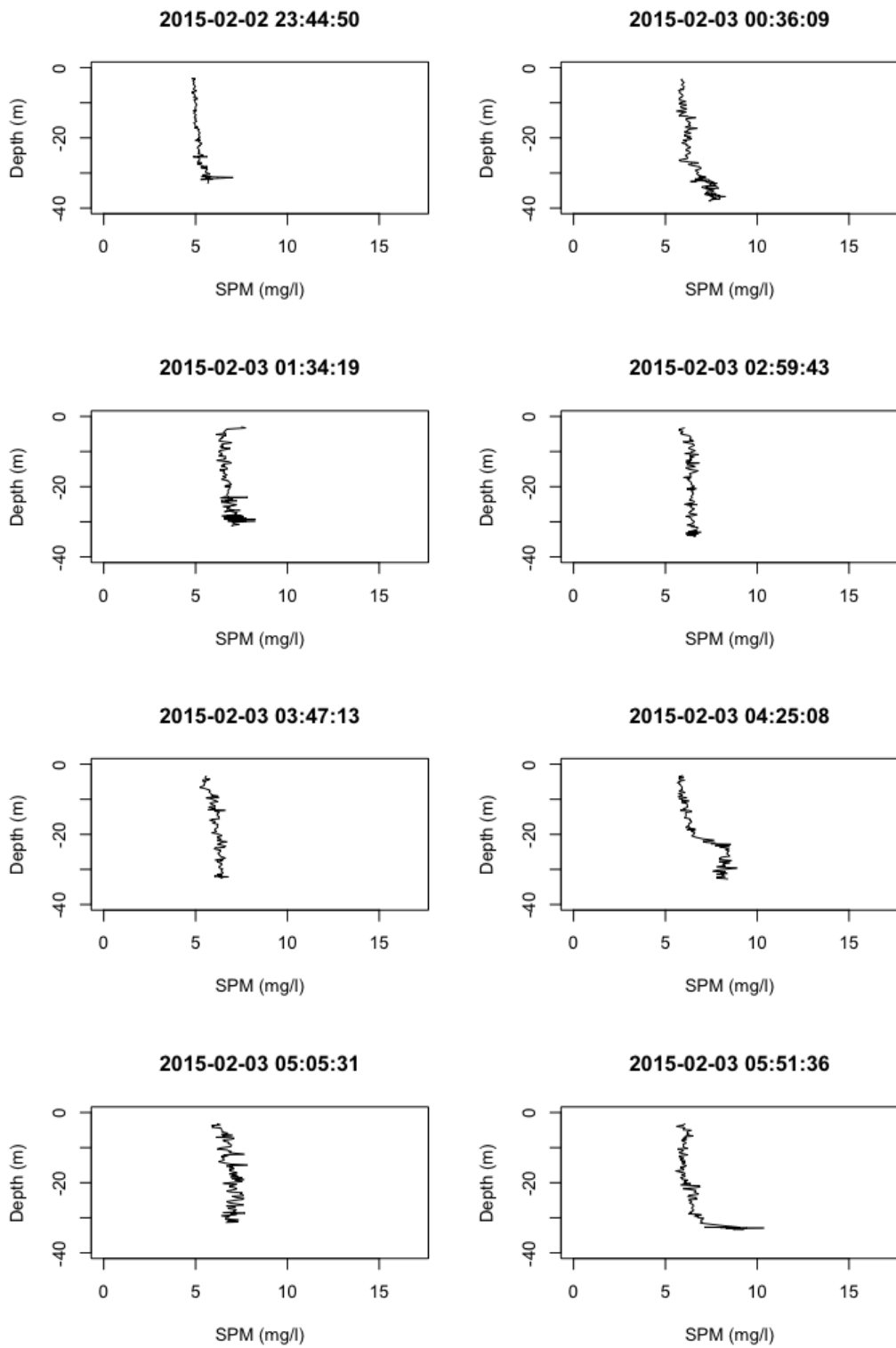


Figure 37. SPMC along vertical profiles taken in the gullies east and west of the Westhinder sandbank (ST1502, 2015-02-02 17:15 – 2015-02-03 07:20). Timestamp is related to the closest valid value to the seabed.

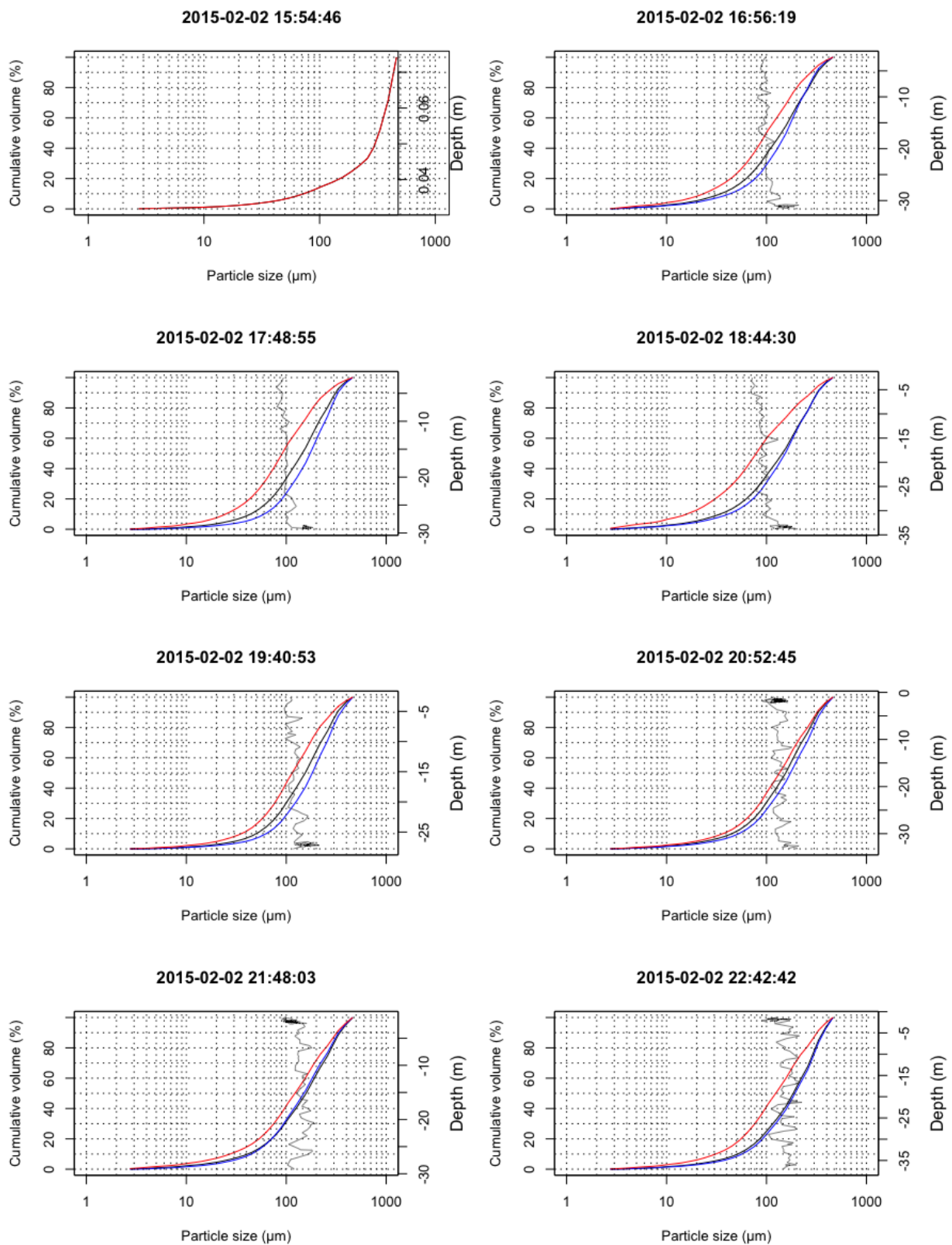


Figure 38. Cumulative particle-size distributions (PSD) in the water column (LISST profiling). See next page for full caption.

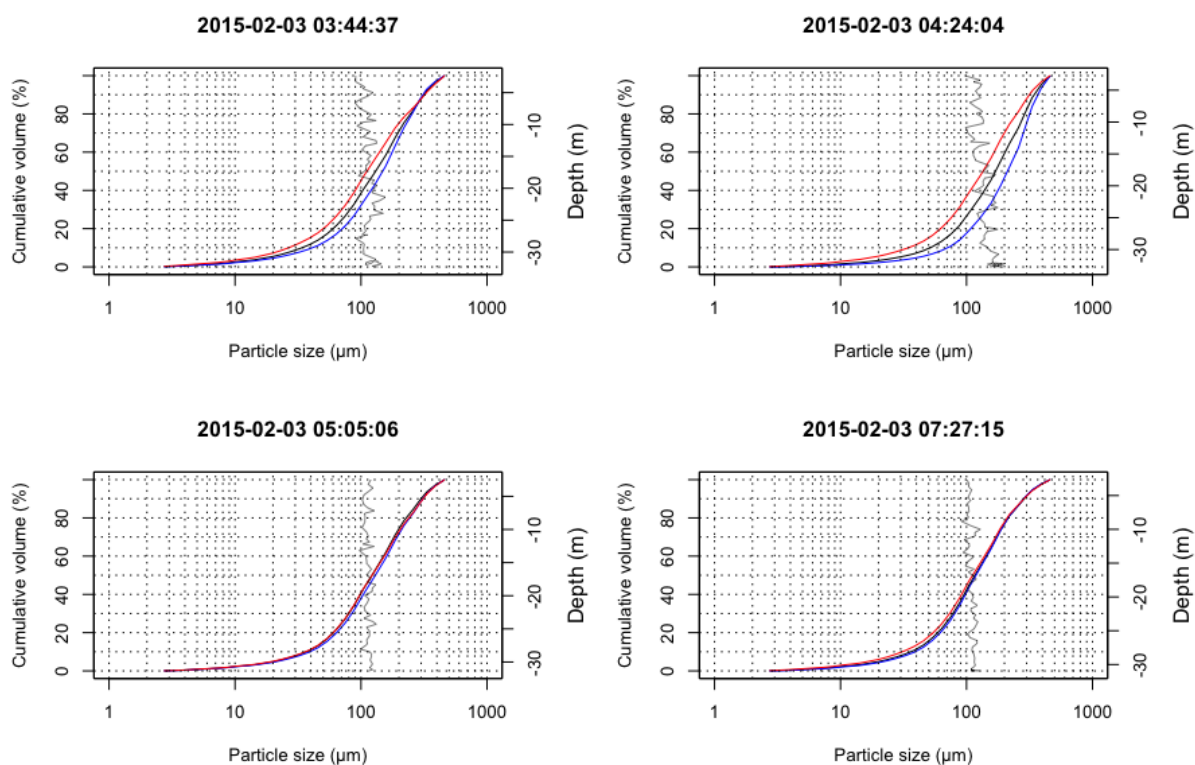


Figure 39. Cumulative particle-size distributions in the water column (LISST profiling) (black: average particle size, red: top 10%, blue: bottom 10%) together with median grain size (grey) of each individual profile taken during the measurement cycle. Timestamp is related to the value that maximum depth was reached.

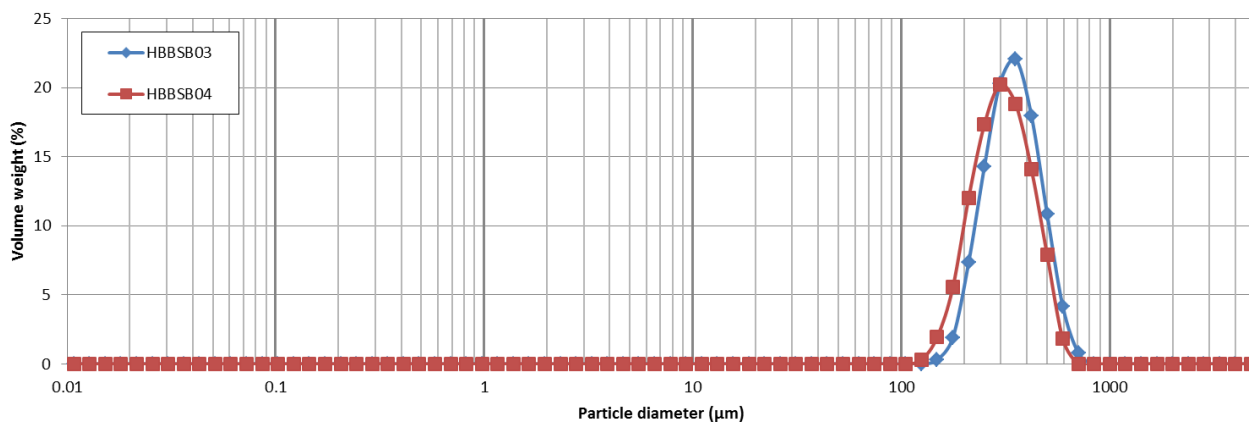


Figure 40. Particle-size analysis of samples taken in subarea HBBSB, east of the Westhinder kink area. A Hamon grab was used for the sampling. See cruise report ST1507 for pictures of the samples taken.

Overall summary:

- Current and backscatter data from ADCP measurements, showed increased SPMC, both caused by resuspension and advection.
- The advection event can occur directly after the resuspension, and can deposit at the following slack tide. Sometimes, this occurred after flood; sometimes after ebb. Hitherto, no systematic patterns have been revealed.
- Advection events have been seen under both spring and mid tidal conditions and the source direction is both flood and ebb oriented.
- Importance of wind-driven currents, e.g., persistent winds from the southwest strengthen the flood current and can, for the typical ebb-dominated steep slope of the Oosthinder sandbank, reverse the residual current to flood dominant.
- The gravel fields in the barchan dunes of the Habitat Directive area are subdued to a dominance of the flood current, though the flood current was decelerated near the bed, potentially pointing to a vortex structure along the steep side of the barchans.

4.2. Human-induced variation

4.2.1. Introduction

In relation to the physical impacts of marine aggregate extraction, one can expect two major alterations: (1) abrasion of the seabed; and (2) dispersion and deposition of sediment plumes, affecting both the water column and seabed. Three types of dredge plumes exist, each having a typical behaviour (Spearman et al., 2011): (1) a surface plume dispersing away from the vessel (i.e., TSHD); (2) a dynamic plume, representing the coarser part of the initial plume, and descending in the near field; and (3) a passive plume, bringing together the finest fractions from the surface and dynamic plumes, and from a near-bed plume caused by the draghead. The dispersion of the passive plume can easily extend several km from the vessel. In the study area of the Hinder Banks, first observations of such plumes were made in 2013 using the unmanned surface vehicle Wave Glider. The descent of a passive plume was evidenced, but also large huge natural variability of turbidity events in the water column (Van Lancker & Baeye, 2015). Results on the sediment plume study were reported in Year 2 (Van Lancker et al., 2015), including the characteristics of the TSHDs as operated in the MOZ4 area.

4.2.2. Near-field impacts

In the report of Year 2, observations were discussed of sediment plumes, both regarding their extent and their nature in terms of particle-size. First results of PSDs nearby TSHDs and in their overflow showed a main particle mode in the range of 5-10 μm . Importantly, changes in sediment characteristics were shown in the near field of the main extraction site (Sector 4c). On the one hand detailed core analyses showed more heterogeneous sediments near the dredge tracks, than outside of the dredging zone. Additionally, some fining trend was observed

in the top surface of the seabed. It was evidenced that some of the *in-situ* sediments contained mud fractions, especially near the western edge of Sector 4c. At one location, 25.3 % mud content was measured at 6.5 cm depth. Noteworthy also were the higher particle sizes at the western edge, pointing to the admixture of shells. Correlation with geological data showed the shallowness of the Top Pleistocene deposits downslope of the sandbank. Finally, it was also attempted to detect changes in sediment transport during the period of multiple marine aggregate extraction events, however the analyses of currents, SPMC and bottom shear stresses against aggregate extraction data did not reveal significant relationships.

4.2.3. Far-field impacts

An important concern in the monitoring was the investigation of a potential smothering process of the gravel beds in the Habitat Directive Area. Available historic data were presented in the report of Year 2 (Van Lancker et al., 2015), as well as first observations and results were discussed within the monitoring period 2011-2014. Seabed samples pointed to an enrichment of mud in the sand fraction, whilst video imagery showed a predominance of sand in the gravel areas. An increasing sand thickness was also reported in Yr2 when comparing diver measurements from 2004 against those of 2014. This could point to a loss of the gravel areas, by overtopping with sands. Since Belgium, in its MSFD commitment, stated that the ratio hard substrate versus the surrounding soft sediments, should not show a decrease, it was important to monitor changes over time and this was the driver of the consecutive multibeam recordings. Since the last dataset was only acquired in december 2015, results will be available in the next report. The multiple video observations of 2015 showed again the predominance of sand in the gravel bed areas. Seabed samples and the video images taken in 2015 confirmed the enrichment of a fine fraction in the sand matrix (e.g., sediment clouds) (see Annex B for video footage).

4.3. Modelling of changing hydrographic conditions

See Report Year 2 on the validation of advection-diffusion sediment transport models, as well as on the validation of sand transport models (Report Year 2, Annex C). Here, emphasis is on the modelling of changing bottom shear stress in relation to various scenarios of aggregate extraction. See Van den Eynde, Annex C for a full report; here only the main results are synthesized.

The effect of extraction of marine aggregates on the bottom shear stress was evaluated in the framework of the European Marine Strategy Framework Directive (MSFD). In the Belgian implementation of this directive, and related to descriptor 7 on hydrographic conditions, it was stated that a human impact needs consideration when the bottom shear stress, calculated by a validated mathematical model over a spring-neap tidal cycle: 1) increases by more than 10 %, or 2) that the ratio of the period for erosion and the period for deposition is larger than -5 % or +5 %. Furthermore, it was stated that the impact, that needs consideration, should

stay in a distance less than the square root of the area of the zone of activity, measured from the boundary of the area ('within distance' area). To test whether the 10 % threshold would not be exceeded outside this area *w.r.t.* Zone 4 of the Hinder Banks, a validation was first executed of some numerical models. Furthermore some scenarios were simulated to test the effect of aggregate extraction on the changes of the bottom shear stress.

Validation of hydrodynamic and wave models

The hydrodynamic and wave models were described first, after which their validation was discussed. For this validation all of the current measurements as conducted in the period 2011-2014 were used (see report Yr1 and Yr2 for details). Results showed that the currents at the station east of the Oosthinder sandbank (BM-ADCP measurements near Sector 4c) were modelled well. However, for the station in the southern part of the Oosthinder sandbank (BM-ADCP measurements in the trough of the barchan dunes), the results were less good. This is probably due to complex hydrodynamics in this area, as showed again in the measurements section of this report. Waves were modelled satisfactorily.

Bottom shear stress calculations and its modelling

Analysis of the bottom shear stress calculations, as derived from the BM-ADCP measurements, showed that 5 m of the lowest part of the water column should be taken into account when calculating bottom stress from the measured current profile. Furthermore, it was recommended to apply a moving average filter, with a window of about 2 hours, to filter out the high frequency fluctuations in the measurements. Within a confidence limit of 95 %, the calculated bottom shear stress varied between 0 and 0.5 Pa for the minimum and 1.5 to 3.0 Pa for the maximum bottom shear stress. No clear influence of the significant wave height was found on the bottom shear stress as derived from the measurements at the two stations. This is mainly due the overall higher water depths.

The validation of the bottom shear stress model showed that the bottom shear stress could be reasonably modelled by the numerical models. Using a constant bottom roughness, best results were obtained by the Soulsby model, using a constant bottom roughness length of 0.01 m. Similar results were obtained by other models, with for station BM01, a bias of around 0.20 Pa, and a RMSE of about 0.35 Pa. In more than 90 % of the time, the modelled bottom shear stress was within the 95 % confidence limits. Less good results were obtained again for the station in the barchan dune area. When the bottom roughness length was calculated by the model itself, the modelled bottom roughness length seemed to be too high, resulting in too high bottom shear stresses. When scaling the calculated bottom roughness length with a factor of 0.10 better results were obtained. However, also after scaling the bottom roughness length, results were not significantly better than using the constant bottom roughness length of 0.01 m. Therefore, using a constant bottom roughness length is recommended.

Scenario analyses in relation to marine aggregate extraction

Three scenarios were simulated to investigate the influence of large-scale ex-

traction of marine aggregates (35 million m³) on the bottom shear stress in zone 4 of the Hinder Banks. The first scenario used a similar maximal extraction depth in the four extraction sectors; in the second scenario the four sectors were extracted until the same final water depth; in the third scenario, all the extraction was executed in Sector 4c. The simulations showed that for the three scenarios, the changes of the bottom shear stress in the area, where no impact was allowed ('outside distance'), remained limited to around 6 %, hence less than the maximum allowance of 10 % as specified within the Belgian implementation of MSFD. This is likely due to the relatively deep waters in the Hinder Banks area. For a full description, see Van den Eynde (Annex C).

Table 4. For the three simulations, minimum and maximum change in bottom shear stress (in percentage) in the different areas (extraction sector, area within a distance from the border as defined in the MSFD implementation; area outside this distance).

	In the Sector		Within distance		Outside distance	
	Min	Max	Min	Max	Min	Max
Sim 1	-27.33	9.71	-4.89	15.05	-2.16	3.52
Sim 2	-38.90	14.45	-6.48	26.80	-3.02	6.46
Sim 3	-35.59	12.62	-7.87	21.50	-3.46	2.58

5. Integrated assessment of the monitoring 2011-2015

5.1. Introduction

The MOZ4 monitoring programme started in 2013, though since 2011 integrated monitoring of sediment processes is in place allowing a first assessment of the impacts of marine aggregate extraction in the Hinder Banks region and evaluating the compliancy of the activities with what is stipulated in European Directives. One of the issues is to assess Good Environmental Status (GES) to comply with Europe's Marine Strategy Framework Directive (MSFD), and therefore a number of indicators needed evaluation. These indicators relate to seafloor integrity (e.g., sediment changes), and hydrographic conditions (e.g., changes in current regime). It needs emphasis that the monitoring series is only 4 years long, implying that most of the impact hypotheses can yet not be tested fully. The assessment here presented focuses primarily on hydrodynamics and sediment transport (RBINS OD Nature), albeit with relevance to the geomorphological (FPS Economy, SMEs, Self-Employed and Energy), and biological (ILVO) monitoring.

5.2. Integrated monitoring approach

Measurements were acquired, in view of (1) characterizing the spatial and temporal variability in seabed nature; (2) building up knowledge on sediment processes in zone 4; and (3) first testing of impact hypotheses, in which the investigation of cause-effect relationships was important.

Throughout the monitoring, a series of instrumentation and approaches have been used to study both naturally- and human-induced variability in sediment processes. Data prior to this period was scarce, and little was known on the sandbank dynamics, as well as of the water properties in the region ('blue clear waters'). Therefore, in 2011-2013 emphasis was put on the spatial variability of water and sediment processes in zone 4 and measurements were made along transects over the sandbanks in all sectors, albeit in combination with measurements on fixed locations. The spatial approach was important to characterise the T_0 situation. An innovative experiment took place in 2013, using a Wave Glider (Liquid Robotics). In a period of 30-days the autonomous surface vehicle sailed around Sector 4c and monitored turbidity events under naturally- and anthropogenically-steered conditions (see Van Lancker and Baeye, 2015). Also seabed mapping was invested in using a combination of acoustic measurements, seabed samples and visual observations. Complementary to the multibeam monitoring conducted by FPS Economy, multibeam depth and backscatter were acquired focussing mostly on the gullies in and out of the Habitat Directive Area. Here, also time series were recorded. From 2013 onwards, visual observations were conducted also, mostly in the ecologically important gravel beds in the Habitat Directive Area, but also in other parts of the gullies in the bigger study area. Video frames (VLIZ) were deployed, and diving operations (RBINS-OD Nature) were conducted. In both 2014 and 2015, opportunities were taken to obtain seabed imagery with a

remote operated vehicle (Genesis ROV, operated by VLIZ). With respect to sediment transport measurements, some stationary measurements, albeit short-term, were conducted in the period 2014-2015, focussing on Sector 4b-4c and on the gravel beds in the Habitat Directive Area. However, emphasis was also on the gullies to investigate the seabed substrate in more detail. Experience showed that results from measurements along transects or on drift complicated largely the interpretation as well as the quantitative correlative analyses of the data. This is due to the complex sandbank environment where sediment resuspension and advection may vary strongly with morphological position. This was shown especially with the Wave Glider. This platform captured a multitude of turbidity increases in the water column, both naturally- and human-induced, but also evidenced important lag effects between such increases and their drivers.

Regarding the mathematical models, results were obtained from a number of new modules that are under development in the framework of the ZAGRI programme. These were developed in view of assessing changes in seafloor integrity and hydrographic conditions, two key descriptors in the definition of GES (MSFD):

1. A new workflow for sediment plume modelling was developed coupling technical specifications of a series of trailing suction hopper dredgers (TSHD) and data on extraction activities to an advection-diffusion model that predicts the extent and total mass / concentration of sediment fractions released from the TSHDs. Effects of differences in extraction practices, particularly related to the use of small (2,500 m³), medium (4,500 m³) and large (> 10,000 m³) TSHDs were modelled.
2. The suite of hydrodynamics and sediment transport models were validated with the newly acquired measurements to optimize modelling in zone 4 of the Hinder Banks.
3. Regarding bottom shear stress, a variety of calculations from measurements and modelling approaches were revisited. Recommendations were formulated when using bottom shear stress models in impact predictions under various scenarios of extraction.

See monitoring report Year 2, Van Lancker et al. (2015) for detailed results on sediment plume modelling, see Annex C of this report for detailed results on the bottom shear stress modelling.

5.3. Physical impact assessment

5.3.1. Monitoring results

The following results were obtained on a first assessment of near- (in and around the sectors of extraction) and far-field impacts toward the south, where ecologically sensitive gravel habitats occur in a Habitat Directive Area. First some characteristics of TSHD are provided, typical for the operations in zone 4. Subsequently, some factual observations are listed. Finally, some hypothetical impact relationships are put forward that were further tested.

TSHD characteristics and their operations

1. TSHD typically operated under the ebbing phase of the tide, hence when the current was SW-directed (at least for the coastal safety-related extraction).
2. Deposition of dynamic sediment plumes was observed using acoustic imagery (multibeam and ADCP).
3. Deposition of a passive plume was observed acoustically also, 3 hrs after an extraction event.
4. Modelling of the overflow plume showed that most of the sandy material deposits in the near field. In a tidal cycle, the finer fractions of the overflow can deposit in the ecologically valuable gravel beds in the Habitat Directive Area, though modelling results would simulate a resuspension of the material under agitated conditions (e.g., spring tide, or enhanced current-wave interaction).
5. Since the start of extraction in 2012, and especially in 2014, the activity was intense per period of extraction (high amount and extraction by multiple vessels), but was followed by long, intermittent periods, of no extraction.

See monitoring report Year 2, Van Lancker et al. (2015) for detailed results.

Hydrodynamics and sediment transport

6. From 30-days current measurements around Sector 4c using a Wave Glider, and conform to the other measurements, flood and ebb tidal currents were overall quasi equally strong. Still, at the sandbank level, the western slopes are flood dominated; the eastern slopes ebb dominated. However, hydro-meteo conditions are able to reverse the residual current direction.
7. Peaks in SPMC were linked mostly to peaks in current strength, both in the gullies, and across the sandbank crest. During spring tide, SPMC is high throughout the water column, with highest values near the seabed.
8. Tidally-induced SPMC was similar under NE- and SW-directed currents, though higher concentrations were generally measured under flood (NE) conditions. In the upper water layers, at -10 m, median values of SPMC reached about 0.010 gl^{-1} . Concentrations in the surface waters were around 0.001 to 0.002 gl^{-1} , for neap and spring tide respectively. Median SPMC in the lower waters was 0.011 to 0.015 gl^{-1} in the deepest areas and up to 0.019 gl^{-1} over the sandbank crests.
9. Under wave conditions, SPMC is high throughout the water column.
10. SPMC during extraction activities showed increases with a factor of 1.25 greater than the natural background values, hence the concentrations fall within the envelope of natural variability.
11. The gravel fields in the barchan dunes of the Habitat Directive area are subdued to a dominance of the flood current, though the flood current was decelerated near the bed, potentially pointing to a vortex structure along the steep side of the barchans.
12. As a conclusion, natural variability of sediment processes in the Hinder Banks region was much more variable than previously expected. This applied to bedform migration, bottom shear stress, as well as SPMC in the wa-

ter column. This contrasts the opinions raised before the start of the monitoring: blue clear waters and low seabed dynamics because of water depth.

See monitoring reports Year 1, 2, 3 Van Lancker et al. (2014, 2015, 2016).

Seabed substrate

13. Medium sands dominated most of the aggregate sectors on the sandbanks. Shallow seabed cores did show some finer grained layers in the upper 10-30 cm. The topzone of Sector 4c witnessed merely fine to medium sands, whilst downslope, near the foot of the gentle side of the Oosthinder sandbank, shell layers were evidenced. Combining this with geological data (UGent, RCMG), outcropping of Pleistocene deposits was shown downslope of the sandbank. Importantly, it was shown that some downslope taken cores also contained muddy layers. These constrain the extent of the extractable resource potential to the main body of the sandbank.
14. In the gullies, adjacent to the aggregate sectors, medium to coarse sands predominated with shell hash deposits and geogenic gravel, locally. The Hamon grabs, that take a full sediment volume of the seabed, did show an enrichment of silt-clay in the seabed matrix. This was confirmed by video observations that showed resuspension clouds when the video frame hit the seafloor. Mostly, this fine fraction had a mode around 10 μm . Video imagery taken in March 2015 (ST1507) also showed deposits of organic matter.

See monitoring reports Year 1, 2, 3 Van Lancker et al. (2014, 2015, 2016) for detailed results.

Status of the gravel beds (habitat type 'Reef', code 1170)

The gravel beds are located in the far field of the extraction activities, with the major known hotspot of biodiversity (main gravel refugium) lying 8 km southwards of the nearest extraction sector (4c). With respect to Sector 4c, the gravel bed refugia are located along the axis of the tidal stream, and modelling showed that deposition of fine-grained material from Sector 4c is possible (see point 4, above).

15. The gravel bed refugia, as described by Houziaux et al. (2008,) are both positioned within the troughs of barchan dunes. Barchan dunes are very steep dunes that are typical for coarse substrates, where currents are high, and where there is sediment available to transport. The dunes are 6 to 8 m in height, with wavelengths of 150 to 200 m. Locally, their steep side is 20°. The height/slope dimensions are known to generate turbulent flow with counteracting near bed flow. In such flow separation zones, the sand cover is minimal, but fine-grained sediments are able to settle. This was partially demonstrated from new measurements and modelling in the study area.
16. Seabed samples and video observations in the gravel bed refugia showed enrichment of silt-clay particles, and the sampled sediment-water interface clearly witnessed brown waters. Though, video data did not show a surficial

smothering of fine-material at the seabed surface. Instead, the fine-grained material was buffered within the sandy substrate. This was evidenced by re-suspension of sediment clouds when the seabed was agitated.

17. In the gravel bed refugia, much more sand was observed visually than expected from previous visual observations (diving observations of 2006, OD Nature, Norro). The new measurements showed a very patchy distribution of the gravel blocks and they seemed partially buried in the sand. Nearest to the lee side of the dunes, in the flow separation zone, the density in gravel, at least at the surface, was somewhat higher. In 2006, sand thickness measured by divers was zero. Sand thickness at present is yet to be determined.
18. Above findings apply mainly to the main gravel bed refugium; the barchan dunes hosting the northernmost refugium was much smaller in dimensions. Video data only showed the presence of sands and some shell hash.
19. Multibeam time series (depth and backscatter) were recorded over the main gravel bed substrate. Their analyses are underway, since firstly a standardized workflow needed development. Aim is to quantify the ratio of hard versus soft substrate in line with one of the MSFD indicators.

See monitoring reports Year 1, 2, 3 Van Lancker et al. (2014, 2015, 2016) for detailed results.

Key findings in terms of near- and far-field effects are summarized below.

Table 5. Key findings on the near- and far-field monitoring (PSD: Particle-size distribution).

<p>Near-field</p> <p>Settling of dynamic plume</p> <ul style="list-style-type: none"> • <i>In-situ</i> sediment can contain higher mud contents; at the lower slope 30% mud was measured near 6.5 cm depth; • Plumes very limited in width; • Local increase of SPM concentrations; • Re-deposition of <i>in-situ</i> sediment through overflow; • Some fining in grain-size was observed, but no organic enrichment. This effect will become clear only on the longer term; • Water samples have multimodal PSD; under increased human pressure the ~10 µm mode becomes more important; <p>Settling of passive plume was observed (ref. Wave Glider data)</p> <p>Far-field</p> <p>Habitat Directive area</p> <ul style="list-style-type: none"> • Under agitated conditions, simulations do not show an important deposition of fines; though • Seabed sediments up to 22 % mud locally; bimodal PSDs with extra mode around 10 µm; • Significant increase in sand thickness compared to 2006; • Mud is buffered within the permeable coarse sediment, but might be released under agitated conditions. <p>Belgian part of the North Sea</p> <ul style="list-style-type: none"> • Simulations showed that the fine fraction deposits mostly in the area of the windmill farms; mud enrichment has been found in the predicted area of mud deposition.
--

5.3.2. Hypothetical cause-effect relationships

The sampling of fine-grained material in the offshore area triggered the investigation of cause-effect relationships with the aggregate extraction activities. Since multiple evidence became available on the presence of fine-grained material in the near field, as well as modelling results that showed the potential of deposition of the fine-grained material in the far field, underlying processes were investigated. Most important was to investigate whether the extraction activities would induce a smothering on the ecologically valuable gravel beds in the Habitat Directive Area.

1. Hypothesis 1: **Fine-grained material can be trapped in morphologically complex areas due to enhanced tide-topography interaction (Van Lancker, 2017)**. Fine-grained material was sampled in the troughs of barchan dunes along the western flank of the Oosthinder sandbank, at 8 km from the aggregate sector. As indicated in previous paragraph, the height/slope dimension of the dunes has the potential to generate gyres or eddies in their lee side (steep side). A flow separation zone exists characterized by low sand dynamics near the bed, but where material from the water column can settle. It is hypothesized that the more fine-grained material exists in the water column, the more material will be trapped in the trough of the dunes. Monitoring data have indeed shown the existence of a near-bed low dynamics zone, which was confirmed by modelling results (see first part of this report). The resolution of the measurements and the modelling did not allow showing increased SPMC in this particular zone. However, fine-grained material was sampled and was found to be buffered within the coarser grained permeable sand matrix. Concerns are raised whether this may clog the pores of the permeable bed, ultimately affecting biogeochemical fluxes. It needs emphasis that the origin of the fine-grained material cannot be unambiguously linked to the extraction activities in zone 4. Cumulative and in-combination effects may exist.
2. Hypothesis 2: **Aggregate extraction, in combination with bottom trawling, extends the far field dispersal of sediment plume deposits (*in-combination effect*)**. It may be argued that 8 km is a too far distance to relate deposition of fine-grained material from sediment plumes to aggregate extraction activities. The monitoring showed that also in the gullies nearer to the extraction activity fine sediment clouds resuspended when agitating the seabed. During the monitoring this agitation was caused by a grounding of the video frame or ROV, or by agitation by divers. It is clear that bottom trawling, omni-present, would give rise to huge sediment clouds that are subsequently transported away by current-wave action. Important to reiterate is the fact that in the gullies there was much more sand than expected from previous seabed mapping that predicted the occurrence of gravel mainly. Geologically, the Paleogene substrate would be outcropping, represented by a rough, hard surface. Multiple observations now show a sand cover. Quantification of the sand thickness is yet to be done. Based on expert advice from a scientist investigating bottom trawling impacts (pers. comm.) it is ar-

gued that thin sand covers over harder substrates would have been winnowed away if indeed bottom trawling, already active since 150 yrs, would be the sole pressure. However, if there is a new source of sediment, the whole winnowing process restarts.

Both hypotheses combine in a **step-wise impact hypothesis**:

1. Excess of fine-grained material and sand from overflow of trailing suction hopper dredgers;
2. Deposition in the near field and in the gullies along the tidal stream axis;
3. Resuspension by beam trawling;
4. Longer lasting deposition in morphologically complex areas that preferentially trap fine-grained sediments.

It is clear that the source of the fine-grained sediment cannot be unambiguously related to aggregate extraction. It may be a cumulative effect, hence with sediments originating from different locations where aggregate extraction takes place, and supplementary to fisheries, other in-combination effects may exist, e.g., wind-mill farms that also give rise to turbidity plumes (Baeye & Fettweis, 2015). Figure 41 provides an overview of the location of the gravel beds in the Habitat Directive Area in relation to other activities.

Regarding the source of fine-grained material, it can also be argued that geological sources may exist that are resuspended under current-wave action. Figure 42 shows the presence of silt and clay in the upper meter of available geological cores in the broader study area, hence showing potential sources of fine-grained material. Importantly, the cores show no silt or clay layering in the sandbanks themselves, but only in the gullies. Noteworthy is the trajectory near the Westhinder navigation channel, where in 2018, the trenching of an electricity cable will start. This is roughly 4 km away from the ecologically valuable gravel beds. Future monitoring will need to account for this extra pressure.

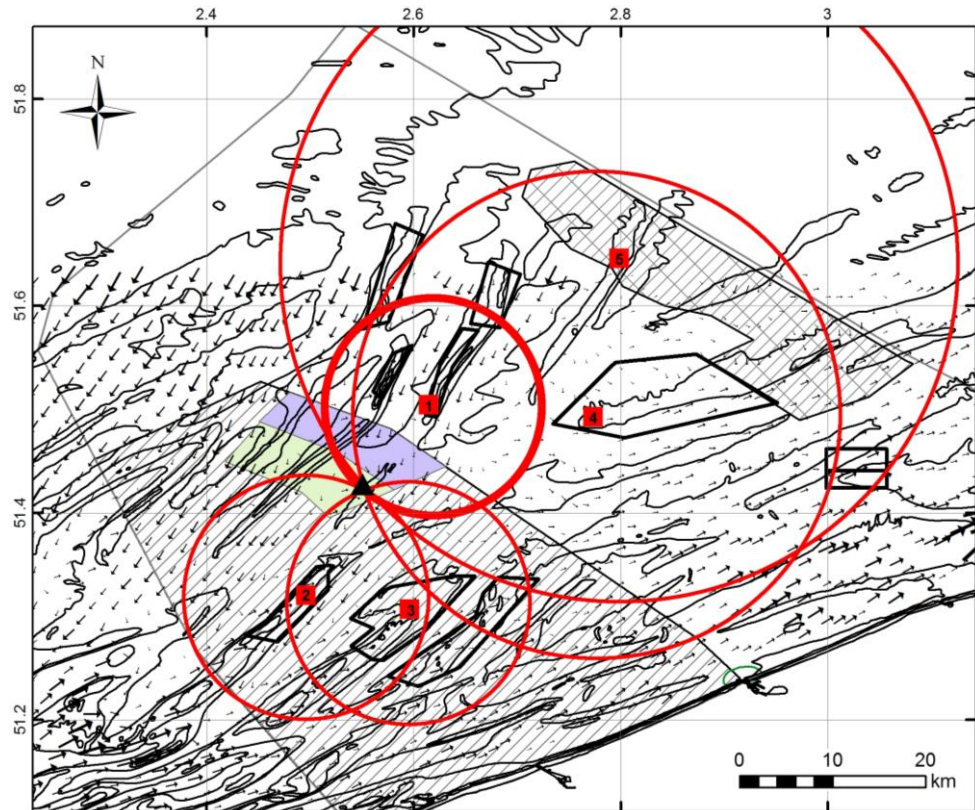


Figure 41. Ecologically valuable gravel beds in the Habitat Directive Area (triangle) with the distances to the different pressures (red squares). (1) Extraction in Sector 4c, Hinder Banks; (2) and (3) Extraction in zone 2: Oostdijk and Buiten Ratel; (4) Extraction in zone 1 Thornton Bank. All of these may act cumulatively. In-combination effects may also exist, hence deposition may exist from turbidity plumes generated around the windmill structures (5). Note that these are minimally 30 km away. Importantly to note is the omni-presence of fisheries activities. On the BPNS, the influence of these activities on water column turbidity and seabed texture has not been assessed yet. To give insight in the spreading of fine-grained material, the direction and magnitude of maximum currents are indicated. Fisheries management areas are indicated also, in the north part (purple) fisheries will be prohibited in the future; in the south part (green) only alternative fishing will be allowed.

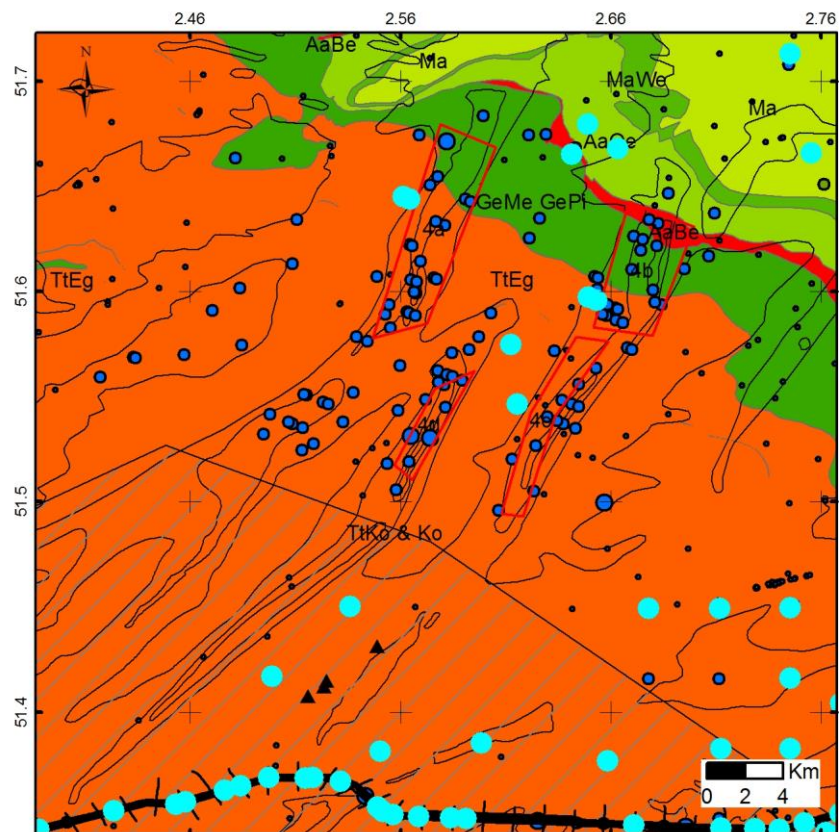


Figure 42. Overview of core locations (circles with size reflecting core length) with an indication of those having clay or silt in the upper 1 m (cyan) (extracted from TILES geological databases, Kint and Van Lancker, 2016). Background is the pré-Quaternary outcrop map (Paleogene formations: TtKo & Ko: Tielt and Kortrijk formations composed of hard clay; TtEg: Tielt–Egem: with locally more sand; GeMe & GePi: mainly clayey Gentbrugge Formation with the Merelbeke and Pittem Member; AaBe, AaOe: mainly sandy Aalter Formation, Members Beernem and Oedelem; Ma, MaWe: mainly clayey Maldegem Formation with the Wommel Member (Le Bot et al., 2003). Note that the southernmost cores were taken along the trajectory of the NEMO cable (UK-BE electricity cable (black)) (data courtesy NEMO-Link). Important to note is that the cores did not show any silt or clay layering in the sandbanks themselves, but only in the gullies. Extent of the Habitat Directive Area is indicated also (hatched), as well as the gravel refugia (triangles).

5.3.3. Relevance of results w.r.t. to other monitoring

In this section, results on hydrodynamics and sediment transport are discussed in concertation with the other actors concerned by this monitoring. Hence, a first reflection is made on the relevance of the results on bathymetrical and morphological changes, as well as on benthos, in function of MSFD requirements. It needs emphasis that only first reflections are presented here, since significant information on the geomorphological and biological follow-up of zone 4 will only become available mid 2017, to be presented at the ‘Studiedag Zandwinning’ of June 9th 2017.

For the period 2012-2015, FPS Economy monitored changes in depth and backscatter using multibeam technology in the monitoring area HBMC in Sector

4c (see box, FPS Economy/COPCO, 2015). Two main results were obtained: (1) Dune migration (water depths of -15 to -20 m MLLWS): consistently to the NE (\pm 30 and 20 m /yr for a profile transecting the dunes on the western slope of HBMC, north and south part respectively), lowering and flattening of the dunes. Compared to the reference situation of 2005, the dunes migrated roughly 85 m and 65 m respectively. (2) Changes in backscatter pointing to a fining of the seabed, significantly being observed from March 2014 onwards (Figure 43).

ADCP measurements along the western slope of the sandbank section in Sector 4c were reported in year 2 of the monitoring (Van Lancker et al., 2015). For a mid-tide period (coefficient 57), flood currents were measured up to 0.75 ms^{-1} , (highest observations of SPMC), against ebb currents of up to 0.5 ms^{-1} . Generally, the western slope of the sandbank is indeed flood dominant causing bedform migration to the NE. In a later phase the magnitude of the migration will be compared with similar environments (naturally- and anthropogenically-influenced).

In relation to the results of the fining in sediments, as derived from the BS analyses, it is not clear yet what the nature of the BS change means physically. Some of the shallow cores taken in the monitoring, discussed in this report, showed locally relatively high mud percentages close to the seabed. Extra cores were taken in December 2015, but were not yet analysed. From the BS change mapping, the change could be related to deposition of the dynamic plume of TSHDs. The associated depth time series (COPCO) did show important migration and decrease in depth level of the large to very-large dunes occurring higher up the slope. Reorganization of winnowed sediments and their deposition is hence also plausible. In this sense, the higher absorption of the acoustic signal might also be related to a difference in compaction level of the sediments. Finally, it should be further investigated whether the abrasion by extraction led to a surfacing of a deeper lying geological substrate that is less coarse in texture. In any case the newly emerging sediment surface, will be more prone to resuspension and transport by currents and waves to be deposited elsewhere.

For the period 2010-2013, hence before the intensive extraction activities of 2014, the biological monitoring of ILVO in the aggregate sectors showed that the benthos recovers well from the extraction activities. The results confirmed previous findings that the current benthic sandy ecosystem of the BPNS is resilient enough to buffer aggregate dredging when performed at low or at high, but infrequent intensities. The latter is the case for the extraction in Sector 4c. However, it is highlighted that dredging, focused on a small surface area, and when performed at high and frequent intensities, this will likely result in changes in sediments that subsequently result in clear biological changes (De Backer et al., 2014; and references therein).

Multibeam monitoring results FPS Economy

For the period 2012-2015, FPS Economy analysed multibeam backscatter (BS) time series for Sector 4c, HBMC area. Compared to time-series analyses on the Flemish Banks, a clear evolution in backscatter values was observed, particularly when the occurrence of fine against coarse acoustic seabed types was evaluated. The finer seabed type was representative of sediments along the topzone of the sandbank, whilst the coarser seabed type mostly occurred downslope of the sandbank. From results obtained in March 2014 onwards, a relative gradual increase was seen in the finer seabed type. This continued in May 2014. In November 2014 a fair extent of the finer seabed class was present downslope of the sandbank and was still observed in May 2015. The areal extent of the zone of BS change fell completely within the area where extraction activities were above 2500 m³ per 2500 m³.

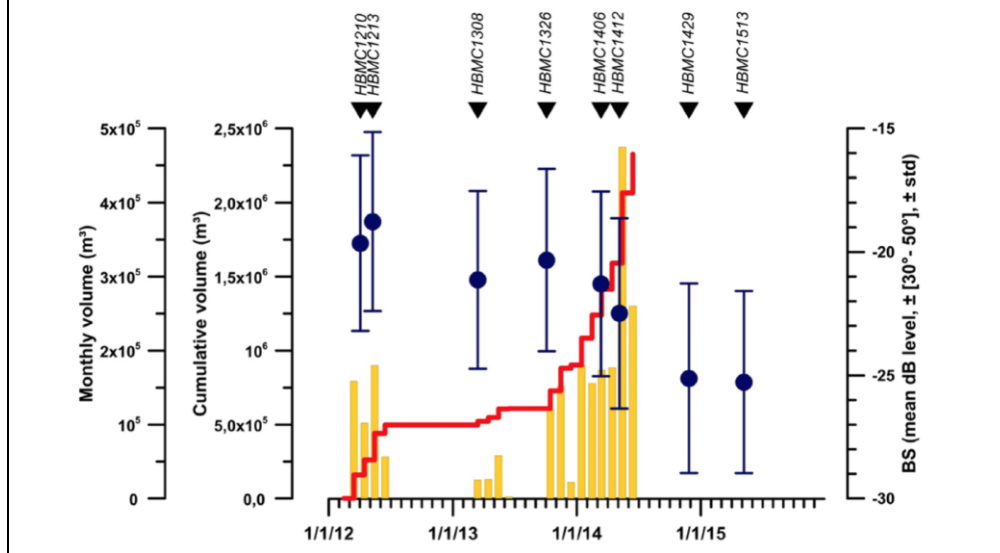


Figure 43. HBMC extraction area and BS evolution. BS values are derived following a standardized processing. Note the important drop in BS values (increase in finer sediments) after the peak extraction of 2014 (FPS Economy/COPCO, 2015).

Biological monitoring of the hard substrates is carried out by OD Nature in the context of the implementation of MSFD. This monitoring is aligned with the monitoring presented in this report. As such, from many of the samples taken in this monitoring also biological analyses will be performed. Results are foreseen in Spring 2017 to align with the MSFD assessment deadlines. Furthermore, the MOZ4 monitoring will be pivotal for establishing a base line and follow-up of a fisheries management zone, designated to the north of the Habitat Directive Area (e.g., coloured polygons in Figure 41). This comprises two areas: a northern zone where it is projected to prohibit fishing activities; a southern zone where only alternative fishing gear will be allowed. Follow-up of these areas will clarify whether gravel flora and fauna can re-establish under decreased to no pressure from fishing activities.

5.4. Assessment of impacts w.r.t. the Belgian MSFD environmental targets

In this section, the compliancy of the marine aggregate extraction activities versus the environmental targets, defined by Belgium in its implementation of the Marine Strategy Framework Directive, is reflected upon. Purpose was to test the usefulness and efficiency of the targets and associated indicators that parametrize the state of the physical seafloor within the descriptors of seafloor integrity and hydrographic conditions, respectively. For both, the Belgische Staat (2012) also put forward monitoring programmes, hence these needed testing too.

It needs emphasis that the MSFD assessment procedure is entirely new for the Member States and that guidance is still underway. The assessments are due officially by June 2018, but taken into account internal review, as well as public consultation, the reports need delivery by June 2017. Hence, at this stage, only some preliminary reflections are put forward and, importantly, harmonization of all findings will be needed before any final assessments can be made.

5.4.1. Evaluation

Seafloor integrity (GES descriptor 6)

Following the Commission Decision 2010/477/EU on this descriptor, seafloor integrity should be at a level that ensures that the structure and functions of the ecosystems are safeguarded and benthic ecosystems, in particular, are not adversely affected. The objective is that human pressures on the seabed do not hinder the ecosystem components to retain their natural diversity, productivity and dynamic ecological processes, having regard to ecosystem resilience.

For the pressure part of seafloor integrity, the Commission put forward three primary criteria that need assessing: 1) Physical loss; 2) Physical damage and 3) Spatial extent of adverse effects from physical disturbance on benthic broad habitats. For (1) and (2) the spatial extent and distribution need quantification. Physical loss defines a permanent change to the seabed which has lasted or is expected to last for a period of two reporting cycles (12 years) or more. Physical disturbance is a change to the seabed which can be restored if the activity causing the disturbance pressure ceases.

Most challenging, and recognized in the Commission Decision is the scale of assessment because of the patchy nature of the features of some benthic ecosystems and of several human pressures. As such, they put forward that assessment and monitoring needs to be carried out further to an initial screening of impacts and threats to biodiversity features and human pressures at the most appropriate scale. Later, an integration of assessment results is needed from smaller to broader scales, covering where appropriate a subdivision, a sub-region or region. The marine region under concern is the North-East Atlantic Ocean; the sub-region is the Greater North Sea.

Related to the seafloor integrity criteria physical loss and damage, the Belgian State (2012) defined two targets/indicators, together with their monitoring programmes. Since these were all newly developed, the present study aimed at a first evaluation, in the context of aggregate extraction.

1. The areal extent and distribution of EUNIS level 3 Habitats (sandy mud to mud; muddy sand to sand and coarse sediments), as well as of the gravel beds, remain within the margin of uncertainty of the sediment distribution, with reference to the Initial Assessment. (*Environmental Target 'ET' 7 within the Belgian MSFD reporting*).

To monitor this indicator, at the scale of the Belgian part of the North Sea, it was put forward to carry out (i) a full-coverage seabed mapping of a selection of areas, where the delineation of the EUNIS level 3 habitats has a high confidence; (ii) transect seabed mapping crossing the EUNIS Level 3 habitats and the gravel beds. For the methodology, a combination of multibeam bathymetry / backscatter and seabed sampling, in a stratified random sampling approach, was proposed. At least 1 mapping round per MSFD cycle (6 yrs) should be procured.

2. Within the gravel beds⁹ (in test zones), the ratio of the surface of hard substrate (i.e., surface colonized by hard substrata epifauna) against the ratio of soft sediment (i.e., surface on top of the hard substrate that prevents the development of hard substrata fauna), does not show a negative trend. (*Environmental Target 'ET' 17 within the Belgian MSFD reporting*)

For this indicator an annual monitoring (June/July) was proposed to enable linking observed changes to human activities. Also multibeam bathymetry / backscatter were proposed as methodology, in combination with visual observations and seabed sampling; the latter following a stratified random sampling approach.

For ET 7 the indicator implies that no transitions are allowed from the class sandy mud to mud towards muddy sand to sand and vice versa, as well as from muddy sand to sand towards mixed or coarse sediments and vice versa (Figure 44). Specifically related to coarse sediment, incl. gravel, enrichment of mud should not lead to muddy sandy Gravel (mixed sediment). Also, it is put forward that the extent of the gravel beds should be safeguarded. The latter targets the prevention of the loss of gravel beds. Changes need evaluation against the Initial Assessment. Herewith was also stated that changes should remain within the margin of uncertainty. This quantification of uncertainty is still on-going and is only foreseen to be ready by mid 2017, hence no final statements can be made.

From the monitoring in zone 4, most samples fall within the classes sand,

⁹ For the monitoring of this indicator, the Belgian State defined two testzones in the Habitat Directive Area: one along the southern Oosthinder sandbank ('barchan dune' area, here discussed); one in-between the Kwinte Bank and Buiten Ratel sandbank ('KWGS' area).

coarse sediment and gravel. The monitoring did depict a new class ‘mixed sediments’ which was not mapped in the Initial Assessment. Mixed sediments typically contain an admixture of mud. Referring to the Folk diagramme (Figure 44) sediments are classified as mixed sediments when in the gravel range of 5 % to 80 % gravel, the sand to mud ratio is lower than 9 to 1. In Table 6 the threshold of mud percentage is shown per major gravel percentage. For the higher gravel percentages, only a minor addition of mud results in mixed sediments.

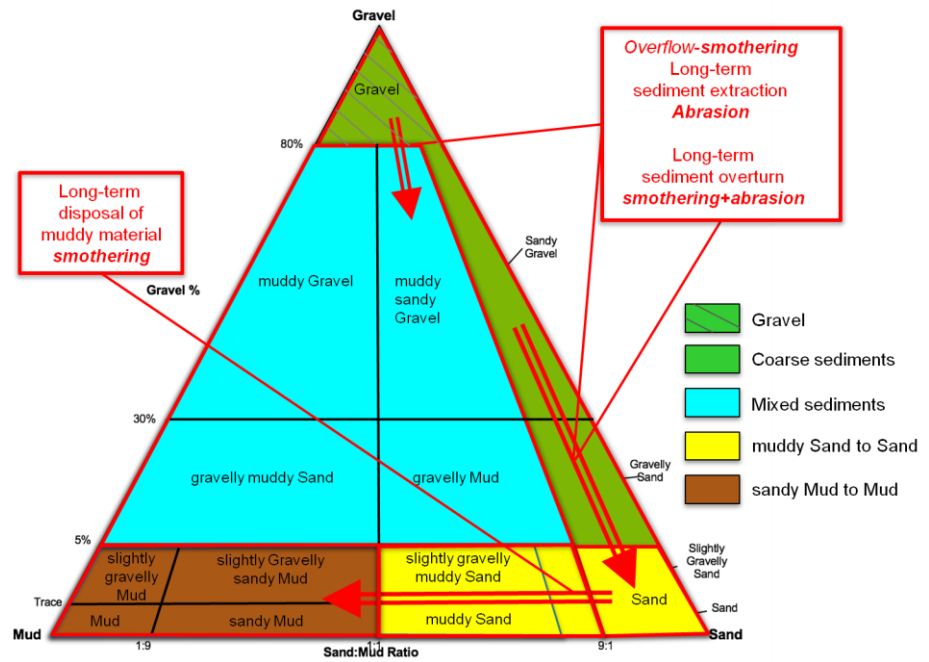


Figure 44. Relationships between EUNIS Level 3 Habitats (sandy mud to mud; muddy sand to sand; mixed sediments and coarse sediments) as derived from a grouping of the 14 Folk substrate classes. For the Belgian MSFD implementation, gravel is also considered individually. Regarding changes in this indicator of seafloor integrity, possible transitions are indicated that can occur under the influence of human activity.

Table 6. Threshold of allowable mud percentage per major gravel percentage. Higher mud percentages result in lower sand to mud ratios, classifying sediments into mixed sediments instead of coarse sediments.

% gravel	% sand	% mud	sand:mud ratio
5	85.5	9.5	9
10	81	9	9
20	72	8	9
30	63	7	9
40	54	6	9
50	45	5	9
60	36	4	9
70	27	3	9
80	18	2	9

In the databases containing grain-size distribution data (RBINS Sedi-CURVE@SEA; Van Lancker 2009) there are no samples having elevated mud percentages in the gravel areas. However, the present monitoring showed that the mud was retained in the sand matrix (within the interstitial pores). This complies with the multiple observations of 'brown waters' and appearance of sediment clouds when stirring the sediment (with ROV or video frame landings, or agitation by divers).

Furthermore, monitoring in the gravel rich areas showed more sand than the expected gravel clasts, resulting in a classification of sand rather than gravel. This is especially the case in areas with low gravel percentages, where an overtopping sand layer would easily prevent the detection of gravel clasts.

Preliminary results on the multibeam monitoring did not show major changes, although the development of standardized change detection methods is still underway, as well as the sensitivity analysis of the technology ('discrimination potential) with respect to the Folk classification.

Some remarks regarding the evaluation of the indicators:

- Gravel percentages are very hard to measure correctly (very patchy in nature), as well as percentages of mud particles in the low percentage range. Appropriate sampling gear is needed that retains a volume of sediment. Historically, Van Veen grabs were taken with jaws that could not retain bigger clasts and allowing mud to be mostly washed away by the time the grab was hauled on deck. The Hamon grab, used in the present monitoring, captures a full sediment volume retaining maximally what is on the seafloor. This complicates comparison with historical data.
- Also, the monitoring of the gravel distribution and extent remains difficult and needs further evaluation. Existing maps were qualitative only, showing areas where gravel may occur. They were based on a combination of the underlying geology, seabed samples, diving observations, as well as acoustic data (multibeam). The latter was pivotal for the gravel mapping (Van Lancker et al. 2007) since it allowed the mapping of a continuum based on a similar classification of the backscatter of the acoustic signal. Occurrence of gravel is generally associated with areas that have a strong seabed return, though those areas also have a typical hillhocky or bumpy morphology that also results in stronger reflections. Hence, if a sandy layer overtops the gravel, it will be difficult to distinguish from the acoustic signature alone. The present monitoring, and particularly the visual observations, showed mostly sand in the areas where gravel was expected acoustically in the gullies, and only sporadically gravel patches and/or blocks were seen. Since the existing maps (Van Lancker et al., 2007) were hardly verified with visual observations, it cannot be reported how much sand was on top of the gravel at that time. An additional quantification of various terrain indices of the seafloor (calculated from digital terrain models) could help in this assessment: the more gravel has a surficial expression, the rougher the seabed will be; the more sand that is overtopping the gravel, the smoother the seabed will be.

Biologically, this makes sense too, since structural complexity (roughness *s.l.*) is important for ecological successional phases to occur (Houziaux et al. 2007).

To conclude, evaluation of the ET 7 indicator is difficult in areas with gravel and uncertainty in the mapping will remain high. However, since the sediment is a first proxy of many species and biological communities, further follow-up is needed.

For the evaluation of ET 17 on the monitoring of the ratio of the surface area of hard versus soft substrata, the development of a standardized workflow is ongoing. Aim is to enable evaluation of changes in multibeam backscatter within a series of repetitive measurements along the biodiversity rich gravel beds in the Habitat Directive Area. Seven time series are available in the period 2004-2015 with two surveys prior to extraction, 3 during extraction and 2 post extraction. Since the last survey dates from December 2015, results will only be reported in the next phase of the project.

Hydrographic conditions (GES descriptor 7)

For descriptor 7 on hydrographic conditions, the Commission only put forward two secondary criteria to be assessed: (1) Spatial extent and distribution of permanent alteration of hydrographical conditions; and (2) Spatial extent of adverse effects on benthic habitats from permanent alteration of hydrographical conditions. To that end the Belgian State (2012) defined three indicators, mainly in the view of preventing permanent changes to hydrographic conditions.

1. It was stated that a human impact demands consideration if one of the following conditions – related to the bottom shear stress on a 14 days spring tide/neap tide cycle as computed by validated mathematical models – is met: i) there is an increase of more than 10 % of the mean bottom shear stress; ii) the variation of the ratio between the duration of the bottom shear stress and the duration of the erosion is outside the “-5%, +5%” range. (*Environmental Target ‘ET’ 29 within the Belgian MSFD reporting*).

2. The impact, that needs consideration, should remain within a distance equal to the root square of the surface occupied by this activity and taken from its external limit (*Environmental Target ‘ET’ 30 within the Belgian MSFD reporting*).

3. All developments must comply with the existing regulatory regime (e.g., EIA, SEA, and Habitats Directives) and regulatory assessments must be undertaken in such a way that it takes into consideration any potential impacts arising from permanent changes in hydrographical conditions, including cumulative effects, at the most appropriate spatial scales following the guidance prepared to this end. (*Environmental Target ‘ET’ 31 within the Belgian MSFD reporting*).

Monitoring of these changes needs execution within the permitting procedure, during the preparation of the environmental impact assessment, or during its evaluation. It will determine whether new activities will impact on the hydrodynamics and whether this requires further research (ET 29). In that case, it is expected that the impact remains limited to the environment of the activity (ET 30). It is also stipulated that depth, 3D currents and bottom shear stress need to be evaluated. Use should be made of a validated numerical model with an adapted resolution and model validation will be done using in-situ measurements acquired in the area for which the permit is asked for. To evaluate the cumulative impact, a database will be developed and maintained to register the bathymetrical evolution, as well as the human activity at sea that needs consideration (ET 31).

All of the above is new for the Belgian part of the North Sea, hence the applicability and efficiency need full testing.

Applied to the MOZ4 study area, in-situ data on bathymetry, currents and bottom shear stresses were collected and used for the validation of the numerical models. Next a workflow was established on how to evaluate changes in bottom shear stress, compliant with the prescriptions set in the MSFD context. In a first research phase, some extraction scenarios were then simulated in zone 4 of the Hinder Banks and their changes in bottom shear stress was evaluated. Following the permit, in total 35 million m³ of sands can be extracted in the area over a 10-yr period. In a first scenario a similar maximal extraction depth was used in the four extraction sectors to reach the total volume; in the second scenario the four sectors were extracted until the same final water depth; in the third scenario, all the extraction was executed in Sector 4c. The simulations showed that for the three scenarios, changes in bottom shear stress did get higher than 10 % where extraction activities took place (ET 29), though the changes of the bottom shear stress in the area, where no impact was allowed ('outside distance' or within the buffer zone), the change remained limited to around 6 %, hence less than the maximum allowance of 10 %, as specified within the Belgian implementation of MSFD (ET 30). No research has yet been carried out on how this combines with other human activities in the area (ET 31).

5.4.2. Recommendations on the MSFD indicators, monitoring and evaluation

In this section recommendations on potential refinements of the MSFD environmental targets related to descriptor 6 and 7 are considered.

The MSFD indicators, here specified, were set-up in view of enabling a monitoring of human activities, albeit with the criterion that human activities are allowed, but that major alterations, from which the seabed and its biodiversity would not recover, would be prevented.

Regarding seafloor integrity both the indicator on changes in EUNIS Level 3

habitats (ET 7) and on the ratio of hard to soft substrata (ET 17) makes sense *w.r.t.* the expected changes that marine aggregate extraction can induce, whether or not in combination with other activities and in concert with natural variability; e.g., in the direct near field, exposure of another type of sediment (abrasion process); in the far field deposition of more fine-grained material, sand overtopping. Next to that, long-term monitoring will provide insight into the recovery potential of the seabed after disturbance, an important component of seafloor integrity. More specifically, seabed mobility as well as the natural envelope of natural processes are studied. Seabed recovery processes are important for the resilience of macro-benthic communities.

However, the proposed monitoring using multibeam technology, has some shortcomings:

- Multibeam technology can only detect surficial changes in seabed texture. If fine-grained material is buffered in the parent bed, it will not be detected.
- In gravel areas, multibeam imaging merely depicts the overall landscape that is typical for gravel areas (heterogeneous and patchy in nature); a sand cover is difficult to detect (e.g., in 30 m water depth, the bathymetric vertical uncertainty with ± 95 % confidence levels of the depth measurements is 0.33 m for the EM3002D echosounder). If ripples develop in the sand cover, detection will depend on their size *w.r.t.* the footprint of the echosounder used.

From this it would be recommended to test the use of additional sampling and observations techniques, especially if a smothering process is suspected (recommendations, see last paragraph in section 5.5.1).

The indicator on allowable bottom shear stress changes (ET 29), related to the descriptor on hydrographic conditions, allowed a preliminary investigation of where the effects of large-scale extraction would be most severe. It serves the purpose of being an early warning and helps steering targeted substrate and biological monitoring. Two remarks can be made on the basis of the experiences gained: (1) the allowable buffer of change varies proportionally with the areal extent of the activity, which implies that huge areas would be allowed to be affected; (2) there is considerable freedom in the way bottom shear stresses are calculated and modelled (e.g., skin friction or total friction, see Annex C). For sound evaluations, more guidance is needed on the approaches.

As a conclusion, it needs emphasis that the MSFD monitoring here presented are all related to new indicators and newly set-up monitoring programmes that are still in a testing phase. Preliminary results show that the monitoring is able to quantify changes, at least partially. At this early stage of the monitoring, no reformulations are advised.

5.5. Lessons learned and recommendations for the continuation of extraction practices

5.5.1. Lessons learned

Knowledge and data gaps

The MSFD requires that all EU Member States take measures to ensure that human pressures do not exceed the capacity of the marine ecosystem to withstand human-induced changes, whilst enabling the sustainable use of the marine environment for present and future generations. The whole approach is new, and especially its application in offshore waters is highly challenging since these areas suffer from data scarcity, and subsequently knowledge on the marine environment is far less than in coastal areas. This was already recognized by the Commission Decision 2010/477 EU in which it was put forward that there is a substantial need to develop additional knowledge and system understanding to implement the concept of GES in a truly science-based way. In any case, assessing the status of an environment is very difficult, the more it provides limited insight in how it should be managed. Instead it is much more practical to focus on quantifying pressures (perturbations) and their presumed impacts (i.e. changes in the state of the ecosystem), since these are in most cases manageable. A number of data and knowledge gaps were identified in the present monitoring that hamper the provision of adequate assessments:

(1) Baseline – natural variability

Compared to the coastal area, data availability is rather poor in offshore areas, and there is only a fragmented knowledge on habitats and ecosystem functioning. Generally, time-series datasets are scarce. Mostly existing data have highly varying spatial and temporal scales implying huge uncertainties in the overall dataset. This is challenging to resolve in complex sandbank environments, where seabed nature and dynamics vary with morphological position.

Regarding knowledge on the state of the environment the main issues related to (i) Poor prior knowledge on fine-grained fractions in the seabed, mostly due to the use of sampling gear not allowing appropriate quantitative sampling of both the fine- and coarse-grained part of the sediments. (ii) Limited to no knowledge on the sand cover overtopping the gravel lag. Video data in the gravel areas mostly showed the presence of sand with sporadically gravel occurrences. Since sand overtopping prevents biodiversity to flourish on gravel beds there is an urgent need for sand thickness estimation, which is probably only do-able by divers. A major lesson learned was the importance of knowing the geological substrate and realizing its importance in predicting habitat change (e.g., change in sediments at the lower slopes of the sandbanks).

Little is known on water column and seabed dynamics, as well as on the processes involved. Knowledge on natural processes is important for the understanding of recovery and resilience of ecosystems. How are sediments redistributed, where can fine sediments be trapped and buffered? A major effort has now been made to start building up data and information on natural variability ('natural envelope'). Next, coupling of the observations to hydro-meteo forcing is

needed. Main issues already encountered are the observed lag effects between turbidity events observed in the data and the major drivers. In this regard, the importance of the Coriolis force, and Ekman veering needs further investigation. Hence, surface and bottom processes are not necessarily equal.

Last, but not least, there is no information on long-term variability introduced by climate change or long-term cycles in sediment dynamics (e.g., 18.6 yr lunar cycle). This might also be a factor in explaining the varying sand layer observations overtopping the gravel lags in the gullies.

(2) Cause-effect relationships

Mostly related to more adequate quantification of far field impacts, three main caveats were identified: (i) Pressure-related information need more adequate quantification. This relates to the nature, release and spreading of fine-grained material. (ii) Process knowledge needs improving to understand the fate of the fine-grained material and how this may affect habitats and ecosystem functioning. E.g., what is the mechanism of uptake and release of fine-material in the seabed and the importance of buffering of fine material in the seabed. This could affect functional biodiversity with implications for biogeochemistry and food webs. This is now investigated in the Belspo project, FACE-It. In this project also the relevance on the larger scale of the North Sea will be studied. (iii) Estimation of cumulative and in-combination effects, since the origin of the fine-grained material cannot be unambiguously linked to the extraction activities in zone 4. What are indeed the effects of different combinations of stressors (aggregate-extraction at multiple sites; fishing; dredging and disposal of dredged material; windmill farms), as also climate change? It is also important to realize that an impact is not always directly related to a pressure and the typical response time of the ecosystem is largely unknown. This needs careful consideration in the monitoring phases.

(3) Significance of the effects on larger scales

For the time being the status and dynamics of the MOZ4 environment is mostly studied at the small scale, given the importance to better understand potential changes. However, at a later phase it will be critical to assess the significance of the observed changes on a regional scale. The observed buffering of fine sediments will be up-scaled to the North Sea in the Belspo FACE-It project. The use of multibeam monitoring of seabed changes is presently under discussion at European level and may require standardization of the approaches, as well as of data analyses.

Implications for monitoring approaches

Establishing most suitable monitoring approaches in offshore areas is very difficult. This is due to the high spatial and temporal variability of sandbank environments, as well as the difficulty of safe deployments of instrumentation. Additionally, fair weather conditions are far less occurring than in the coastal area. Hence, it remains a challenge to implement time- and cost-efficient approaches

and keep the effort manageable.

To improve on the baseline further investments are needed in accurate seabed mapping, repeated in time, and combining most appropriate measuring and observational techniques. Probability mapping of sediment distributions is underway (Belspo project TILES) and will provide better insights in the accuracy of seabed maps in the area. A standardized approach for the analysis of repetitive multibeam data is currently worked out in the Belspo project INDI67. Belspo TILES will also provide best available knowledge (and associated uncertainty) on the geological substrate. Video data will be further acquired, mainly to assess the status of the gravel beds.

To study cause-effect relationships in more detail, it is recommended to opt, at key locations, for longer-term fixed deployments of instrumentation (e.g., with benthic landers). This strategy would provide less biased data on natural variability over spring-neap tidal cycles, and these datasets can then be analysed statistically against external data, e.g., on aggregate extraction, fishing intensity. Such landers would also allow measurements up to the bottom which is needed for adequate calculations of bottom shear stresses. Hitherto, such data are hardly available in the offshore area. However, in open sea, such as in zone 4 of the Hinder Banks region, there is no protection for the landers and creative solutions need to be sought for safe deployments. A prerequisite remains that the fixed locations are chosen well. This should be based on a regional assessment of currents and sediment transport in relation to the impact predictions.

Regarding process knowledge, there is a need to better understand the composition and behaviour of particles in the overflow, which determines the settling velocity and dispersal. Therefore, samples need to be taken in the weir of the TSHDs and when entering the surrounding water mass. These data are needed to further refine the outcome of the sediment plume models. An important development will be the use of a 3D advection-diffusion model, instead of a 2D depth-averaged model as used now. This would allow accounting for the difference between overflow at the surface (small TSHD) and below the hull of a vessel (large TSHD). Subsequently, a regional probability assessment of deposition of fine material from TSHD overflow is needed, in combination with ground-truth validation at most critical locations. From the experience so far, it is important to understand morphological trapping of fine-grained material and to determine criteria on where this is most likely to occur on the BPNS.

In a next phase, the study of cumulative and in-combination effects becomes important. The quest remains whether or not, per location, the origin of the fine material can be traced. Therefore, it will be attempted to take shallow cores, although this may prove very difficult given the coarse substrate. For the analyses of the cores several techniques exist that could help in identifying the nature and potentially the source of sediments (e.g., microscan; hyperspectral cameras; microscopy).

Clearly, the above recommendations imply a drastic increase in time/effort and costs. This will need to be balanced against the relevance of the expected impacts and how this improves on the management of the marine environment, as well as on advising on better practices for the continuation of extraction.

5.5.2. Recommendations for the continuation of extraction

The monitoring programme, set-up for zone 4, generates data and knowledge to assist in minimising the physical damage of the substrate types within zone 4. Particularly, and especially on the long-term, the following items are considered:

- (1) Ensuring a fast recovery of the seabed after disturbance (resilience of the system), i.e. no significant disturbance of natural processes:
→ *Monitoring is too short for advise. Future research will comprise the evaluation of depletion/ regeneration rates in the sectors for extraction and compare those to other areas with similar environmental characteristics. This information will be used in conjunction with time-series of depth registrations using multibeam technology.*
- (2) Preventing alterations to the habitat types (e.g. sediment related):
→ *Concerning Sector 4c, the present rates of extraction will not lead to abrasion inducing habitat changes, except on the lower slope of the sandbanks, where the depth to the Top Pleistocene is minimal. It is advised to restrict extraction to the middle and top part of the sandbank where the geological resource is thickest.*
→ *In the far field fining of sediments may occur under persistent extraction on Sector 4c during the ebbing phase of the tide. Most of the initial extraction took place on Sector 4c being the southernmost sector, hence nearest to the Habitat Directive Area. Whenever possible, it is advised to spread the activity over different sectors. The potential smothering process needs follow-up.*
- (3) Preventing unnatural fragmentation of the seabed:
→ *Monitoring is too short for advise.*
- (4) Preventing permanent alteration of the hydrographic conditions:
→ *Monitoring is too short for advise.*

6. Outreach

Results have been presented at national and international conferences and events, see Annex E. Results of the Wave Glider experiment, conducted in 2013, were published in 2015 (Van Lancker & Baeye, 2015) in PlosONE. A book chapter on the relation between bedforms and habitat occurrences was prepared, but will only be published in 2017 (Van Lancker, 2017). In Winter 2016, a paper on the detection of habitat changes in the Habitat Directive area will be submitted to the A1 Journal of Marine Geophysical Research (Montereale-Gavazzi et al.).

7. Acknowledgments

Flemish Authorities, Agency Maritime Services and Coast, Coast, are acknowledged for financially contributing to the monitoring activities (MOZ4). Full support is provided by the continuous monitoring programme ZAGRI, paid from the revenues of extraction activities. The BELSPO Brain-be INDI67 project (contract BR/143/A2/INDI67) contributed to the modelling of bottom shear stresses and the quantification of benthic habitat changes from multibeam data.

RV Belgica shiptime was provided by RBINS OD-Nature and Belgian Science Policy (BELSPO). The commander and crew are acknowledged for their support during the measuring campaigns. Lieven Naudts, and other team members of the Measuring Service Ostend (MSO) (OD Nature) are thanked for their logistical support, especially during the deployment of the bottom-mounted ADCPs. Special thanks goes to Reinhilde Van den Branden for her continuous support throughout all measurements, and for providing, together with Gregory De Schepper, processed data on the dredging activities.

Flanders Marine Institute, VLIZ, is thanked for the use of its LISST instrument and the Hamon grab for gravel sampling. Additionally, a video frame was provided for visual observations, and their Remote Operated Vehicle, GENESIS. RV Simon Stevin was used as base ship.

Ghent University, Renard Centre of Marine Geology, is acknowledged for providing laboratory facilities. Particularly, Sébastien Bertrand is thanked for his assistance during the sediment analyses.

Furthermore several OD Nature teams are acknowledged for their contributions: ECOCHEM for the analyses of the filtrations of the water samples; MFC, Sébastien Legrand, for modelled hydro-meteorological data.

Measurements of hydro-meteorological data were acquired from IVA MDK - afdeling Kust - 'Meetnet Vlaamse Banken'.

Continental Shelf Department (COPCO), FPS Economy, Self-Employed, SMEs and Energy are thanked for assistance with multibeam data processing, and active cooperation in general.

Last, but not least, numerous students (Msc Oceans & Lakes) are thanked for assisting in the measurements at sea and in the post-processing of the data.

This work contributes also to the Brain-be project TILES (Transnational and Integrated Long-term marine Exploitation Strategies), funded by BELSPO under contract BR/121/A2/TILES.

8. References

- Baeye, M. & Fettweis, M. (2015). In situ observations of suspended particulate matter plumes at an off-shore wind farm, southern North Sea. *Geo-Marine Letters* 35 (4), 247–255.
- Belgische Staat, 2012. Determination of Good Environmental Status and establishment of environmental Targets for the Belgian marine waters. Art. 9 & 10: 33 pp. Brussels: Federal Public Service Health Food Chain Safety and Environment.
- De Backer, A., Hillewaert, H., Van Hoey, G., Wittoeck, J. and Hostens, K. (2014). Structural and functional biological assessment of aggregate dredging intensity on the Belgian part of the North Sea, in: De Mol, L. and Vanderycken, H. (Ed.) 'Which future for the sand extraction in the Belgian part of the North Sea?'. Study day, 20 October 2014, Belgium Pier - Blankenberge. pp. 29-58.
- FPS Economy/COPCO (2015). HBMC Monitoring area. Results period 2012-2015. Presentation at MOZ4 meeting of 30/10/2015 (internal document only).
- Houziaux, J.-S., Kerckhof, F., Degrendele, K., Roche, M.F. & Norro, A. 2008. The Hinder banks: yet an important area for the Belgian marine biodiversity?: 248 pp. Brussels: Belgian Science Policy.
- Kint, L. & Van Lancker, V. (2016). SediLITHO@SEA v2 (06/10/2016). Database lithological descriptions, with relevance to Belgian part of the North Sea. Brussels: Royal Belgian Institute of Natural Sciences.
- Lefebvre, A., A. J. Paarlberg, and C. Winter (2014), Flow separation and shear stress over angle-of-repose bed forms: A numerical investigation, *Water Resour. Res.*, 50, 986–1005, doi:10.1002/2013WR014587.
- Le Bot, S., Van Lancker, V., Deleu, S., De Batist, M., & Henriët, J. P. (2003). Tertiary and Quaternary geology of the Belgian continental shelf. Scientific support plan for a sustainable development policy, SPSD II. PPS Science Policy, Brussels, 75 pp.
- Omidyeganeh, M., Piomelli U., Christensen K. T. & Best J.L. (2013) Large eddy simulation of interacting barchan dunes in a steady, unidirectional flow . *Journal of Geophysical Research-Earth Surface* 118(4), 2089-2104.
- Papili, S, Jenkins, C, Roche, M, Wever, T, Lopera, O, and Van Lancker, V. (2015). Influence of shells and shell debris on backscatter strength: investigation using modeling, sonar measurements and sampling on the Belgian Continental Shelf. In: *Seabed and Sediment Acoustics: Measurements and Modelling*, ed. by Blondel et al., vol. 37(1), pp. 304-310, University of Bath, Bath, Institute of Acoustics. Proceedings of the Institute of Acoustics.
- Sea-Bird Electronics Inc. (2013). Application note no. 48. Entering calibration coefficients for the Sea-point Turbidity Meter. Available at: www.seabird.com
- Sequoia Scientific, 2008. <http://www.sequoiasci.com/article/processing-lisst-100-and-lisst-100x-data-in-matlab/>
- Van den Branden, R., De Schepper, G. & Naudts, L. (2016). Zand- en grindwinning op het Belgisch deel van de Noordzee. Electronic Monitoring System (EMS) voor de monitoring van de aggregaatextractie: jaarrapport 2014-2015. RBINS-OD Nature-MSO. Report MDO/2016-02/ZAGRI , 60 pp.
- Van Lancker, V. (2009). SediCURVE@SEA: a multiparameter sediment database, in support of environmental assessments at sea. In: Van Lancker, V. et al. QUantification of Erosion/Sedimentation patterns to Trace the natural versus anthropogenic sediment dynamics (QUEST4D). Final Report Phase 1. Science for Sustainable Development. Brussels: Belgian Science Policy 2009 – 63p + Annexes.

- Van Lancker, V. & Baeye, M. (2015). Wave glider monitoring of sediment transport and dredge plumes in a shallow marine sandbank environment. *PloS one*, 10(6), e0128948.
- Van Lancker, V., Baeye, M., Fettweis, M., Francken, F., & Van den Eynde, D. (2014). Monitoring of the impact of the extraction of marine aggregates, in casu sand, in the zone of the Hinder Banks. Scientific Report 1 - January - December 2013. RBINS OD Nature report MOZ4-ZAGRI/X/VVL/201401/EN/SR01.
- Van Lancker, V., Baeye, M., Evangelinos, D. & Van den Eynde, D. (2015). Monitoring of the impact of the extraction of marine aggregates, in casu sand, in the zone of the Hinder Banks. Period 1/1 - 31/12 2014. Brussels, RBINS-OD Nature. Report <MOZ4-ZAGRI/I/VVL/201502/EN/SR01>, 74 pp. (+5 Annexes, 109 pp).
- Van Lancker, V, Du Four, I, Verfaillie, E, Deleu, S, Schelfaut, K, Fettweis, M, Van den Eynde, D, Francken, F, Monbaliu, J, Giardino, A, Portilla, J, Lanckneus, J, Moerkerke, G. & Degraer, S (2007). Management, research and budgetting of aggregates in shelf seas related to end-users (Marebasse). Brussel (B), Belgian Science Policy (D/2007/1191/49), 139 pp. + DVD GIS@SEA.
- Van Lancker, V.R.M., Bonne, W., Bellec, V., Degrendele, K., Garel, E., Brière, C., Van den Eynde, D., Collins, M.B. & Velegrakis, A.F. (2010). Recommendations for the sustainable exploitation of tidal sandbanks. *Journal of Coastal Research* SI51: 151-161.
- Van Lancker, V. (2017). Bedforms as Benthic Habitats: Living on the Edge, Chaos, Order and Complexity, pp. 195-198. In: Guillén, J, Acosta, J, Chiocci, FL, Palanques, A (Eds). *Atlas of Bedforms in the Western Mediterranean*. Springer International Publishing Switzerland. ISBN: 978-3-319-33938-2. DOI 10.1007/978-3-319-33940-5_30.

9. Annexes

Annex A. RV Belgica Campaign Reports

Annex B. Video footage 2015

Annex C. Impact of extraction on the bottom shear stress in zone 4

Annex D. Monitoring results HBMC, FPS Economy

Annex E. Publications

COLOPHON

This report was issued in August 2016

Its reference code is MOD code.

Status draft
 final version
 revised version of document
 confidential

Available in English
 Dutch
 French

If you have any questions or wish to receive additional copies of this document, please send an e-mail to vera.vanlancker@naturalsciences.be, quoting the reference, or write to:

Royal Belgian Institute of Natural Sciences
OD NATURE
100 Gulledelle
B-1200 Brussels
Belgium
Phone: +32 2 773 2111
Fax: +32 2 770 6972
<http://www.odnature.naturalsciences.be/>

The typefaces used in this document are Gudrun Zapf-von Hesse's *Carmina Medium* at 10/14 for body text, and Frederic Goudy's *Goudy Sans Medium* for headings and captions.

Annex A

Cruise reports RV Belgica 2015

ST1502-ST1507-ST1517-ST1533

This Annex forms part of the report:

Van Lancker, V., Baeye, M., Montereale-Gavazzi, G. & Van den Eynde, D. (2016). Monitoring of the impact of the extraction of marine aggregates, in casu sand, in the zone of the Hinder Banks. Period 1/1 - 31/12 2015 and Synthesis of results 2011-2015. Brussels, RBINS-OD Nature.

RV BELGICA CRUISE 2015/02 – CRUISE REPORT

Subscribers:	Koen Degrendele (KD), Vera Van Lancker (VV), Sonia Papili (SP)
Institutes:	FPS Economy, SMEs, self-employed and Energy, Continental Shelf Department (CSS) Operational Directorate Natural Environment (OD NATURE) Belgian Navy: DGMR-RMA-NMWMSC (DGMR)
Addresses:	CSS: NGII - Koning Albert II Laan 16 , 1000 Brussels OD NATURE-BRU : Gulledelle 100, 1200 Brussels OD NATURE: 3de & 23ste Linierregimentsplein, 8400 Oostende DGMR: Naval base Zeebrugge, Graaf Jansdijk 1, B-8380 Zeebrugge
Telephones:	+32(0)2 2778411 (KD) +32(0)2 50558368 (SP)
E-mails:	koen.degrendele@economie.fgov.be , vera.vanlancker@mumm.ac.be , sonia.papili@mil.be

*Legend: Black: fixed lay-out
Red: example and to fill in
Blue: to fill in*

Geology: 02/02/2015 - 04/02/2015

1. Cruise details
2. List of participants
3. Scientific objectives
4. Operational course
5. Track plot
6. Measurements and sampling
7. Remarks
8. Data storage

1. CRUISE DETAILS

1.	Cruise number	2015/02
2.	Date/time	Zeebrugge TD: 02/02/2015 at 12h00 Zeebrugge TA: 04/02/2015 at 13h10
3.	Chief Scientist Participating institutes	Marc Roche CSS, OD NATURE, DGMR
4.	Area of interest	Belgian part of the North Sea

2. LIST OF PARTICIPANTS

INSTITUTE	NAME	02/02 - 04/02/15
CSS	Lies DE MOL	X
	Marc ROCHE	X
OD Nature	Vera VAN LANCKER	X
	Nathan TERSELEER	X
	Kevin HINDRYCKX	X
	Jeroen DE BISSCHOP	X
DGMR	Sonia PAPILI	X
	Ives REGENT	X
	Gino DECEUNINCK	X
	Freddy PRIEM	X
		10

3. SCIENTIFIC OBJECTIVES

CSS-KD

Implementation of the continuous investigation laid down in section 3, §2, subsection 3, of the law of June 13th 1969, concerning the exploration and exploitation of non-living resources on the Belgian Continental Shelf, and the concession decisions.

The follow up of the repercussions of the sand extraction on the stability of the sand banks en surrounding area in the exploitation zones, in order to formulate policies concerning the exploitation in the concession zones on a scientific base. The sediments of the Belgian continental shelf will be investigated in order to:

1. Establish the impact of sand extraction on the sand budget and seabed sediments.
2. Survey the sand winning sites to detect significant changes of the seabed sediments and the morphology of the seabed and sand banks in order to guarantee the availability of sand to extract in the future.

OD NATURE-VVL

INDI67/SEACoP – Monitoring MSFD indicators on seafloor integrity and hydrographic conditions / Joint seabed mapping

Within Europe's Marine Strategy Framework Directive (MSFD), progress towards Good Environmental Status (GES) needs monitoring in a most time- and cost-effective way. For the GES descriptors 6 and 7, on seafloor integrity and hydrographic conditions, respectively, new integrative indicators (i.e. bottom shear stress, turbidity and seabed/habitat type) need developing. To advance the mapping of seabed/habitat types, a Community of Practice (CoP) on seabed mapping will be established, investigating the main issues preventing joint mapping of the seabed.

Within SEACoP (CoP on 'Surveying for Environmental Assessments') the following objectives are targeted: a) estimation of the precision, sensitivities and repeatability of the acoustic devices to detect changes in seabed/habitat types; b) quantification of the external sources of variance in the acoustic signature, including the influence of near-bed and water column suspensions on backscatter data; c) definition of best practice in ground-truthing the acoustic signal, with emphasis on visual techniques; and d) innovation in collaborative seabed mapping.

DGMR-OL

MRN09 & MRN10 – Detection and classification of mines using high resolution SAS images

Those projects aim to determine the limits for the detection and classification of seabed objects, in particular mines. In the frame of the Long Term Critical Requirement 21 (Fast detection and neutralization of a minefield) and following the development of autonomous underwater vehicles (AUV), it is necessary to develop classification procedures. This work will focus on two points: first, the study of synthetic aperture sonar (SAS) images to validate SAS image processing algorithms, which will be developed; second, the study of magnetometer data to detect sea-bottom targets. Data (high resolution SAS images and magnetometer data) will be collected using the available equipment (modern mine hunters and sensors from the Mine Warfare Data Center) during the measurement campaigns that will be planned in collaboration with the study of YVP.

DGMR-YVP

Collection of bathymetric seabed information of Belgian EEZ with the use of the systems of project MRN09 – MRN10 and multi beam (MBES) survey in areas with priority 1 for the Naval Mine Warfare Mission Support Center. Meanwhile fine tuning of software and development of procedures for use of the systems of the Mine Warfare Data Center (MWDC). Most of our clients, Belgian and Dutch mine hunters as our NATO partners come to exercise into these areas. Therefore our intention is to procure them a picture of all the possible items that they can encounter within these waters. With this project we are going to try to have as much as possible relevant information about these areas. The information is also used to produce AML's (who is our main tasks).

DGMR-SP

The actual bottom-types doctrinal is legacies from the 1950's mine warfare (NMW) and anti-submarine warfare (ASW). At that time sonar systems performed similarly having more or less the same capabilities and specification. Nowadays, there is a wide variety of sonar systems' types, displays etc. (side-scan, low-frequency wide band (LFWB), high-frequency wide-band (HFWB), synthetic aperture sonar (SAS), as well as much refined forward looking sonar systems). These different sonar types can and do perform very differently against the same target in the same water and bottom conditions. The main purpose of the current work is to classify the sea bottom considering a wide spectrum of parameters. The different parameters will be combined in relation to their influence on backscatter and reverberation response on different instruments. In this way the available instruments will be properly tuned to the sea-floor. As last result, the sensors will be more reliable on defining the bottom type, even in unknown region. Beside the contribution of the sea bottom, the volume reverberation caused by the backscattering from the water column impacts as well the sonar image. To estimate this component, also water column properties will be analyzed.

OD NATURE-LN (AUMS)

The AUMS (Autonomous Underway Measurement System) project is inspired by the success of similar systems deployed on various ships of opportunity in the framework of the European Union FerryBox project (www.ferrybox.org). The instrumentation will greatly enhance the continuous oceanographic measurements made by RV Belgica by taking advantage of the significant technological improvements since the design of the existing (salinity, temperature, fluorescence) systems. In particular, many new parameters can now be measured continuously including important ecosystem parameters such as nitrate, ammonia, silicate, dissolved oxygen and CO₂, turbidity, alkalinity and phytoplankton pigments. In addition, the new equipment allows automatic acquisition and preservation of water samples, rendering RV Belgica operations significantly more efficient by reducing onboard human resources. Data will be available in near real-time via OD NATURE's public web site and following quality control, from the Belgian Marine Data Centre.

ESA-MC (GNSS)

For the European Space Agency continuous GNSS (Global Navigation Satellite system) data is autonomously acquired in the maritime environment for performance evaluation under different conditions.

4. OPERATIONAL COURSE

All times are given in local time. All coordinates in WGS84.

Throughout the campaign, measurements are made with the AUMS system.

Monday 02/02/2015

08h00-10h00	Embarkation of instruments and personnel
12h00	Departure from Zeebrugge
	Transit to Westhinder (HBBSB area)
15h40-17h15	Multibeam and seacat tests
17h15-02h40	Multibeam survey and seacat sampling on HBBSB area (CSS-KD and OD-Nature-VVL)

Tuesday 03/02/2015

02h40-03h55	Transit to HBBSA area
03h55-09h50	Multibeam survey and seacat sampling on HBBSA area (CSS-KD and OD-Nature-VVL)
09h50-11h50	Multibeam calibration (DGMR)
11h50-12h55	Transit to KWGS area
12h55-14h00	Multibeam calibration on KWGS (DGMR)
14h20-16h40	Shadows test and measurements – failed and aborted (DGMR)
17h30-08h30	13h Cyclus and multibeam survey on KWGS (CSS-KD and OD-Nature-VVL)

Wednesday 04/02/2015

08h30-10h30	Multibeam test on KWGS (DGMR)
10h30	Transit to Zeebrugge
13h10	Arrival at Zeebrugge
	Debarcation of participants and material

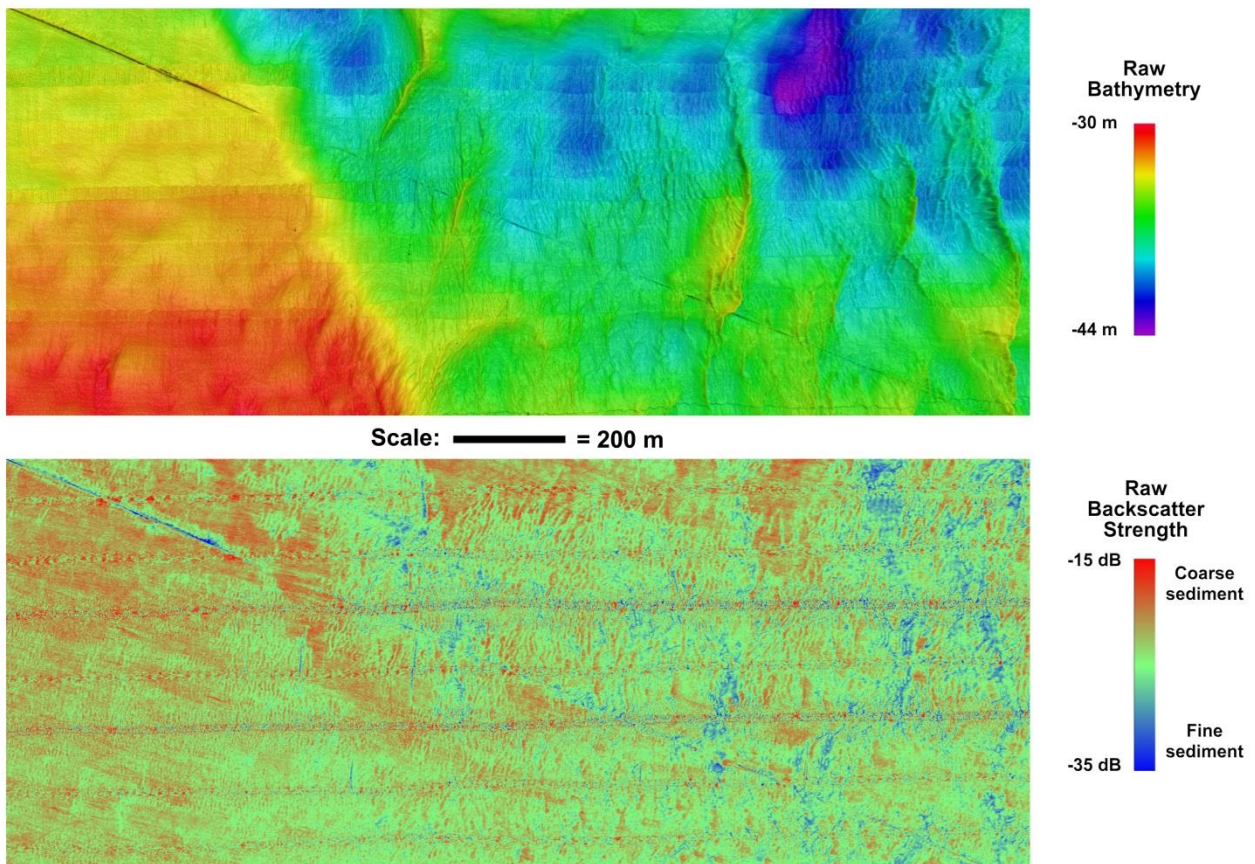
- End of campaign 2015/02 -

5. TRACK PLOT

Figure 1: Track plot of campaign 2015/02

6. MEASUREMENTS AND SAMPLING

6.1. CSS-KD



Multibeam surveys in the channel between West and Oost Hinder (Franpipe is visible).

6.2. OD NATURE-VVL

Hydrodynamic and sediment transport related measurements and observations in two reference areas where gravel beds occur: (1) Hinder Banks, gully in-between Westhinder and Oosthinder; and (2) KWGS area, gully in-between Kwinte Bank and Buiten Ratel. The following measurements were carried out:

1. Hinder Banks reference area (see also COPCO):
Seacat profiles (CTD, OBS (Seapoint), LISST100 instrumentation (VLIZ) and a 10l Niskin bottle for water sampling) at the end of each multibeam line. At the end of the line the hull-mounted ADCP (RDI WH300 kHz; 0.25 m bin size) was switched on unitl after the sampling and vertical profiling of oceanographic parameters. Water samples were filtered for suspended particulate matter (SPM).
2. KWGS area (see also COPCO):
Seacat profiles (CTD, OBS (Seapoint), LISST100 instrumentation (VLIZ) and a 10l Niskin bottle for water sampling) were taken \pm every 30' at the beginning and end of a centrally lying reference line in the KWGS area. The hull-mounted ADCP ADCP (RDI WH300 kHz; 0.25 m bin size) was switched on in-between the multibeam recordings. Water samples were filtered for SPM.
3. No continuous AUMS registrations were made, nor centrifuge samples were taken because of a malfunctioning of the seawater pump.

Table x: Timestamp of the vertical profiles and water samples (with volume filtered) taken in the Hinder Banks reference area.

Station	Gear	OdasTime	SPM (ml)	Remark
WH01	SBE19-L-10l-LISST-SEAPOINT	2015-02-02 15:59:30	1500	
WH02	SBE19-L-10l-LISST-SEAPOINT	2015-02-02 16:56:40	1500	
WH03	SBE19-L-10l-LISST-SEAPOINT	2015-02-02 17:49:00	1500	
WH04	SBE19-L-10l-LISST-SEAPOINT	2015-02-02 18:44:50	1500	

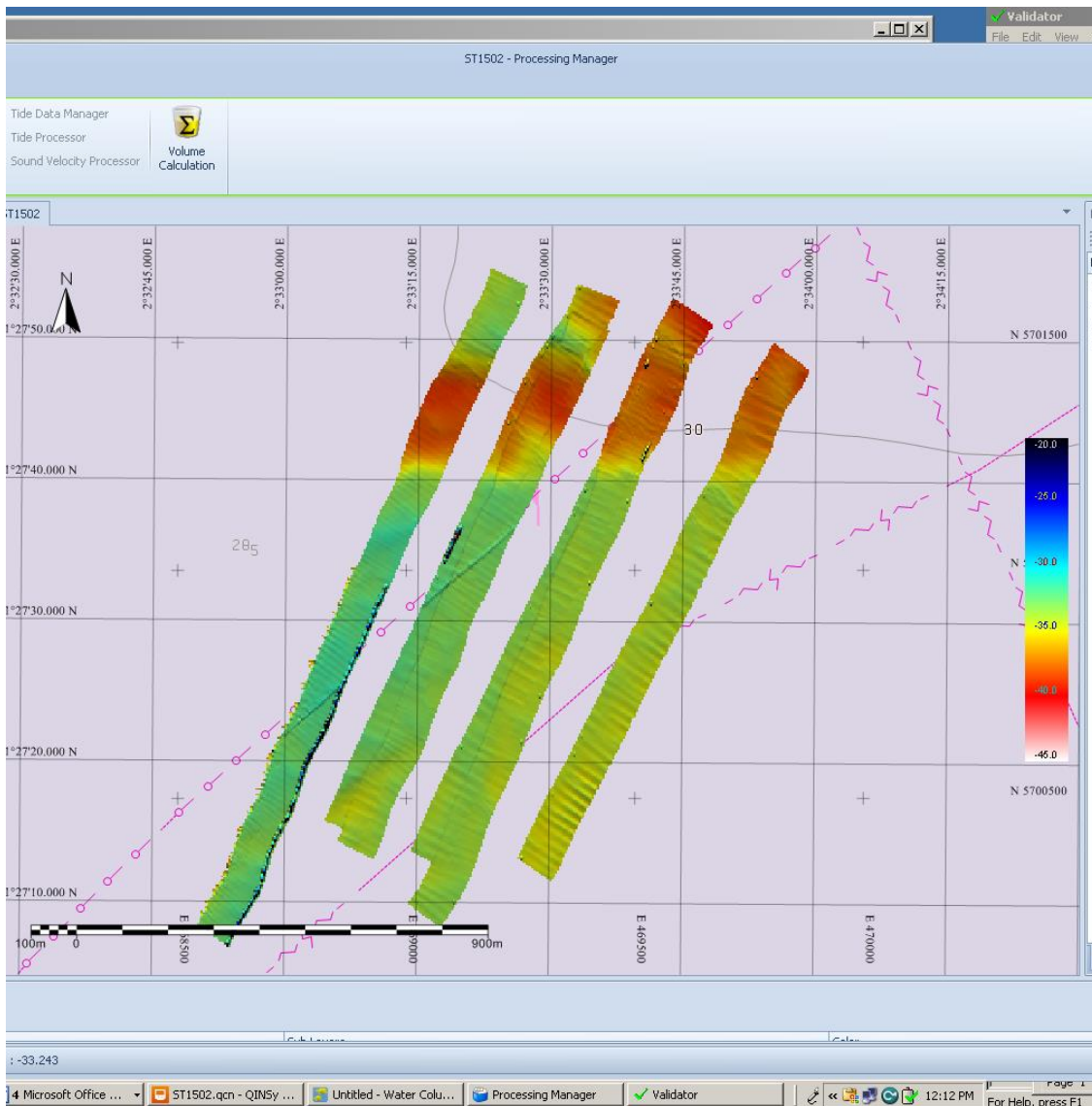
WH05	SBE19-L-10I-LISST-SEAPOINT	2015-02-02 19:40:20	1500	
WH06	SBE19-L-10I-LISST-SEAPOINT	2015-02-02 20:52:50	1500	
WH07	SBE19-L-10I-LISST-SEAPOINT	2015-02-02 21:49:30	1500	
WH08	SBE19-L-10I-LISST-SEAPOINT	2015-02-02 22:43:30	1500	
WH09	SBE19-L-10I-LISST-SEAPOINT	2015-02-02 23:44:40	1500	
WH10	SBE19-L-10I-LISST-SEAPOINT	2015-02-03 00:36:30	1500	
WH11	SBE19-L-10I-LISST-SEAPOINT	2015-02-03 01:34:00	1500	
WH12	SBE19-L-10I-LISST-SEAPOINT	2015-02-03 02:59:00	1500	
WH13	SBE19-L-10I-LISST-SEAPOINT	2015-02-03 03:46:50	1500	First filter was missed
WH14	SBE19-L-10I-LISST-SEAPOINT	2015-02-03 04:24:40	1500	
WH15	SBE19-L-10I-LISST-SEAPOINT	2015-02-03 05:05:10	1500	
WH16	SBE19-L-10I-LISST-SEAPOINT	2015-02-03 05:51:10	1500	
WH17	SBE19-L-10I-LISST-SEAPOINT	2015-02-03 06:41:00	1500	
WH18	SBE19-L-10I-LISST-SEAPOINT	2015-02-03 07:31:30	1500	

Table x: Timestamp of the vertical profiles and water samples (with volume filtered) taken in the KWGS reference area.

Station	Gear	OdasTime	SPM (ml)	Remark
KWGS01	SBE19-L-10I-LISST-SEAPOINT	2015-02-03 16:36:40	1500	
KWGS02	SBE19-L-10I-LISST-SEAPOINT	2015-02-03 17:09:10	1500	
KWGS03	SBE19-L-10I-LISST-SEAPOINT	2015-02-03 17:40:10	1500	
KWGS04	SBE19-L-10I-LISST-SEAPOINT	2015-02-03 18:03:10	1000	
KWGS05	SBE19-L-10I-LISST-SEAPOINT	2015-02-03 18:30:20	1000	
KWGS06	SBE19-L-10I-LISST-SEAPOINT	2015-02-03 18:59:20	1000	
KWGS07	SBE19-L-10I-LISST-SEAPOINT	2015-02-03 19:35:10	1000	
KWGS08	SBE19-L-10I-LISST-SEAPOINT	2015-02-03 20:03:40	1000	
KWGS09	SBE19-L-10I-LISST-SEAPOINT	2015-02-03 20:36:40	1000	
KWGS10	SBE19-L-10I-LISST-SEAPOINT	2015-02-03 20:58:00	1000	
KWGS11	SBE19-L-10I-LISST-SEAPOINT	2015-02-03 21:26:40	1000	
KWGS12	SBE19-L-10I-LISST-SEAPOINT	2015-02-03 21:56:30	1000	
KWGS13	SBE19-L-10I-LISST-SEAPOINT	2015-02-03 22:25:50	500	
KWGS14	SBE19-L-10I-LISST-SEAPOINT	2015-02-03 22:59:50	500	
KWGS15	SBE19-L-10I-LISST-SEAPOINT	2015-02-03 23:31:30	500	
KWGS16	SBE19-L-10I-LISST-SEAPOINT	2015-02-04 00:01:00	1000	Bottle not optimally closed
KWGS17	SBE19-L-10I-LISST-SEAPOINT	2015-02-04 00:36:00	500	
KWGS18	SBE19-L-10I-LISST-SEAPOINT	2015-02-04 01:02:00	1000	
KWGS19	SBE19-L-10I-LISST-SEAPOINT	2015-02-04 01:33:50	1000	Problems with bottle
KWGS20	SBE19-L-10I-LISST-SEAPOINT	2015-02-04 02:00:00	1000	Problems with bottle
KWGS21	SBE19-L-10I-LISST-SEAPOINT	2015-02-04 02:27:00	1000	Problems with bottle
KWGS22	SBE19-L-10I-LISST-SEAPOINT	2015-02-04 02:56:20	1000	Problem fixed
KWGS23	SBE19-L-10I-LISST-SEAPOINT	2015-02-04 03:25:00	1000	
KWGS24	SBE19-L-10I-LISST-SEAPOINT	2015-02-04 03:54:40	1000	
KWGS25	SBE19-L-10I-LISST-SEAPOINT	2015-02-04 04:22:20	1000	
KWGS26	SBE19-L-10I-LISST-SEAPOINT	2015-02-04 04:48:10	1000	
KWGS27	SBE19-L-10I-LISST-SEAPOINT	2015-02-04 05:15:10	1000	
KWGS28	SBE19-L-10I-LISST-SEAPOINT	2015-02-04 05:42:40	1000	
KWGS29	SBE19-L-10I-LISST-SEAPOINT	2015-02-04 06:15:10	1000	
KWGS30	SBE19-L-10I-LISST-SEAPOINT	2015-02-04 06:37:50	750	

6.3. DGMR

MB measurements on HBBSSAB, Head 1.



Shadows:

Shadows preparation was perfect.

When the Shadows was deployed into the water, the 2 servers of the system shut down and the shadows gave an alert. Tests were performed, but the system continues to give alert signal.

Hypothesis on the occurrence of a “ground loop” and ground interferences have to be verified, partly on shore and partly off shore.

MB EM3002 (DGMR system):

- The repaired SVP probe between the 2 heads produces a big interference on the returning signal of Head 2. To be evaluate.
- A shift of 0.5m in height between the 2 heads recordings is encountered.
- The system has to be calibrated

7. REMARKS

The crew of the Belgica is acknowledged for the valuable and greatly appreciated cooperation.

8. DATA STORAGE

All raw multibeam data is stored by FPS Economy – Continental Shelf Department.
For any information contact Koen Degrendele

MB and Shadows data recorded by DGMR-MWDC system is stored in Afdopszeb MWU-REA.
Contact person: Afdopszeb MWU-REA, Sonia Papili and/or Yves Van Peteghem.

RV BELGICA 2015/07 - CRUISE REPORT

Subscribers:	Prof. Dr. Vera Van Lancker ^{1a} / Prof. Dr. Ann Vanreusel ² (Jelle Van Campenhout ²) Dr. Michael Fettweis ^{1a} ; Jan Haelters ^{1b} , Dr. Matthias Baeye ^{1a}
Institutes:	¹ Operational Directorate Natural Environment (OD Nature) ² Ghent University, Section Marine Biology (UGent-SMB)
Addresses:	^{1a} OD Nature-BRU: Gulledele 100, B-1200 Brussels ^{1b} OD Nature-OST: 3de en 23ste Linierregimentsplein, B-8400 Ostend ² UGent-SMB: Krijgslaan 281, B-9000 Ghent
Telephones:	+32(0)2 773 21 29 (VVL); +32(0)9 264 85 21 (AVR); +32(0)9 264 85 24 (JVC) +32(0)2 773 21 32 (MF); +32(0)59 24 20 55 (JH); +32(0)2 773 21 32 (MB)
E-mails:	v.vanlancker@mumm.ac.be , ann.vanreusel@ugent.be , jelle.vancampenhout@ugent.be , m.fettweis@mumm.ac.be , jan.haelters@mumm.ac.be , m.baeye@mumm.ac.be

Monitoring/Geology/Education: 16/03/2015 - 20/03/2015

1. Cruise details
2. List of participants
3. Scientific objectives
4. Operational course
5. Track plot
6. Measurements and sampling
7. Remarks
8. Data storage



Reference to this report:

Van Lancker, V., Van den Branden, R., Terseller Lillo, N., Vigin, L., Van Campenhout, J., Verhelst, P.J., De Smet, G., Hindryckx, K., Vanhaverbeke, W., and students party (2015). *Cruise report RV Belgica ST1507, 16-20/3/2015*. Royal Belgian Institute of Natural Sciences, Operational Directorate Natural Environment, 17p.

1. CRUISE DETAILS

1.	Cruise number	2015/07
2.	Date/time	16/03/2015: 10h40 17/03/2015: T&G Zeebrugge 17h45-19h15 19/03/2015: T&G Zeebrugge 10h30-11h15 20/03/2015: 12h30
3.	Chief Scientist Participating institutes	Prof. Dr. Vera Van Lancker OD Nature / UGent-SMB
4.	Area of interest	Belgian part of the North Sea

2. LIST OF PARTICIPANTS

Institute	Family name	Given name	Gender	16-17/03	17-19/03	19-20/03
RBINS-ODN	Van Lancker	Vera	F	x	x	x
RBINS-ODN	Van den Branden	Reinhilde	F	x		x
RBINS-ODN	Terseleer Lillo	Nathan	M	x	x	
RBINS-ODN	Vigin	Laurence	F		x	
UG-SMB	Van Campenhout	Jelle	M	x	x	x
UG-SMB	Verhelst	Pieter-Jan	M	x		
UG-SMB	De Smet	Guy	M			x
RBINS-ODN	Hindryckx	Kevin	M	T&G		
RBINS-ODN	Vanhaverbeke	Wim	M	T&G		
Students Oceans and Lakes ¹	Aruoriwo Egbo	Great	M	x		
	Aththanayaka	Thamarasi Sachithrangi	F	x		
	Basooma	Rose	F	x		
	De Luca ²	Laura Vittoria	F	x		
	De Wilde ²	Ellen	F	x		
	Green	Jenny	F		x	
	Heynderickx	Hanneloor	F		x	
	Hoegen	Marije	F		x	
	Iglesias González	Alba	F		x	
	Ingeniero ²	Riel Carlo	M	x		
	Islam ²	Md. Jakiul	M	x		
	Janssen ²	Tom	M	x		
	Labatt	Chepkemboi Kabon	F		x	
	Meeremans	Pieter	M	x		
	Mordi	Collins	M		x	
	Mori	Winiel Daniel	M		x	
	Rakotondrazafy	Sariaka Ravaka Andrianavalona	F		x	
	Rottiers ²	Thomas	M		x	
	Rodriguez Levy	Inti Ernesto	M		x	
	Runya	Robert Mzungu	M			x
Seghers	Stephie	F			x	
Slootmaekers	Bart	M			x	
Thilakarathne	Darshana Elle Pathirathnalage,	M			x	

		Nuwan				
	Tran	Thi Lan Anh	F			x
	Vergara	Gabriela	F			x
	Vlaminck	Ellen	F			x
				14	14	14

3. SCIENTIFIC OBJECTIVES

OD NATURE-VVL/UG-SMB - STUDENTS

Students will be trained in the framework of the MSc program Oceans and Lakes, course “In-situ and remote sensing tools in Aquatic Sciences”. They will learn to: (1) conduct most of the stages of a scientific expedition at sea (from sample collection to reporting); (2) apply a multidisciplinary approach in marine research; (3) get acquainted with different techniques of data and sample collection at sea; (4) collaborate in a scientific team including the vessel crew in order to achieve common objectives; and (5) gain insight in some important patterns of temporal variation and spatial gradients present on the Belgian Part of the North Sea (BPNS). Measurements and observations are performed in function of scientific projects (ZAGRI/MOZ4, *see below*).

OD NATURE-VVL-ZAGRI/MOZ4

ZAGRI is a continuous research program on the evaluation of the effects of the exploitation of non-living resources of the territorial sea and the continental shelf. MOZ4 focuses on the monitoring of hydrodynamics and sediment transport in relation to marine aggregate extraction in a far offshore zone. Overall aim is to increase process and system knowledge of this area, with a particular focus on the compliancy of the extraction activities with respect to the European Marine Strategy Framework Directive. More specifically changes in seafloor integrity and hydrographic conditions will be assessed. An important parameter is the bottom shear stress, with knowledge needed on both natural and anthropogenically-induced variability. Results will be used for the validation of mathematical models, necessary for impact quantification.

OD Nature-MOMO

The project "MOMO" is part of the general and permanent duties of monitoring and evaluation of the effects of all human activities on the marine ecosystem to which Belgium is committed following the OSPAR-convention (1992). The goal of the project is to study the cohesive sediments on the Belgian continental shelf 'BCS' using numerical models as well as by carrying out of measurements. Through this, data will be provided on the transport processes which are essential in order to answer questions on the composition, origin and residence of these sediments on the BCS, the alterations of sediment characteristics due to dredging and dumping operations, the effects of the natural variability, the impact on the marine ecosystem, the estimation of the net input of hazardous substances and the possibilities to decrease this impact as well as this in-put.

OD NATURE-JH - Monitoring of offshore windfarms: mooring of PODs

In the framework of the assessments of the effects of the construction and operation of offshore windfarms on small cetaceans, MUMM uses Passive Acoustic Monitoring Devices: porpoise detectors (C-PODs). A C-POD consists of a hydrophone, a processor, batteries and a digital timing and logging system, and has an autonomy of up to four months (www.chelonia.co.uk). Data obtained provide an indication of the (relative) abundance of harbor porpoises in the vicinity of the device, up to a distance of approximately 300m. Data obtained from one POD can give an indication of presence/absence of porpoises, and can be compared to data obtained from PODs moored at other locations. For mooring PODs at MOW1, a tripod is used; the POD is attached vertically to the central column. PODs moored at Gootebank, at the Oostdyck Bank and at other locations are attached to cardinal buoys.

OD NATURE-VVL

INDI67/SEACoP – Monitoring MSFD indicators on seafloor integrity and hydrographic conditions / Joint seabed mapping

Within Europe’s Marine Strategy Framework Directive (MSFD), progress towards Good Environmental Status (GES) needs monitoring in a most time- and cost-effective way. For the GES descriptors 6 and 7, on seafloor integrity and hydrographic conditions, respectively, new integrative indicators (i.e. bottom shear stress, turbidity and seabed/habitat type) need developing. To advance the mapping of seabed/habitat types, a Community of Practice (CoP) on seabed mapping will be established, investigating the main issues preventing joint mapping of the seabed.

Within SEACoP (CoP on 'Surveying for Environmental Assessments') the following objectives are targeted: a) estimation of the precision, sensitivities and repeatability of the acoustic devices to detect changes in seabed/habitat types; b) quantification of the external sources of variance in the acoustic signature, including the influence of near-bed and water column suspensions on backscatter data; c) definition of best practice in ground-truthing the acoustic signal, with emphasis on visual techniques; and d) innovation in collaborative seabed mapping.

UG-SMB: The importance of estuarine and coastal areas for the migration of fish and recovery of populations

Estuaries and coastal areas are subject to anthropogenic activities, as the largest harbours and economic activities are located along river banks and close to shore. Known to have a high habitat diversity, estuaries and coastal areas play a key role in the life cycle of many organisms, including diadromous and marine fish. As such, these areas can serve as transport routes, foraging or nursery areas. In order to conserve these areas in a cost-efficient and sustainable way, a better understanding of the ecosystem functions and services is needed. The Western Scheldt estuary and adjacent coastal area of Belgium are an important migration route and resident area for diadromous and marine fish. We selected Atlantic cod (*Gadus morhua*) and European eel (*Anguilla anguilla*) as two economically important indicator species for resp. marine and diadromous fish species, in order to assess the importance of estuarine and coastal areas as a key habitat for these species. The results of this study will be useful for management measures for the conservation and restoration of the eel and cod stocks.

OD Nature-JERICO

OD Nature's commitment to the European framework program JERICO (www.jerico-fp7.eu/about) is WP 10.6, viz. inter-comparison study between SPM concentrations derived from different platforms and sensors (i.e. surface buoys, benthic frames, satellites). The sensor used for this study is the Campbell Sc. OBS-5+, an optical backscatter point sensor measuring turbidity. It is stand-alone, equipped with an anti-biofouling wiper and installed in a stainless steel frame hanging at about 1.5 m under sea surface. It is a valuable tool towards better understanding SPM dynamics in the high-turbidity area in front of the Belgian coast. Continuous time-series of SPM concentration covers a wide range of hydro-meteo conditions. The AW buoy (51°22.42'N 3°7.05'E) is located at about 6 km off Zeebrugge harbor, in water depth of 10 m LAT and in the direct proximity of the benthic tripod frame with location MOW1.

OD NATURE-LN (AUMS)

The AUMS (Autonomous Underway Measurement System) project is inspired by the success of similar systems deployed on various ships of opportunity in the framework of the European Union FerryBox project (www.ferrybox.org). The instrumentation will greatly enhance the continuous oceanographic measurements made by RV Belgica by taking advantage of the significant technological improvements since the design of the existing (salinity, temperature, fluorescence) systems. In particular, many new parameters can now be measured continuously including important ecosystem parameters such as nitrate, ammonia, silicate, dissolved oxygen and CO₂, turbidity, alkalinity and phytoplankton pigments. In addition, the new equipment allows automatic acquisition and preservation of water samples, rendering RV Belgica operations significantly more efficient by reducing onboard human resources. Data will be available in near real-time via OD Nature's public web site and following quality control, from the Belgian Marine Data Centre.

ESA-MC (GNSS)

For the European Space Agency continuous GNSS (Global Navigation Satellite system) data is autonomously acquired in the maritime environment for performance evaluation under different conditions.

4. OPERATIONAL COURSE

All times are given in local time. All coordinates in WGS84. Throughout the campaign, measurements were performed with the AUMS system.

Sun rise: ~6h30; sun set: ~19h00; nautical twilight: ~5h20 (morning) ~20h15' (evening).

Monday 16/03/2015

High Tide Zeebrugge 09h52, 22h29
High Tide Oostende 09h25, 22h01
Low Tide Oostende 03h31, 16h01

08h30-09h30 Embarkation of instruments and personnel

10h40 Sail off from Zeebrugge

Transit to location **WZ** for acoustic receiver data recovery (UG-SMB)

11h07-11h23 Rhib transfer to WZ location (51° 22.57'; 3° 10.72') and data recovery

Transit to MOW1 for tripod replacement (OD Nature-MF)

12h15-13h30 Recovery and deployment of tripod at MOW1 (51-22. 640 N -- 003-10 .820E)
Recovery of OBS5 at AW buoy

Transit to location **S7** to deploy receiver (UG-SMB)

14h05-14h20 Rhib transfer to S7
Deployment acoustic receiver at location S7 (51° 23.98'; 3° 10.42')

14h35-14h50 Rhib transfer of OD-Nature scientist(s).

Transit to Oosthinder, Sector 4b

17h06-20h08 Reineck boxcoring and onboard slicing (1 cm slices), Sector 4b

20h15 Start centrifuge (2802388-2817807 l; 20h15-09h35) and start HM-ADCP
20h51 13-hrs cycle at **location 6** on Sector 4b. Vertical profiling of oceanographic parameters and water sampling.

Tuesday 17/03/2015

High Tide Oostende 10h32, 23h00
Low Tide Oostende 04h41, 17h09

-09h31 End of measurements

Transit to gully, west of Westhinder, for seabed sampling in area HBBSB

11h01-12h57 Biological sampling with Hamon grab (HBBSA and Area 4 in the barchan dune area)

13h28-14h34 Video frame barchan dune area (**Area 2**)

Transit to Zeebrugge

17h45-19h15 Touch & Go Zeebrugge
Disembarkation students group 1, OD Nature R. Van den Branden, UG-SMB PJ Verhelst
Disembarkation tripod
Embarkation beam trawl
Embarkation students group 2, OD Nature Laurence Vigin

Transit to Oosthinder sandbank, natural reefs area

21h47 Full-coverage multibeam over fisheries zone

Wednesday 18/03/2015

*High Tide Oostende 11h26, 23h48
Low Tide Oostende 05h45, 18h08*

-09h40 End of measurements

10h19-10h29 Beam trawling in sandy areas in fisheries zone
Sampling failed at first location, at foot of the eastern slope of the Westhinder, probably because of stones.

10h47-10h57 Beam trawling over Oosthinder sandbank.

Seastate did not allow taking Hamon grabs. Therefore, it was decided to continue multibeam echosounding.

11h48-15h15 Continuation multibeam echounding in fisheries zone.

15h32-17h21 Video frame gully in-between Oosthinder and Westhinder

Transit to Oosthinder, natural reefs area

17h58 Continuation full-coverage multibeam over fisheries zone

Thursday 19/03/2015

*High Tide Oostende 12h12
Low Tide Oostende 06h37, 18h56*

-06h51 End of measurements

Transit to Zeebrugge harbor

10h30-11h15 Touch & Go Zeebrugge
Disembarkation students group 2, OD Nature Laurence Vigin, Nathan Terseleer
Embarkation students group 3
Embarkation OD Nature, Reinhilde Van den Branden; UG-SMB Guy De Smet
Embarkation Reineck boxcorer

Transit to Oosthinder sandbank, HBBSA area

14h46 Arrival at point HB6 for Hamon grab sampling. However, waves were too high for sampling. It was decided to sail MBES lines until currents were sufficiently low for video imaging.

15h05-16h04 Multibeam continuation in gully, west of the Westhinder sandbank (HBBSA area).

- 16h17-18h00 Video frame gully, west of the Westhinder sandbank. Timing of the slack water window was later than expected from the tide tables. This might be due to persistent NNE wind conditions throughout the week.
- 18h53-19h45 Continuation multibeam recordings along a transect in gully East of Westhinder.
- 20h01-21h26 Reineck boxcoring Sector4c, Oosthinder sandbank (onboard slicing of subcores)
- 22h21- Hull-mounted ADCP profiling over a series of barchan dunes. Speed \pm 5 kt. Water sampling and vertical profiling of oceanographic parameters. Only 2 profiles were taken (at 23h and 23h43). At 23h32, the Seacat cable came off the drum and the frame fell to the bottom. Seacat was recovered manually; cable is damaged and instruments need inspection. ADCP measurements were continued. Filtration was now done on seawater from the seawater pump (@3.2 m), every 30'.

Friday 20/03/2015

*High Tide Zeebrugge 01h01, 13h25
 High Tide Oostende 00h31, 12h55
 Low Tide Oostende 07h22, 19h41
 New moon max 22/03*

08h *Evaluation of weather conditions for POD recovery. Waves are still too high for safe operations, so cancelled.*

-09h30 End of ADCP measurements

Transit to harbor

12h30 Zeebrugge Harbor

End of campaign

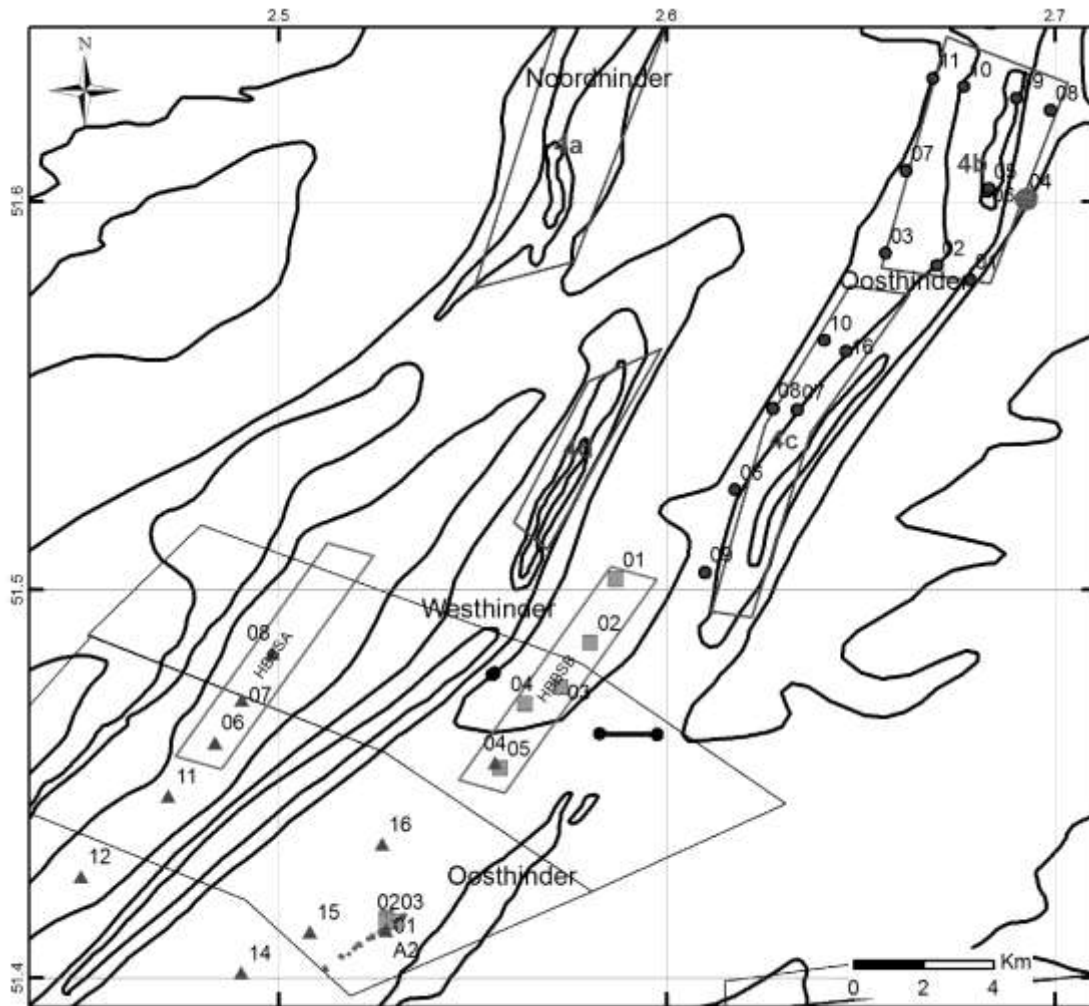


Figure 6.1.1. Overview of sampling and observations. Reineck boxcoring (dots) in Oosthinder Sector 4c (south) and Sector 4b (north); Hamon grabs (rectangles) in the gully between Westhinder and Oosthinder, as also Video imaging (triangles). Water sampling (small dots) during 13 hrs in Sector 4b, and along a transect in the southern part of the Oosthinder sandbank. Beam trawling (thick line). Fisheries management area is indicated, comprising two areas, HBBSA and HBBSB, where multibeam monitoring was conducted during ST1502.

Table 6.1.1. Timestamp, coordinates and depth of all sampling and observations (RC: Reineck core; SBE19 10L: water sampling and vertical profiling of oceanographic parameters; GPUMP: water sampling of surficial waters (@3.2m); BT: beam trawling). Coordinates are corrected for gear position relative to antenna.

id	gear	Timestamp	start/end	wg84_x_f	wg84_y_f	eadepth33
4B01	RC	2015-03-16 16:06:00		477706	5714373	-25,05
4B02	RC	2015-03-16 16:21:20		477114	5714775	-22,65
4B03	RC	2015-03-16 16:36:50		476196	5715129	-30,26
4B07	RC	2015-03-16 17:07:00		476569	5717492	-31,68
4B06	RC	2015-03-16 17:33:20		478014	5716909	-21,29
4B05	RC	2015-03-16 17:38:00		478044	5716976	-21,81
4B04	RC	2015-03-16 17:58:10		478678	5716676	-30,48
4B08	RC	2015-03-16 18:23:30		479150	5719203	-32,57
4B09	RC	2015-03-16 18:33:20		478544	5719554	-15,32
4B10	RC	2015-03-16 18:54:40		477617	5719900	-24,12
4B11	RC	2015-03-16 19:07:50		477069	5720145	-33,77
4B_LOC06	CENTRIFUGE	2015-03-16 19:15:10	start	477055	5720118	0,00

4B00	SBE19-L-10l	2015-03-16 19:51:30		478751	5716602	-35,01
4B01	SBE19-L-10l	2015-03-16 19:56:40		478761	5716627	-32,66
4B02	SBE19-L-10l	2015-03-16 20:30:50		478762	5716712	-32,81
4B03	SBE19-L-10l	2015-03-16 20:57:50		478753	5716722	-32,56
4B04	SBE19-L-10l	2015-03-16 21:27:40		478754	5716727	-32,58
4B05	SBE19-L-10l	2015-03-16 21:57:00		478745	5716740	-32,78
4B06	SBE19-L-10l	2015-03-16 22:28:30		478741	5716742	-32,34
4B07	SBE19-L-10l	2015-03-16 22:58:10		478773	5716730	-33,10
4B08	SBE19-L-10l	2015-03-16 23:28:00		478745	5716743	-32,01
4B09	SBE19-L-10l	2015-03-16 23:59:40		478701	5716752	-31,02
4B10	SBE19-L-10l	2015-03-17 00:28:30		478706	5716751	-31,34
4B11	SBE19-L-10l	2015-03-17 00:59:30		478701	5716747	-30,28
4B12	SBE19-L-10l	2015-03-17 01:28:10		478690	5716740	-30,30
4B13	SBE19-L-10l	2015-03-17 01:58:00		478695	5716739	-30,28
4B14	SBE19-L-10l	2015-03-17 02:30:00		478661	5716717	-29,81
4B15	SBE19-L-10l	2015-03-17 03:04:20		478658	5716680	-28,13
4B16	SBE19-L-10l	2015-03-17 03:28:40		478654	5716672	0,00
4B17	SBE19-L-10l	2015-03-17 03:58:10		478664	5716649	-29,21
4B18	SBE19-L-10l	2015-03-17 04:28:10		478672	5716643	-29,47
4B19	SBE19-L-10l	2015-03-17 05:00:20		478669	5716609	-30,74
4B20	SBE19-L-10l	2015-03-17 05:30:20		478682	5716597	-31,23
4B21	SBE19-L-10l	2015-03-17 05:59:20		478685	5716584	-31,52
4B22	SBE19-L-10l	2015-03-17 06:29:20		478690	5716581	-32,20
4B23	SBE19-L-10l	2015-03-17 07:00:30		478686	5716582	-31,95
4B24	SBE19-L-10l	2015-03-17 07:30:00		478682	5716587	-32,10
4B25	SBE19-L-10l	2015-03-17 07:59:30		478712	5716591	-33,12
4B26	SBE19-L-10l	2015-03-17 08:30:20		478728	5716721	-32,72
4B_LOC06	CENTRIFUGE	2015-03-17 08:35:00	end	478697	5716718	0,00
HBBSB01	Hamon grab	2015-03-17 10:01:20		471323	5705814	-40,34
HBBSB02	Hamon grab	2015-03-17 10:15:10		470860	5703994	-39,57
HBBSB03	Hamon grab	2015-03-17 10:31:00		470321	5702705	-40,09
HBBSB04	Hamon grab	2015-03-17 10:45:10		469688	5702249	-39,56
HBBSB05	Hamon grab	2015-03-17 11:01:40		469227	5700409	-34,55
Area4_01	Hamon grab	2015-03-17 11:42:30		467172	5696119	-34,28
Area4_02	Hamon grab	2015-03-17 11:49:50		467168	5696024	-29,16
Area4_03	Hamon grab	2015-03-17 11:57:50		467292	5696029	-33,78
Area2	Video frame	2015-03-17 12:28:00	start	467161	5695767	-34,50
Area2	Video frame	2015-03-17 13:34:00	end	467161	5695810	-33,22
BT01	BT	2015-03-18 09:25:40	start	469094	5703078	-31,50
BT01	BT	2015-03-18 09:26:20	end	469141	5703141	0,00
BT02	BT	2015-03-18 09:47:30	start	472049	5701356	-32,24
BT02	BT	2015-03-18 09:56:40	end	471019	5701382	-27,57
hb15	Video frame	2015-03-18 14:32:00	start	465797	5695734	-33,07
hb15	Video frame	2015-03-18 14:41:00	end	465621	5695773	0,00
hb14	Video frame	2015-03-18 14:54:00	start	464560	5694574	0,00
hb14	Video frame	2015-03-18 15:04:20	end	464580	5694406	0,00
hb16	Video frame	2015-03-18 15:38:00	start	467102	5698245	0,00

hb16	Video frame	2015-03-18 15:52:00	end	467054	5698131	0,00
hbbsb04	Video frame	2015-03-18 16:17:20	start	469137	5700566	0,00
hbbsb04	Video frame	2015-03-18 16:21:20	end	469163	5700499	0,00
hbbsa08	Video frame	2015-03-19 15:17:30	start	465178	5703735	-37,54
hbbsa08	Video frame	2015-03-19 15:24:30	end	465164	5703673	0,00
hbbsa07	Video frame	2015-03-19 15:41:10	start	464626	5702393	0,00
hbbsa07	Video frame	2015-03-19 15:47:50	end	464477	5702454	-38,37
hbbsa06	Video frame	2015-03-19 16:01:10	start	464126	5701171	0,00
hbbsa06	Video frame	2015-03-19 16:13:10	end	463828	5701097	-32,98
hb11	Video frame	2015-03-19 16:27:40	start	463289	5699647	-32,68
hb11	Video frame	2015-03-19 16:35:40	end	463202	5699540	0,00
hb12	Video frame	2015-03-19 16:53:40	start	461707	5697358	-33,34
hb12	Video frame	2015-03-19 17:01:40	end	461699	5697279	-32,68
4C09	RC	2015-03-19 19:01:30		472921	5706005	-27,19
4C06	RC	2015-03-19 19:22:40		473473	5708369	NA
4C08	RC	2015-03-19 19:43:50		474159	5710701	-31,80
4C07	RC	2015-03-19 19:55:20		474595	5710657	-24,20
4C16	RC	2015-03-19 20:12:20		475474	5712329	NA
4C10	RC	2015-03-19 20:26:10		475084	5712638	-31,28
HM-ADCP01	SBE19-L-10I	2015-03-19 22:00:40		467195	5695742	0,00
HM-ADCP02	SBE19-L-10I	2015-03-19 22:43:00		467155	5695874	0,00
HM-ADCP02	GPUMP	2015-03-19 23:07:50		467076	5695779	0,00
HM-ADCP03	GPUMP	2015-03-19 23:34:20		467500	5696202	0,00
HM-ADCP04	GPUMP	2015-03-20 00:04:00		467300	5696019	0,00
HM-ADCP05	GPUMP	2015-03-20 00:40:20		466687	5695344	0,00
HM-ADCP06	GPUMP	2015-03-20 01:04:00		467375	5696056	0,00
HM-ADCP07	GPUMP	2015-03-20 01:33:40		467465	5696188	0,00
HM-ADCP08	GPUMP	2015-03-20 02:14:50		466577	5695252	0,00
HM-ADCP09	GPUMP	2015-03-20 02:35:20		467457	5696138	0,00
HM-ADCP10	GPUMP	2015-03-20 03:04:30		467039	5695713	0,00
HM-ADCP11	GPUMP	2015-03-20 03:33:30		466379	5695013	0,00
HM-ADCP12	GPUMP	2015-03-20 04:04:20		466832	5695537	0,00
HM-ADCP13	GPUMP	2015-03-20 04:34:40		466904	5695624	0,00
HM-ADCP14	GPUMP	2015-03-20 05:06:00		466660	5695388	0,00
HM-ADCP15	GPUMP	2015-03-20 05:33:20		466050	5694720	0,00
HM-ADCP16	GPUMP	2015-03-20 06:03:30		466341	5695046	0,00
HM-ADCP17	GPUMP	2015-03-20 06:33:10		466071	5694649	0,00
HM-ADCP18	GPUMP	2015-03-20 07:03:30		466485	5695098	0,00
HM-ADCP19	GPUMP	2015-03-20 07:30:40		466913	5695564	0,00
HM-ADCP20	GPUMP	2015-03-20 07:59:10		466607	5695292	0,00

6.2. OD NATURE-MF (MOMO)

Recovering and deployment of tripods

The tripod deployed at MOW1 (51°N 21.586', 3°E 6.937') on 27/01/2015 has been recovered on Monday 16/03; another one was deployed at the same location.

Table 6.2.1: Position and time of tripod recuperation/ deployment.

ID	Instrument	Date (local time)	Lat_wgs84	Lon_wgs84
MOW1	Tripod recuperation+deployment	16/03/2015 12h15-13h30	51°N 21.640'	3°E 6.820'

6.3. OD NATURE-JH (MONIWIND)

Replacement of PODs at cardinal buoys at the following locations.

Table 6.3.1: Position and time of POD recuperation/ deployment

ID	Instrument	Date (local time)	Lat_wgs84	Lon_wgs84
Gootebank	POD replacement	Recovered during earlier campaign	51°N 26.953'	002°E 52.723'
Oostdyck W	POD replacement	Not possible because of adverse weather conditions	51°N 17.15'	002°E 26.32'

6.4. UG-SMB Importance of estuarine and coastal areas for the migration of fish and recovery of populations

Data recovery and deployment of acoustic receivers in the Belgian part of the North Sea. Only locations W Z and S7 were within reach for such operations.

Table 4.4.1. Coordinates of the receiver locations.

Name Buoy	Lat	Long	Lat DD.MMM	Long DD.MMM	Owner
W Z	51.376167	3.178666667	51° 22.57'	3° 10.72'	VLOOT
S 7	51.399667	3.173666667	51° 23.98'	3° 10.42'	VLOOT

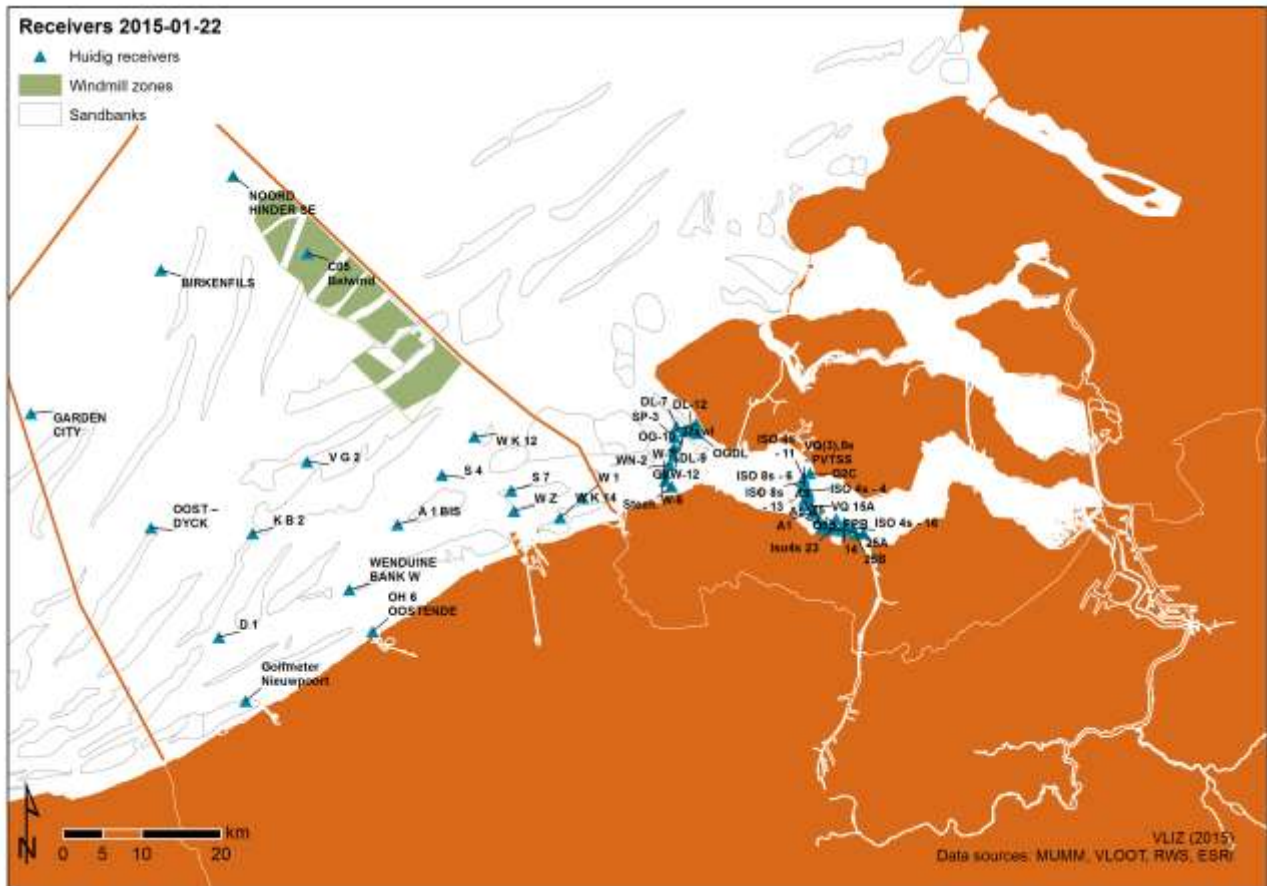


Figure 6.4.1. Location of the acoustic receivers.

6.5. OD NATURE MB Jericho

An OBS5+ was replaced mounted at AW buoy (51°22.42'N 3°7.05'E), located at about 6 km off Zeebrugge harbor, in a water depth of 10 m LAT and in the direct proximity of the benthic tripod frame with location MOW1.

7. REMARKS

Officers and crew are thanked warmly for the skillful handling of the operations and student assistance.

8. DATA STORAGE

OD NATURE

- Multibeam echosounding: on hard disk OD NATURE-BRU; copy will be provided to BMDC. Contact person: Vera Van Lancker (271 nm).
- ADCP: on hard disk MUMM-BRU; copy RBINS-ODN MDO. Contact person: Vera Van Lancker (48 nm)
- Water samples: Integration BMDC via MARCHEM (27 samples in Sector 4b; 21 in barchans dune area)
- Seabed samples; integration into BMDC. Contact person: Vera Van Lancker (Reineck cores: 11 in Sector 4b; 6 in Sector 4c; Hamon grab: 5 in HBBS area; 3 in Area 4, barchan dune area)
- SBE19 data: 29(x2) profiles. Contact RBINS-ODN MDO
- LISST data: 29(x2) profiles. Contact Vera Van Lancker
- Tripod data. Contact RBINS-ODN MDO

Annex – Pictures

Table A1: Hamon grabs gully Westhinder-Oosthinder

	
<p>HG01</p>	<p>HG01</p>
	
<p>HG01</p>	<p>HG02</p>
	
<p>HG02</p>	<p>HG02</p>
	
<p>HG02</p>	<p></p>



HG03



HG03



HG04



HG04



HG05



HG05



HG05



HG05



HG06



HG06



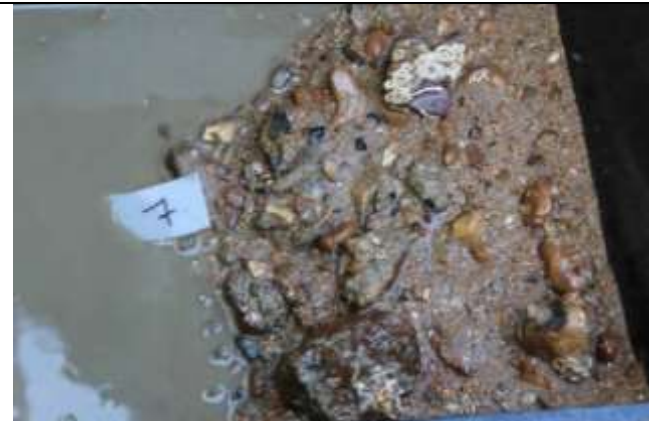
HG06



HG06



HG07



HG07



HG07



HG07



HG08



HG08



HG08

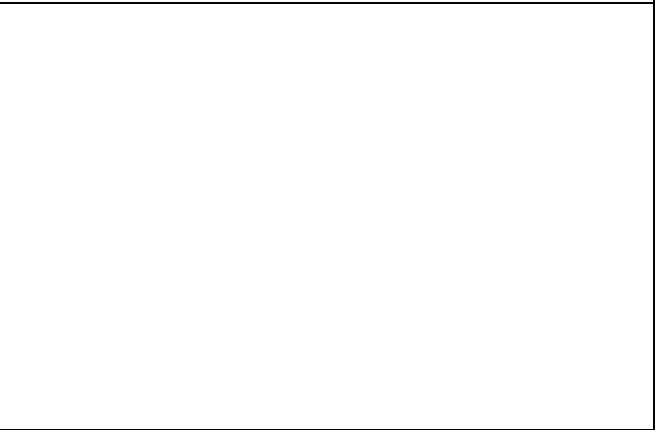


Table A2. Oosthinder gravel area. Centrifuge sample.



RV BELGICA CRUISE 2015/17 – CRUISE REPORT

Subscribers:	Koen Degrendele (KD) ¹ ; Dr. Lies De Mol (LDM) ¹ ; Sonia Papili (SP) ^{2a} ; Dr. Olga Lopera (OL) ^{2b} ; Yves Van Peteghem (YVP) ³ ; Dr. Vera Van Lancker (VVL) ^{4a} ; Dr. Michael Fettweis (MF) ^{4b}
Institutes:	¹ FPS Economy, SMEs, Self-employed and Energy - Continental Shelf Service ^{2a} Ministerie van Defensie - DGMR - Mine Counter Measure - AFDOPSZEB / MWU - REA ^{2b} Ministerie van Defensie - DGMR - Mine Counter Measure - Signal and Image Centre - CISS Department - Royal Military Academy ³ Ministerie van Defensie - COMOPSNAV - AFDOPSZEB-MWU/REA (Mine Warfare Unit/Rapid Environmental Assessment) - NMWMSC (Nato Mine Warfare Mission Support Centre) ⁴ Royal Belgian Institute of Natural Sciences - Operational Directorate Natural Environment
Addresses:	¹ Koning Albert II-laan 16, 1000 Brussel ^{2a} Graaf Jansdijk 1, 8380 Zeebrugge ^{2b} Renaissancelaan 30, 1000 Brussel ³ Graaf Jansdijk 1, 8380 Zeebrugge ^{4a} Gulledele 100, 1200 Brussel ^{4b} 3de en 23ste Linieregimentsplein, 8400 Oostende
Telephones:	+32(0)2 2778411 (KD); +32(0)2 2779578 (LDM); +32(0)50 558368 (SP); +32(0)2 7426666 (OL); +32(0)50 558368 (YVP); +32(0)2 7732129 (VVL); +32(0)2 7732132 (MF)
E-mails:	koen.degrendele@economie.fgov.be ; lies.demol@economie.fgov.be ; sonia.papili@mil.be ; olopera@elec.rma.ac.be ; yves.vanpeteghem@mil.be ; vera.vanlancker@naturalsciences.be ; m.fettweis@mumm.ac.be

Geology: 22/06/2015 – 26/06/2015

-
1. Cruise details
 2. List of participants
 3. Scientific objectives
 4. Operational course
 5. Track plot
 6. Measurements and sampling
 7. Remarks
 8. Data storage



1. CRUISE DETAILS

1.	Cruise number	2015/18
2.	Date/time	Zeebrugge TD: 22/06/2015 at 11h15 Zeebrugge TA: 22/06/2015 at 21h15 Zeebrugge TD: 23/06/2015 at 13h00 Zeebrugge TA: 26/06/2015 at 10h00
3.	Chief Scientist Participating institutes	Dr. Lies De Mol CSS/UG-RCMG, DGMR, MSC, OD Nature
4.	Area of interest	Belgian part of the North Sea

2. LIST OF PARTICIPANTS

INSTITUTE	NAME	22/06/2015	22/06 - 26/06/2015
CSS UG-RCMG	Lies DE MOL	X	X
	Koen DE RYCKER	X	X
	Vasileios CHADEMENOS	X	X
DGMR/MSC	Sonia PAPILI	X	X
	Olga LOPERA	X	X
	Christophe PEISKER	X	X
	Freddy PRIEM	X	X
	Gino DECEUNINK	X	X
	Ives REGENT	X	X
	Fred BLAISE	X	X
OD Nature	Vera VAN LANCKER	X	X
	Reinhilde VAN DEN BRANDEN	X	X
	Matthias BAEYE	X	X
	Maura RYCKEBUSCH	X	X
	Wim VANHAVERBEKE	X	
	Kevin HINDRYCKX	X	
Total number of participants:		16	14

3. SCIENTIFIC OBJECTIVES

CSS-KD

Implementation of the continuous investigation laid down in section 3, §2, subsection 3, of the law of June 13th 1969, concerning the exploration and exploitation of non-living resources on the Belgian Continental Shelf, and the concession decisions.

The follow up of the repercussions of the sand extraction on the stability of the sand banks and surrounding area in the exploitation zones, in order to formulate policies concerning the exploitation in the concession zones on a scientific base. The sediments of the Belgian continental shelf will be investigated in order to:

1. Establish the impact of sand extraction on the sand budget and seabed sediments.
2. Survey the sand winning sites to detect significant changes of the seabed sediments and the morphology of the seabed and sand banks in order to guarantee the availability of sand to extract in the future.

DGMR-SP

The actual bottom-types doctrinal is legacies from the 1950s mine warfare (NMW) and anti-submarine warfare (ASW). At that time sonar systems performed similarly, having more or less the same capabilities and specifications. Nowadays, there is a wide variety of sonar systems' types, displays etc. (side-scan, low-frequency wide band (LFWB), highfrequency wide-band (HFWB), Synthetic Aperture Sonar (SAS), as well as much refined forward looking sonar systems). These different sonar types can and do perform very differently against the same target in the same water and bottom conditions. The main purpose of the current work is to classify the sea bottom considering a wide spectrum of parameters. The different parameters will be combined in relation to their influence on backscatter and reverberation response on different instruments. In this way, the available instruments will be properly tuned to the sea-floor. As last result, the sensors will be more reliable on defining the bottom type, even in unknown region. Beside the contribution of the sea bottom, the volume reverberation caused by the backscattering from the water column, impacts as well the sonar image (Lurton, 2002). To estimate this component, also water column properties will be analyzed.

DGMR-OL

This project aims to determine the limits for the detection and classification of seabed objects, in particular mines. In the frame of the Long Term Critical Requirement 21 (Fast detection and neutralization of a minefield) and following the development of autonomous underwater vehicles (AUV), it is necessary to develop classification procedures. This work will focus on the study of synthetic aperture sonar (SAS) images to validate SAS image processing algorithms which will be developed. Data (high resolution SAS images) will be collected using the available equipment (modern minehunters and sensors from the Mine Warfare Data Center) during the measurement campaigns which will be planned in collaboration with the projects of Sonia PAPILI (progr. 17) and Eric MERSCH (progr. 19).

MSC-YVP

Collection of bathymetric seabed information of Belgian EEZ with the use of EM 3002D Multibeam Echo Sounder, SHADOWS Synthetic Aperture Sonar and SEAQUEST Gradiometer in areas with priority 1 for the NMW MSC. Meanwhile fine tuning of software and procurement of procedures for use of the systems for upgrade of the Mine Warfare Data Center (MWDC). Most of our clients, Belgian and Dutch minehunters as our NATO partners come to exercise into these areas. Therefore our intention is to procure them a picture of all the possible items that they can encounter within these waters. With this project we are going to try to have as much as possible information about these areas. The information is also used to produce Additional Military Layers (AML's).

OD Nature-VVL (ZAGRI/MOZ4)

ZAGRI is a continuous research program on the evaluation of the effects of the exploitation of non-living resources of the territorial sea and the continental shelf. MOZ4 research focuses on the hydrodynamics and sediment transport in a marine aggregate extraction zone, far offshore, and its impact on an adjacent Habitat Directive Area. Overall aim is to increase process and system knowledge of both areas, with particular focus on the compliancy of the extraction activities with respect to the European Marine Strategy Framework Directive. More specifically changes in seafloor integrity and hydrographic conditions need assessment.

OD Nature-VVL (INDI67/MONIT.BE)

Within Europe's Marine Strategy Framework Directive (MSFD), progress towards Good Environmental Status (GES) needs monitoring in a most time- and cost-effective way. For the GES descriptors 6 and 7, on seafloor integrity and hydrographic conditions, respectively, new integrative indicators (i.e. bottom shear stress, turbidity and seabed/habitat type) need developing. To advance the mapping of seabed/habitat types, a Community of Practice (CoP) on seabed mapping will be established, investigating the main issues preventing joint mapping of the seabed. Within SEACoP (CoP on 'Surveying for Environmental Assessments') the following objectives are targeted: a) estimation of the precision, sensitivities and repeatability of the acoustic devices to detect changes in seabed/habitat types; b) quantification of the external sources of variance in the acoustic signature, including the influence of near-bed and water column suspensions on backscatter data; c) definition of best practice in ground-truthing the acoustic signal, with emphasis on visual techniques; and d) innovation in collaborative seabed mapping.

OD Nature-MF (MOMO)

The project "MOMO" is part of the general and permanent duties of monitoring and evaluation of the effects of all human activities on the marine ecosystem to which Belgium is committed following the OSPAR-convention (1992).

The goal of the project is to study the cohesive sediments on the Belgian continental shelf 'BCS' using numerical models as well as by carrying out of measurements. Through this, data will be provided on the transport processes which are essential in order to answer questions on the composition, origin and residence of these sediments on the BCS, the alterations of sediment characteristics due to dredging and dumping operations, the effects of the natural variability, the impact on the marine ecosystem, the estimation of the net input of hazardous substances and the possibilities to decrease this impact as well as this in-put.

OD NATURE-MF (AUMS)

The AUMS (Autonomous Underway Measurement System) project is inspired by the success of similar systems deployed on various ships of opportunity in the framework of the European Union FerryBox project (www.ferrybox.org). The instrumentation will greatly enhance the continuous oceanographic measurements made by RV Belgica by taking advantage of the significant technological improvements since the design of the existing (salinity, temperature, fluorescence) systems. In particular, many new parameters can now be measured continuously including important ecosystem parameters such as nitrate, ammonia, silicate, dissolved oxygen and CO₂, turbidity, alkalinity and phytoplankton pigments. In addition, the new equipment allows automatic acquisition and preservation of water samples, rendering RV Belgica operations significantly more efficient by reducing onboard human resources. Data will be available in near real-time via OD NATURE's public web site and following quality control, from the Belgian Marine Data Centre.

ESA-MC (GNSS)

For the European Space Agency continuous GNSS (Global Navigation Satellite system) data is autonomously acquired in the maritime environment for performance evaluation under different conditions.

RBINS & OD Nature-Detection of bats

New equipment is installed on RV Belgica to detect the presence of bats at sea with a focus on the effects of windmill farms on the behavior, trekking routes of these animals.

4. OPERATIONAL COURSE

All times are given in local time. All coordinates in WGS84.

Throughout the campaign, measurements are made with the AUMS system.

Monday 22/06/2015

09h00-10h30	Embarkation of instruments and personnel
11h15	Departure Zeebrugge + Transit to Sierra Ventana (New QR area)
12h00	Measurements cancelled due to bad weather
17h00	Transit to Wandelaar
17h30-19h00	Test multibeam system DGMR for shift error due to GPS (DGMR-SP)
19h00	Transit to MOW1
19h30-20h15	Recuperation of tripod at MOW1 (OD Nature-MF)
20h15	Transit to Zeebrugge
21h15	Arrival to Zeebrugge – Replacement tripod/shadows and disembarkation of MOMO team In harbor due to bad weather

Tuesday 23/06/2015

13h00	Departure Zeebrugge + Transit to Kwintebank
15h30-23h00	Seismic investigations in combination with multibeam on the Kwintebank (CSS-KD)
23h00	Transit to Westhinder shell hash area

Wednesday 24/06/2015

01h00-05h00 Seismic investigations in combination with multibeam in the Westhinder shell hash area (CSS-KD)
05h00-08h00 Multibeam recordings in the Westhinder-Oosthinder gully (OD Nature-VVL)
08h00-10h15 Hamon grabs Westhinder-Oosthinder gully and Westhinder shell hash area (OD Nature-VVL)
10h15-14h15 Video recordings in the Westhinder shell hash area (OD Nature-VVL)
14h15-17h00 Sting measurements in the Westhinder shell hash area (DGMR-SP)
17h00-20h00 Multibeam recordings in the Westhinder shell hash area (DGMR-SP)
20h00 Transit to Kwintebank
22h30-24h00 Seismic investigations in combination with multibeam on the Kwintebank (CSS-KD)

Thursday 25/06/2015

00h00-07h30 Seismic investigations in combination with multibeam on the Kwintebank (CSS-KD)
07h30 Transit to barchan dune area
08h30-11h00 Hamon grabs in the barchan dune area (OD Nature-VVL)
08h45-11h30 REMUS recordings in the barchan dune area (DGMR-SP)
11h30-14h30 Video recordings in the barchan dune area (OD Nature-VVL/DGMR-SP)
14h30 Transit to KWGS area
15h30-18h30 Shadows recordings in the KWGS area (DGMR-OL)
19h00 Transit to Kwintebank
19h30-22h30 Seismic investigations in combination with multibeam on the Kwintebank (CSS-KD)
22h30 Transit to Thorntonbank
23h30-24h00 Seismic investigations in combination with multibeam on the Thorntonbank (CSS-KD)

Friday 26/06/2015

00h00-07h30 Seismic investigations in combination with multibeam on the Thorntonbank (CSS-KD)
07h30 Transit to Zeebrugge
10h00 Arrival to Zeebrugge

- End of campaign 2015/17 -

5. TRACK PLOT

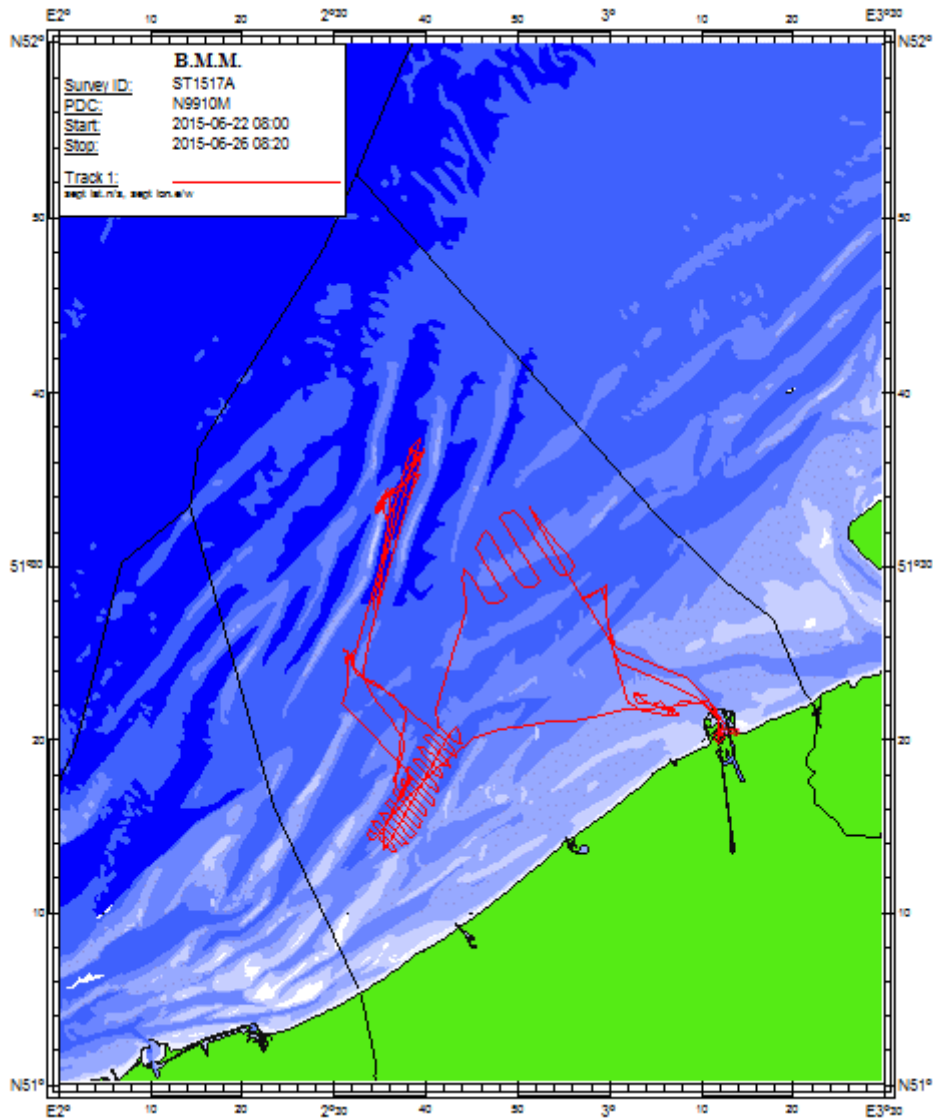


Figure 1: Track plot of campaign 2015/17

6. MEASUREMENTS AND SAMPLING

6.1. CSS-KD

Cartography and 3D modeling of the sand reserves inside the extraction areas (collaboration with UGent-RCMG): seismic profiles in extraction areas 1 (Thorntonbank), 2 (Flemish Banks) and 4 (Hinderbanks). Simultaneous EM3002D multibeam measurements were performed.

Equipment and seismic characteristics

Two seismic sources were used during the campaign: the Centipede and the SIG sparker (Table 1).

Table 1: Characteristics of the seismic equipment used during the survey

Equipment	Frequency range	Vertical resolution	Penetration
Centipede sparker	1.1 – 1.2 kHz	> 35 cm	Sandy seafloor, up to 50 m
SIG sparker	800 – 900 Hz	> 50 cm	Sandy seafloor, up to 100 m

Table 2: Settings of the seismic equipment during the survey

Source	SIG or CENTIPEDE
Energy	400 J
Offset source vessel	30 m
Receiver	SIG single channel streamer 75 m
Acquisition	Krohnhite 3750
Analogue bandpass filter	250-6000 Hz
Elics	
Sampling frequency	10 kHz
Shooting interval	750 ms
Record length	300 ms

Recorded network

The final recorded seismic network is about 180 km in total length. Due to the bad weather at the beginning of the cruise the data quality of the lines obtained during the first night (23-24/06) is not optimal. However the data quality of the next two nights are very high with a very good resolution. The data covers mainly the Kwintebank (Figure 2) as well as a few lines in the Westhinder shell hash area (Figure 3) and on the Thorntonbank (Figure 4).

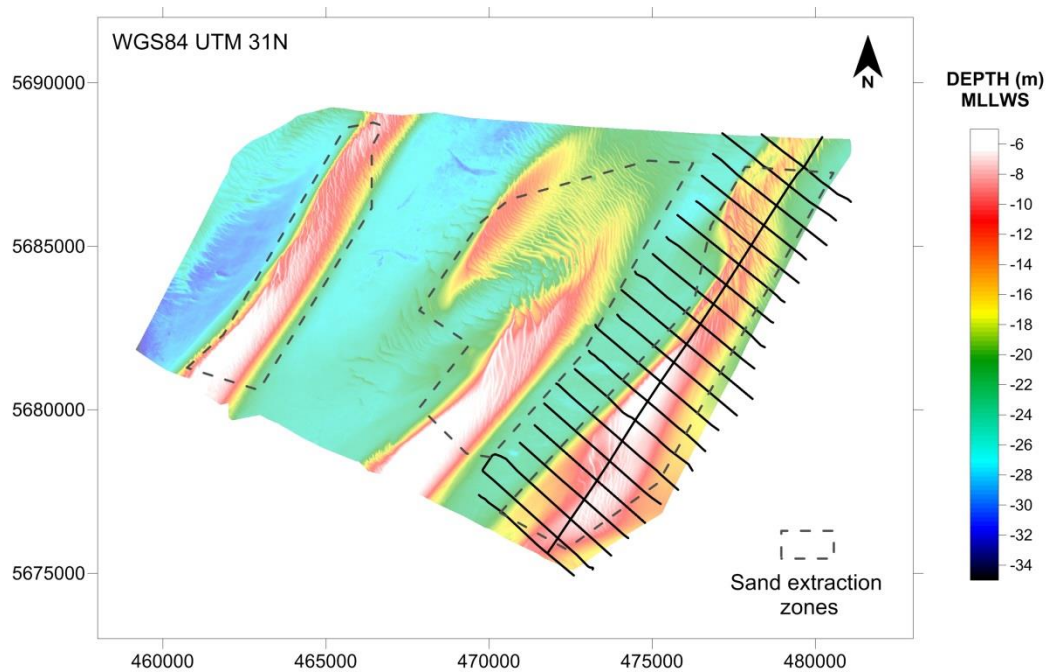


Figure 2: Seismic network on the Kwintebank

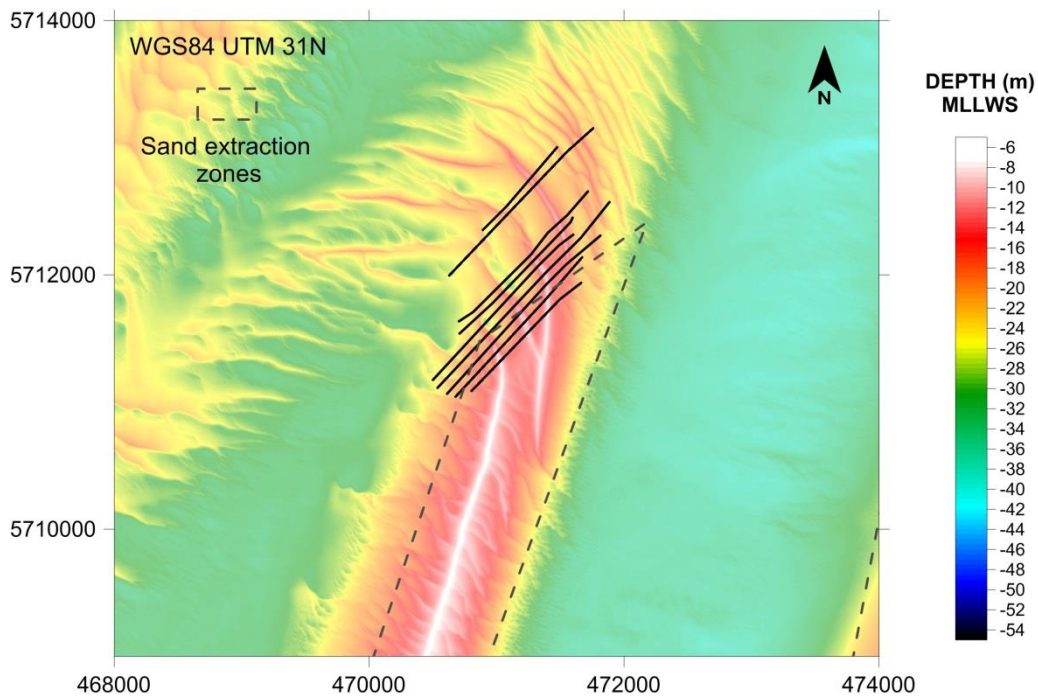


Figure 3: Seismic network in the Westhinder shell hash area

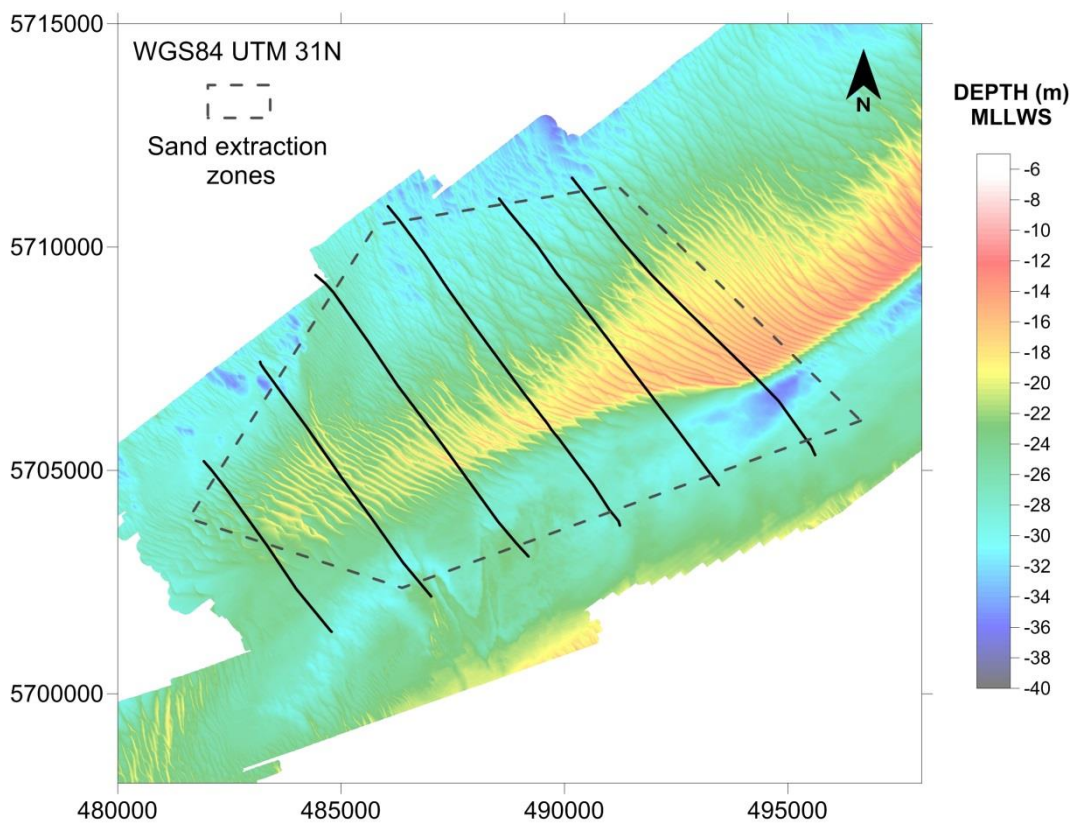


Figure 4: Seismic network on the Thorntonbank

Table 3: Details on the seismic survey lines

Date	Seastate	Source	Energy (J)	Offset (m)			
23-24/06	3-4	SIG 75 m	400	30			
Time (UTC)	Shot nr	Latitude	Longitude	Water depth (m)	Velocity (knots)	Heading (degrees)	Remarks
14:12	0	51°14'49.53	2°33'56.54				SOL FB_L03
14:40	1640	51°14'48.26	2°33'58.85				EOL FB_L03

14:47	0	51°13'36.55	2°36'56.81				SOL FB_L04
15:46	4768	51°15'28.04	2°34'30.91				EOL FB_L04
15:47	0	51°15'27.52	2°34'32.23	27	4.3	305	SOL FB_L05
16:22	2805	51°13'48.03	2°37'32.26	19	4.3	142	EOL FB_L05
16:32	0	51°14'09.00	2°35'04.50	19	4.3	305	SOL FB_L06
17:20	3668	51°15'57.14	2°37'45.18	26	4	142	EOL FB_L06
17:25	0	51°52'55.00	2°35'30.20	28	4	305	SOL FB_L07
17:59	2604	51°14'20.00	2°38'39.20	19	4	142	EOL FB_L07
18:13	0	51°14'42.00	2°38'43.22	18	3.2	305	SOL FB_L08
18:59	3722	51°16'22.00	2°35'34.19	27	3.7	305	EOL FB_L08
19:08	0	51°16'39.00	2°36'03.10	27	3.5	133	SOL FB_L09
19:48	3208	51°14'54.38	2°39'16.46	17	3.5	133	EOL FB_L09
19:58	0	51°15'15.47	2°39'31.26	18	3.2	330	SOL FB_L10
20:40	3274	51°16'54.67	2°36'27.14				EOL FB_L10
23:20	0	51°33'49.30	2°35'26.27	23	4.2	213	SOL HB_L01
23:30	775	51°33'14.30	2°34'21.28	30	4.2	213	EOL HB_L01
23:40	0	51°31'16.30	2°34'42.14	24	4.2	44	SOL HB_L02
23:57	1345	51°33'46.24	2°35'25.40	23	4	44	EOL HB_L02
00:14	0	51°33'38.89	2°35'20.10	18	4	227	SOL HB_L03
00:24	796	51°33'00.27	2°34'28.10	28	4	227	EOL HB_L03
00:27	0	51°33'02.17	2°34'30.20	24	4	46	SOL HB_L04
00:56	2281	51°33'49.22	2°35'42.50	24	4	46	EOL HB_L04
01:00	0	51°33'38.25	2°35'32.10	24	4	223	SOL HB_L05
01:11	861	51°32'57.38	2°34'33.40	22	4	223	EOL HB_L05
01:16	0	51°32'59.20	2°34'39.07	20	4	45	SOL HB_L06
01:36	1653	51°33'34.54	2°35'30.56	24	4	45	EOL HB_L06
01:40	0	51°33'26.75	2°35'23.80	18	4	227	SOL HB_L07
01:48	664	51°32'59.59	2°34'39.20	21	4	227	EOL HB_L07
02:01	0	51°33'31.62	2°34'38.47	27	4	41	SOL HB_L08
02:19	1442	51°34'07.82	2°35'36.70	24	4	41	EOL HB_L08
02:26	0	51°34'00.28	2°35'14.45	26	4	219	SOL HB_L09
02:33	535	51°33'40.16	2°34'45.68	27	4	219	EOL HB_L09
Date	Seastate	Source	Energy (J)	Offset (m)			
24-25/06	3	SIG 75 m	400	30			
Time (UTC)	Shot nr	Latitude	Longitude	Water depth (m)	Velocity (knots)	Heading (degrees)	Remarks
20:50	0	51°17'11.61	2°36'51.60	27	4	128	SOL FB_11
21:30	3152	51°15'33.74	2°39'57.96	17	4	128	EOL FB_11
21:38	0	51°15'56.56	2°40'10.08	20	3.6	302	SOL FB_12
22:13	2786	51°17'40.50	2°37'01.81	23	3.6	302	EOL FB_12
22:21	0	51°17'47.94	2°37'36.45	26	3.1	135	SOL FB_13
22:59	3089	51°16'08.36	2°40'49.61	17	3.3	135	EOL FB_13
23:07	0	51°16'26.90	2°41'04.67	18	3.7	309	SOL FB_14
23:41	2750	51°18'15.81	2°37'38.72	22	3.7	309	EOL FB_14
23:48	0	51°18'30.98	2°38'02.75	24	4	137	SOL FB_15
00:33	3384	51°16'56.59	2°41'13.74	22	4	137	EOL FB_15
00:36	0	51°17'18.84	2°41'20.76	22	4	309	SOL FB_16
01:08	2502	51°18'51.20	2°38'29.93	25	4	309	EOL FB_16
01:12	0	51°19'05.24	2°38'53.13	26	3.9	130	SOL FB_17

01:47	2629	51°17'41.86	2°41'41.21	22	4	130	EOL_FB_17
02:01	0	51°18'02.23	2°41'57.07	23	4.1	312	SOL_FB_18
02:26	2110	51°19'28.30	2°39'06.09	28	4	312	EOL_FB_18
02:37	0	51°19'44.02	2°39'31.38	29	4	119	SOL_FB_19
03:07	2363	51°18'21.32	2°42'23.32	23	4	119	EOL_FB_19
03:16	0	51°18'42.39	2°42'35.30	23	4	314	SOL_FB_20
03:50	2623	51°20'10.00	2°39'44.28	28	4	314	EOL_FB_20
03:57	0	51°20'29.78	2°40'01.26	27	4	124	SOL_FB_21
04:27	2419	51°18'58.27	2°43'07.41	24	4	124	EOL_FB_21
04:35	0	51°19'23.97	2°43'16.47	25	4	306	SOL_FB_22
05:20	3582	51°20'50.57	2°40'12.93	27	4	306	EOL_FB_22
Date	Seastate	Source	Energy (J)	Offset (m)			
24-25/06	2	CENTIPEED	400	30			
Time (UTC)	Shot nr	Latitude	Longitude	Water depth (m)	Velocity (knots)	Heading (degrees)	Remarks
17:49	0	51°15'05.20	2°37'02.35	13	4	34	SOL_FB_25
19:26	7852	51°20'48.23	2°43'00.87	22	4	34	EOL_FB_25
19:53	0	51°19'42.52	2°43'40.02	26	4	307	SOL_FB_23
20:23	2452	51°20'49.42	2°41'16.10	27	4	307	EOL_FB_23
21:42	0	51°29'50.48	2°44'26.62	32	3.8	133	SOL_TB_01
22:21	3122	51°27'49.08	2°46'50.43				EOL_TB_01
22:40	0	51°28'16.12	2°48'42.20	26	3.1	329	SOL_TB_02
23:29	3994	51°31'05.55	2°45'28.74	32	4	329	EOL_TB_02
23:50	0	51°32'06.50	2°46'33.24	30	3	128	SOL_TB_03
00:56	5305	51°28'43.31	2°50'42.67	26	4	139	EOL_TB_03
01:19	0	51°29'06.61	2°52'25.33	28	3	326	SOL_TB_04
02:32	5780	51°47'57.10	2°48'00.71	32	4	326	EOL_TB_04
02:55	0	51°33'04.53	2°50'05.39	32	4	140	SOL_TB_05
03:53	4672	51°29'33.31	2°54'23.06	29	4	140	EOL_TB_05
04:18	0	51°29'57.63	2°56'10.22	28	4	326	SOL_TB_06
05:26	5446	51°33'19.54	2°51'25.01	33	4	326	EOL_TB_06

6.2. DGMR-SP

Table 4: List of Hamon grabs in the Westhinder shell hash area

ID	Date and time	Latitude	Longitude	Depth (33 kHz)
WHS01	2015-06-24 07:35:09	51.56605657	2.587687433	-26.45
WHS02	2015-06-24 07:49:17	51.56245042	2.582911167	-21.65
WHS03	2015-06-24 08:07:01	51.55732485	2.582363133	-17.77



WHS01



WHS02



WHS03



WHS03

Figure 5: Pictures of Hamon grabs in the Westhinder shell hash area

Table 5: List of video recordings in the Westhinder shell hash area

ID	Start			End		
	Date and time	Latitude	Longitude	Date and time	Latitude	Longitude
WHS03	2015-06-24 07:35:09	51.5571977	2.581333167	2015-06-24 08:47:00	51.55785472	2.583029933
WHS02	2015-06-24 07:49:17	51.56251933	2.582993317	2015-06-24 09:07:48	51.56219698	2.582592017

Six sting measurements were performed in the Westhinder shell hash area (Table 6).

Table 6: List of sting measurements

ID	Date and time	Latitude	Longitude	Depth (33 kHz)	Remarks
WHS6	2015-06-24 13:28:11	51.5672732	2.5879036	-24.50	2 nd attempt
WHS1	2015-06-24 13:39:32	51.56639265	2.586701967	-26.04	2 nd attempt
WHS3	2015-06-24 13:57:48	51.56399778	2.583701833	-25.43	
WHS2	2015-06-24 14:15:09	51.56242243	2.582170617	-22.44	
WHS4	2015-06-24 14:36:28	51.5600895	2.58309275	-24.07	
WHS5	2015-06-24 14:53:00	51.55764758	2.581539917	-22.15	

REMUS recordings were performed in the barchan dune area in the Westhinder-Oosthinder gully (Table 7).

Table 7: Coordinates of the REMUS recordings area

ID	Latitude	Longitude
A1	51°24.693'	2°31.628'
A2	51°24.779'	2°31.701'
A3	51°24.744'	2°31.476'

A4	51°24.829'	2°31.549'
----	------------	-----------

Table 8: List of video recordings in the barchan dune area

ID	Start			End		
	Date and time	Latitude	Longitude	Date and time	Latitude	Longitude
REMUS contact	2015-06-25 12:06:33	51.41180852	2.52797165	2015-06-25 12:27:17	51.41173375	2.52785645

6.3. DGMR-OL

Several lines were recorded over KWGS using the SHADOWS and MB system. The generated map can be seen in Figure 6 and 7. Several details can be observed, including different zones in the seabed and trawling lines.

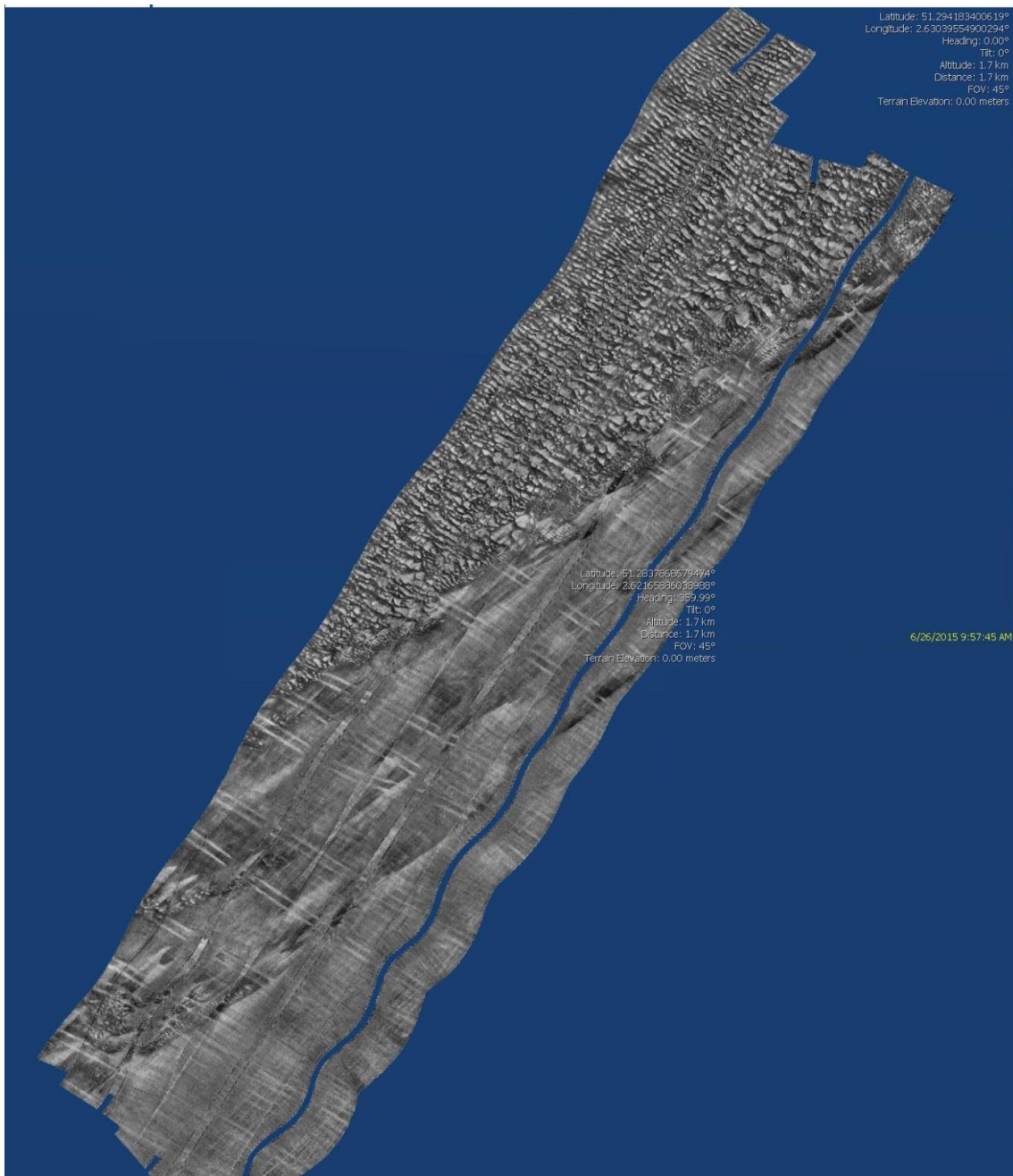


Figure 6: SHADOWS mapping of area KWGS

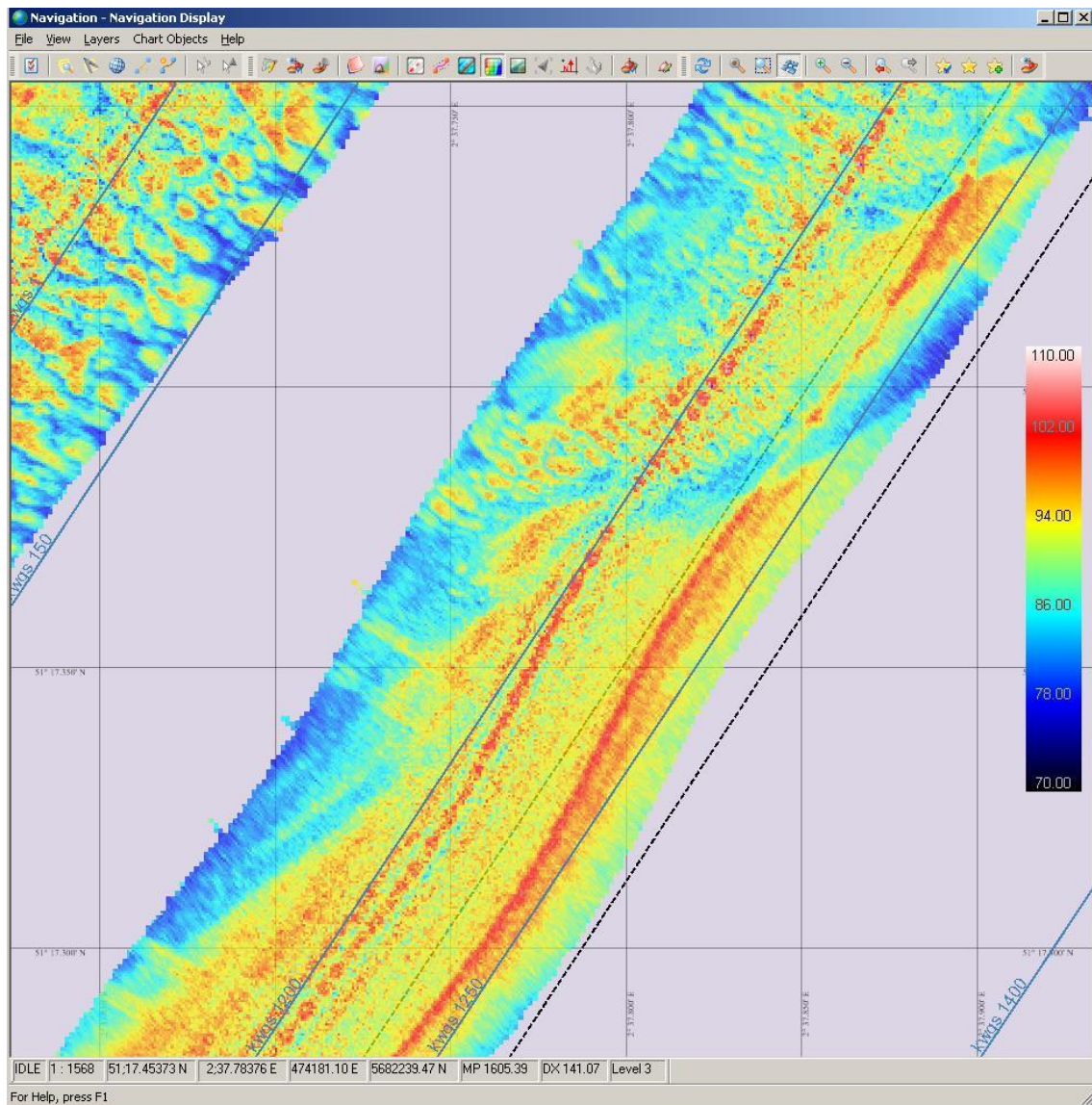


Figure 7: MB backscatter mapping of area KWGS

6.4. MSC-YVP

The multibeam recordings were cancelled due to bad weather.

6.5. OD Nature-VVL

Hydrodynamic and sediment transport related measurements and observations in marine aggregate concession zone 4, Hinder Banks region and adjacent Habitat Directive Area 'Flemish Banks'.

Measurements and observations:

- a. **Multibeam bathymetry and backscatter:**
 - Long tracklines parallel to the axis of the Westhinder-Oosthinder gully
- b. **Seabed sampling**
 - **Hamon Grab**, for sampling of biological and sediment data in patches of coarse sands and gravel, Westhinder-Oosthinder gully, and in and around barchan dune area, west of the southern part of Oosthinder sandbank.
 - **Sting measurements** at selected locations Westhinder-Oosthinder gully

- c. **Video frame. High resolution imagery of gravel rich areas.**
- Westhinder-Oosthinder gully near aggregate Sector 4b
 - Westhinder-Oosthinder gully in and around barchan dune area, west of the southern part of Oosthinder sandbank.
- d. **Centrifuge sampling**
- Westhinder-Oosthinder gully near aggregate Sector 4b (2015-06-24 07:15 to 2015-06-24 19:35; discharge 0.2999 l s^{-1}).
 - Westhinder-Oosthinder gully in and around barchan dune area, west of the southern part of Oosthinder sandbank (2015-06-25 07:08 to 2015-06-24 19:35; discharge 0.2999 l s^{-1}).
- e. **AUMS registrations (continuous)**

Table 9: NE-SW Tracklines along the axis of the Westhinder-Oosthinder gully ($\pm 10 \text{ nm}$ each)

ID	Start		End	
	Latitude	Longitude	Latitude	Longitude
1	51° 36.899' N	2° 39.767' E	51° 27.309' N	2° 34.537' E
2	51° 37.187' N	2° 39.240' E	51° 27.596' N	2° 34.010' E
3	51° 37.474' N	2° 38.713' E	51° 27.883' N	2° 33.483' E

Table 10: List of Hamon grabs near Sector 4B (in gully west of Oosthinder sandbank)

ID	Biological sample nr	Date and time	Latitude	Longitude	Depth (33 kHz)
4B1	1	2015-06-24 06:16:14	51.60843557	2.6602801	-32.57
4B2	2	2015-06-24 06:28:00	51.61012955	2.648860167	-40.58
4B3	3	2015-06-24 06:42:24	51.61329828	2.638150533	-42.81
4B4	4	2015-06-24 07:05:40	51.58940938	2.648775233	-36.65

Table 11: List of video recordings near Sector 4B (in gully west of Oosthinder sandbank)

ID	Start			End		
	Date and time	Latitude	Longitude	Date and time	Latitude	Longitude
4B09	2015-06-24 09:31:23	51.57380232	2.617141217	2015-06-24 09:34:49	51.5735845	2.617553967
4B08	2015-06-24 09:47:35	51.57033082	2.62728475	2015-06-24 09:54:52	51.57010548	2.626838433
4B07	2015-06-24 10:13:00	51.56615182	2.6360087	2015-06-24 10:20:40	51.5664388	2.636766567
4B04	2015-06-24 10:52:36	51.58936348	2.649444333	2015-06-24 10:59:00	51.58903122	2.649026483
4B05	2015-06-24 11:15:32	51.59147568	2.638512167	2015-06-24 11:20:20	51.59101638	2.639121
4B06	2015-06-24 11:40:20	51.59382833	2.628854117	2015-06-24 11:48:00	51.5939963	2.628571067
4B01	2015-06-24 12:06:00	51.60836577	2.65971705	2015-06-24 12:18:55	51.60803845	2.659661867

Table 12: List of Sting measurements near Sector 4B (in gully west of Oosthinder sandbank)

ID	Date and time	Latitude	Longitude	Depth (33 kHz)	Remarks
4B1	2015-06-24 12:17:03	51.60798288	2.659635667	-32.09	
4B5	2015-06-24 12:42:43	51.59149703	2.638912717	-38.73	2 nd attempt
4B9	2015-06-24 12:57:08	51.57328618	2.617560317	-37.41	

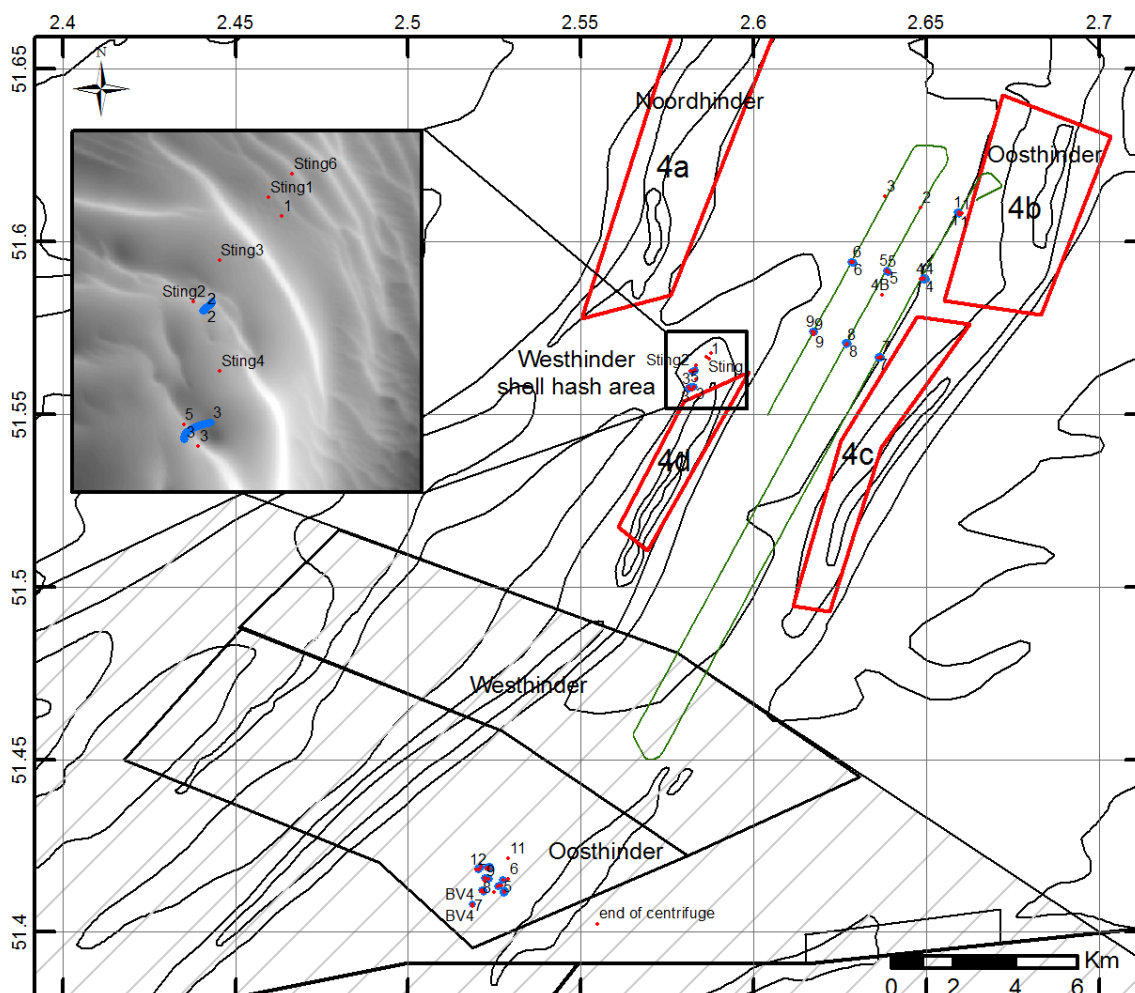


Figure 8: Overview of the samples and observations in the Hinder Banks area: Hamon grabs and Sting penetration tests (red); video imaging (blue) and multibeam echosounding (green). Insert: detailed view of the Westhinder shell hash area. Further indicated: marine aggregate extraction sectors (4a to 4d; red); Habitat Directive Area (hashed) and fisheries management areas (black polygons).

Table 13: List of Hamon grabs in the barchan dune area, west of southern Oosthinder sandbank

ID	Biological sample nr	Date and time	Latitude	Longitude	Depth (33 kHz)
BV5	5	2015-06-25 06:30:55	51.41359838	2.52745285	-35.42
BV6	6	2015-06-25 06:58:38	51.41539878	2.529352567	-35.01
BV4	7	2015-06-25 07:34:00	51.40773812	2.519117233	-34.81
BV3	8	2015-06-25 07:57:55	51.41211307	2.521493283	-35.96
BV2	9	2015-06-25 08:14:44	51.41485773	2.522656767	-35.16
BV1	10	2015-06-25 08:31:59	51.41843313	2.523058317	-34.98
VV2	11	2015-06-25 08:46:29	51.42152493	2.529318233	-34.67
VV3	12	2015-06-25 08:58:51	51.41816025	2.5201472	-34.65

Table 14: List of video recordings in the barchan dune area, west of southern Oosthinder sandbank

ID	Start			End		
	Date and time	Latitude	Longitude	Date and time	Latitude	Longitude
VV3	2015-06-25 09:47:45	51.41798108	2.520508317	2015-06-25 09:54:10	51.41868363	2.520824933
BV1	2015-06-25 10:09:35	51.41849288	2.523221583	2015-06-25 10:17:13	51.41829618	2.5234754
BV2	2015-06-25 10:29:47	51.4151825	2.523302717	2015-06-25 10:36:00	51.41537107	2.522256467

BV3	2015-06-25 10:50:49	51.41194433	2.521446483	2015-06-25 10:59:00	51.41135483	2.522032933
BV4	2015-06-25 11:12:18	51.40790468	2.51883595	2015-06-25 11:15:00	51.40784632	2.518896733
BV5	2015-06-25 11:30:15	51.41335805	2.5265892	2015-06-25 11:37:00	51.4132122	2.526198583
BV6	2015-06-25 11:48:50	51.41508167	2.527557367	2015-06-25 11:52:15	51.4150725	2.527911117

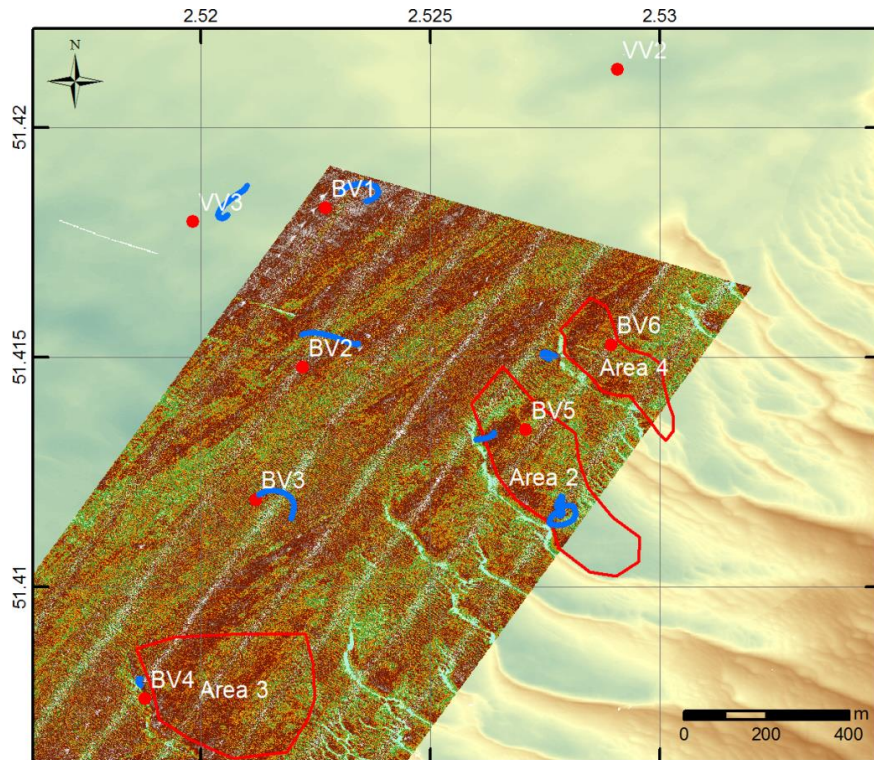


Figure 9: Detailed view of the samples (red) and video observations (blue) in the barchan dune area, west of the southern part of the Oosthinder sandbank. Area 2, 3 and 4 represent areas of higher biodiversity (ref. ST1407).

6.6. OD Nature-MF

1. Recovering of tripod

The tripod deployed at MOW1 during campaign 2015/13 was recovered on 22/06/2015 (Table 15).

Table 15: Position and time of tripod recuperation

ID	Instrument	Date (local time)	Latitude	Longitude
MOW1	Tripod recuperation	22/06 19h42	51°21.620'	3°06.815'

2. Collection of data with AUMS and hull-mounted ADCP along pre-defined tracks

Data was automatically collected using the AUMS and the hull-mounted ADCP (Figure 10).

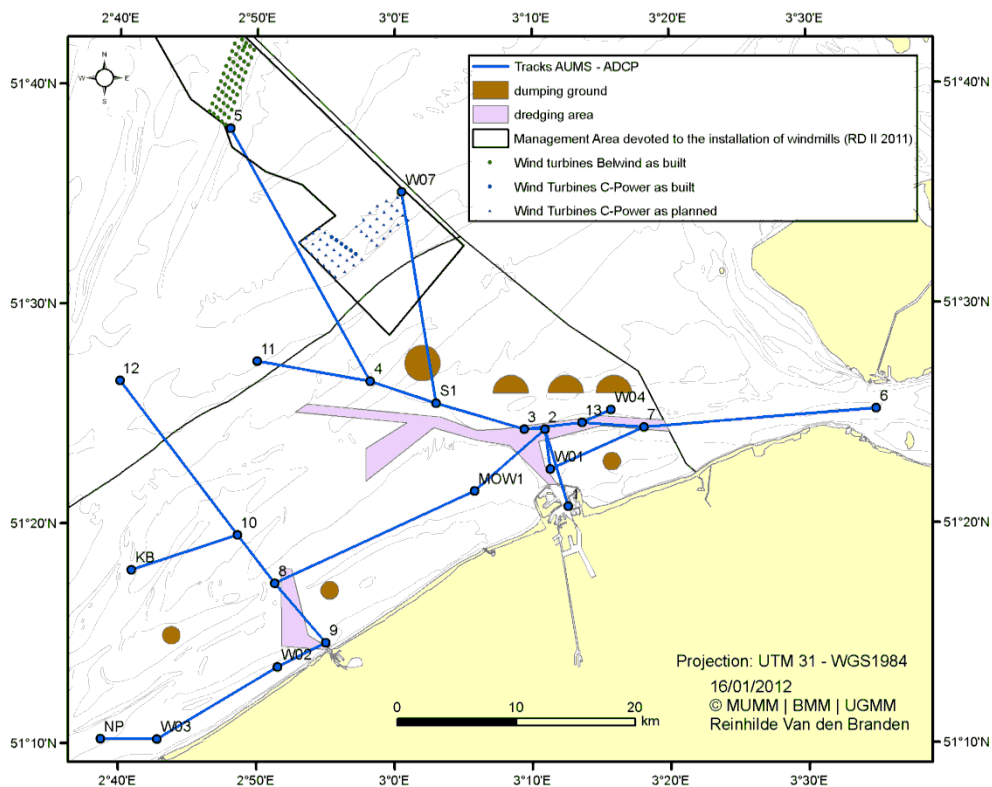


Figure 10: Map with AUMS tracks

7. REMARKS

Officers and crew are thanked warmly for the skillful handling of the operations.
24h lost due to bad weather at the beginning of the cruise.

8. DATA STORAGE

OD NATURE

- Multibeam echosounding: on hard disk OD NATURE-BRU; copy will be provided to BMDC. Contact person: Vera Van Lancker (120 nm)
- Seabed samples; integration into BMDC. Contact person: Vera Van Lancker (Hamon grabs: 4 near Sector 4b; 8 in and around barchan dune area)
- Sting measurements. Contact person: Vera Van Lancker (3 near Sector 4b)
- Video imagery. Contact person: Vera Van Lancker (7 shots near Sector 4b; 7 in and around barchan dune area)
- Centrifuge sample. Contact person: Vera Van Lancker (1 near Sector 4b; 1 barchan dune area)
- Tripod data. Contact person: Michael Fettweis

CSS/UG-RCMG

- Multibeam recordings (180 km): COPCO. Contact person: Koen Degrendele
- Seismics (180 km): UG-RCMG. Contact person: David Van Rooij

Annex – Pictures RBINS-OD Nature VVL



4B_01



4B_01



4B_02



4B_03



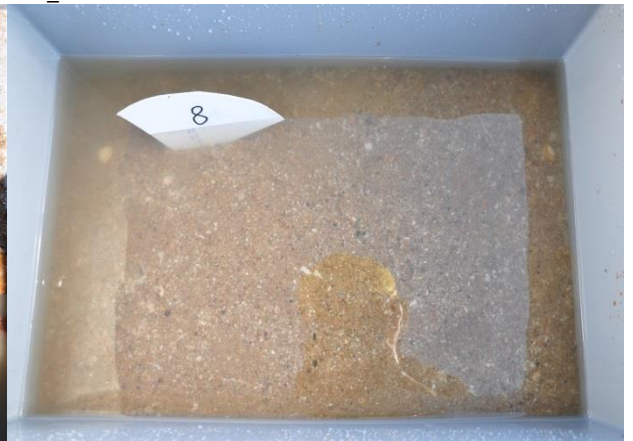
4B_04



BV1_10



BV2_09



BV3_08



BV4_07



BV5_05



BV6_02



VV2_11



VV3_12



VV3_12

Figure A1: Picture of Hamon grabs.



Figure A2: Oosthinder Sector 4B area. Centrifuge sample.

RV BELGICA CRUISE 2015/33 – CRUISE REPORT

Subscribers	CSS:	Koen Degrendele (KD);
	OD Nature:	Dr. Vera Van Lancker (VVL);
Institutes	CSS:	FPS Economy, SMEs, self-employed and Energy, Continental Shelf Department
	OD Nature:	Royal Belgian Institute of Natural Sciences - Operational Directorate Natural Environment
Addresses	CSS:	NGII - Koning Albert II Laan 16 , 1000 Brussels
	OD Nature:	Gulledelle 100, 1200 Brussels
Telephones	CSS:	+32(0)2 2778411 (KD);
	OD Nature:	+32(0)2 7732129 (VVL)
E-mails	CSS:	koen.degrendele@economie.fgov.be ;
	OD Nature:	vera.vanlancker@naturalsciences.be

Reserve: 15/12/2015 - 18/12/2015

1. Cruise details
2. List of participants
3. Scientific objectives
4. Operational course
5. Track plot
6. Measurements and sampling
7. Remarks
8. Data storage



Reference to this report

Degrendele, K., De Mol, L., Roche, M., Montereale-Gavazzi, G., Terseleer N., and Van Lancker, V. (2016). *RV Belgica campaign ST1533. Cruise Report. 15-18/12/2015*. Royal Belgian Institute of Natural Sciences, Operational Directorate Natural Environment, **38p**.

1. CRUISE DETAILS

1.	Cruise number	2015/33
2.	Date/time	Zeebrugge TD: 15/12/2015 at 10h15 Zeebrugge TA: 18/12/2015 at 12h00
3.	Chief Scientist Participating institutes	Koen Degrendele/ Vera Van Lancker FPS Economy-CSS, OD Nature
4.	Area of interest	Belgian part of the North Sea

2. LIST OF PARTICIPANTS

INSTITUTE	NAME	15/12 – 18/12/2015
CSD	Koen DEGRENDELE	X
	Lies DE MOL	X
	Marc ROCHE	X
OD Nature	Vera VAN LANCKER	X
	Giacomo MONTEREALE-GAVAZZI	X
	Nathan TERSELEER	X
Total number of participants		6

3. SCIENTIFIC OBJECTIVES

CSS-KD

Implementation of the continuous investigation laid down in section 3, §2, subsection 3, of the law of June 13th 1969, concerning the exploration and exploitation of non-living resources on the Belgian Continental Shelf, and the concession decisions.

The follow up of the repercussions of the sand extraction on the stability of the sand banks and surrounding area in the exploitation zones, in order to formulate policies concerning the exploitation in the concession zones on a scientific base. The sediments of the Belgian continental shelf will be investigated in order to:

1. Establish the impact of sand extraction on the sand budget and seabed sediments.
2. Survey the sand winning sites to detect significant changes of the seabed sediments and the morphology of the seabed and sand banks in order to guarantee the availability of sand to extract in the future.

OD Nature-VVL (ZAGRI/MOZ4)

ZAGRI is a continuous research program on the evaluation of the effects of the exploitation of non-living resources of the territorial sea and the continental shelf. MOZ4 research focuses on the hydrodynamics and sediment transport in a marine aggregate extraction zone, far offshore, and its impact on an adjacent Habitat Directive Area. Overall aim is to increase process and system knowledge of both areas, with particular focus on the compliancy of the extraction activities with respect to the European Marine Strategy Framework Directive. More specifically changes in seafloor integrity and hydrographic conditions need assessment.

OD Nature-VVL (INDI67/MONIT.BE)

Within Europe's Marine Strategy Framework Directive (MSFD), progress towards Good Environmental Status (GES) needs monitoring in a most time- and cost-effective way. For the GES descriptors 6 and 7, on seafloor integrity and hydrographic conditions, respectively, new integrative indicators (i.e. bottom shear stress, turbidity and seabed/habitat type) need developing. To advance the mapping of seabed/habitat types, a Community of Practice

(CoP) on seabed mapping will be established, investigating the main issues preventing joint mapping of the seabed. Within SEACoP (CoP on 'Surveying for Environmental Assessments') the following objectives are targeted: a) estimation of the precision, sensitivities and repeatability of the acoustic devices to detect changes in seabed/habitat types; b) quantification of the external sources of variance in the acoustic signature, including the influence of near-bed and water column suspensions on backscatter data; c) definition of best practice in ground-truthing the acoustic signal, with emphasis on visual techniques; and d) innovation in collaborative seabed mapping.

OD Nature-LN (AUMS)

The AUMS (Autonomous Underway Measurement System) project is inspired by the success of similar systems deployed on various ships of opportunity in the framework of the European Union FerryBox project (www.ferrybox.org). The instrumentation will greatly enhance the continuous oceanographic measurements made by RV Belgica by taking advantage of the significant technological improvements since the design of the existing (salinity, temperature, fluorescence) systems. In particular, many new parameters can now be measured continuously including important ecosystem parameters such as nitrate, ammonia, silicate, dissolved oxygen and CO₂, turbidity, alkalinity and phytoplankton pigments. In addition, the new equipment allows automatic acquisition and preservation of water samples, rendering RV Belgica operations significantly more efficient by reducing onboard human resources. Data will be available in near real-time via OD Nature's public web site and following quality control, from the Belgian Marine Data Centre.

ESA-MC (GNSS)

For the European Space Agency continuous GNSS (Global Navigation Satellite system) data is autonomously acquired in the maritime environment for performance evaluation under different conditions.

4. OPERATIONAL COURSE

*All times are given in local time (UTC+1H). All coordinates in WGS84.
Throughout the campaign, measurements are made with the AUMS system.*

Tuesday 15/12/2015

09h00-11h00	Embarkation of instruments and personnel.
11h12-11h51	Survey boxcorer near Zeebrugge
13h35-15h42	Calibration of EM3002D near Thorntonbank
16h50-22h26	Multibeam survey on TBMA B
23h07-03h50	Multibeam survey on HBMC (sector 4c)

Wednesday 16/12/2015

Because of bad weather, transit to coastal area for multibeam surveying and sampling (RBINS-ODN)

05h55-10h05	MBES Coastal area, main gully west of Ostend, up to French border (2 overlapping lines)
10h53-15h55	Van Veen grab sampling coastal area

Transit to KWGS area for multibeam surveying (FPS Economy)

17h05-17h45	Multibeam BS calibration survey on KWGS
18h00-23h18	Multibeam survey on BRMA
23h33-03h47	Multibeam survey on BRMC

Thursday 17/12/2015

Transit to Hinder Banks south for Van Veen grab sampling (RBINS-ODN)

07h06-08h14	Van Veen grab sampling Hinder Banks south – barchan dune area
08h34-10h00	Video imaging Hinder Banks south
10h17-14h50	MBES survey Hinder Banks south

15h08-15h33 Van Veen grab sampling Hinder Banks south (continuation)

Transit to Hinder Banks Sector 4c for Reineck boxcoring (RBINS-ODN)

16h40-17h50 Reineck boxcorers Sector 4c

Transit to Thornton Bank (FPS Economy)

19h00-02h14 Multibeam survey on TBMA B

Friday 18/12/2015

07h00-11h00 Recuperation of boxcorer near Zeebrugge

11h12-11h28 Multibeam calibration survey in Vandammesluis

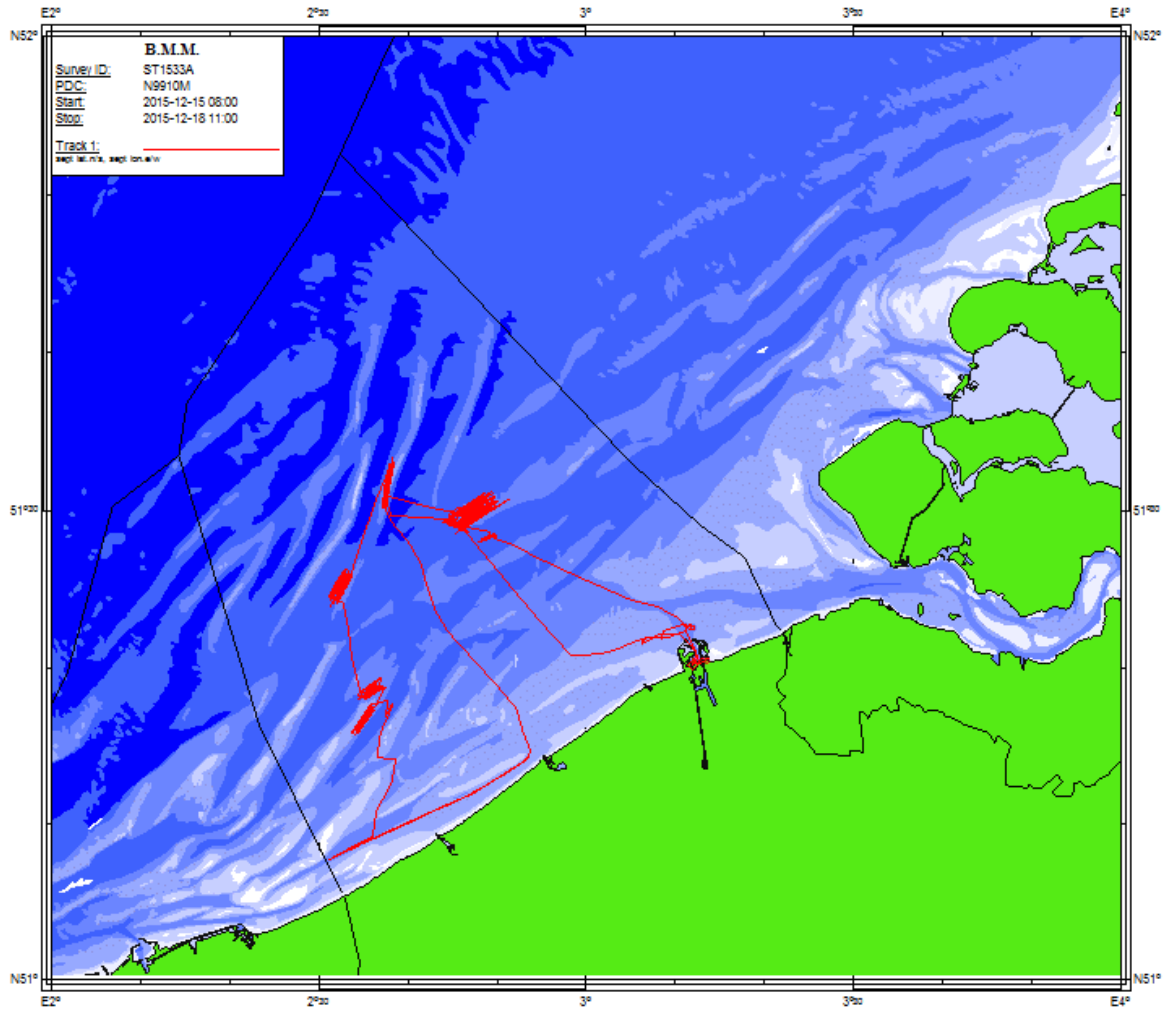
12h00 Arrival at Zeebrugge

Debarcation of participants and material

- End of campaign 2015/33 -

5. TRACK PLOT

Figure 1: Track plot of campaign 2015/33



6. MEASUREMENTS AND SAMPLING

6.1. CSS-KD

1. Box corer detection using the MBES EM3002D

1. First MBES track based on the coordinates provided by the CO:

51° 22.603' N – 03° 11.193' E

2. 4 Tracks:

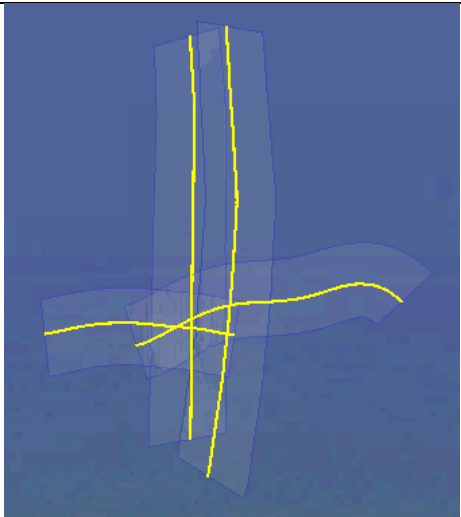
Lines	Map	
0001_20151215_101500_Belgica.all 0002_20151215_102616_Belgica.all 0003_20151215_103750_Belgica.all 0004_20151215_104650_Belgica.all		

Figure 2: Boxcorer survey

3. Clear target detection at 51° 22.589'N 3° 11.162'E visible on each lines

4. Raw bathymetry:

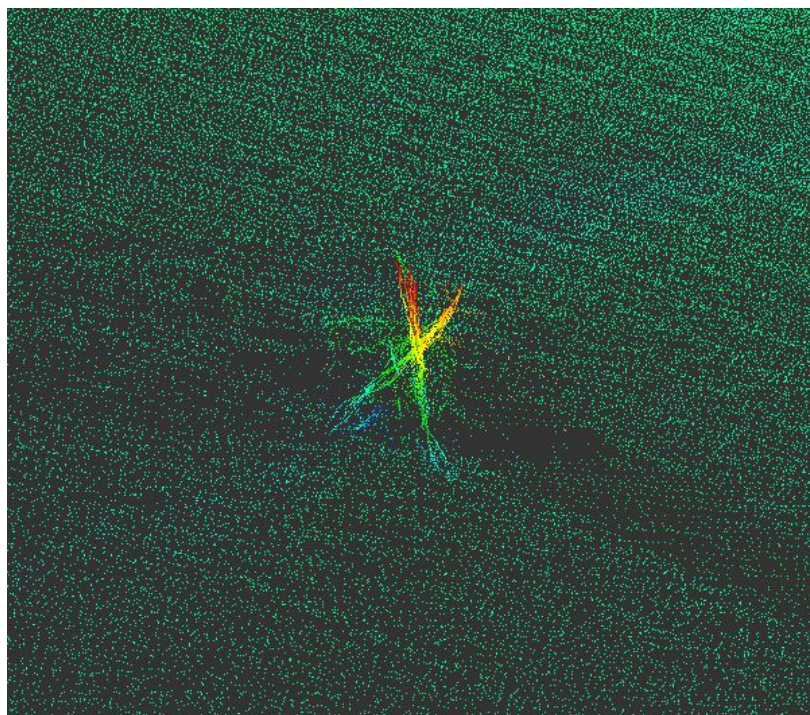


Figure 3: Detailed bathymetry of target near provided position. Lines 1 and 3 are visualized.

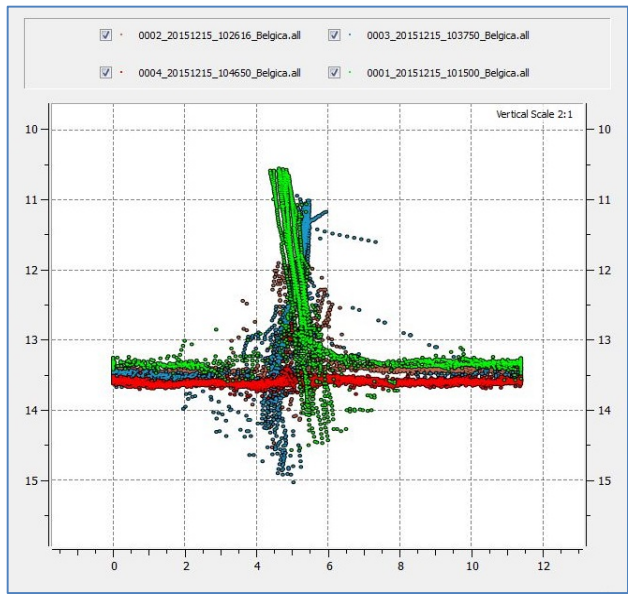


Figure 4: Profile across the detected object on the four lines.

5. MBES Seabed-Sonar image:

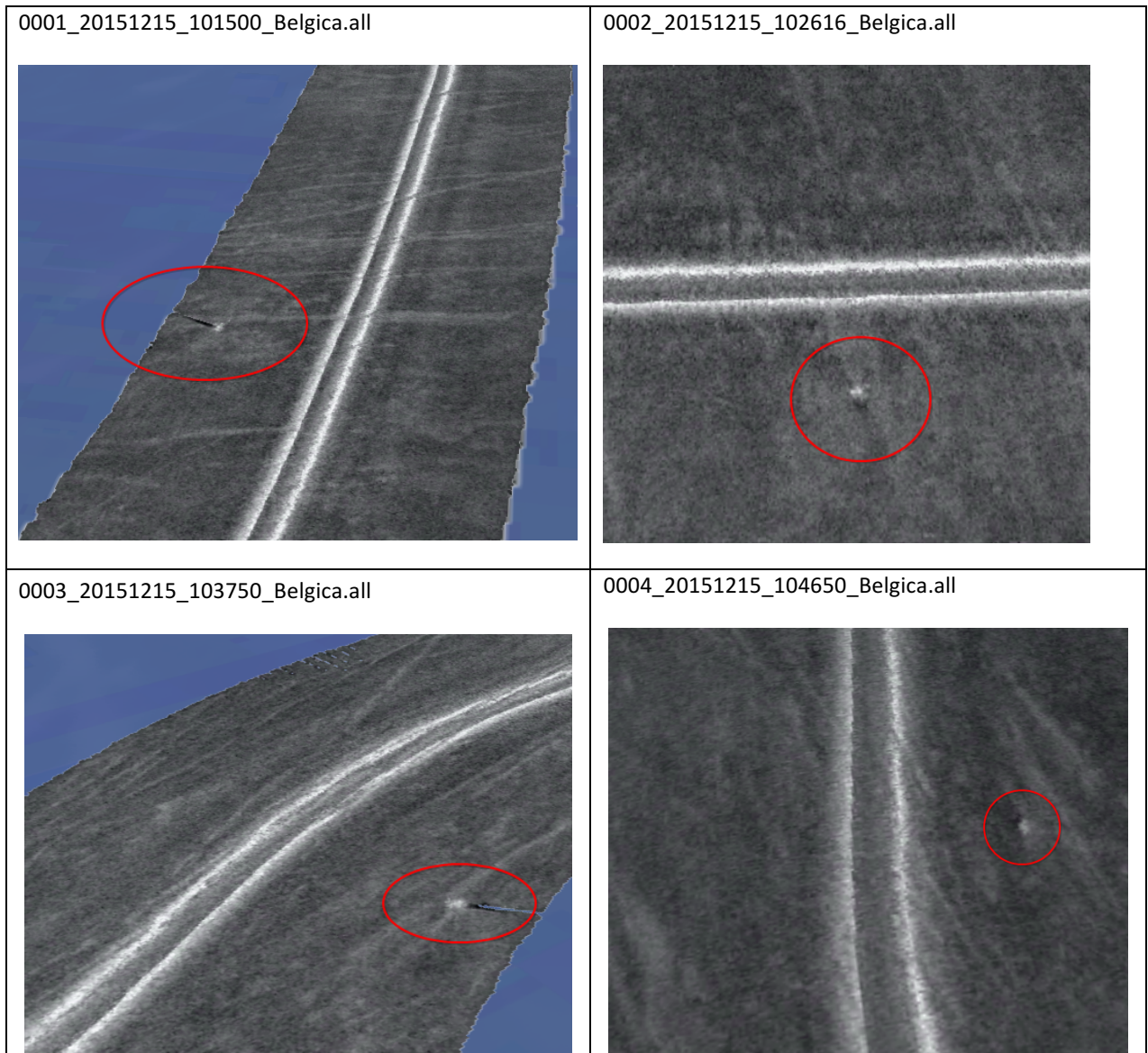


Figure 5: Sonar image

2. Calibration of the EM3002D

New installation parameters:

Location offset (m)			
	Forward (X)	Starboard (Y)	Downward (Z)
Pos, COM1:	-6.569	-3.643	-15.202
Pos, COM3:	0.00	0.00	0.00
Pos, COM4/UDP2:	0.00	0.00	0.00
Sonar head 1:	-5.807	-2.296	0.984
Sonar head 2:	-5.813	2.319	0.990
Attitude 1, COM2/UDP5:	0.00	0.00	0.00
Attitude 2, COM3/UDP6:	0.00	0.00	0.00
Waterline:			-3.112
Depth Sensor:	0.00	0.00	0.00

Offset angles (deg.)			
	Roll	Pitch	Heading
Sonar head 1:	34.395	1.1	359.5
Sonar head 2:	-34.135	0.8	2.5
Attitude 1, COM2/UDP5:	0	0	0
Attitude 2, COM3/UDP6:	-0.20	2.00	0
Stand-alone Heading:			-0.25

Figure 6: Installation parameters for campaign 1533

3. Multibeam survey of TBMA area

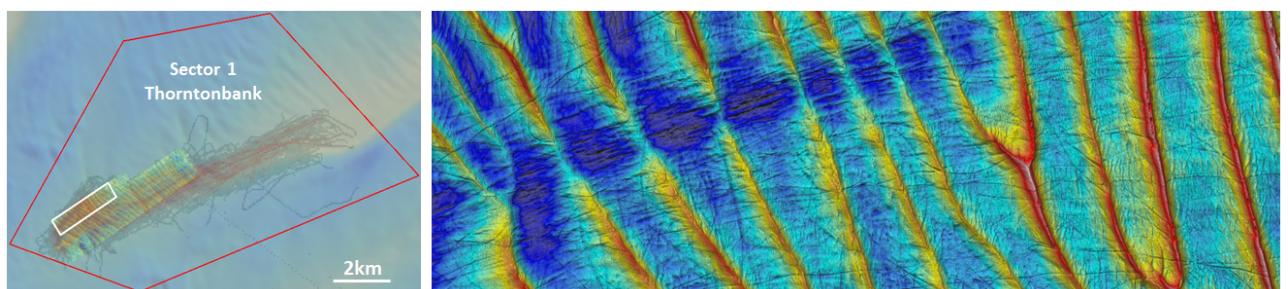


Figure 7: Multibeam survey on Thorntonbank (TBMA)

4. Multibeam survey of HBMC area

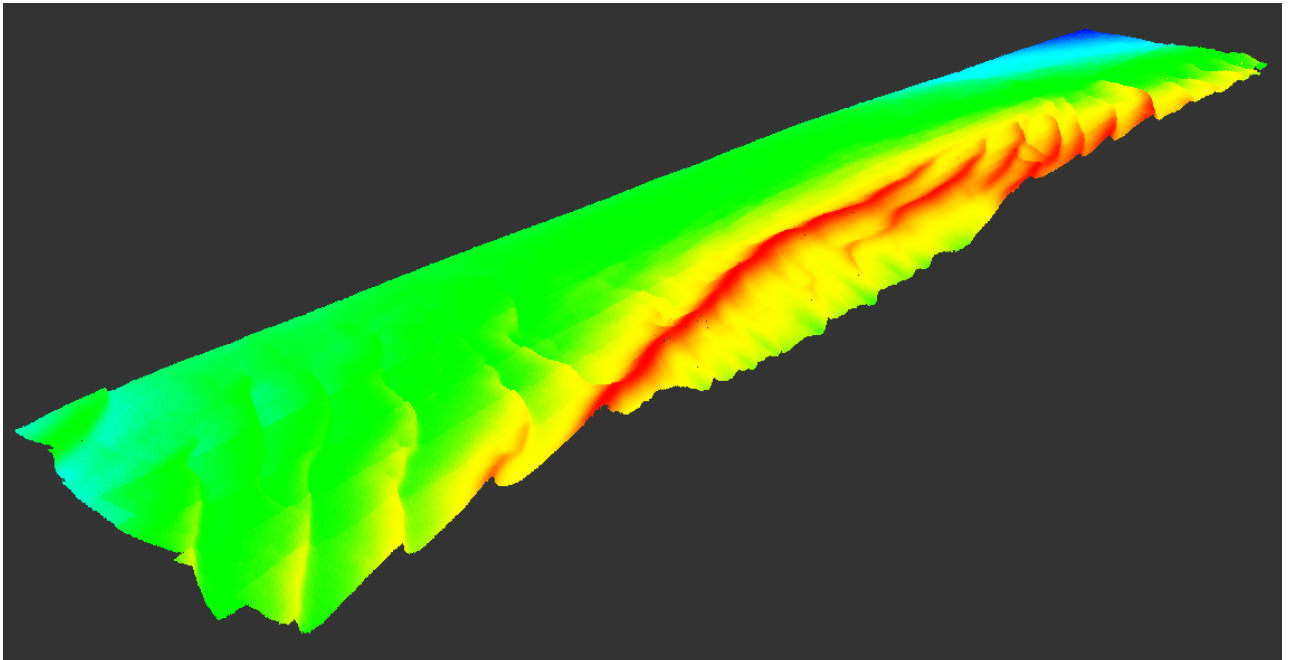


Figure 8: Multibeam survey on Oosthinder (HBMC)

5. Multibeam BS calibration survey of KWGS area

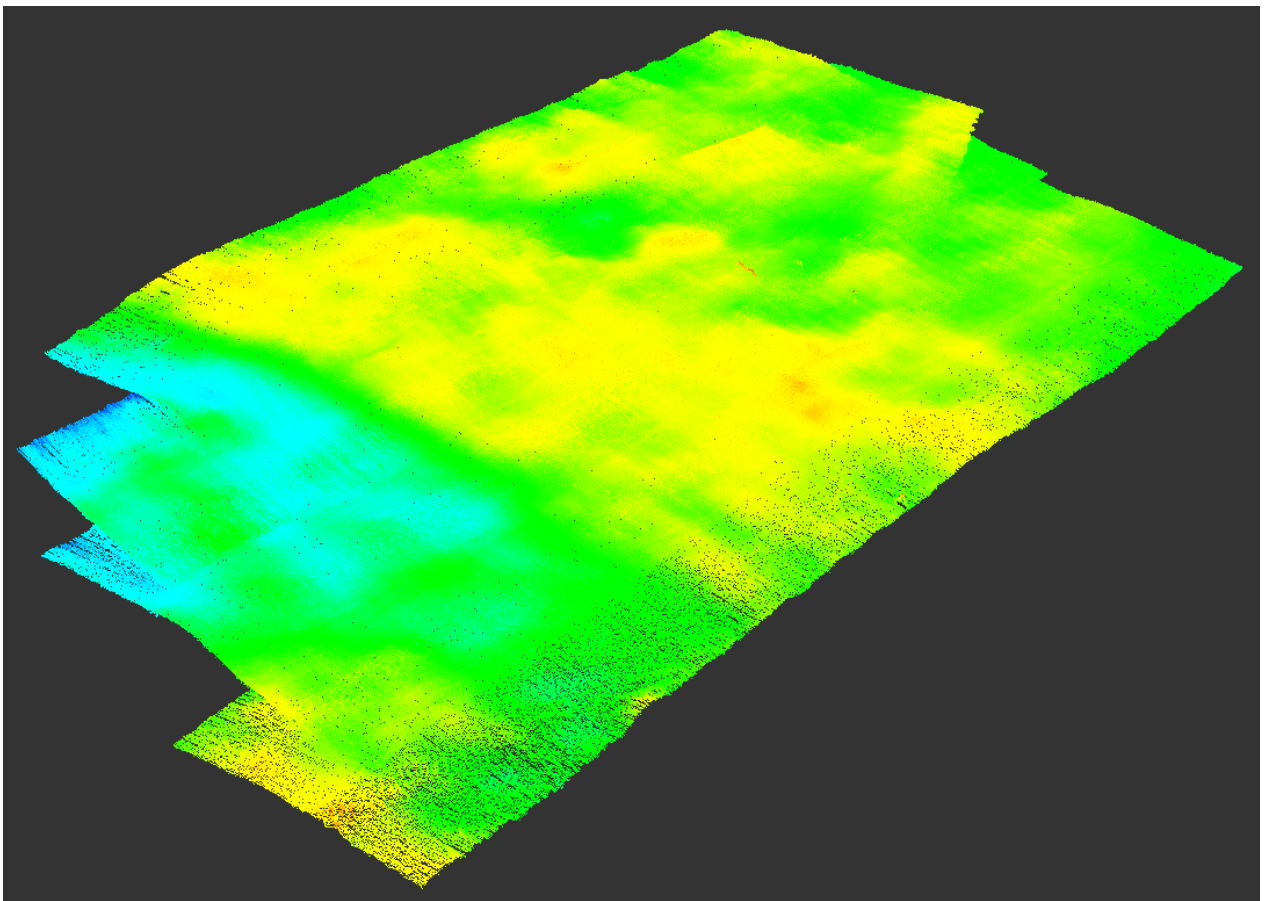


Figure 9: Multibeam BS calibration survey on KWGS

6. Multibeam survey of BRMA area

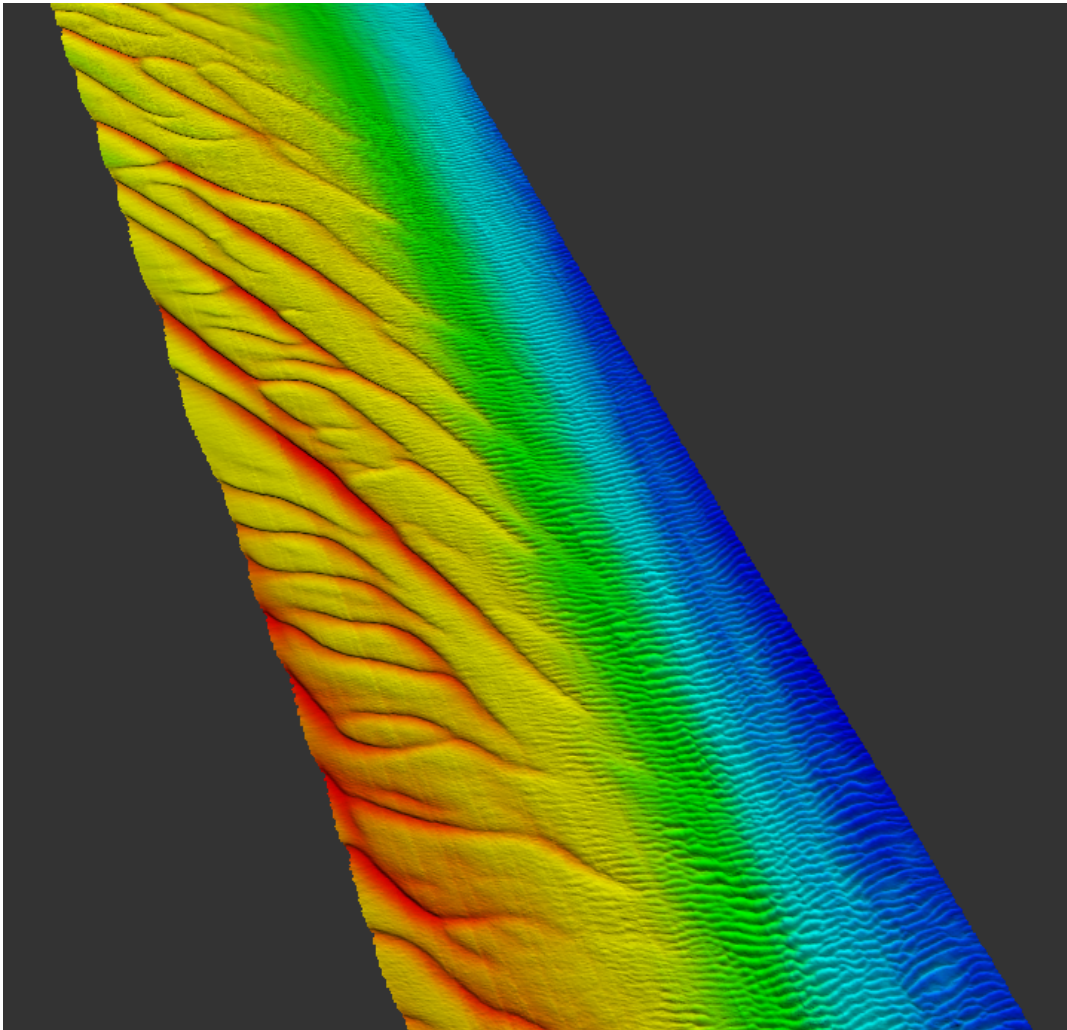


Figure 10: Multibeam survey on Buiten Ratel (BRMA)

7. Multibeam survey of BRMC area

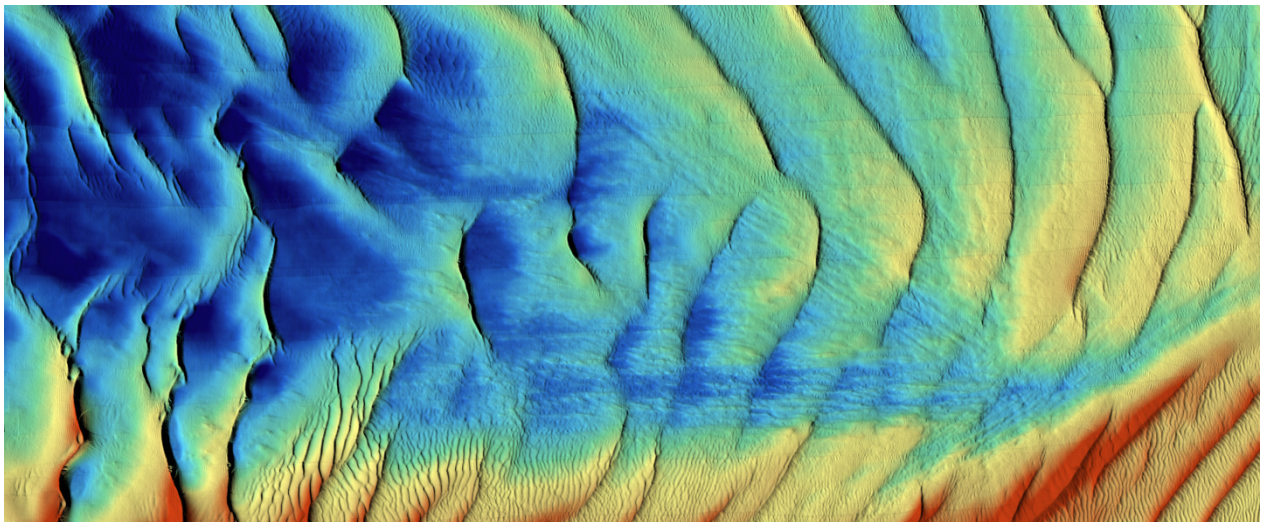


Figure 11: Multibeam survey on Buiten Ratel (BRMC)

8. Multibeam calibration survey of Vandammesluis

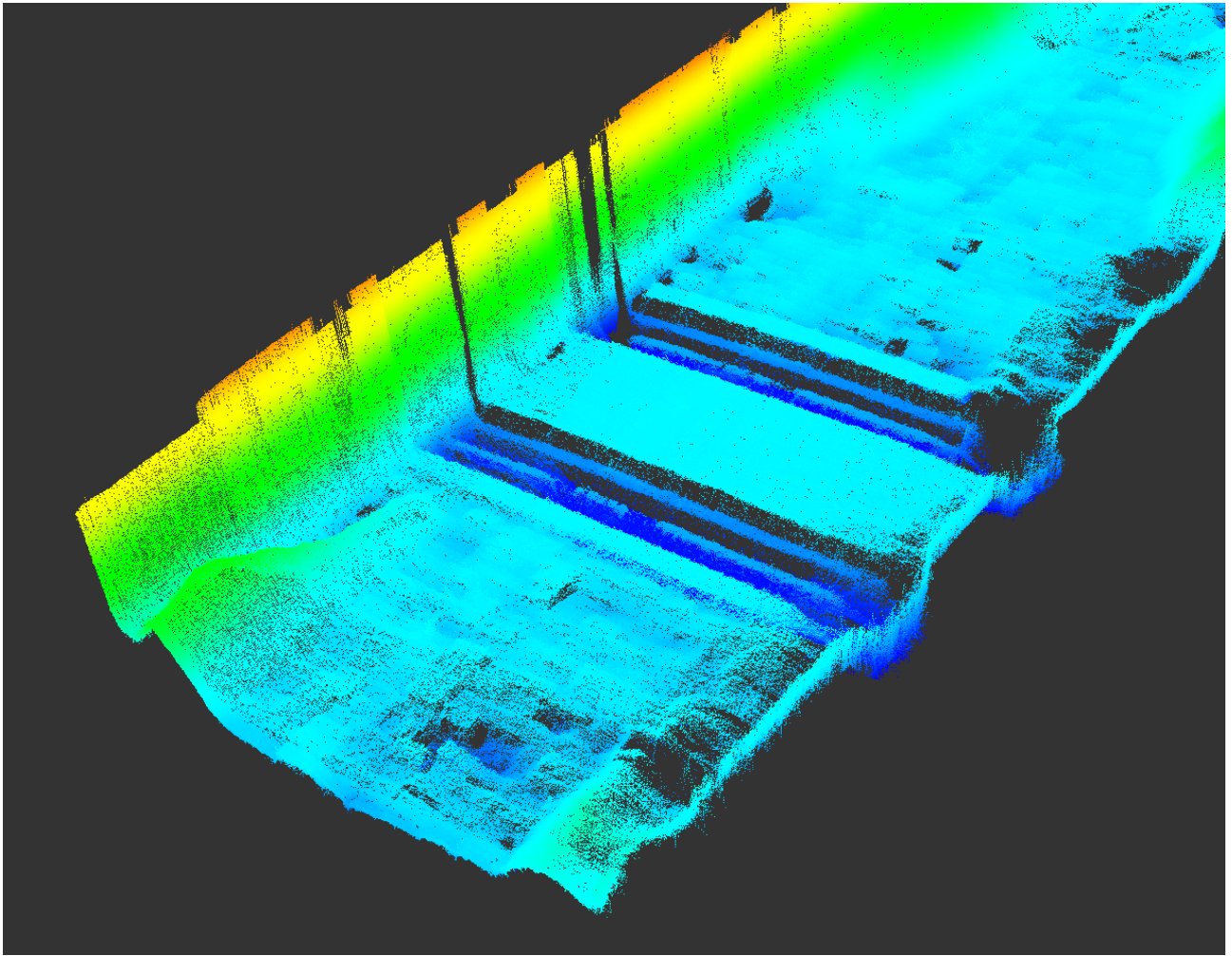
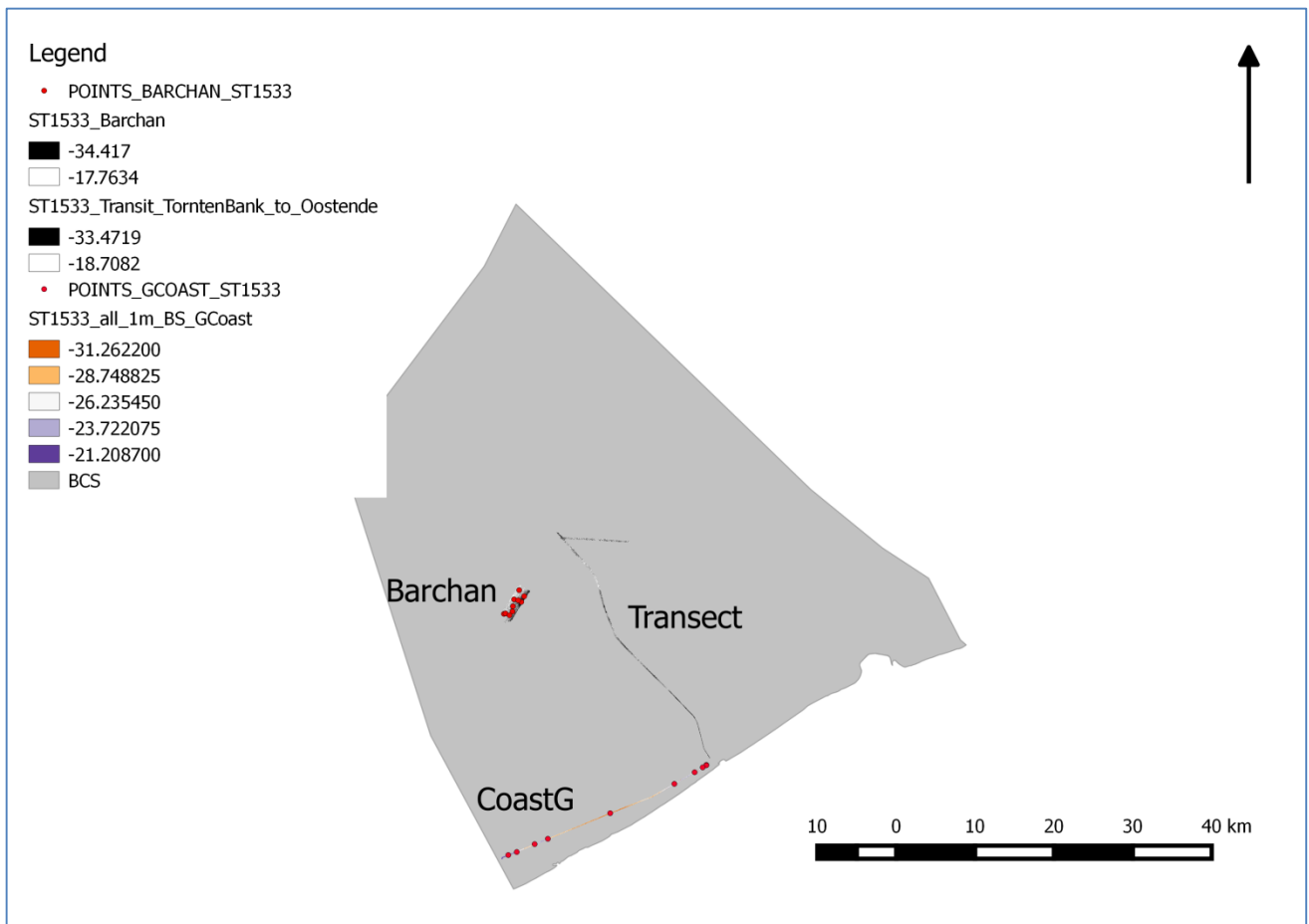


Figure 12: Multibeam bathymetry calibration survey in the Vandammesluis

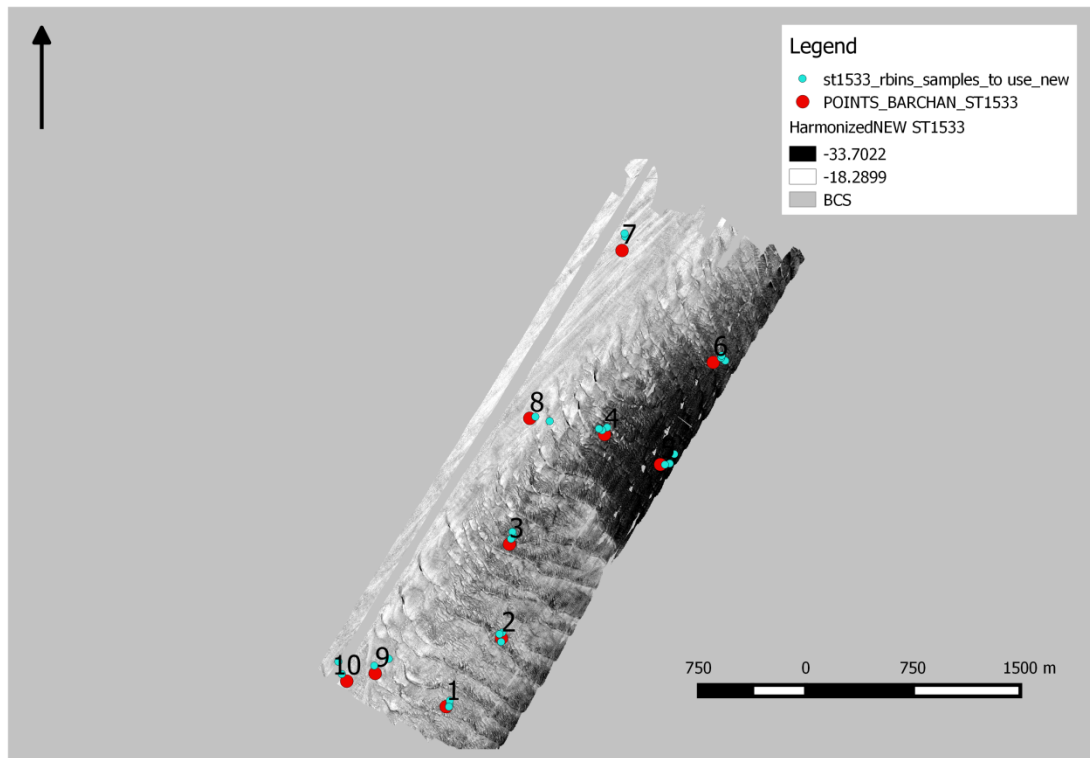
6.2. OD Nature-VVL-GMG-NTL

A map summarizing the overall Multibeam surveys in the coastal area, and along the barchan dune area in the southern part of the Hinder Banks. Multibeam data were also recorded along the main transects between survey areas.

6.2.1 General overview of the RBINS multibeam survey areas



6.2.2 Hinder Banks - Barchan Area



6.2.3 CoastG Area

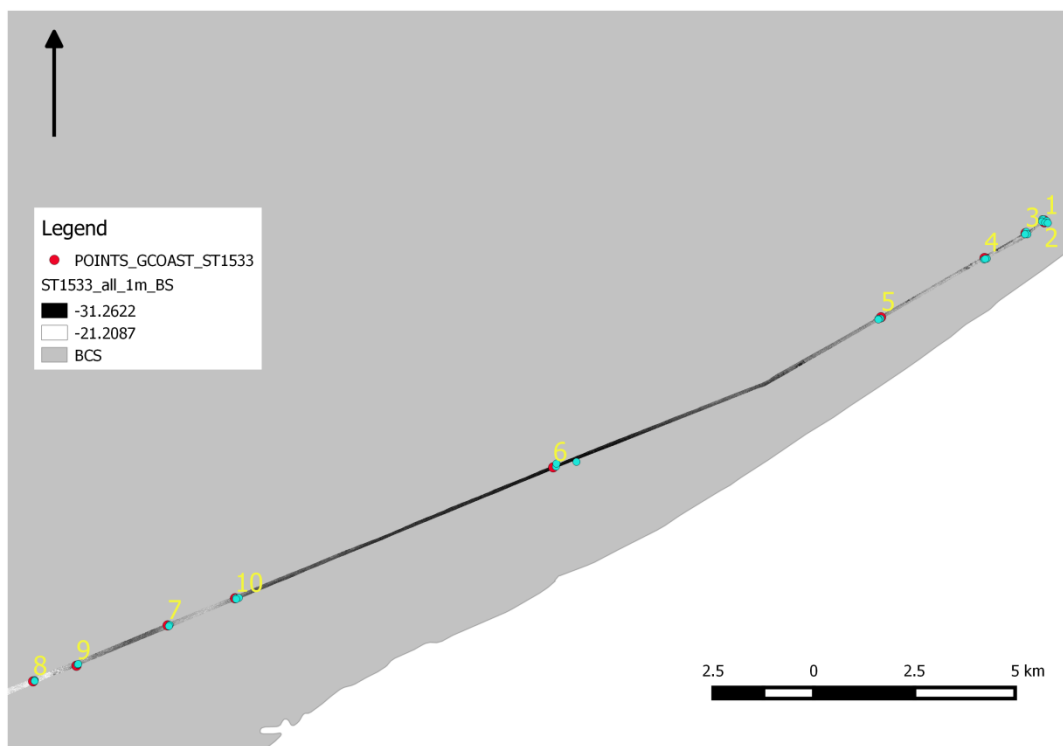


Figure 15: RBINS multibeam survey area near coast

6.3 In Situ Sampling

6.3.1 On-board sampling protocol:

Van Veen grab sampling

Table 1. Items used for the Van Veen sampling.

Items	Used for
Transparent sealable plastic bags	Preserve samples and replicates
Permanent marker	Write sample ID on bags
Portable whiteboard	Write sample ID in picture background
Kitchen spoon	Collect the first 1 to 2 cm of substrate
Spatula	Slice the full substrate sample profile
Bucket	Wash hands and keep biological specimen for observation
Watch	Record time of each sample to later couple to ODAS
Photographic camera	Take in situ pictures of samples and replicates

For each sample, 3 replicates were collected with the Van Veen grab. Two types of sub-samples were prepared. Firstly, when the grab was retrieved on board, a spoon was used to collect the very surficial substrate of the sample. These were named as e.g. GC01a-SUR. Secondly, part of the main bulk of the sample was sliced using a spatula. These were named as e.g. GC01a-B. The ID of each sample was written with a permanent marker on the plastic bags they were collected. The portable whiteboard reporting the sample ID was used in the background of each photograph. For each sample, the time was recorded as to later couple it with the ODAS information to obtain the most correct positioning. Sample locations corrected for antenna layback and corresponding *in situ* pictures are reported below. Overall, 18 samples were gathered: 10 Grabs In the CoastG dataset and 6 Grabs and 2 Video-Frames in the Barchan Dataset.

Reineck sampling

Reineck boxcoring was performed along 5 locations in marine aggregate sector 4c on the Hinder Banks. Locations were chosen close to previous sampling locations, but within the area constrained by the multibeam recording of FPS Economy during this campaign (see figure in the following pages). For these samples, only one, but successful core sample was retained. A subcore was taken per sample. Subsequently, in the wet lab, the subcore was turned and the sediment column was pushed upwards. Per 1-cm a slice was retained with the spatula, hence number 1 on the plastic bags corresponds with the lowest sample retrieved. Sometimes the last sample was not 1-cm, but somewhat less. From the full sample in the corer itself, a vertical cut was made with a spatula and photographed (see pictures below).

Table 2. Coordinates of all samples. Positions are in WGS84 and are corrected for the position of the sampler (12m along axis; 7m across).

id	id_short	gear	utc_from	depth	X	Y	
CoastG	1a	Van Veen	2015-12-16 09:55:00	-8.5	2.8894048	51.236762	
CoastG	1b	Van Veen	2015-12-16 10:04:00	-8.33	2.8897411	51.236728	
CoastG	1c	Van Veen	2015-12-16 10:08:28	-8.4	2.889335	51.236244	
CoastG	2a	Van Veen	2015-12-16 10:14:23	-7.95	2.8909637	51.236385	
CoastG	2b	Van Veen	2015-12-16 10:19:50	-8.17	2.8904158	51.236028	
CoastG	2c	Van Veen	2015-12-16 10:23:48	-8.07	2.8913658	51.235916	
CoastG	3a	Van Veen	2015-12-16 10:34:04	-8.84	2.8836996	51.233941	
CoastG	3b	Van Veen	2015-12-16 10:37:56	-8.62	2.8841143	51.233396	
CoastG	3c	Van Veen	2015-12-16 10:43:53	-8.77	2.8832721	51.233398	
CoastG	4a	Van Veen	2015-12-16 11:00:49	-9.32	2.8687097	51.227778	
CoastG	4b	Van Veen	2015-12-16 11:05:10	-9.14	2.8696771	51.22795	
CoastG	4c	Van Veen	2015-12-16 11:09:08	0	2.8691331	51.227883	
CoastG	5a	Van Veen	2015-12-16 11:28:28	0	2.8319133	51.214532	
CoastG	5b	Van Veen	2015-12-16 11:33:45	-10.68	2.8311759	51.214477	
CoastG	5c	Van Veen	2015-12-16 11:37:30	-10.65	2.8311729	51.214338	
CoastG	6a	Van Veen	2015-12-16 12:10:00	-10.75	2.7240633	51.182365	
CoastG	6b	Van Veen	2015-12-16 12:19:27	-11.84	2.7167829	51.181285	
CoastG	6c	Van Veen	2015-12-16 12:23:48	-11.84	2.7169428	51.181961	
CoastG	7a	Van Veen	2015-12-16 13:10:27	-17.76	2.5797531	51.145419	
CoastG	7b	Van Veen	2015-12-16 13:14:42	-17.96	2.5798773	51.145554	
CoastG	7c	Van Veen	2015-12-16 13:19:28	-18.37	2.5796083	51.145286	
CoastG	8a	Van Veen	2015-12-16 13:45:14	-20.54	2.5321347	51.133061	
CoastG	8b	Van Veen	2015-12-16 13:49:36	-20.53	2.532067	51.133031	
CoastG	8c	Van Veen	2015-12-16 13:55:57	-20.88	2.5320683	51.132861	
CoastG	9a	Van Veen	2015-12-16 14:13:10	-20.08	2.5473557	51.136586	
CoastG	9b	Van Veen	2015-12-16 14:19:13	0	2.5472497	51.136612	
CoastG	9c	Van Veen	2015-12-16 14:23:02	-19.9	2.5474886	51.136703	
CoastG	10a	Van Veen	2015-12-16 14:46:25	0	2.6033313	51.151632	
CoastG	10b	Van Veen	2015-12-16 14:50:54	-16.35	2.6043907	51.151693	
CoastG	10c	Van Veen	2015-12-16 14:55:22	-16.42	2.6034299	51.151391	
HB	1a	Van Veen	2015-12-17 06:06:07	-30.48	2.531171	51.406381	
HB	1b	Van Veen	2015-12-17 06:10:26	-29.79	2.5312049	51.406644	
HB	1c	Van Veen	2015-12-17 06:14:20	-30.1	2.5311202	51.406261	
HB	2a	Van Veen	2015-12-17 06:25:41	-29.71	2.5363317	51.410358	
HB	2b	Van Veen	2015-12-17 06:29:54	0	2.536429	51.410937	
HB	2c	Van Veen	2015-12-17 06:33:16	-30.24	2.5361579	51.410842	
HB	3a	Van Veen	2015-12-17 06:44:30	-28.35	2.5374929	51.416992	

HB	3b	Van Veen	2015-12-17 06:48:08	-33.01	2.5373974	51.417271	
HB	3c	Van Veen	2015-12-17 06:51:25	-30.87	2.5372577	51.416828	
HB	4a	Van Veen	2015-12-17 07:07:18	-27.99	2.5468569	51.423865	
HB	4b	Van Veen	2015-12-17 07:11:19	-29.61	2.5463523	51.423687	
HB	4c	Van Veen	2015-12-17 07:14:30	-30.31	2.5460374	51.423779	
HB	5a	Van Veen	2015-12-17 14:08:48	0	2.5531806	51.421625	
HB	5b	Van Veen	2015-12-17 14:12:27	-20.75	2.5536341	51.422216	
HB	5c	Van Veen	2015-12-17 14:15:47	-19.21	2.5526948	51.421552	
HB	6a	Van Veen	2015-12-17 14:27:11	-23.53	2.5587064	51.428103	
HB	6b	Van Veen	2015-12-17 14:30:22	-25.83	2.558282	51.428284	
HB	6c	Van Veen	2015-12-17 14:33:53	-25.11	2.558335	51.42842	
HB_4C	1	Reineck	2015-12-17 15:40:06	-27.78	2.6335692	51.547301	
HB_4C	2	Reineck	2015-12-17 15:50:00	0	2.6307756	51.541029	
HB_4C	3	Reineck	2015-12-17 16:10:57	-23.75	2.6240576	51.524317	
HB_4C	4	Reineck	2015-12-17 16:24:48	-16.07	2.6288775	51.522687	
HB_4C	4	Reineck	2015-12-17 16:33:04	-15.74	2.6292269	51.5226	
HB_4C	5	Reineck	2015-12-17 16:50:18	-24.9	2.62027	51.51522	
HB	ST1533_1	Videoframe	2015-12-17 07:37:27	-32.69	2.5485575	51.4358635	start
HB	ST1533_1	Videoframe	2015-12-17 07:45:42	-32.3	2.5484968	51.43605512	end
HB	ST1533_2	Videoframe	2015-12-17 08:01:17	-29.3	2.5396268	51.4245116	start
HB	ST1533_2	Videoframe	2015-12-17 08:08:10	-29.5	2.5410784	51.42423592	end
HB	ST1533_3	Videoframe	2015-12-17 08:28:16	-32.8	2.5235835	51.4088131	start
HB	ST1533_3	Videoframe	2015-12-17 08:37:17	-33.1	2.5250356	51.40924772	end
HB	ST1533_4	Videoframe	2015-12-17 08:44:49	-32.9	2.5203316	51.4082728	start
HB	ST1533_4	Videoframe	2015-12-17 08:58:52	-33	2.5199694	51.4090538	end

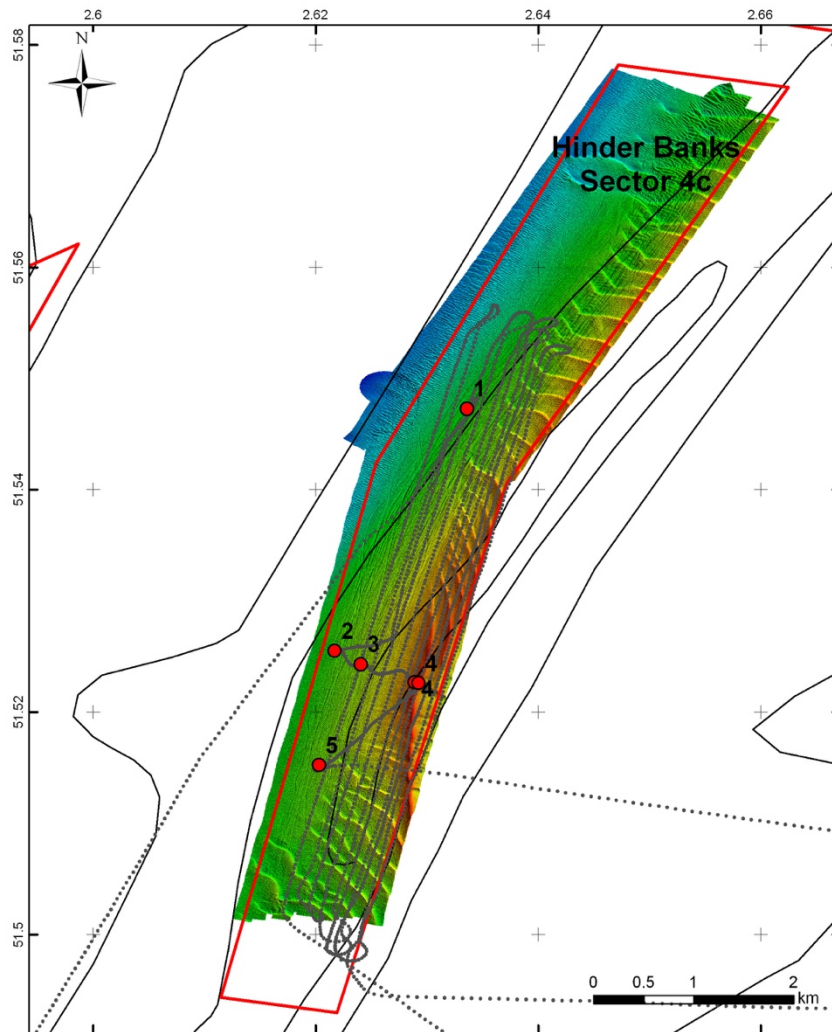


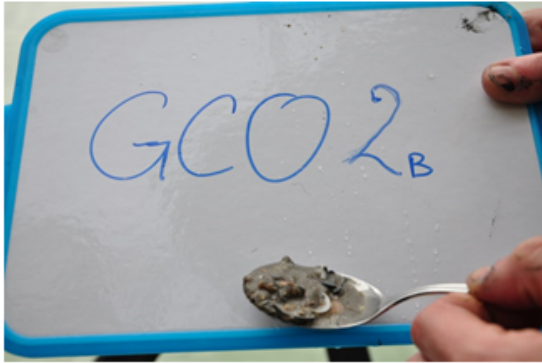
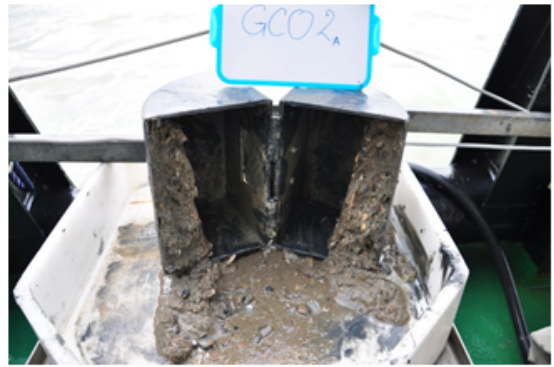
Figure 16. Reineck boxcoring along Hinder Banks marine aggregate sector 4c (5 samples). Indicated also are the tracklines of the multibeam survey carried out in this area during this survey (FPS Economy). Background multibeam bathymetry is derived from FPS Economy (RV Belgica ST1406).

GCoast Area Grab samples 16-12-2015 (n = 10s x 3r)

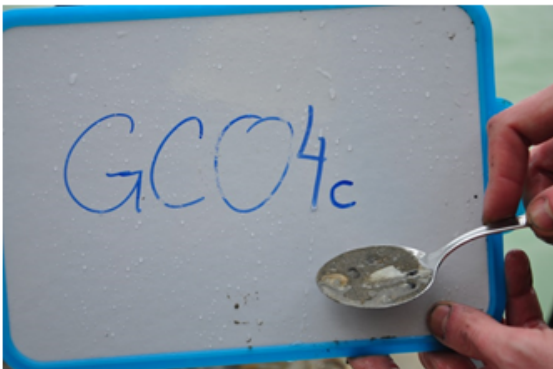




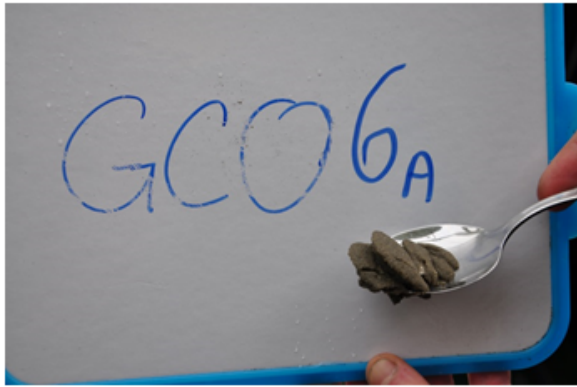
Barnea lactea (Linneaus 1758)– Pholadidae– IUCN Red List

















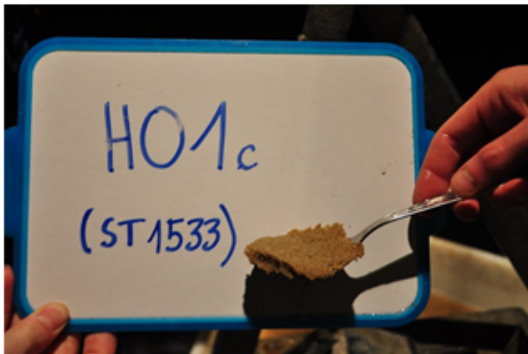
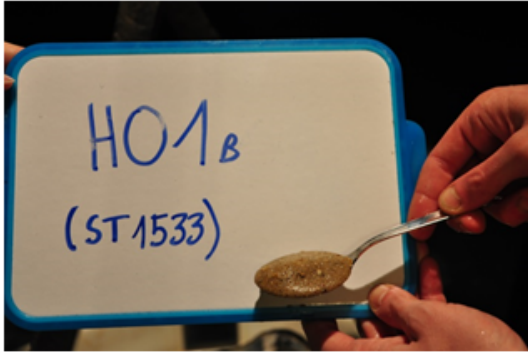
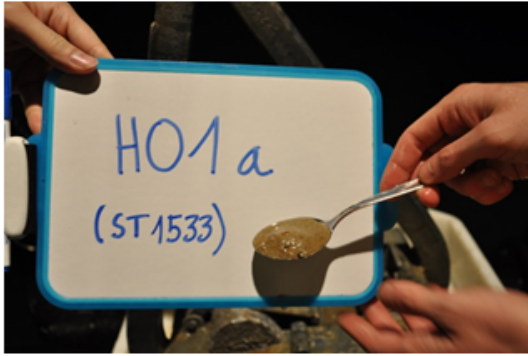
Echinocardium cordatum



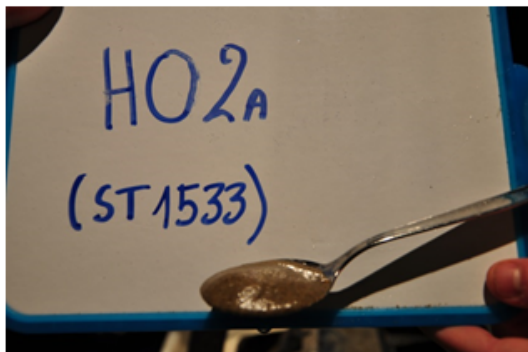
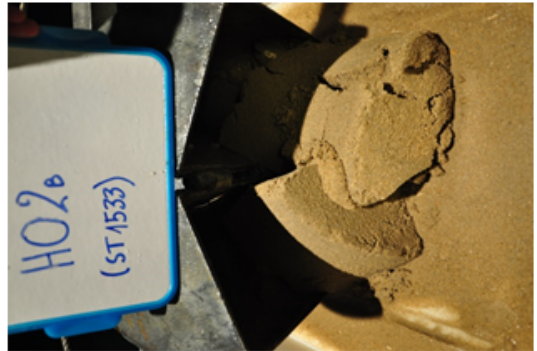
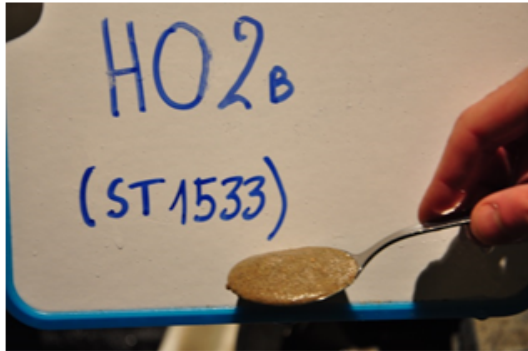
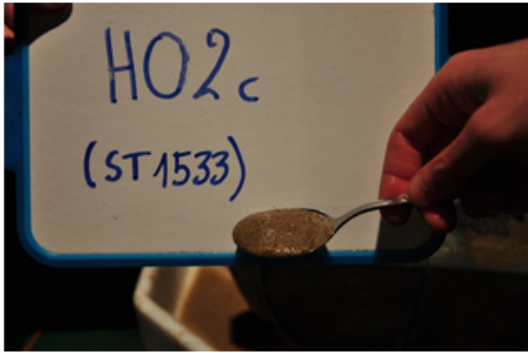
Anphiura sp. Ophiuridae

Barchan Area Grab samples 17-12-2015 (n= 6s x 3r + 4df)

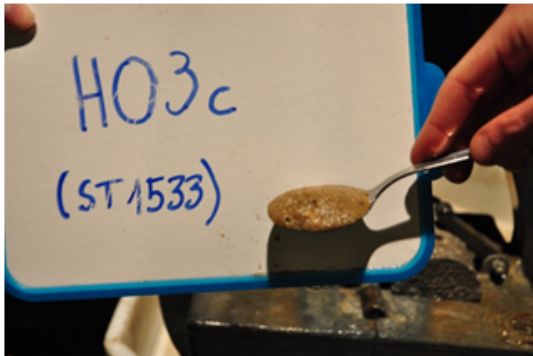
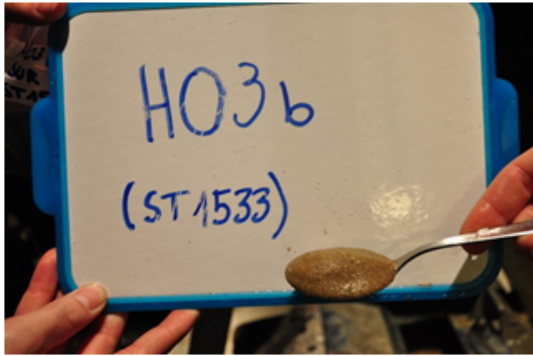
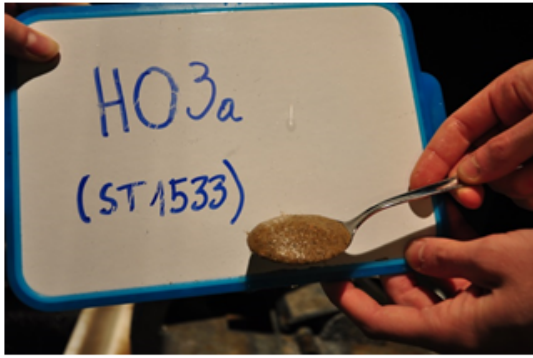




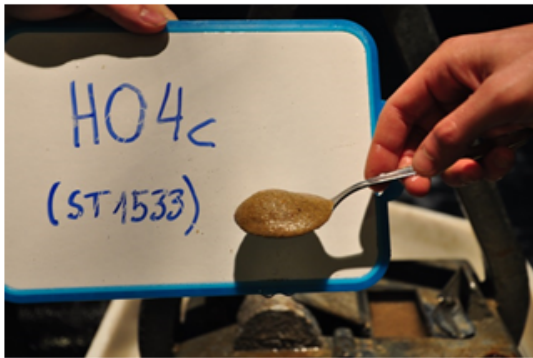
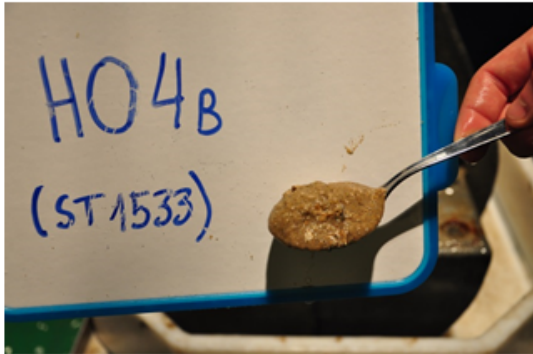
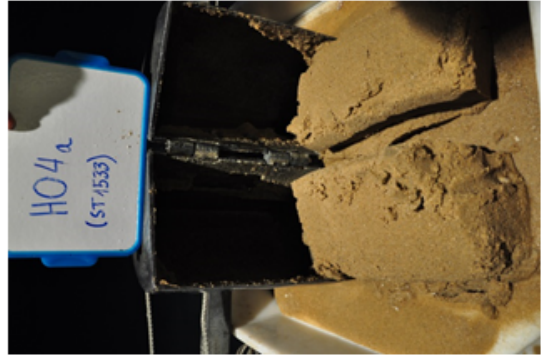
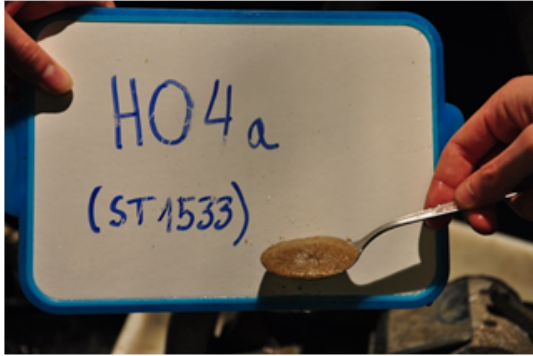
Sample H01a, b, c



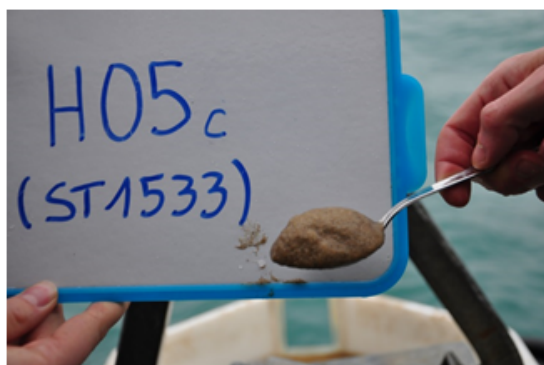
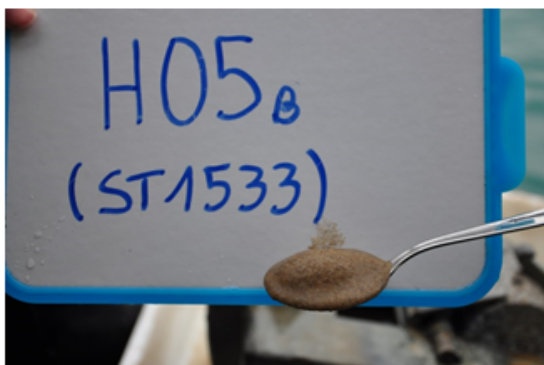
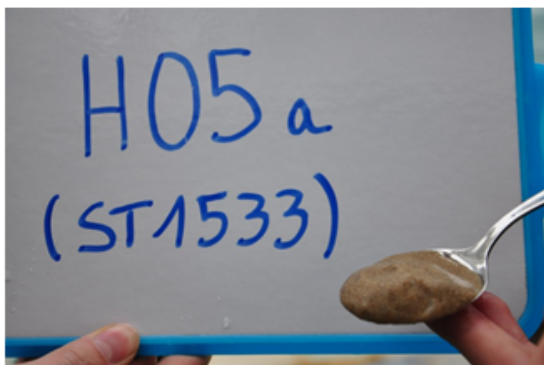
Sample HO2a, b, c



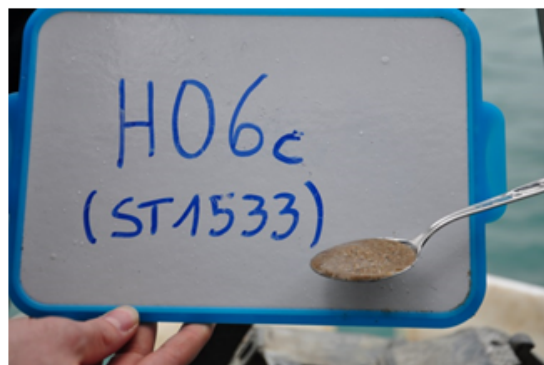
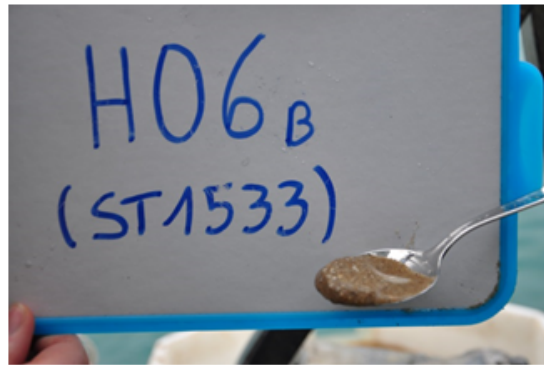
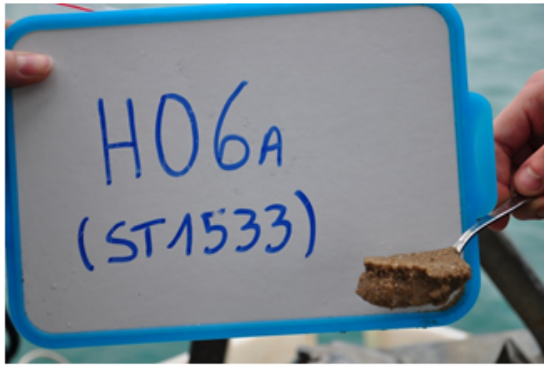
Sample H03a, b, c



Sample H04a, b, c

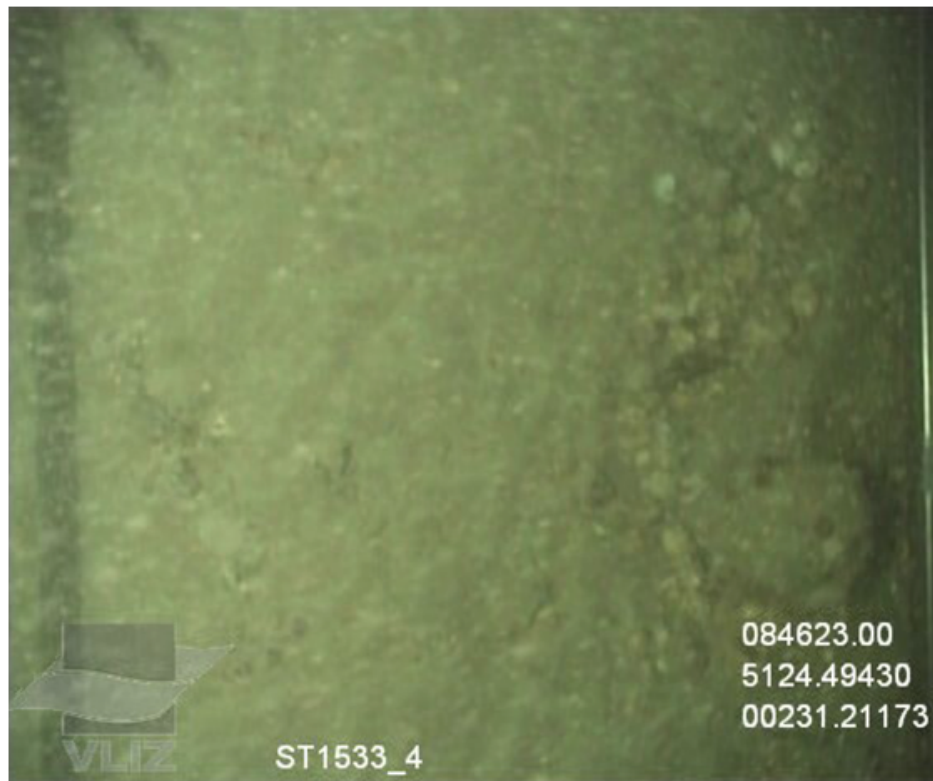


Sample H05a, b, c



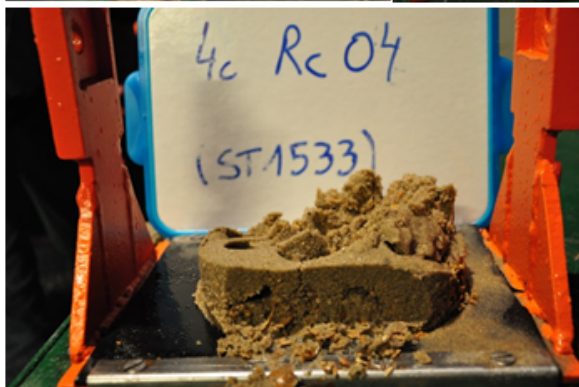
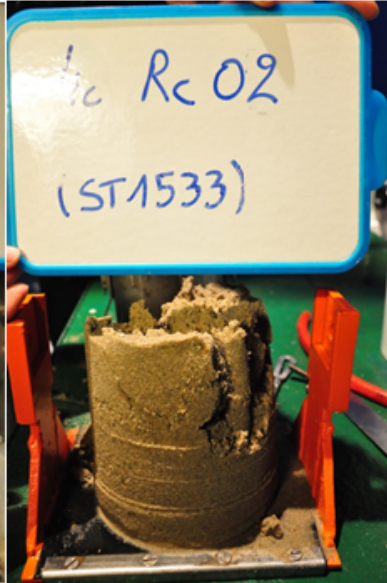
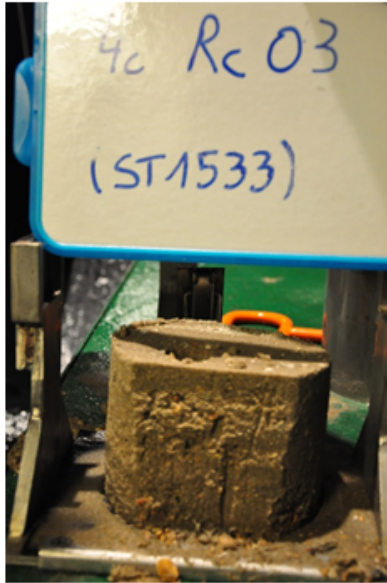
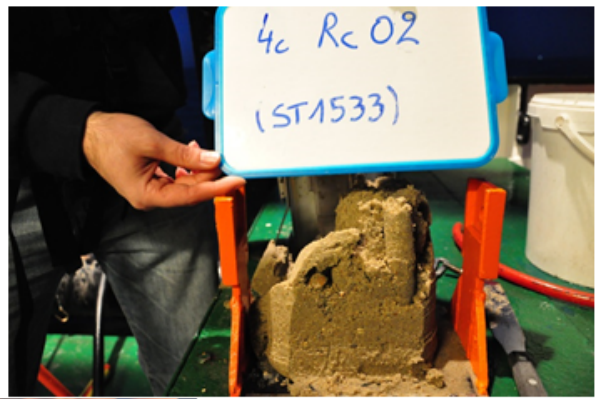
Sample H06a, b, c





Reineck Cores 4c Area 17- 12-2015 (n = 5, r = NA)





7. REMARKS

The crew of the Belgica is acknowledged for the valuable and greatly appreciated cooperation.

8. DATA STORAGE

All raw multibeam data from the Belgica EM3002D is stored by FPS Economy – Continental Shelf Department. For all information contact Koen Degrendele

Seabed samples – Coast, Hinder Banks - Barchan area, and Hinder Banks – Sector 4c will be analyzed for grain-size distribution. Results will be stored in BMDC.

Multibeam echosounder data RBINS-OD Nature were stored on hard drive of RBINS OD Nature. Contact person VVL or GMG

Annex B

Video footage 2015

This Annex forms part of the report:

Van Lancker, V., Baeye, M., Montereale-Gavazzi, G. & Van den Eynde, D. (2016). Monitoring of the impact of the extraction of marine aggregates, in casu sand, in the zone of the Hinder Banks. Period 1/1 - 31/12 2015 and Synthesis of results 2011-2015. Brussels, RBINS-OD Nature.

Annex B. Overview of video footage 2015

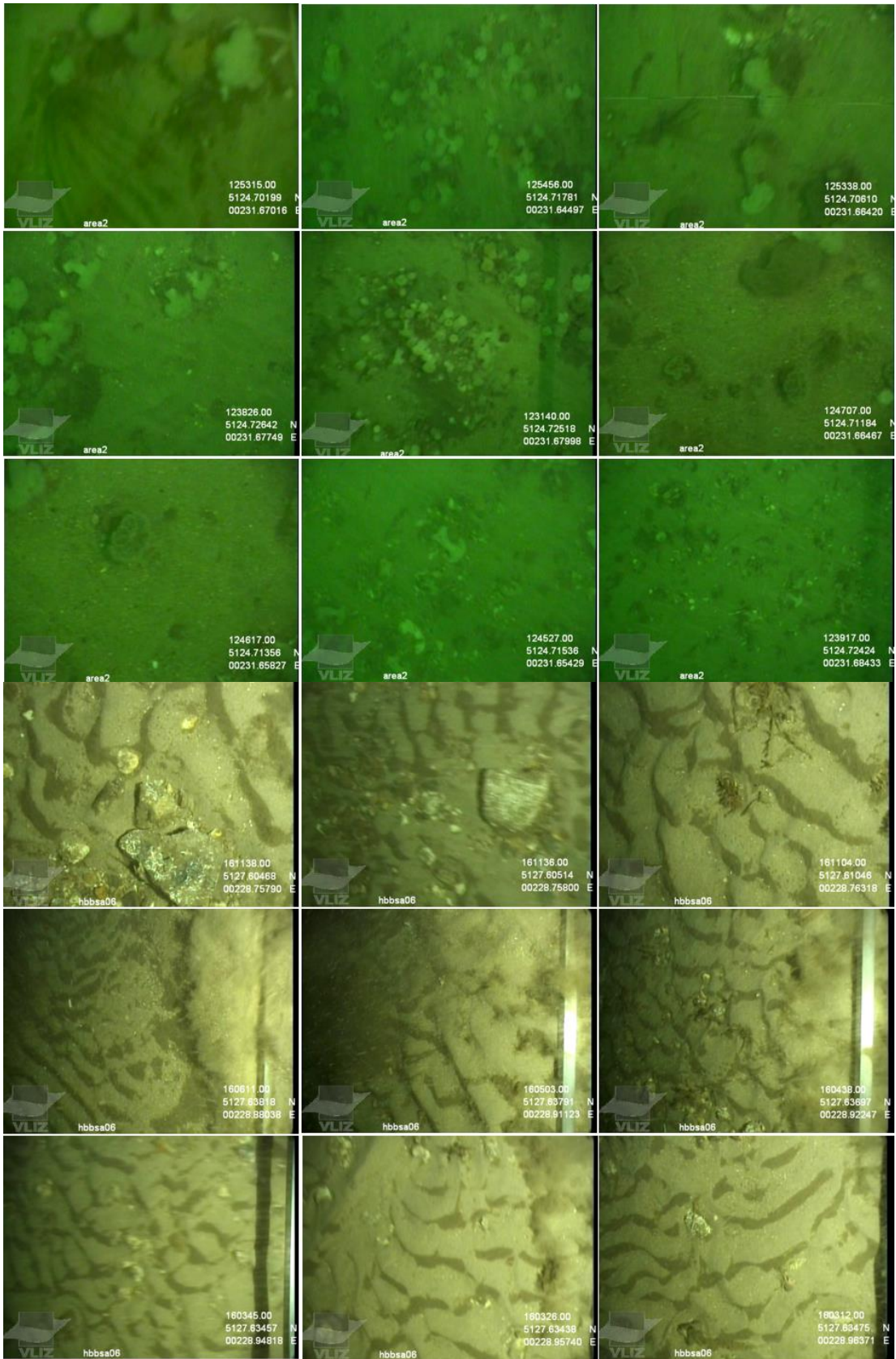
RV Belgica ST1507

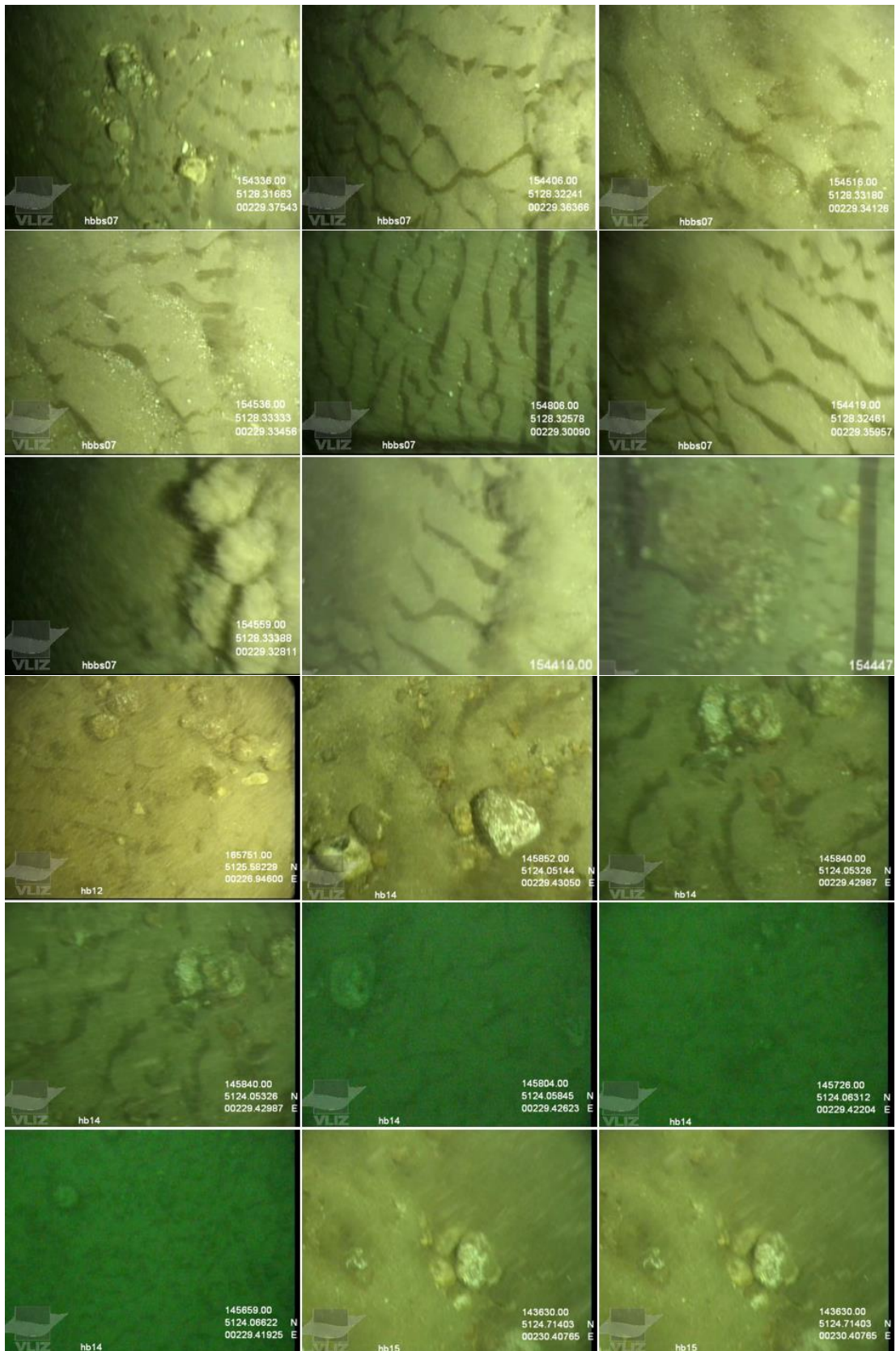


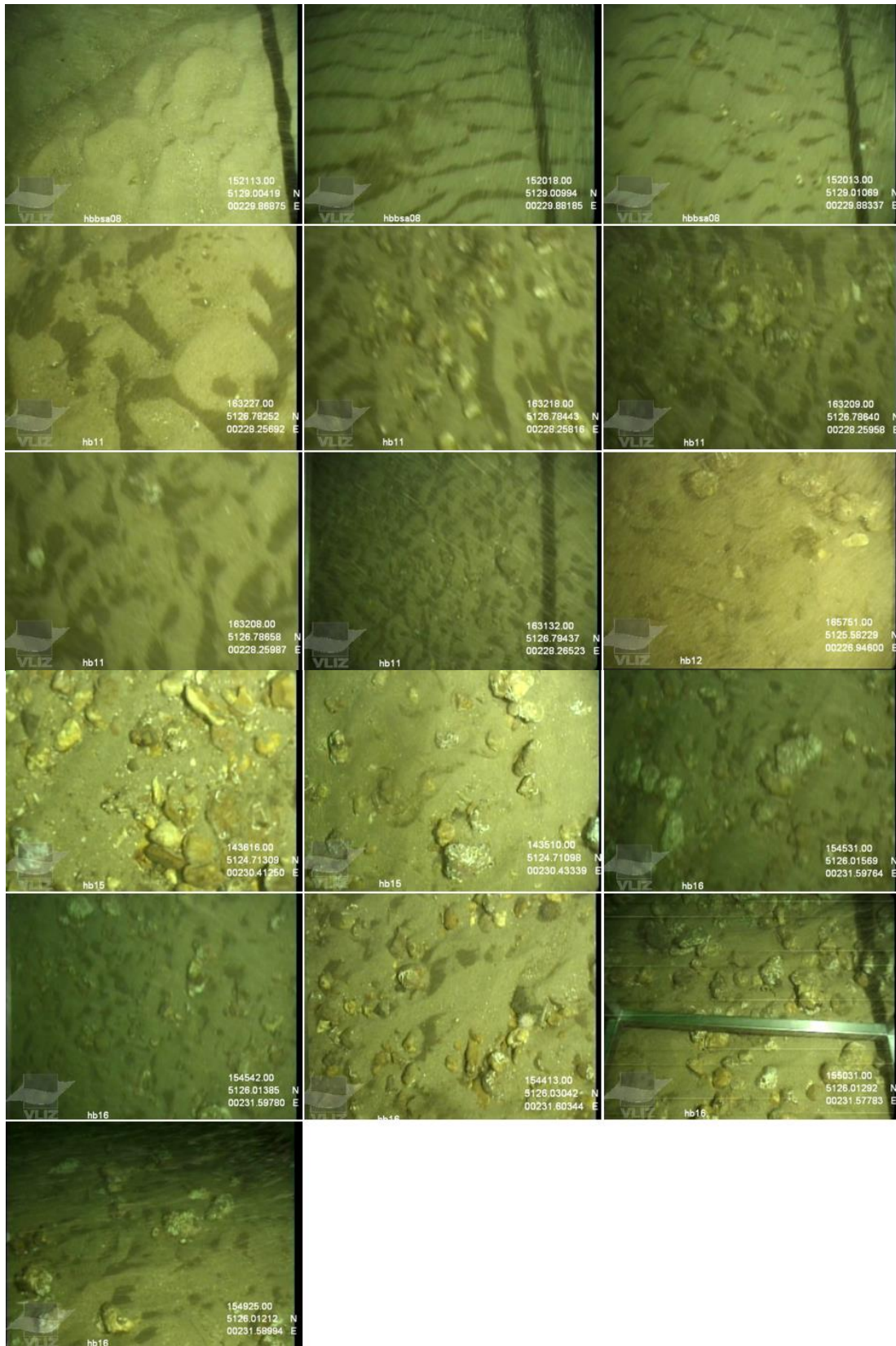
ST1507 - Overview of sampling and observations. Reineck boxcoring (dots) in Oosthinder Sector 4c (south) and Sector 4b (north); Hamon grabs (rectangles) in the gully between Westhinder and Oosthinder, as also Video imaging (triangles). Area 2 is the triangle closest to the western part of the Oosthinder sandbank and is within the main gravel bed refugium. Fisheries management area is indicated, comprising two areas, HBBSA and HBBSB, where multibeam monitoring was conducted during ST1502.

Video footage ST1507. Timestamp, coordinates and depth of the observations. Coordinates are corrected for gear position relative to antenna.

id	gear	Timestamp	start/end	wg84_x_f	wg84_y_f	eadepth33
Area2	Video frame	2015-03-17 12:28:00	start	467161	5695767	-34,50
Area2	Video frame	2015-03-17 13:34:00	end	467161	5695810	-33,22
hb15	Video frame	2015-03-18 14:32:00	start	465797	5695734	-33,07
hb15	Video frame	2015-03-18 14:41:00	end	465621	5695773	0,00
hb14	Video frame	2015-03-18 14:54:00	start	464560	5694574	0,00
hb14	Video frame	2015-03-18 15:04:20	end	464580	5694406	0,00
hb16	Video frame	2015-03-18 15:38:00	start	467102	5698245	0,00
hb16	Video frame	2015-03-18 15:52:00	end	467054	5698131	0,00
hbbsb04	Video frame	2015-03-18 16:17:20	start	469137	5700566	0,00
hbbsb04	Video frame	2015-03-18 16:21:20	end	469163	5700499	0,00
hbbsa08	Video frame	2015-03-19 15:17:30	start	465178	5703735	-37,54
hbbsa08	Video frame	2015-03-19 15:24:30	end	465164	5703673	0,00
hbbsa07	Video frame	2015-03-19 15:41:10	start	464626	5702393	0,00
hbbsa07	Video frame	2015-03-19 15:47:50	end	464477	5702454	-38,37
hbbsa06	Video frame	2015-03-19 16:01:10	start	464126	5701171	0,00
hbbsa06	Video frame	2015-03-19 16:13:10	end	463828	5701097	-32,98
hb11	Video frame	2015-03-19 16:27:40	start	463289	5699647	-32,68
hb11	Video frame	2015-03-19 16:35:40	end	463202	5699540	0,00
hb12	Video frame	2015-03-19 16:53:40	start	461707	5697358	-33,34
hb12	Video frame	2015-03-19 17:01:40	end	461699	5697279	-32,68







RV Belgica ST1517

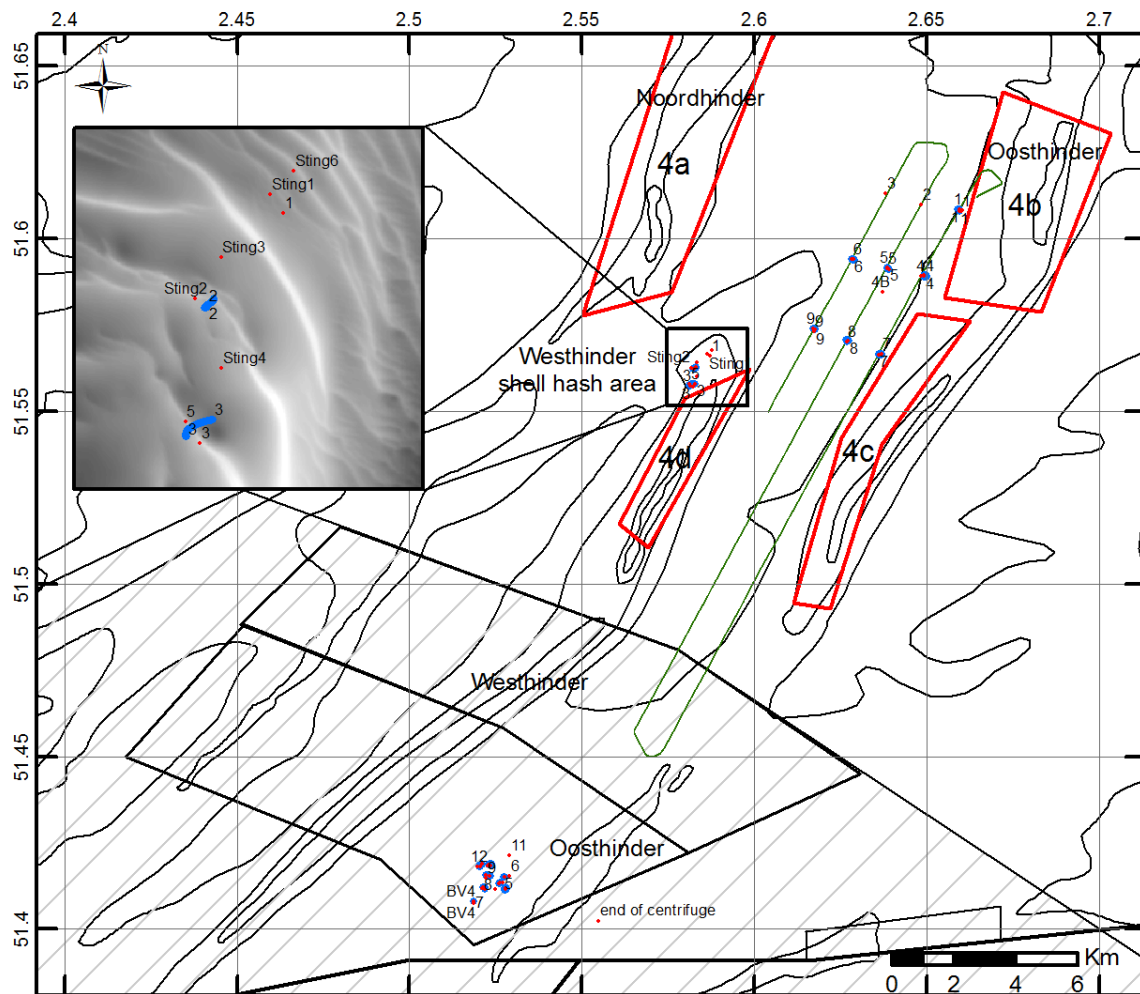
ST1517 - List of video recordings near Sector 4B (in gully west of Oosthinder sandbank)

ID	Start			End		
	Date and time	Latitude	Longitude	Date and time	Latitude	Longitude
4B09	2015-06-24 09:31:23	51.57380232	2.617141217	2015-06-24 09:34:49	51.5735845	2.617553967
4B08	2015-06-24 09:47:35	51.57033082	2.62728475	2015-06-24 09:54:52	51.57010548	2.626838433
4B07	2015-06-24 10:13:00	51.56615182	2.6360087	2015-06-24 10:20:40	51.5664388	2.636766567
4B04	2015-06-24 10:52:36	51.58936348	2.649444333	2015-06-24 10:59:00	51.58903122	2.649026483
4B05	2015-06-24 11:15:32	51.59147568	2.638512167	2015-06-24 11:20:20	51.59101638	2.639121
4B06	2015-06-24 11:40:20	51.59382833	2.628854117	2015-06-24 11:48:00	51.5939963	2.628571067
4B01	2015-06-24 12:06:00	51.60836577	2.65971705	2015-06-24 12:18:55	51.60803845	2.659661867

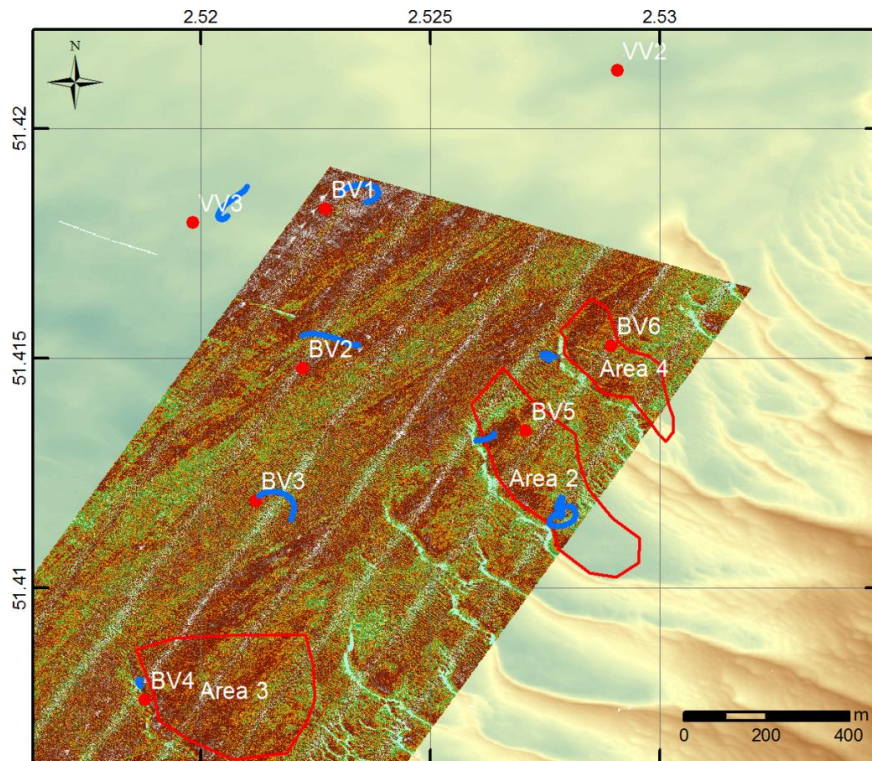
ST1517 - List of video recordings in the barchan dune area, west of southern Oosthinder sandbank

ID	Start			End		
	Date and time	Latitude	Longitude	Date and time	Latitude	Longitude
VV3	2015-06-25 09:47:45	51.41798108	2.520508317	2015-06-25 09:54:10	51.41868363	2.520824933
BV1	2015-06-25 10:09:35	51.41849288	2.523221583	2015-06-25 10:17:13	51.41829618	2.5234754
BV2	2015-06-25 10:29:47	51.4151825	2.523302717	2015-06-25 10:36:00	51.41537107	2.522256467
BV3	2015-06-25 10:50:49	51.41194433	2.521446483	2015-06-25 10:59:00	51.41135483	2.522032933
BV4	2015-06-25 11:12:18	51.40790468	2.51883595	2015-06-25 11:15:00	51.40784632	2.518896733
BV5	2015-06-25 11:30:15	51.41335805	2.5265892	2015-06-25 11:37:00	51.4132122	2.526198583

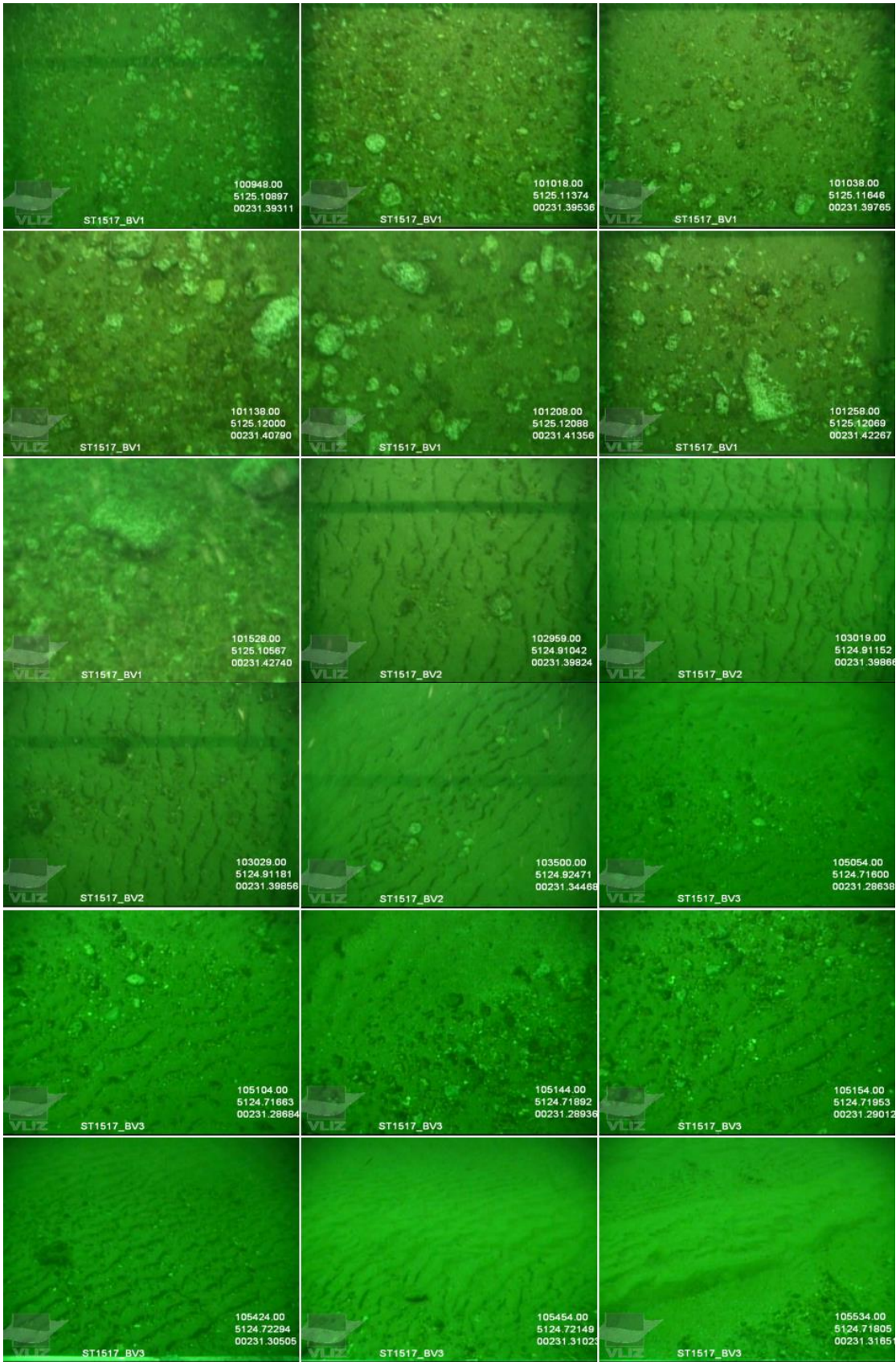
BV6	2015-06-25 11:48:50	51.41508167	2.527557367	2015-06-25 11:52:15	51.4150725	2.527911117
REMUS contact 'Sonia 1' = Area 2	2015-06-25 12:06:33	51.41180852	2.52797165	2015-06-25 12:27:17	51.41173375	2.52785645

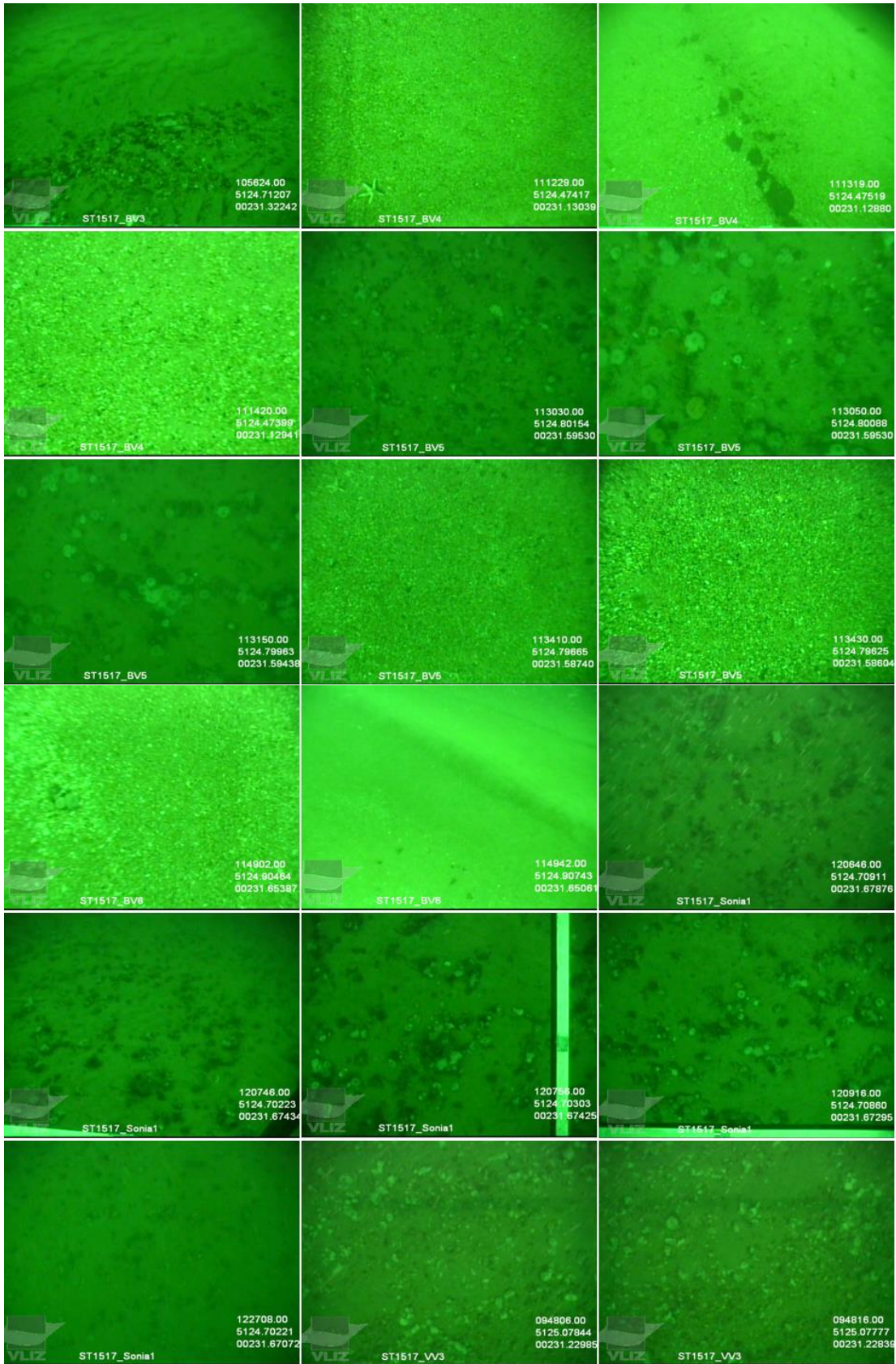


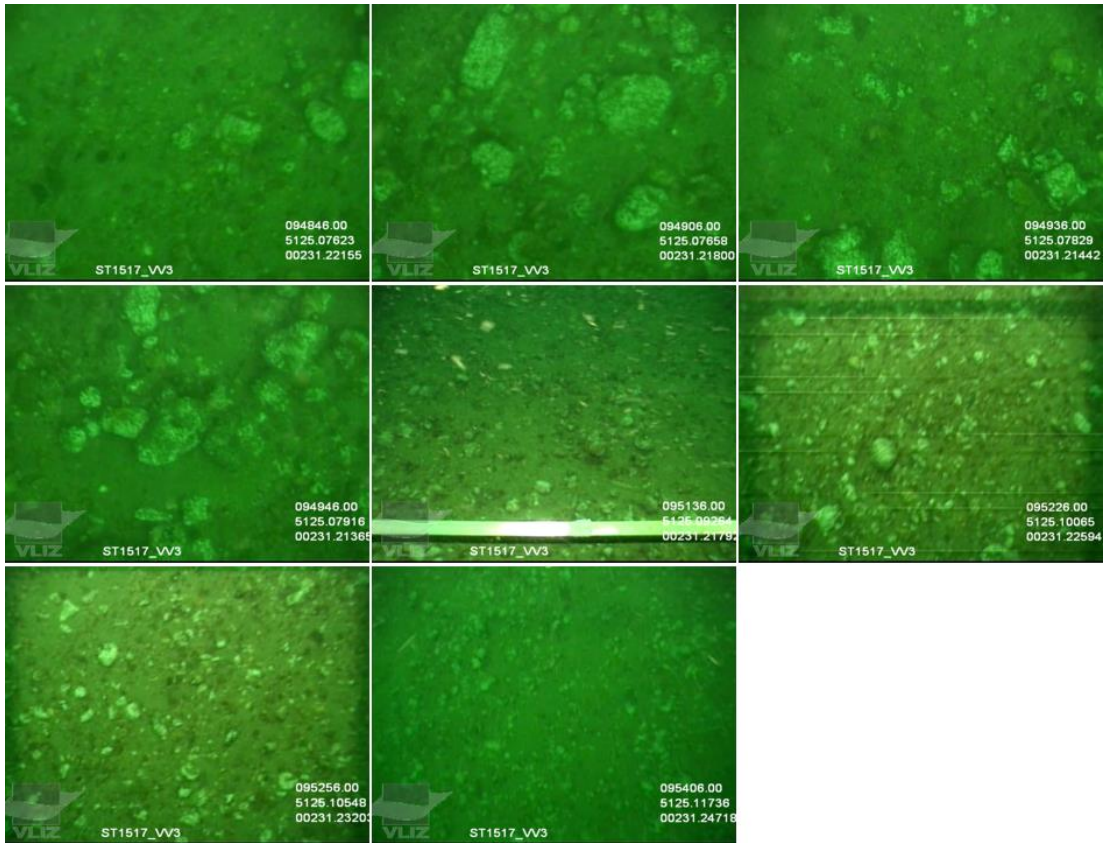
ST1517 - Overview of the samples and observations in the Hinder Banks area: Hamon grabs and Sting penetration tests (red); video imaging (blue) and multibeam echosounding (green). Insert: detailed view of the Westhinder shell hash area. Further indicated: marine aggregate extraction sectors (4a to 4d; red); Habitat Directive Area (hashed) and fisheries management areas (black polygons).

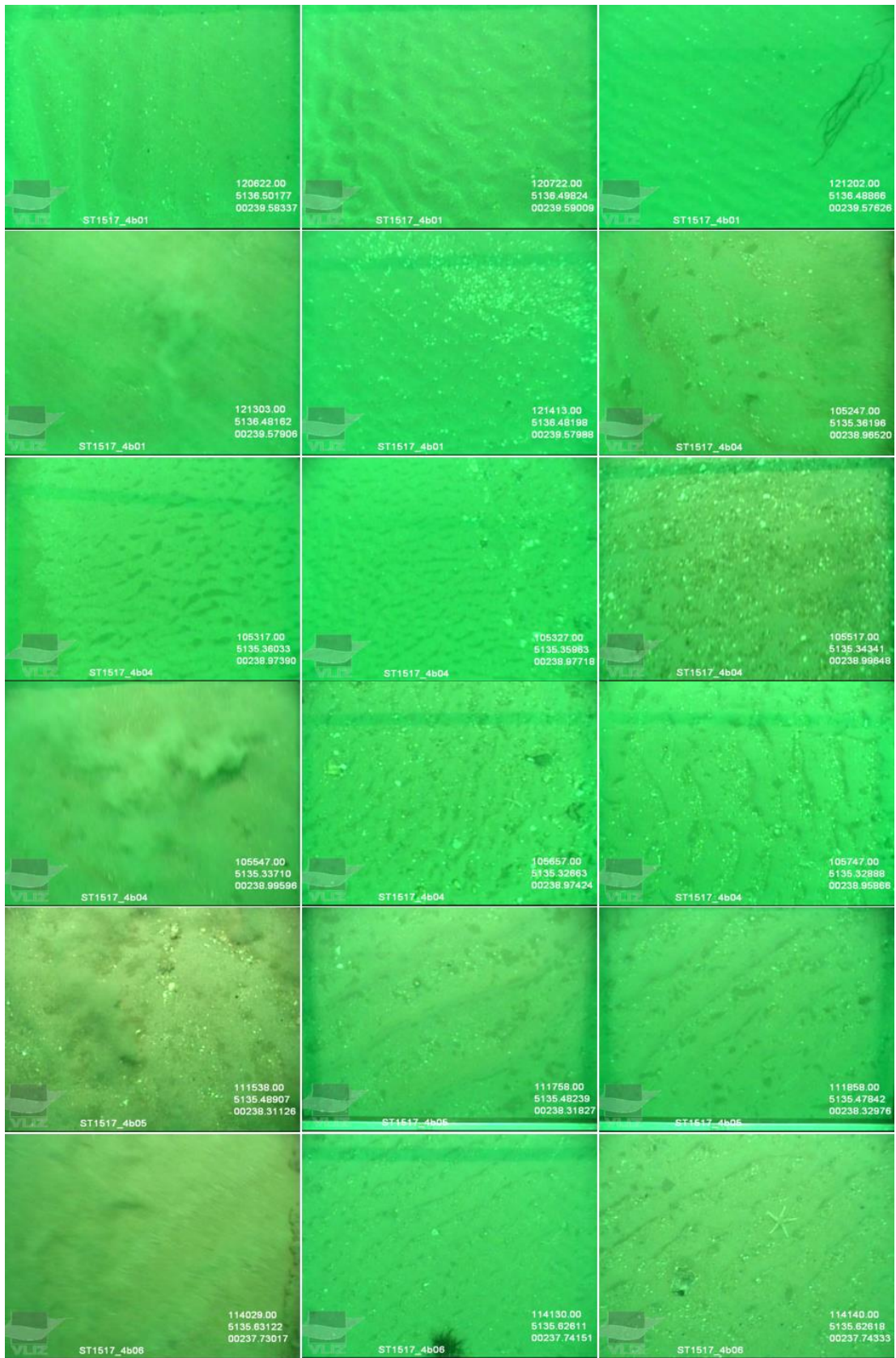


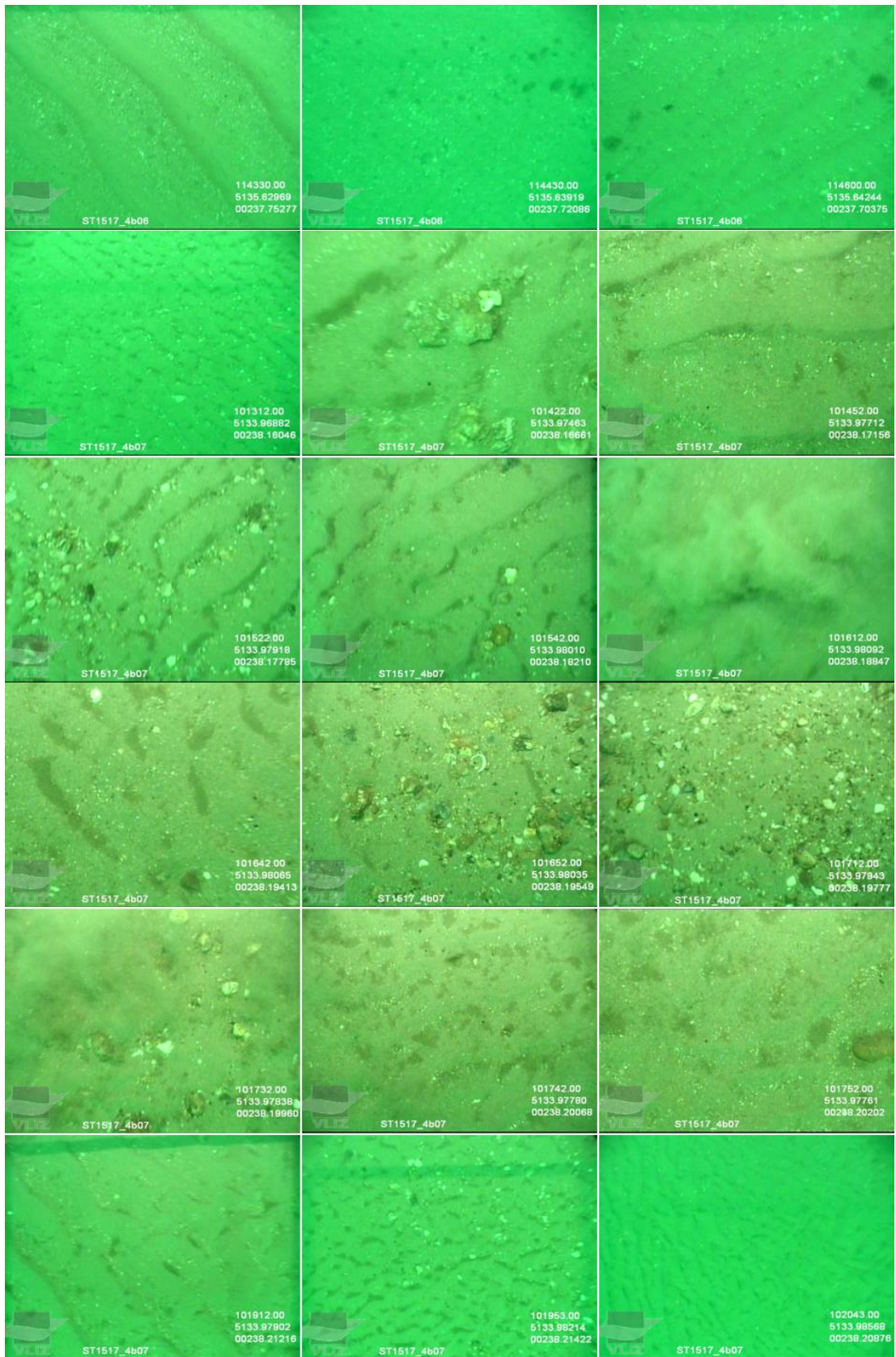
Detailed view of the samples (red) and video observations (blue) in the barchan dune area, west of the southern part of the Oosthinder sandbank. Area 2, 3 and 4 represent areas of higher biodiversity.

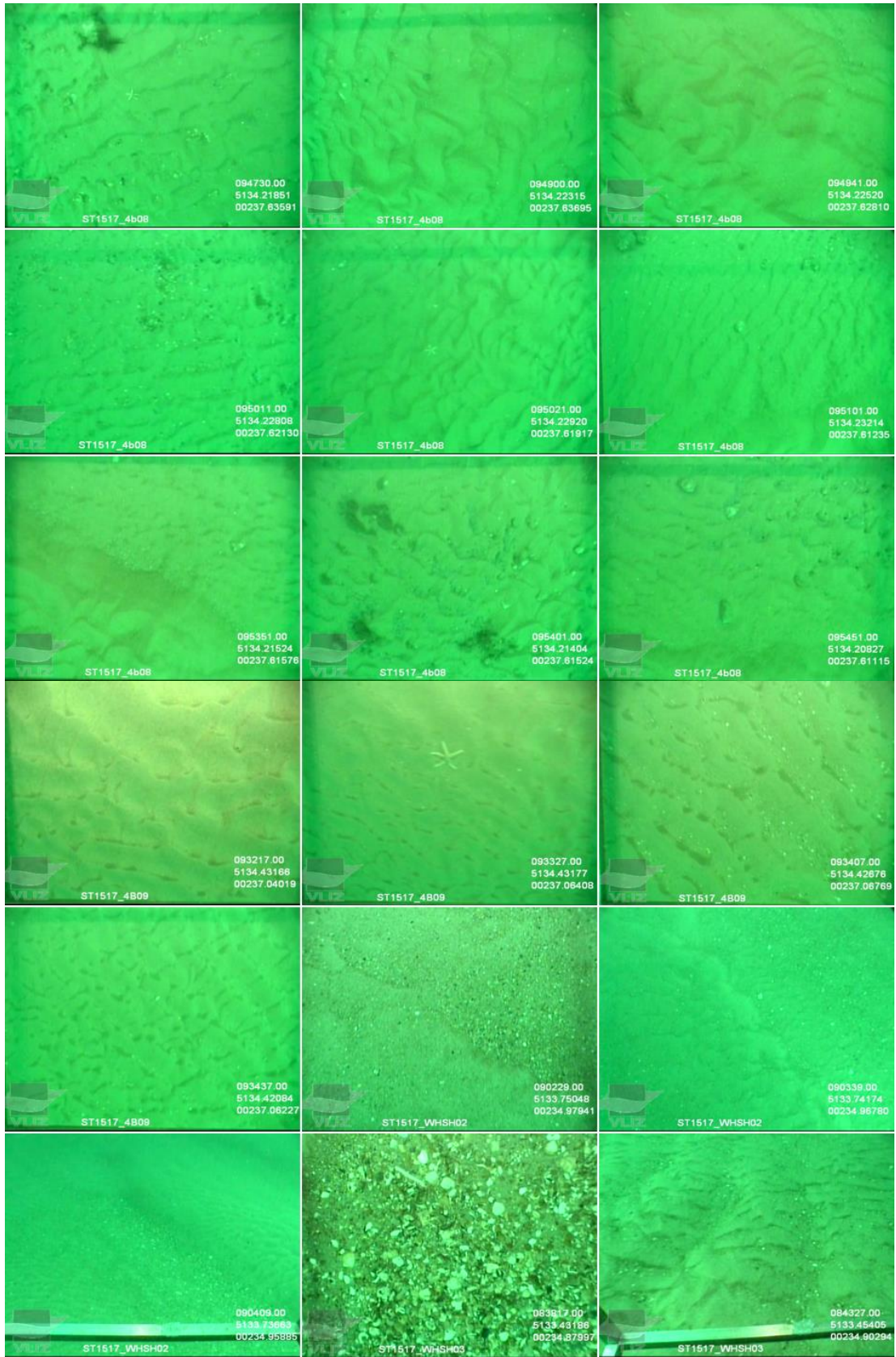








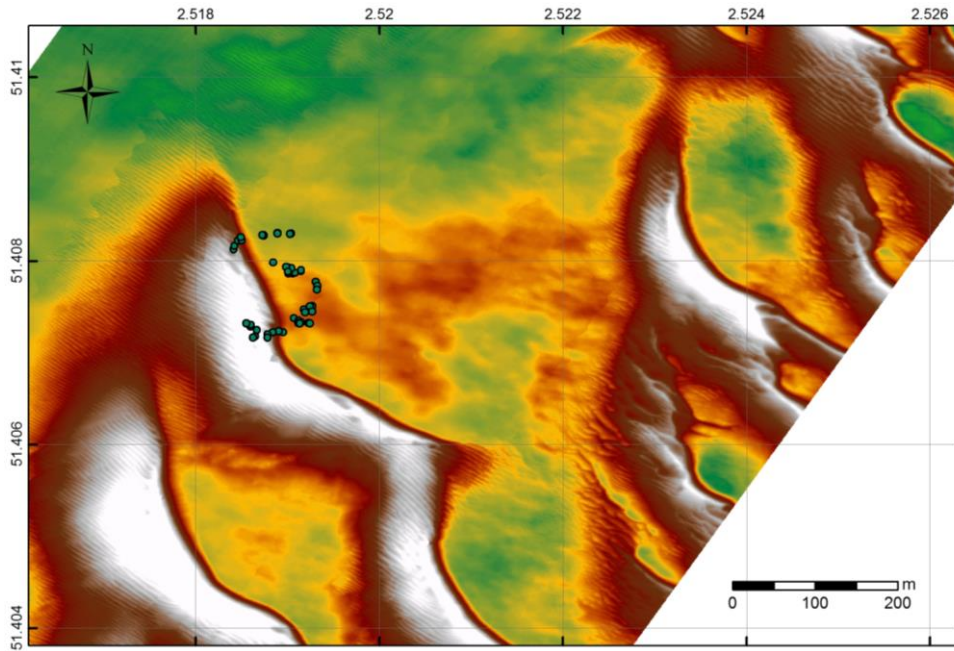




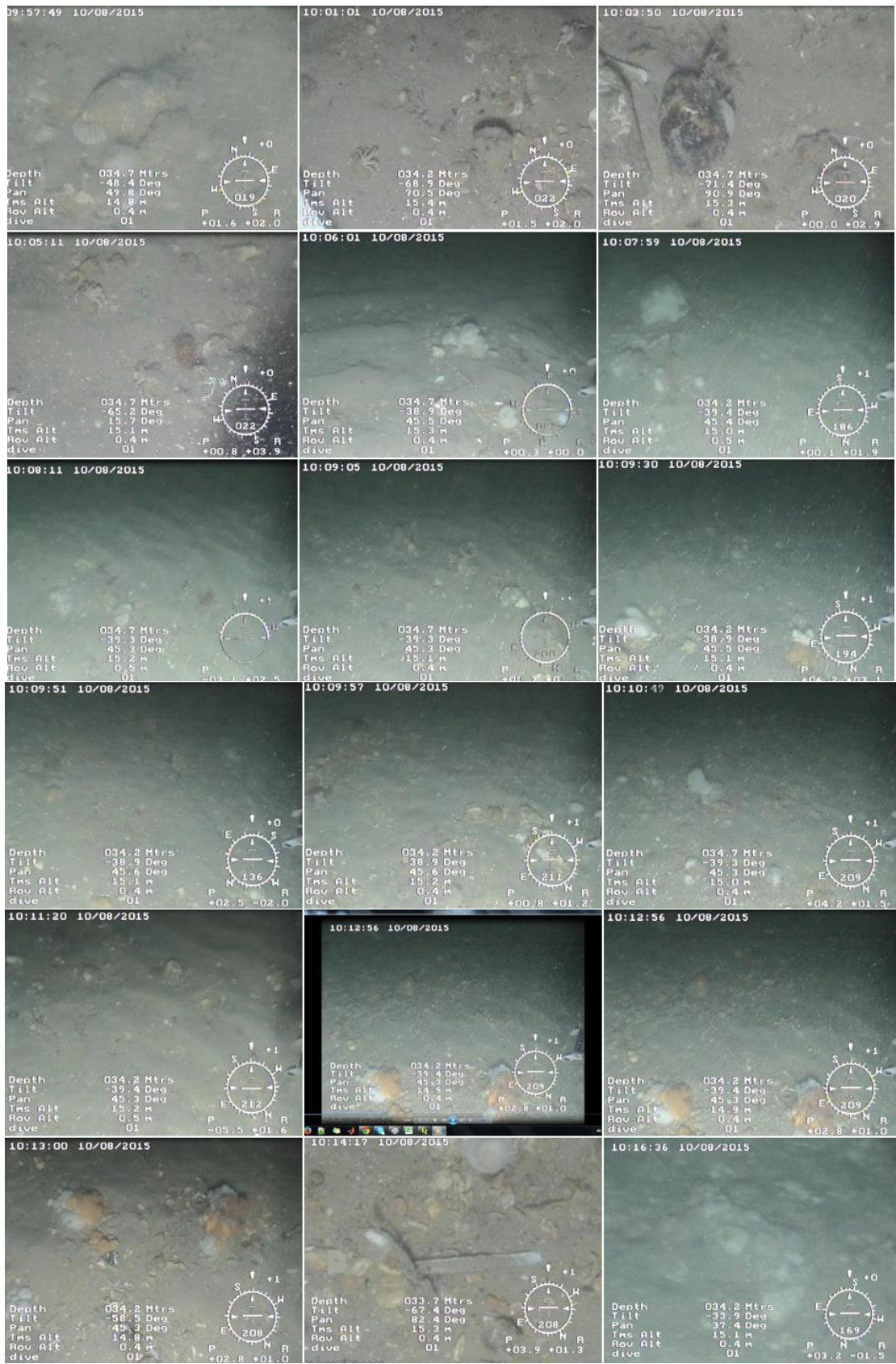
RV Simon Stevin – GENESIS ROV

Visual observations in the Habitat Directive area (Area 4) with GENESIS ROV, deployed from RV Simon Stevin.

Period	Equipment	Platform	Modus
2015-08-10	ROV GENESIS	RV Simon Stevin cruise SS15-540	Drift



Track of the ROV GENESIS (deployed from RV Simon Stevin on 10/08/2015) in area 4, the southernmost gravel bed area.



RV Belgica ST1533

ST1533 – Video footage. Positions are in WGS84. Upper images: 1 and 2; lower images 3 and 4.

id_short	gear	utc_from	depth	X	Y	
ST1533_1	Videoframe	2015-12-17 07:37:27	-32.69	2.5485575	51.4358635	start
ST1533_1	Videoframe	2015-12-17 07:45:42	-32.3	2.5484968	51.43605512	end
ST1533_2	Videoframe	2015-12-17 08:01:17	-29.3	2.5396268	51.4245116	start
ST1533_2	Videoframe	2015-12-17 08:08:10	-29.5	2.5410784	51.42423592	end
ST1533_3	Videoframe	2015-12-17 08:28:16	-32.8	2.5235835	51.4088131	start
ST1533_3	Videoframe	2015-12-17 08:37:17	-33.1	2.5250356	51.40924772	end
ST1533_4	Videoframe	2015-12-17 08:44:49	-32.9	2.5203316	51.4082728	start
ST1533_4	Videoframe	2015-12-17 08:58:52	-33	2.5199694	51.4090538	end



Annex C

This Annex forms part of the report:

Van Lancker, V., Baeye, M., Montereale-Gavazzi, G. & Van den Eynde, D. (2016). Monitoring of the impact of the extraction of marine aggregates, in casu sand, in the zone of the Hinder Banks. Period 1/1 - 31/12 2015 and Synthesis of results 2011-2015. Brussels, RBINS-OD Nature.

ROYAL BELGIAN INSTITUTE FOR NATURAL SCIENCES
OPERATIONAL DIRECTORATE NATURAL ENVIRONMENT

Section Ecosystem Data Analysis and Modelling
Suspended Matter and Sea Bottom Modelling and Monitoring Group (SUMO)
and
Management Unit of the North Sea Mathematical Models (MUMM)



The impact of extraction on the bottom shear stress in Zone 4

Dries Van den Eynde

ZAGRI-MOZ4-INDI67/1/DVDE/201604EN/TR01

Prepared for the ZAGRI and MOZ4 projects

Prepared for the INDI67 project

RBINS-OD Nature
100 Gulledelle
B-1200 Brussels
Belgium

Table of Contents

1. INTRODUCTION	3
2. NUMERICAL MODELS.....	4
2.1. INTRODUCTION	4
2.2. HYDRODYNAMIC MODEL OPTOS-FIN.....	4
2.3. WAVE MODEL WAM.....	5
2.4. CALCULATION OF THE BOTTOM SHEAR STRESS	5
2.4.1. <i>Introduction</i>	5
2.4.2. <i>Bottom stress under the influence of currents</i>	6
2.4.3. <i>Bottom shear stress under the influence of waves</i>	7
2.4.4. <i>Bottom shear currents under influence of currents and waves</i>	7
2.4.5. <i>Calculation of the bottom roughness</i>	8
3. ADCP MEASUREMENTS OF CURRENTS AND BOTTOM STRESS.....	10
3.1. CURRENT AND WATER DEPTH MEASUREMENTS.....	10
3.2. MEASUREMENTS OF THE BOTTOM SHEAR STRESS	11
4. VALIDATION OF THE HYDRODYNAMIC AND WAVE MODEL RESULTS.....	13
4.1. TOTAL WATER DEPTH	13
4.2. DEPTH-AVERAGED CURRENTS	13
4.2.1. <i>Wave height</i>	17
5. VALIDATION OF THE BOTTOM SHEAR STRESS MODEL RESULTS.....	19
5.1. BOTTOM STRESS CALCULATION	19
5.2. VALIDATION OF THE MODEL RESULTS	24
5.2.1. <i>Bottom shear stress with constant bottom roughness</i>	24
5.2.2. <i>Bottom shear stress with bottom roughness calculated</i>	26
5.3. INFLUENCE OF WAVES ON BOTTOM SHEAR STRESS	28
5.4. CONCLUSIONS	29
6. MODELLING THE EFFECT OF EXTRACTION ON BOTTOM STRESS.....	31
6.1. INTRODUCTION	31
6.2. SIMULATIONS	31
6.3. RESULTS.....	33
6.3.1. <i>Scenario 1</i>	33
6.3.2. <i>Scenario 2</i>	36
6.3.3. <i>Scenario 3</i>	39
6.3.4. <i>Conclusions</i>	43
7. CONCLUSIONS	44
8. REFERENCES.....	47

1. Introduction

In the Belgian implementation of the European Marine Strategy Framework Directive (Belgian State, 2012), it was stated that human impacts need consideration when the bottom shear stress, calculated with a validated numerical model, changes with more than 10% at a specified distance of the activity. In this report, the impact of extraction of marine aggregates in zone 4, Hinder Banks, is evaluated with this respect.

Since in the Belgian implementation, it is explicitly stated that the evaluation has to be executed with a validated numerical model, an evaluation of the quality of the bottom shear stress models is executed in a first part of the report. In a first section, the numerical models are described. The hydrodynamic model that is used to calculate the currents and the wave model, calculating the significant wave height are presented. Furthermore, four different models, that are found in literature to calculate the bottom shear stress under the influence of currents and waves are shortly discussed.

In the second section, the measurement at the Hinderbanks are described. In this study, acoustic doppler current profiler (ADCP) data are used to calculate the bottom shear stress from the logarithmic profile of the currents in the lower part of the water column. Five measurement campaigns were executed at two stations in the Hinder Banks area.

In the next two sections, the validation of the hydrodynamic and wave model and of the bottom shear stress models are discussed. The bottom shear stress measurements are analysed first to enable a comparison with the model data. The quality of the bottom shear stress models is assessed, both when using a constant bottom roughness, or when calculating the bottom roughness with an empirical model. Finally the influence of the waves on the bottom shear stress in the Hinder Banks area is evaluated.

In the second part of the report, the impact of large-scale extraction of marine aggregates is evaluated. Three different scenarios of extraction are modelled and the effect on the bottom shear stress in the area is assessed.

Some conclusions are formulated in the last section.

2. Numerical models

2.1. *Introduction*

To calculate the bottom shear stress under the influence of the currents and the waves, numerical models are used. A three-dimensional hydrodynamic model is used for the calculation of the water elevations and the currents. A third generation wave model is used to calculate the waves. Both models will be discussed shortly.

Furthermore, different methods and models are available in literature to calculate the bottom shear stress from the currents and waves. The different models that are used in this study, together with the models to calculate the bottom roughness under the influence of bottom ripples and bed load, are discussed in the next section.

2.2. *Hydrodynamic model OPTOS-FIN*

The three-dimensional hydrodynamic modelling software COHERENS calculates the currents and the water elevation under the influence of the tides and the atmospheric conditions. The model was developed between 1990 and 1998 in the framework of the EU-MAST projects PROFILE, NOMADS and COHERENS. The hydrodynamic model solves the momentum equations and the continuity equation with, if necessary, equations for the sea water temperature and salinity. The momentum and continuity equations are solved using the ‘mode splitting’ technique. COHERENS disposes over different turbulent closures. A good description of the turbulence is necessary for a good simulation of the vertical profile of the currents. A new version of the COHERENS software has been developed recently (Luyten *et al.*, 2014), mainly allowing the model to use parallel computing, while adding also some new features, such as improving the numerical scheme and adding a wetting-drying mechanism.

The model OPTOS-FIN is based on this COHERENS code and is implemented on the Belgian Continental Shelf with a grid with a resolution of 14.29'' in longitude (272 to 278 m) and 8.33'' in latitude (257 m). This model has a 10 σ -layers distributed over the total water depth. Along the open boundaries, the OPTOS-FIN model is coupled with three regional models. The OPTOS-CSM model comprises the entire Northwest European Continental Shelf and calculates the boundary conditions of the North Sea model OPTOS-NOS. The latter model calculates the boundary conditions of the OPTOS-BCZ model, which is implemented for the Belgian waters with a 3 times coarser resolution than the OPTOS-FIN model. The OPTOS-CSM model calculates the depth-averaged currents and is driven by the water elevations at the open sea boundaries, using four semi-diurnal and four diurnal constituents. The bathymetry of OPTOS-FIN model is shown in Figure 1.

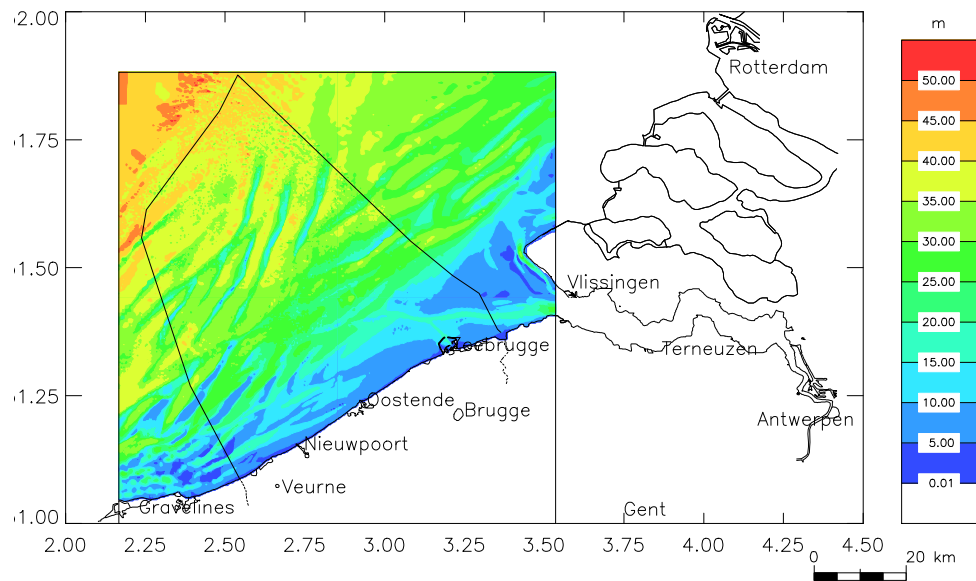


Figure 1: Bathymetry of the OPTOS-FIN model.

The OPTOS-FIN model was validated in the framework of the Marebasse project (Van den Eynde *et al.*, 2010) and the BOREAS project (Mathys *et al.*, 2012). More recently a first validation was executed of the model in the Hinder Banks area, using bottom-mounted ADCP results, hull-mounted ADCP measurements and Wave Glider measurements (Van den Eynde *et al.*, 2014).

2.3. Wave model WAM

The WAM model is a third generation wave model, developed by the WAMDI Group (1988) and described by Günther *et al.* (1992). The WAM model is used both for research and for operational wave forecasting. It includes 'state-of-the-art' formulations for the description of the physical processes involved in the wave evolution. In comparison with the 2nd generation model, the wave spectrum has no restrictions and the wind sea and the swell spectrum are not treated separately.

At the Operational Directorate Natural Environment, the model is running on three coupled model grids. A coarse model grid comprises the entire North Sea, the Fine model models the central North Sea and the Local model calculates the waves in the Southern Bight. The local model has a grid resolution of 0.033° in latitude and 0.022° in longitude. The bathymetry of this local model grid is presented in Figure 2.

2.4. Calculation of the bottom shear stress

2.4.1. Introduction

The calculation of the bottom shear stress is the topic of much research. The bottom shear stresses under the influence of currents alone and under the influence of waves alone over a flat bed are quite well known. However, the calculation of the bottom shear stress under the combined influence of currents and waves, over a

rippled sea bed is complex. First of all, the calculation of the bottom shear stress under the influence of currents and waves is not the simple vector addition of the bottom stress vectors for the currents and the waves alone. Non-linear interactions increase the mean bottom shear stress.

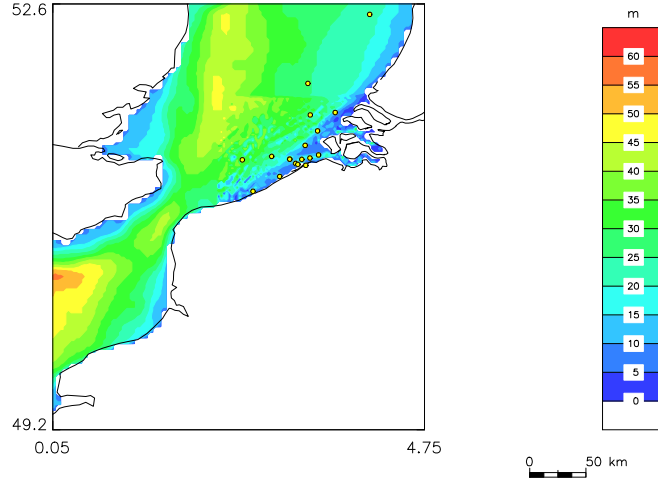


Figure 2: Model grids of the local grid WAM model. The dots indicate the position of the measuring points.

Furthermore, the bottom roughness length, which is an important factor for the calculation of the bottom shear stress, is influenced by different factors. At the bottom itself, the roughness is a function of the grain size. This bottom shear stress, felt by the sediments is called the skin friction. However, at a distance more than a tenth of the length of the bottom ripples, the bottom roughness is also influenced by the bed load and by the height and the length of the bottom ripples. Further away from the bottom, a new logarithmic profile is followed with an apparently increased bottom roughness. The ratio between the skin bottom roughness and the total bottom roughness varies between 1.5 and 20.

In the next sections the bottom shear stress under the influence of the currents, under the influence of the waves and under the influence of the combined effect of currents and waves are discussed separately. Furthermore, also the calculation of the bottom roughness length is discussed in a following section.

The WAM model was recently validated by Van den Eynde (2013).

2.4.2. Bottom shear stress under the influence of currents

The bottom shear stress under the influence of currents can be written as:

$$\tau_c = \rho C_D \bar{u}^2 = \rho \left(\frac{\kappa}{\ln \frac{h}{ez_0}} \right)^2 \bar{u}^2 = \rho u_*^2 \quad (1)$$

with τ_c bottom shear stress under the influence of currents
 C_D drag coefficient

\bar{u}	depth-averaged current
h	water depth
e	2.7182
u_*	shear velocity

As stated above, for the bottom roughness length, a difference has to be made between the skin bottom roughness, felt by the grains itself at the bottom, and the total bottom roughness that is felt by the currents and that is also influenced by the bottom load and by the bottom ripples.

2.4.3. Bottom shear stress under the influence of waves

The bottom shear stress under the influence of waves is calculated using the (maximum) orbital velocity at the bottom. Using linear wave theory, the maximal orbital velocity of a monochromatic wave can be calculated as:

$$u_w = \frac{\pi h_s}{T \sinh(kh)} \quad (2)$$

with	h_s	significant wave height
	T	wave period
	k	wave number

When calculating the wave orbital velocity of a wave spectrum, most of the time the significant wave height and the mean water period are taken as characteristics, although some other recommendations can be found in literature. The wave orbital excursion A can be calculated as:

$$A = \frac{u_w T}{2\pi} \quad (3)$$

The (maximum) bottom shear stress under the influence of waves is then calculated as:

$$\tau_w = \frac{1}{2} \rho f_w u_w^2 \quad (4)$$

with	τ_w	bottom shear stress under the influence of waves
	f_w	wave factor

Also for the wave factor, different theories or models are available, however, with relative small differences.

2.4.4. Bottom shear stress under the influence of currents and waves

For the calculation of the bottom shear stress under the influence of currents and waves, many different models can be found in literature, varying from simple models to very complex iterative models, resolving the stresses in the wave boundary layer and during a complete wave cycle. These very complex models are however very time consuming and not really useful to be used in sediment

transport models. In Van den Eynde en Ozer (1993), different simple models were compared with each other and with the results of more complex models, as they were presented in Dyer and Soulsby (1988). The Bijker (1966) model was selected as a good model, giving realistic model results. This model however does not give realistic results for the bottom shear stress under the influence of waves with very small currents. Additionally, no formulation was given for the mean bottom shear stress over a wave cycle. Therefore, this model is not used in this study.

Recently, more realistic and simple models for the combined bottom shear stress were proposed in literature. Therefore, three new formulations were implemented and tested.

First of all, the Soulsby (1995) formulae were implemented which were the results of a two-coefficient optimisation of a simple model to 131 data points, from more complex theoretical models.

More recently, Soulsby and Clarke (2005) developed a new model, assuming an eddy viscosity varying over the water column, but constant in time. The eddy viscosity varies linearly above the bottom in the thin wave boundary layer and has a parabolic function outside the wave boundary layer. Remark that the eddy viscosity is much higher in the thin wave boundary layer than outside. Furthermore, the eddy viscosity in the wave boundary layer is only a function of waves and currents, so that no iterative calculations are needed.

In the wave boundary layer, the shear stress is constant, outside the wave boundary layer, the shear stress varies linearly, to zero at the water surface. A current profile can be calculated by integration of the current profile over the water depth, giving a quadratic equation that can be used to solve the bottom shear stress. The model of Soulsby and Clarke (2005) gives both a formulation for the maximal bottom shear stress during a wave cycle, and the mean bottom shear stress, averaged over a wave cycle. Furthermore, the theory was developed, both for flow over rough and over smooth bottom.

Finally, Malarkey and Davies (2012) developed the theory of Soulsby and Clarke further to include additional non-linearity in the model, which is present in the more complex theoretical models, but is not found in the Soulsby-Clarke model.

More information and some comparison of the results of the different models can be found in Van den Eynde (2015).

2.4.5. Calculation of the bottom roughness

As indicated above, the bottom shear stress under the influence of currents and waves is a function of the bottom roughness length z_o (for turbulent flow with a rough bottom). A division has to be made between the bottom roughness length at the bottom itself, the skin bottom roughness, caused by the bottom material itself, and the total roughness, felt by the currents and the waves, which are also influenced by the bottom load and the bottom ripples. The skin and the total bottom roughness can be specified by the user itself, or can be calculated by a model. The bottom roughness length, the height above the bottom where the logarithmic current profiles becomes zero, is normally written as a function of the Nikuradse bottom roughness k_s , of the viscosity of the water ν and the friction velocity:

$$z_0 = \frac{k_s}{30} + \frac{\nu}{9u_*} \quad (5)$$

For hydrodynamically rough flows (as is the case for flows over a sandy bed), the second part of the bottom roughness length can be neglected.

The skin bottom roughness is mostly written as a function of the grain-size distribution. A much used formulation is:

$$k_{ss} = 2.5d_{50} \quad (6)$$

with d_{50} the grain size for which 50% is smaller.

Values for the total bottom roughness can be found in tables. Typical values, found in literature, are $k_s=0.2$ mm for a mud bottom or $k_s=6$ mm for a rippled sand bottom. They can however be calculated in the model itself.

For the roughness as a function of the bottom load, a division is made between current-domination and wave-domination. For current-domination, the formula, proposed by Wilson (in Soulsby, 1997) is used. For wave-domination, five different possibilities were implemented, which are: 1) the Grant and Madsen (1982) model; 2) the Soulsby model; 3) the Grant and Madsen (1982) model, assuming wave-domination; 4) the Nielsen model and 5) the Raudkivi formulation (all in Soulsby, 1997). For the exact formulations, the reader is referred to Soulsby (1997).

Finally, the bottom roughness length is a function of the bottom ripples. Normally the bottom roughness, due to bottom ripples is written as:

$$k_{sv} = 27.7 \frac{\eta^2}{\lambda} \quad (7)$$

with η the ripple height
 λ the ripple length

The ripple geometry itself can be calculated by the model again. Also here, a distinction is made between current-dominated ripples and wave-dominated ripples. Two models to calculate the ripple geometry were implemented. The first model uses the ripple geometry, proposed by Soulsby (1997) for the current-dominated ripples and the ripple geometry, proposed by Grant and Madsen (1982) for the wave-dominated ripples. More recently, a new ripple predictor was proposed by Soulsby and Whitehouse (2005). The model was validated against many laboratory and field experiment results and has the advantage that the time evolution of the ripples can be accounted for. Furthermore, for the current-dominated ripples, sheet flow and ripples that are washed out under larger currents are taken into account.

Again more information and some comparison of the results of the different models can be found in Van den Eynde (2015).

3. ADCP measurements of currents and bottom stress

3.1. Current and water depth measurements

For the validation of the bottom shear stress in the Hinder Banks area, different measurement campaigns, using a bottom-mounted ADCP (RDI Workhorse 1200 kHz), have been executed (Van Lancker *et al.*, 2014, 2015). An overview of the different measurements is given in Table 1 and Table 2. The water depth is taken from the hydrodynamical model.

Table 1: ADCP measurements (1/2)

Code	Start	End	Latitude	Longitude	Water depth (m)
BM01	28/06/2012	04/07/2012	51°30.600'N	2°37.940'E	24.87
BM02	29/03/2013	25/04/2013	51°30.600'N	2°37.940'E	24.87
BM03	01/07/2013	03/07/2013	51°24.781'N	2°31.603'E	33.56
BM04	21/10/2013	25/10/2013	51°30.558'N	2°37.814'E	24.87
BM05	26/10/2013	17/04/2014	51°30.558'N	2°37.814'E	24.87
BM06	30/06/2014	03/07/2014	51°24.779'N	2°31.608'E	33.56
BM07	09/02/2015	05/03/2015	51°24.780'N	2°31.614'E	33.56

Table 2: ADCP measurements (2/2)

Code	Start	End	Δt (s)	#	First bin (m)	Binsize (m)
BM01	28/06/2012	04/07/2012	600	79	0.81	0.25
BM02	29/03/2013	25/04/2013	600	119	0.80	0.25
BM03	01/07/2013	03/07/2013	1.5	60	0.82	0.25
BM04	21/10/2013	25/10/2013	600	110	0.81	0.25
BM05	26/10/2013	17/04/2014	3600	30	1.52	1.00
BM06	30/06/2014	03/07/2014	600.5	110	0.81	0.25
BM07	09/02/2015	05/03/2015	2400	29	1.04	0.50

Six measuring campaigns have been executed with a bottom-mounted ADCP. During the campaign from 21/10/2013 till 17/04/2014, the settings of the ADCP changed automatically from a bin size of 0.25 m to a bin size of 1.00 m after four days. Therefore this campaign is split in two separate campaigns (BM04 and BM05). Remark that during campaign BM05, the ADCP was buried by migrating sand dunes and could not be recovered for a long time. It only could be retrieved after interventions by divers. The campaigns BM01, BM02, BM04 and BM05 have been executed on the same place at (51° 30.6' N, 2° 37.94'), along the eastern flank of the Oosthinder. The campaigns BM03, BM06 and BM07 have been executed around a location (51° 24.78'N, 2° 31.61'E) in the Habitat Directive area, in the south part of the Hinderbanks, in the trough of a barchan dune. Both stations are indicated in Figure 3.

The ADCP measurements during campaigns BM01, BM02, BM04 and BM06 had a time step of 10 minutes, while during the campaign BM03 a much higher

time step of 1.5 seconds was used. During the campaigns BM05 and BM07, the bin size was 1.00 m or 0.50 m respectively, which makes it difficult to use these data to calculate the bottom shear stress using a logarithmic profile, while in the other campaigns a bin size of only 0.25 m was used. Furthermore for these two campaigns, the time step was relatively high, i.e. 3600 seconds or 2400 seconds respectively. These measurements were therefore not used in this study. While the ADCP during campaign BM06 was deployed from June 30th 2014 till July 10th 2014, no measurements were obtained from July 4th 2014 onwards. Only the first 4 days could be used in the analysis.

Remark that the measurements of campaigns BM01 and BM02 were already used to validate the OPTOS-FIN model in Van den Eynde *et al.* (2014).

To compare the model results with the measurements of the depth-averaged currents and of the total water depth, the measurements were averaged over a period of 30 minutes.

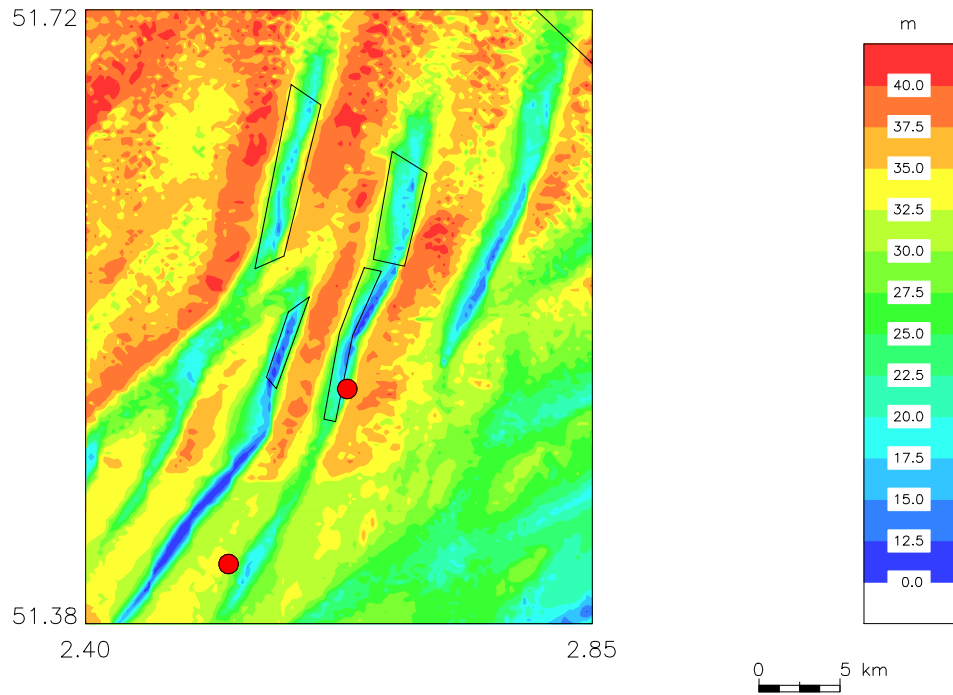


Figure 3: Position of the bottom mounted ADCP

3.2. Measurements of the bottom shear stress

The bottom shear stress can be calculated from the assumed logarithmic profile of the current near the bottom:

$$u = \frac{u_*}{\kappa} \ln \frac{z}{z_0} \quad (8)$$

with u the horizontal current velocity at z m above the bottom, κ the von Kármán constant, equal to 0.4, u_* the shear velocity and z_0 the bottom roughness length.

The shear velocity is related to the bottom shear stress, using the relation:

$$\tau = \rho u_*^2 \quad (9)$$

When the equation is rewritten as:

$$u = \frac{u_*}{\kappa} \ln z - \frac{u_*}{\kappa} \ln z_0 \quad (10)$$

the measured profile can be fitted to this logarithmic profile, using a least squares method.

Wilkinson (1984) furthermore developed expressions for the confidence limits (for a certain degree of confidence) for the estimations of the bottom roughness length and the bottom shear stress, using the Student's t distribution for the number of freedoms, equal to the number of velocities taken into account minus 2. For the exact formulations, the reader is referred to that paper.

4. Validation of the hydrodynamic and wave model results

4.1. Total water depth

The total water depth, as calculated by the model, is compared with the water depth, measured with the ADCP. As an example the results for the campaign BM01 is shown in Figure 4. In Table 3 the bias, unsystematic root-mean-square-error (RMSE) and correlation coefficient are given for the comparison between the measurements and the model results (see Appendix 1 for the definition of the statistical parameters).

Table 3: Number of comparison points (Numb.), Bias, RMSE_u and Corr for the total water depth. (*) The data were shifted over 1/2 hour.

Campaign	Numb.	Bias (m/s)	RMSE_u (m/s)	Corr
BM01	298	0.022	0.163	0.989
BM02	1293	1.674	0.193	0.984
BM03	125	-0.169	0.125	0.992
BM04	175	1.002	0.245	0.973
BM06*	133	1.148	0.660	0.830

One can observe that the bias between the measurements and the model results can be quite large, e.g., the biases for BM02 and BM04 are 1.67 and 1.00 m respectively. This probably has to do with uncertainties in the bathymetry of the model grid. Since the bathymetry of the numerical model is supposed to be a mean water depth over the entire grid cell, while the ADCP measures the water depth in the actual point, some differences in total water depth may occur. Therefore, in this case, the unsystematic RMSE is calculated, not taking into account the effect of the bias (see Appendix 1). The unsystematic RMSE varies between 0.134 m and 0.245 m. Only for campaign BM06 the unsystematic RMSE is much larger, which is due to bad measurements of the total water depth. These results are clearly acceptable. Remark furthermore, that during the analysis, it was shown that for the BM06 campaign, a shift in 0.5 hours occurred in the measurements, see next paragraph.

4.2. Depth-averaged currents

Also the depth-averaged currents from the bottom-mounted ADCP are compared with the model results. As stated above, the measurements are first averaged over depth and further averaged over time, to obtain time series with a time step of 30 minutes. In Figure 4 and Figure 5, the depth-averaged currents and current directions are presented for the five measuring campaigns. The statistical results are presented in Table 4.

Remark first of all that this analysis revealed that the u and v components of the currents were not correctly measured during campaign BM04-BM05. A shift of 90° clockwise occurred, meaning that the u component was not the current to the East, but the current to the South, while the v component was not the current to

the North, but the current to the East. After this shift, the current direction was well modelled by the OPTOS-FIN model.

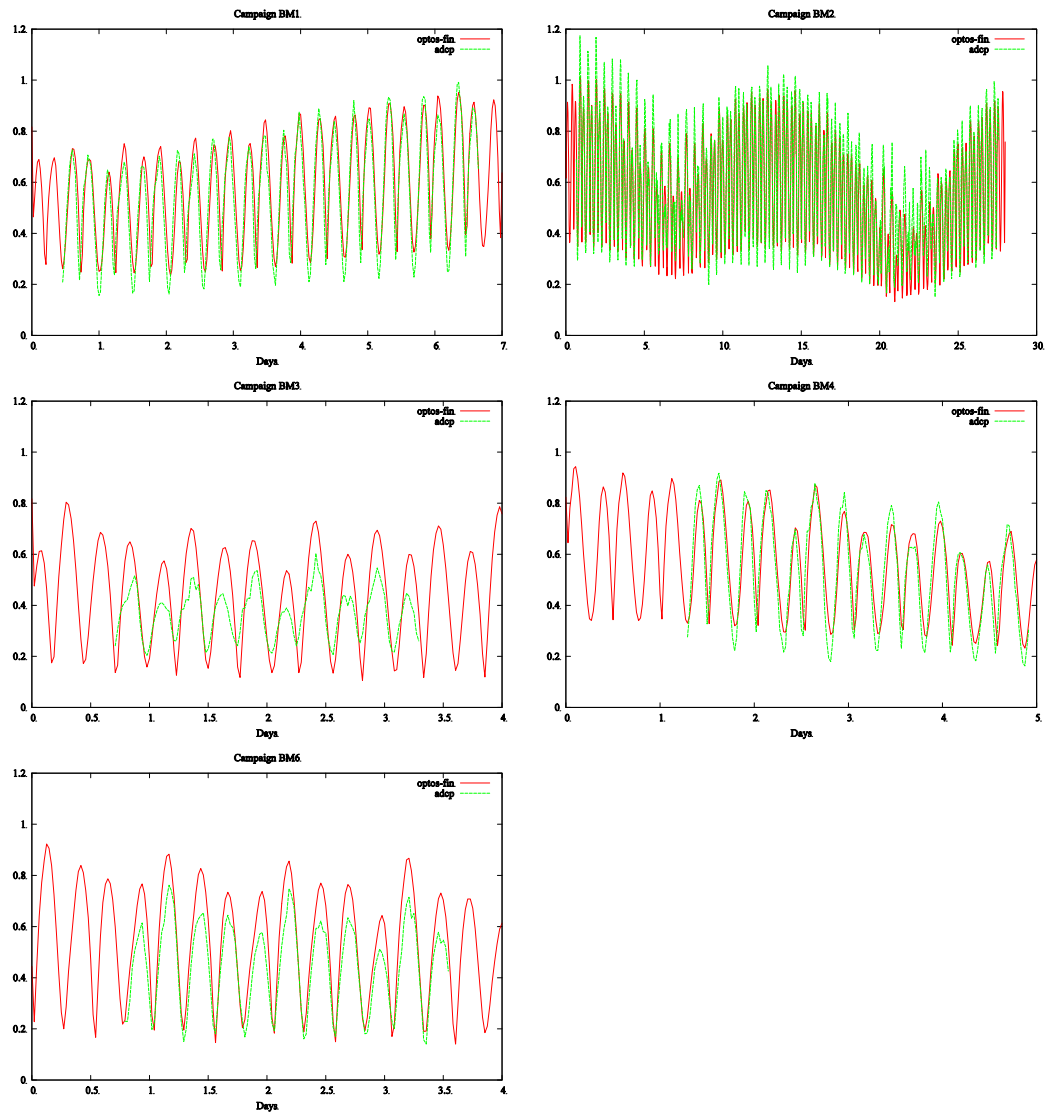


Figure 4: Depth-averaged currents from the bottom-mounted ADCP and from the OPTOS-FIN model for the different campaigns.

Table 4: Number of comparison points (Numb.), Bias, RMSE and S.I. for the depth-averaged current magnitude and direction. (*) The currents were shifted over 90 degrees clockwise for the results of campaign BM04. (**) The data were shifted over 1/2 hour.

Campaign	Numb.	Current magnitude				Current direction		
		Bias (m/s)	RMSE (m/s)	Corr	S.I. (%)	Bias (deg.)	RMSE (deg.)	Corr
BM01	298	0.030	0.086	0.921	15.6	-8.1	17.5	0.990
BM02	1293	-0.034	0.089	0.926	15.1	-4.0	14.1	0.992
BM03	125	0.056	0.118	0.891	31.4	-2.5	15.2	0.991
BM04*	175	0.010	0.082	0.916	15.6	-3.0	14.5	0.991
BM06**	133	0.092	0.110	0.970	24.8	-3.4	9.0	0.996

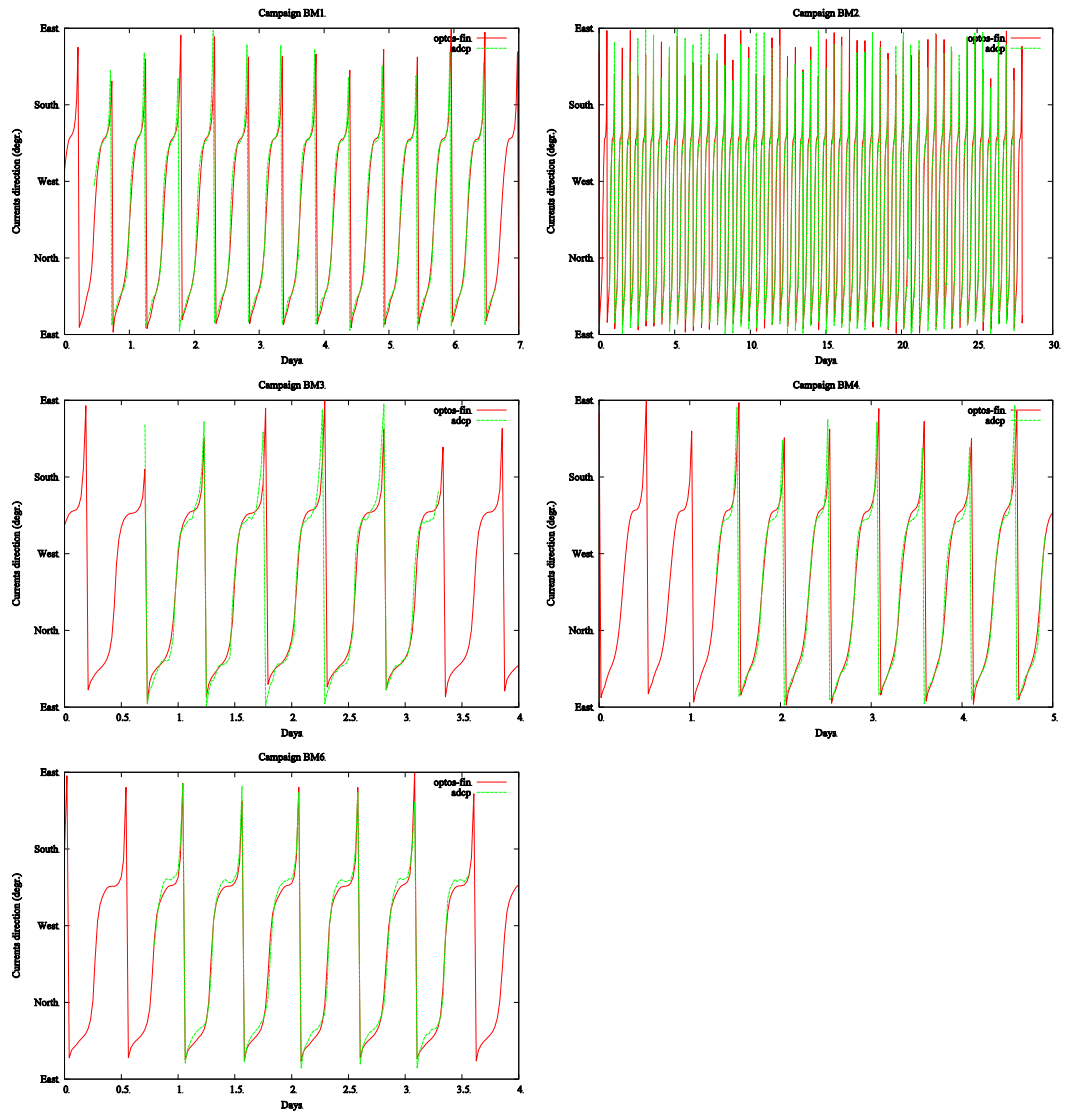


Figure 5: Depth-averaged currents directions from the bottom-mounted ADCP and from the OPTOS-FIN model for the different campaigns.

Furthermore, the analysis showed that for the campaign BM06 a clear shift was found in the currents, compared to the model results. The best results were obtained by shifting the ADCP with $\frac{1}{2}$ hour earlier. This might be an effect of the difference between the local time and the UTC time and thus bad configuration of the ADCP. In this case, the data should be shifted over 1 hour. However, this is consistent with the fact that for some of the other campaigns, slightly better results are obtained by shifting the data with $\frac{1}{2}$ hour later. This is an indication that the model results might, in this region, have a small phase shift.

Overall, the current magnitudes and current directions are quite well reproduced by the model for the measurements at the Hinder Banks, *i.e.* campaigns BM01, BM02 and BM04. In the campaign BM01, the currents were slightly overpredicted, certainly for the slack waters, while in campaign BM02, the overprediction of the currents mainly occurred during high currents. In campaign

BM04, a slight overprediction of the lower currents and an underprediction of the higher currents occurred. This is all clearly illustrated in the scatter plots of Figure 6. The RMSE is less than 0.09 m/s for all these campaigns. Also the current directions are well modelled during these campaigns. Overall, the results of the model are clearly satisfactory at the station east of the Oosthinder.

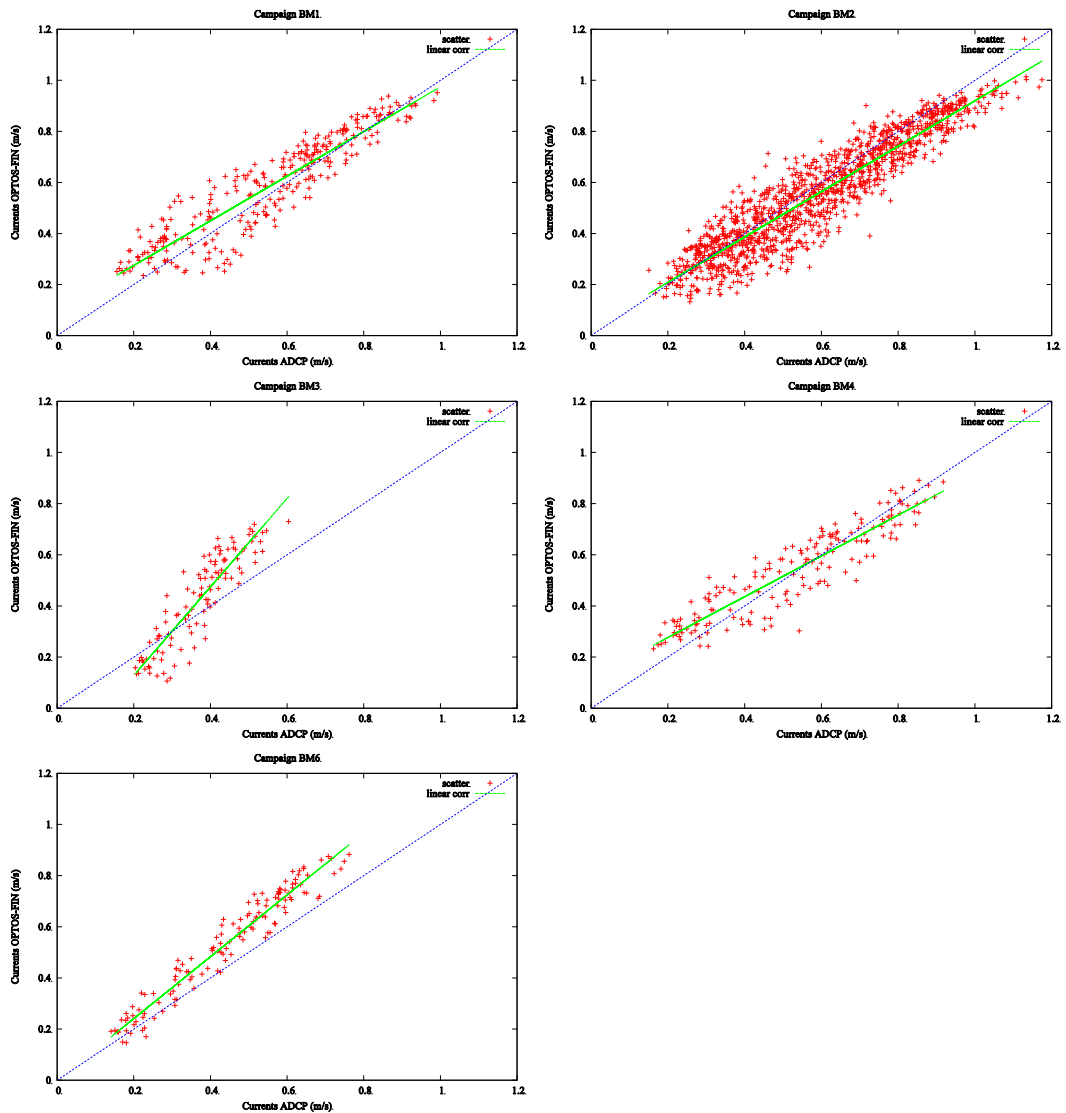


Figure 6: Scatter plots for the depth-averaged current magnitude for the measuring campaigns.

For the measuring campaigns in the Habitat Directive area, south of the Hinder Banks, the results of the model are less satisfactory. Both for the campaign BM03 as for the campaign BM06, the currents by the model clearly overpredict the currents, certainly during high currents. While during campaign BM03, the slack currents are slightly underpredicted by the model, these currents are also slightly overpredicted during campaign BM06. These less satisfactory results are probably due to the specific bathymetry in the area, in the neighbourhood of a large barchan dune, which may slow down the currents in the area, and which is not well

represented in the model bathymetry. This underprediction should be taken into account, when evaluating the model predictions of the bottom shear stress in this area. Remark that the current direction, on the other hand, is well modelled for these two campaigns.

4.2.1. Wave height

The significant wave height, modelled with the WAM model were compared with buoy data at the station MP7 at the Westhinder sand bank (data from Flemish Banks Monitoring Network, Flemish Government, Agentschap Maritieme Dienstverlening en Kust), see Figure 7. Some statistical parameters can be found in

Table 5.

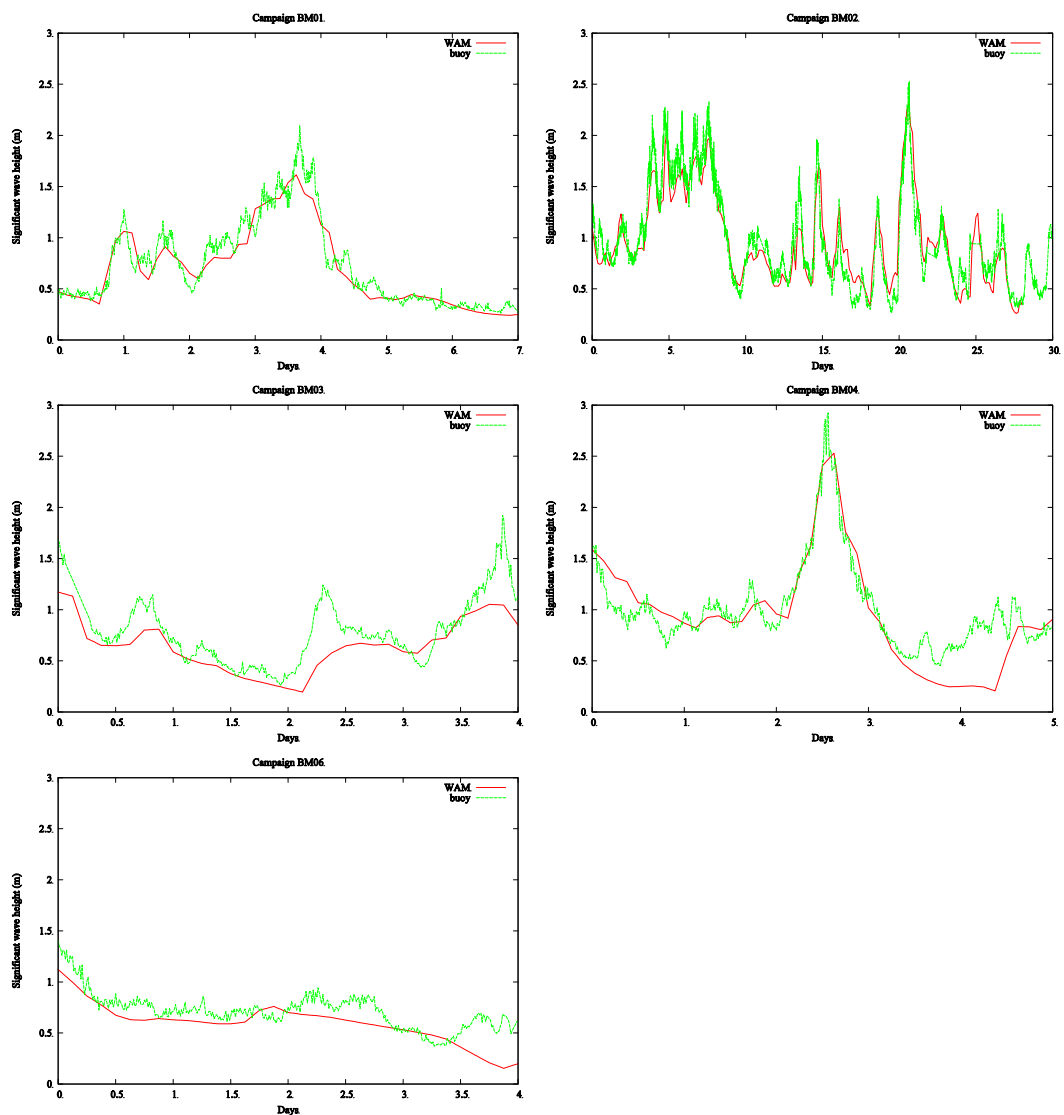


Figure 7: Significant wave height from the WAM model and wave measurements for the different campaigns. Buoy measurements from the Flemish Banks Monitoring Network, Flemish Government, Agentschap Maritieme Dienstverlening en Kust.

Table 5: Number of comparison points (Numb.), Bias, RMSE, Corr and S.I. for the significant wave height.

Campaign	Numb	Bias (m)	RMSE (m)	Corr	S.I. (%)
BM01	314	-0.044	0.130	0.954	17.0
BM02	1240	-0.029	0.175	0.935	17.4
BM03	183	-0.162	0.238	0.848	30.4
BM04	239	-0.068	0.255	0.886	25.0
BM06	191	-0.120	0.179	0.737	25.0

Good results are again obtained for the station at the east flank of the Oosthinder. For campaign BM01 and BM02 a S.I. of only 17% is found; for the BM04 campaign, the scatter index is 25%. Also the bias is always less than 0.07 m. These results are clearly satisfactory. For the station in the Habitat Directive area, the results are again not as good. The bias is higher with an underprediction of 0.12 m and 0.16 m for campaign BM06 and BM03 respectively. Also the S.I. for the BM03 campaign is higher (30%). This probably is again an effect from specific bathymetric conditions at this station.

The waves during the periods of the measurements campaigns remain limited. During the campaign BM01 and BM02, the significant wave height remains most of the time below 2.0 m. During campaign BM04, a peak in significant wave height was reached of about 3.0 m. During the campaigns in the Habitat Directive area, south of the Hinder Banks, the waves remain lower and did not exceed 1.5 m.

5. Validation of the bottom shear stress model results

5.1. Bottom stress calculation

In the section 3.2, it was shortly discussed how to derive the bottom shear stress for the ADCP measurements, using the logarithmic profile in the lower part of the water column. For the campaign BM03, with a time step of the profile measurements of 1.5 second, the mean profile is first calculated over a period of 10 minutes. For the other campaigns, the profiles were measured with a time step of 10 minutes. Using the formulae, described above, the bottom shear stress is then calculated from the (averaged) profile.

In Figure 8 the mean profile in the lowest 6 m of the water column for the entire campaign BM01 is given, as a function of the current direction. The highest currents are the currents in south-south-west direction (ebb) and in north-north-east (flood). For the higher currents, the currents show a relatively nice logarithmic profile. For the slack-water profiles, the current profiles are more constant over the water depth.

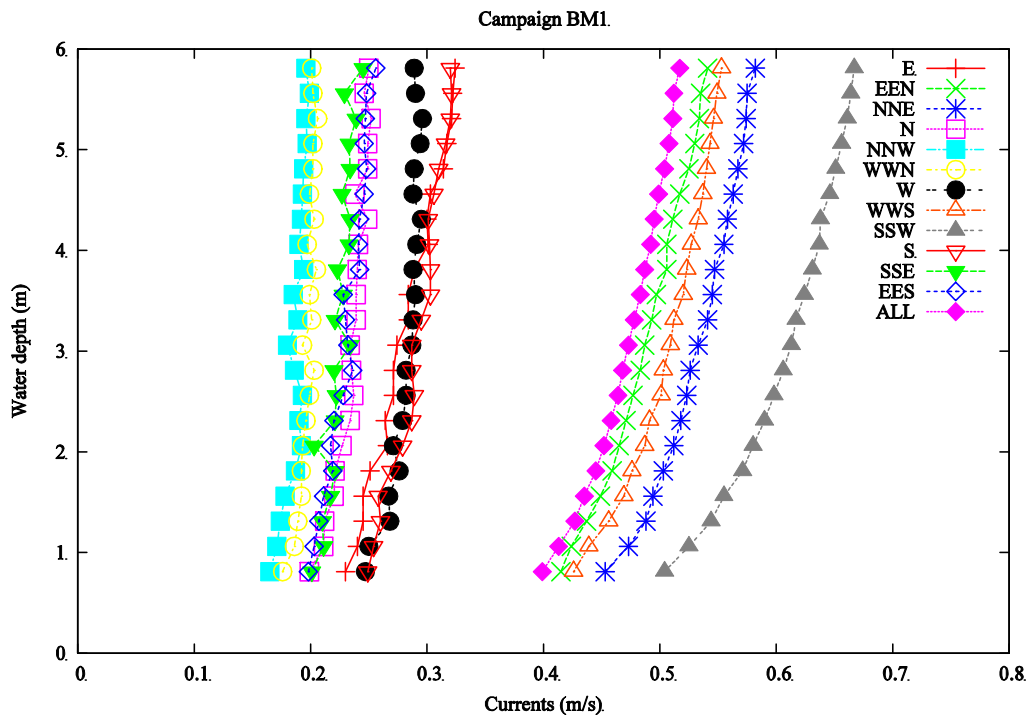


Figure 8: Mean current profiles in the lower part of the water column for campaign BM01, as a function of the current direction.

For the measurements in the Habitat Directive Area, the currents are lower and less logarithmic.

It is clear that the individual profiles can differ more from the logarithmic profile. This is shown in Figure 11 where some of the profiles during campaign BM01 are shown. Some of the profiles have clear disturbances. Furthermore, the logarithmic profile is depending on the part of the water column that is taken into

account to calculate the logarithmic profile. However, most of the current profiles are following a logarithmic profile and only a very limited amount of profiles result in a negative bottom shear stress.

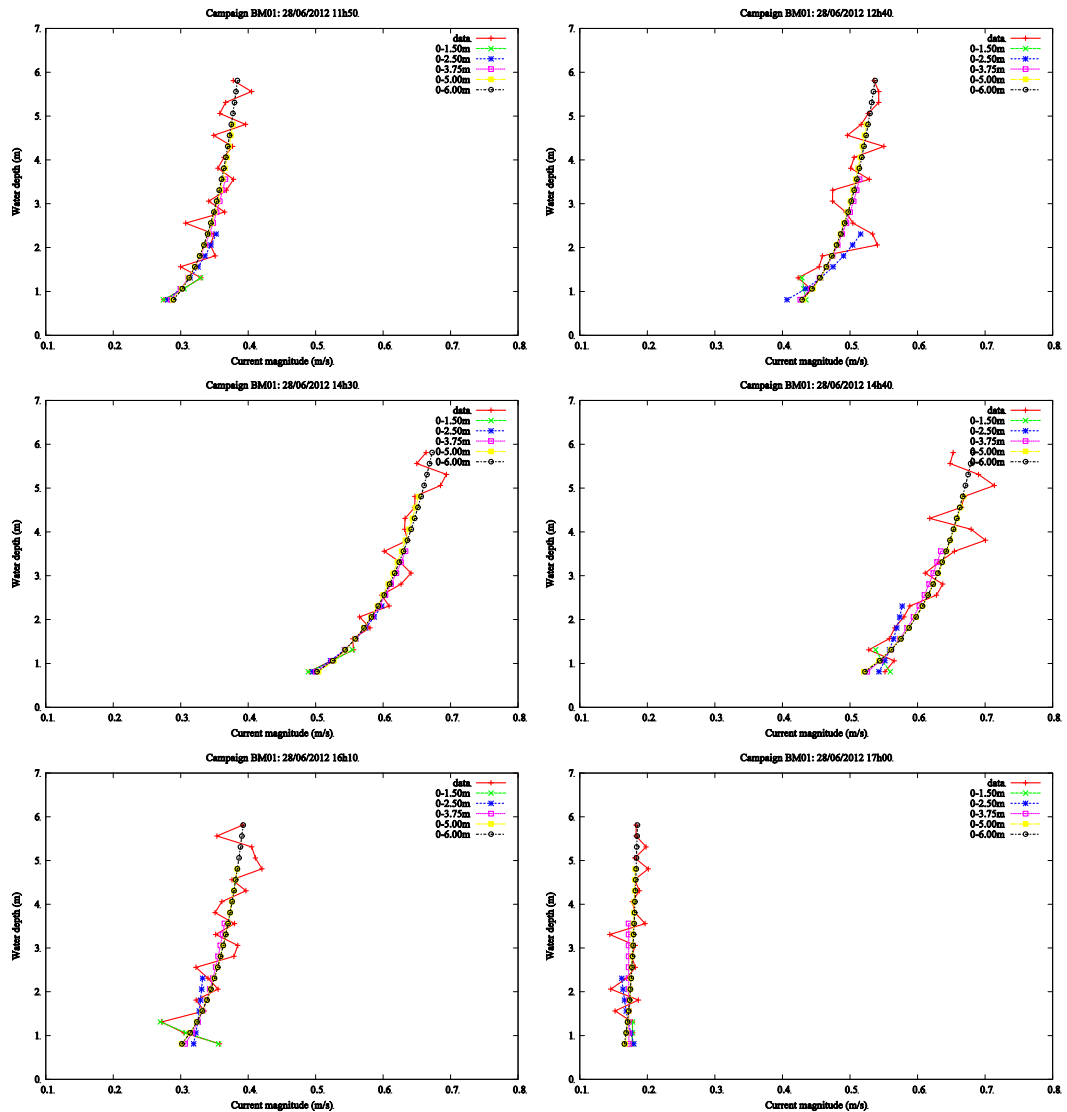


Figure 9: Selected measured current profiles and calculated logarithmic profiles for different parts of the water column (campaign BM01).

The fact that the calculated bottom shear stress is depending on the number of velocities taken into account, i.e., the part of the lower water column, which is used to calculate the bottom shear stress, is also illustrated in Figure 10, where the bottom shear stress is presented during day 1 to day 3 for campaign BM01, using different number of the current measurements that were taken into account. One can clearly observe that when taking a different part of the water column into account, the calculated bottom shear stress varies over a large scale. In Figure 11 for different times, the calculated bottom shear stress is plotted as a function of the highest point in the water column that is taken into account. When only the lowest

water column is taken into account, the bottom shear stress can still change considerably by taking one more velocity measurement into account. From 5 m onwards, the calculated bottom shear stress seems more stable, when more points are taken into account. In this study, the lowest 5 m are taken into account for calculating the bottom shear stress.

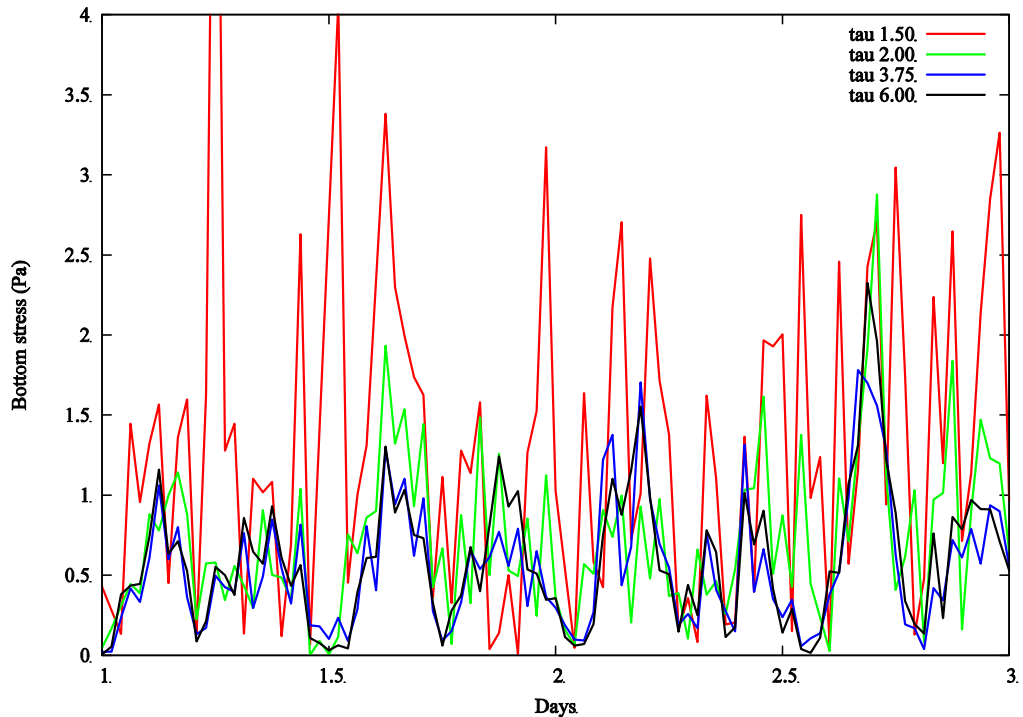


Figure 10: Calculated bottom shear stress for day 1 to 3 for campaign BM01 when taking different parts of the water column (1.50 m, 2.00 m, 3.75 m, 6.00 m) into account.

In Figure 12, the time series of the bottom shear stress, calculated using the lowest 5 m of the water column, is shown for day 1 to day 3 of campaign BM01. One can clearly see that there is still a lot of scatter in these measurements. To remove some of the scatter, a moving average filter is applied to the data with a window of 2 hours.

As indicated above, the method also allows to calculate the confidence limits with a certain degree of certainty, for the derived bottom shear stress. In Figure 13, the ratio between the maximum bottom shear stress with a confidence limit of 95% and the calculated bottom shear stress is presented for the data of campaign BM01. For a bottom stress, higher than 0.5 Pa, this ratio remains lower than a factor 2 and is around 1.55. For lower bottom shear stresses, the ratio can be higher. In Figure 14 the calculated bottom shear stress and the confidence limits (maximum and minimum bottom stress with confidence of 95%) are presented for day 1 to day 3 of campaign BM01, together with the moving averages, both for the bottom shear stress and the confidence limits. Finally, in Figure 15, the time series of the ratio between the moving averaged minimum and maximum bottom shear stress and the moving averaged bottom shear stress is shown for campaign BM01. This ratio for the maximum bottom stress varies between 1.5 and 3, the ratio for the

minimum bottom stress is less than 0.5.

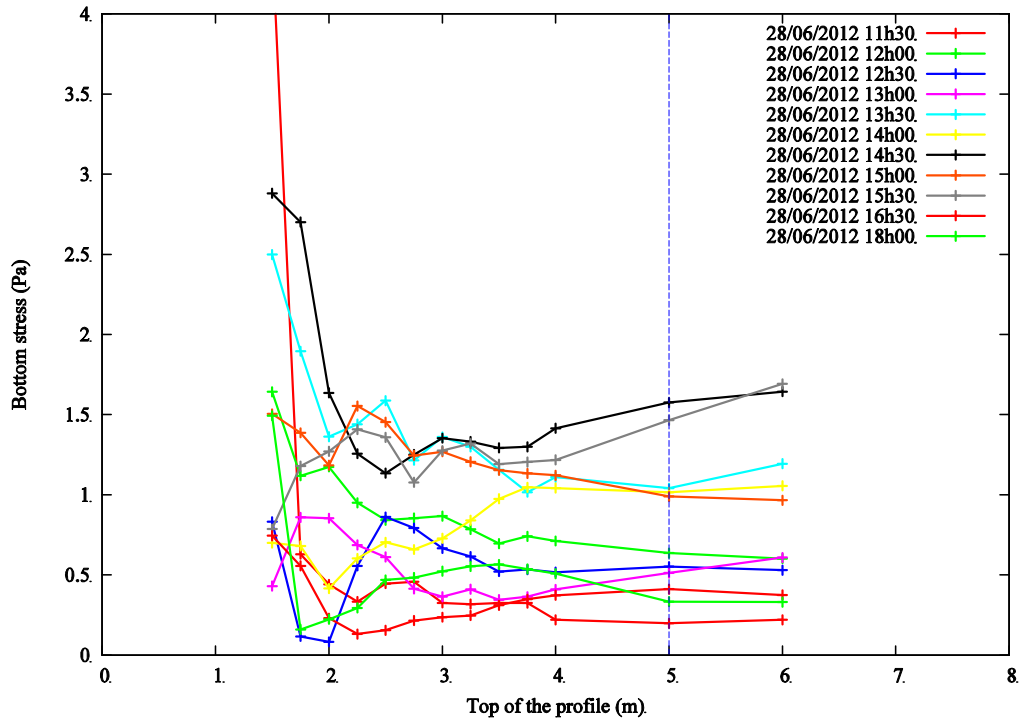


Figure 11: The calculated bottom shear stress for different times during campaign BM01 as a function of the part of the lowest water column taken into account.

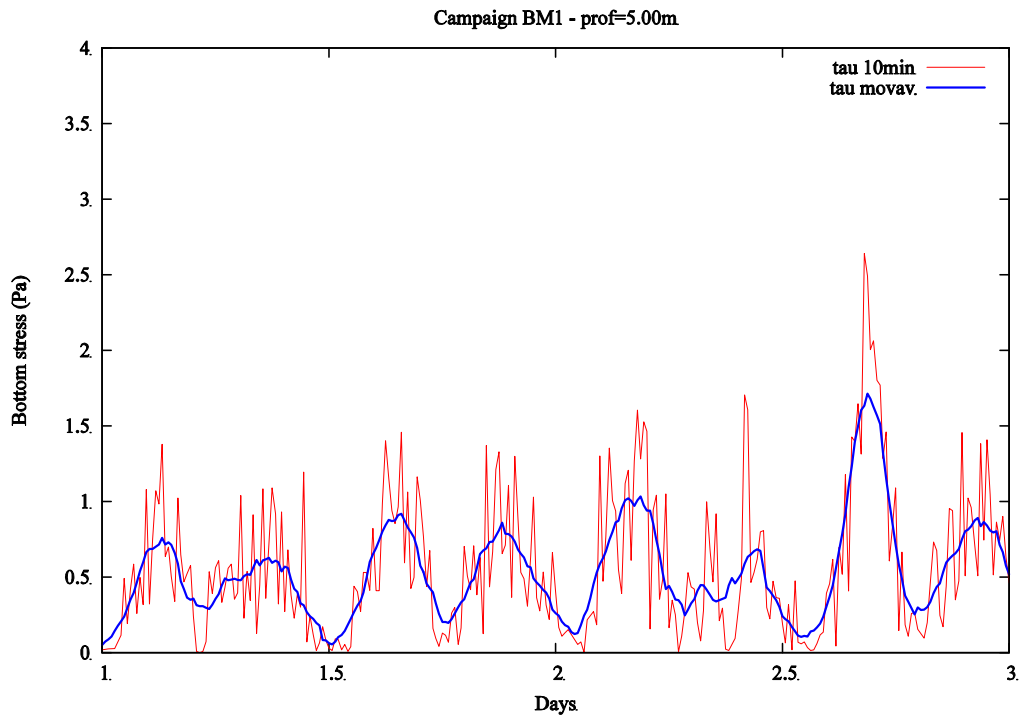


Figure 12: The calculated bottom shear stress (τ) during day 1 to day 3 of campaign BM01, with a time step of 10 minutes and a moving average over 2 hours.

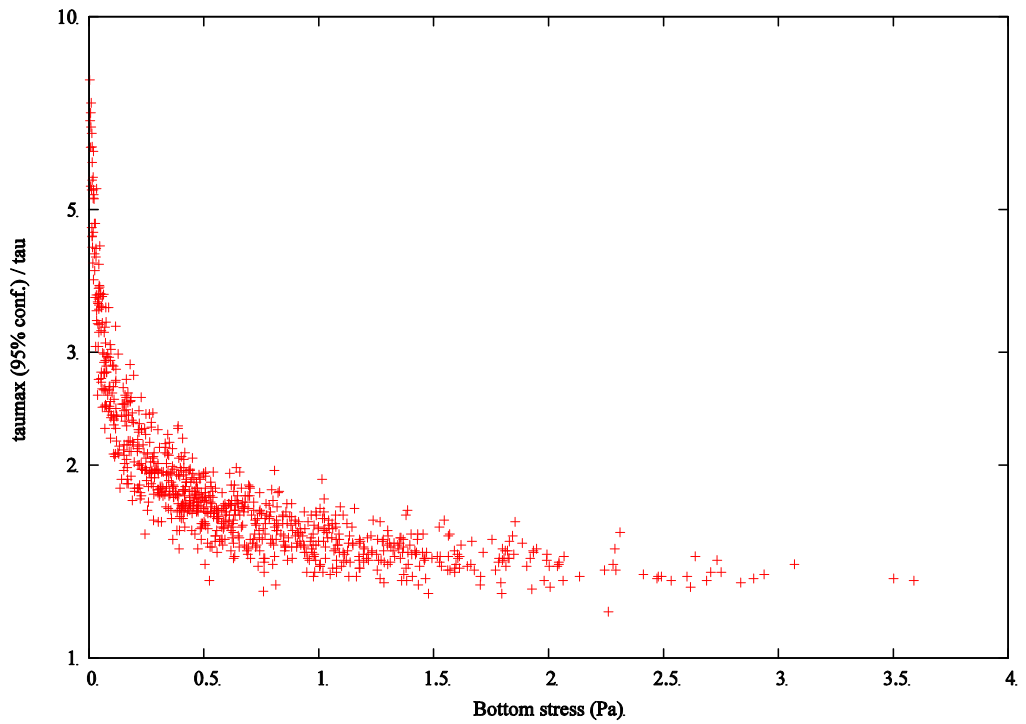


Figure 13: The ratio between the maximum bottom stress with a confidence of 95% (τ_{max}) and the calculated bottom shear stress (τ) for campaign BM01.

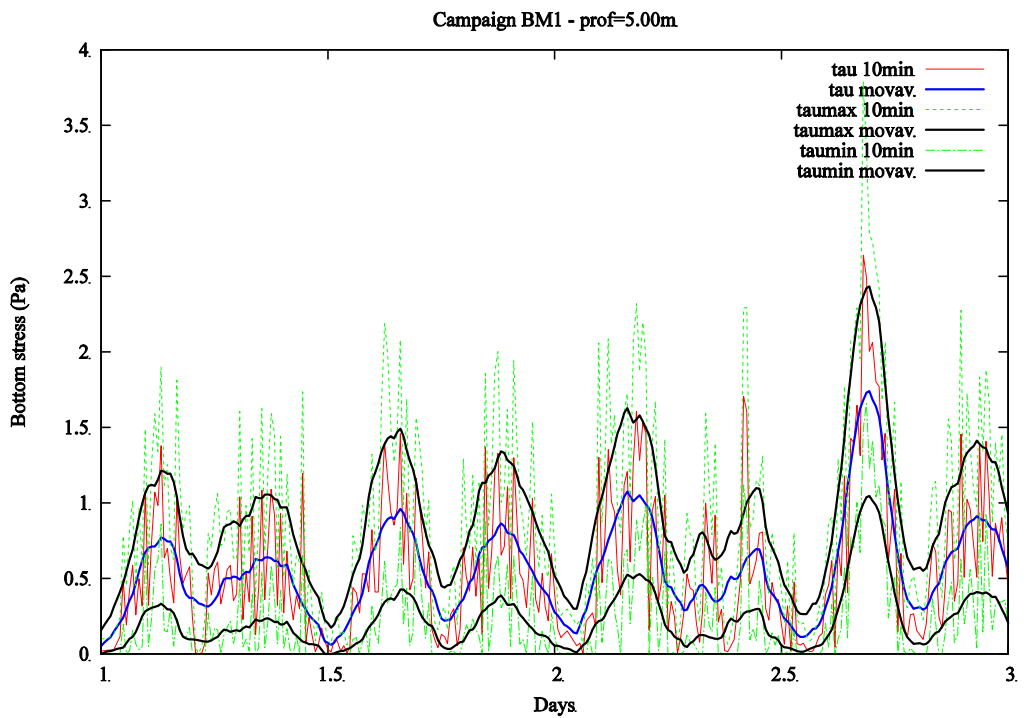


Figure 14: The calculated bottom shear stress (τ) and the maximum and minimum bottom stress with a confidence of 95% (τ_{max} and τ_{min}) during day 1 to day 3 of campaign BM01, with a time step of 10 minutes and moving average over 2 hours.

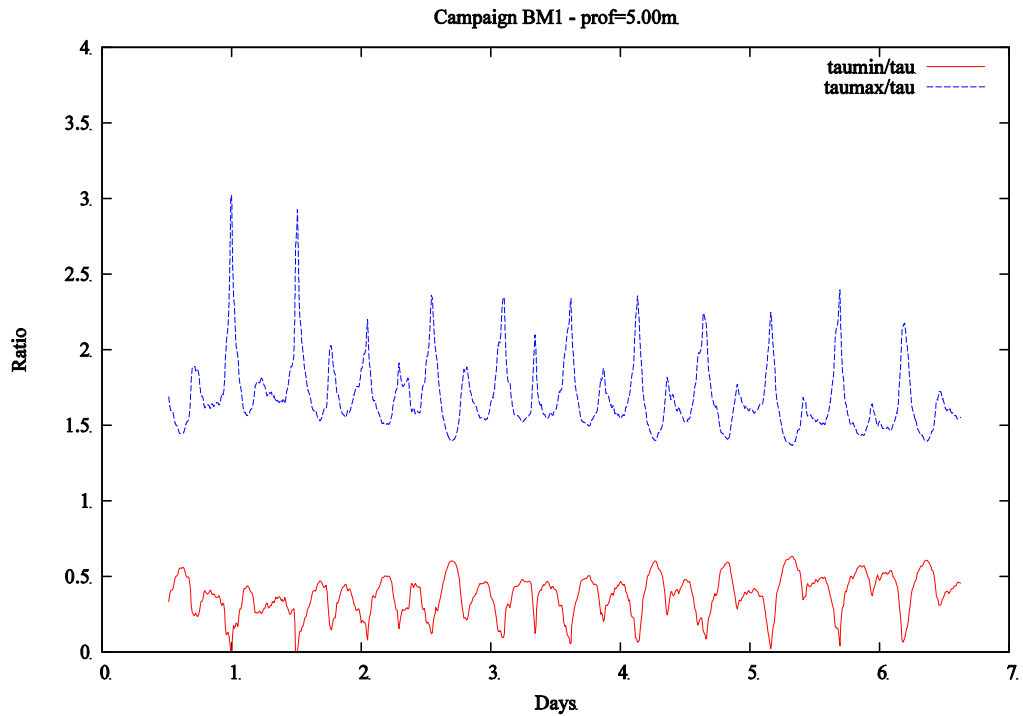


Figure 15: Time series of the ratio between the moving averaged minimum and maximum bottom stress with a confidence of 95% and the moving averaged bottom shear stress for campaign BM01.

5.2. Validation of the model results

5.2.1. Bottom shear stress with constant bottom roughness

To compare the model results of the three models, using a constant bottom roughness length, tests were executed with values of 0.004 m, 0.007 m, 0.01 m, 0.1 m, 0.2 m, 0.3 m, 0.4 m, 0.5 m and 0.6 m. The best overall result (lowest mean RMSE over all campaigns) were obtained with the Soulsby model (see Table 6, ALL), although the results with the Soulsby-Clarke and the Malarkey-Davies model are very comparable. The best results for the 5 separate campaigns are given in Table 6. Remark that the optimal bottom roughness for the campaigns BM03 and BM06, at the station at the Habitat area, are much lower than the bottom roughness for the campaigns BM01, BM02 and BM04, east of the Oosthinder. The optimal bottom roughness for the Malarkey-Davies model for BM01, BM02 and BM04 is 0.01 m, while for the Soulby and Soulsby-Clark model, the optimal bottom roughness for the last two campaigns is higher at 0.03 m. Remark further that the results for the campaign BM03 and BM06 are less good, with a lower correlation. This is probably due to the less good modelled currents at that station, as illustrated above. Also the results at campaign BM04 are less good, with a relative high underestimation of the bottom shear stress (bias of -0.138 Pa) and a relative low correlation coefficient of 0.725.

In Figure 16, the modelled bottom shear stress is given for campaign BM01, together with the measured bottom shear stress. Also the confidence limits (95%) of the measurements are given in the plot. While the height of the peaks may differ considerable, the tidal signal is well reproduced by the model. In more than 92% of

the cases, the model results remains between the 95% confidence limits of the measurements. This is also indicated in Table 6. For the campaigns BM02 and BM04, the model results remains in 84% and 79% of the results between the confidence limits of the measurements. For the campaigns BM03 and BM06, the results are less good.

Overall, one can conclude that using a constant bottom roughness length, the numerical models give satisfactory results. A bottom roughness length of 0.01 to 0.03 m should be used. For the campaigns BM03 and BM06, where the measurements are taken in the Habitat Directive Area, the results are less good, mainly due to the very specific bathymetrical situation.

Table 6: Bias, RMSE and Correlation and Percentage Good for the comparison between numerical model results, using a constant roughness length, and the bottom shear stress, calculated from the logarithmic current profile (lowest 5 m of the water column, moving averaged). For ALL: mean of the absolute value of the bias is given.

Campaign	Model	Roughness (m)	Bias (Pa)	RMSE (Pa)	Corr	PercGood (%)
BM01	Malarkey-Davies	0.010	-0.016	0.235	0.834	92.5
BM02	Soulsby-Clark	0.030	-0.022	0.361	0.822	84.3
BM03	Soulsby	0.004	0.063	0.156	0.660	47.5
BM04	Soulsby-Clark	0.030	-0.138	0.410	0.725	79.3
BM06	Soulsby	0.004	0.062	0.191	0.740	57.4
ALL	Soulsby		0.083	0.255	0.761	

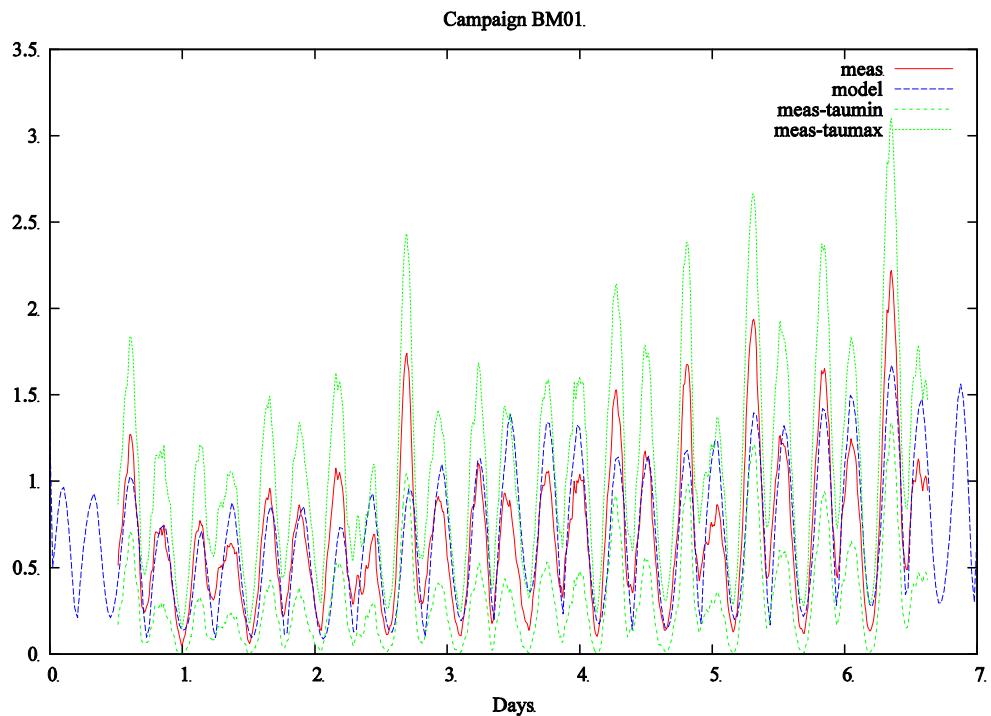


Figure 16: Time series of measured bottom shear stress (with confidence limits of 95%) and modelled bottom shear stress, with a constant bottom roughness length, for campaign BM01.

5.2.2. Bottom shear stress with bottom roughness calculated

As mentioned before, the bottom roughness length can also be calculated by the numerical model itself, based on empirical models for the bottom roughness length, due to bed load and due to bottom ripples. Also the dimensions of the bottom ripples are calculated by empirical models in this case.

When comparing the model results, using different models for the calculation of the bed roughness length as a function of the bed load and the bottom ripples, one can conclude that the simulated bottom roughness seems to be too high. Here again, the Soulsby model and the Soulsby-Clarke model give the best results. The bottom roughness due to bed load seems best predicted by the Grant and Madsen model or with the Grant and Madsen model, assuming wave domination. The bottom ripples are best modelled by the Soulsby-Whitehouse model. Overall, however, the bias is too high, except for the results for campaign BM04. The results are presented in Table 7, while in Figure 17, the results for campaign BM01 are presented.

Table 7: Bias, RMSE and Correlation and Percentage Good for the comparison between numerical model results and the bottom shear stress, calculated from the logarithmic current profile (lowest 5 m of the water column, moving averaged). Roughness length due to bed load: GM= Grant&Madsen model, GMW=Grant&Madsen model with wave-domination. Roughness due to bottom ripples: S-W: Soulsby-Whitehouse model. For ALL: mean of the absolute value of the bias is given.

Campaign	Model	Bedload	Ripple	Bias (Pa)	RMSE (Pa)	Corr	PercGood (%)
BM01	Soulsby-Clarke	GM	S-W	0.205	0.353	0.833	72.4
BM02	Soulsby	GMW	S-W	0.081	0.360	0.773	80.3
BM03	Soulsby	GM	S-W	0.259	0.373	0.660	26.3
BM04	Soulsby	GMW	S-W	0.002	0.468	0.689	82.8
BM06	Soulsby-Clarke	GM	S-W	0.369	0.493	0.739	27.1
ALL	Soulsby			0.183	0.409	0.738	

In Figure 18, the evolution of the bottom roughness length is presented during campaign BM01. From the figure, it is clear that the total bottom roughness length is mainly due to the bottom ripples, while the effect of the bed load is negligible in this case. When using the ripple predictor of Grant-Madsen & Soulsby, the bottom roughness length would even be higher resulting in even higher bottom stresses and a higher bias.

Finally, it is tested whether better results can be obtained by scaling the calculated bottom roughness length with a factor, better results could be obtained. It appeared that best results were obtained by the Soulsby-Clarke model and by scaling the bottom roughness length, using the Grant-Madsen & Soulsby model for calculating the bottom roughness, due to bottom ripples, with a factor 0.10. When using the Malarkey-Davies model, best results are obtained by scaling the Soulsby-Whitehouse model, for calculating the bottom roughness, due to bottom ripples, with a factor of 0.10.

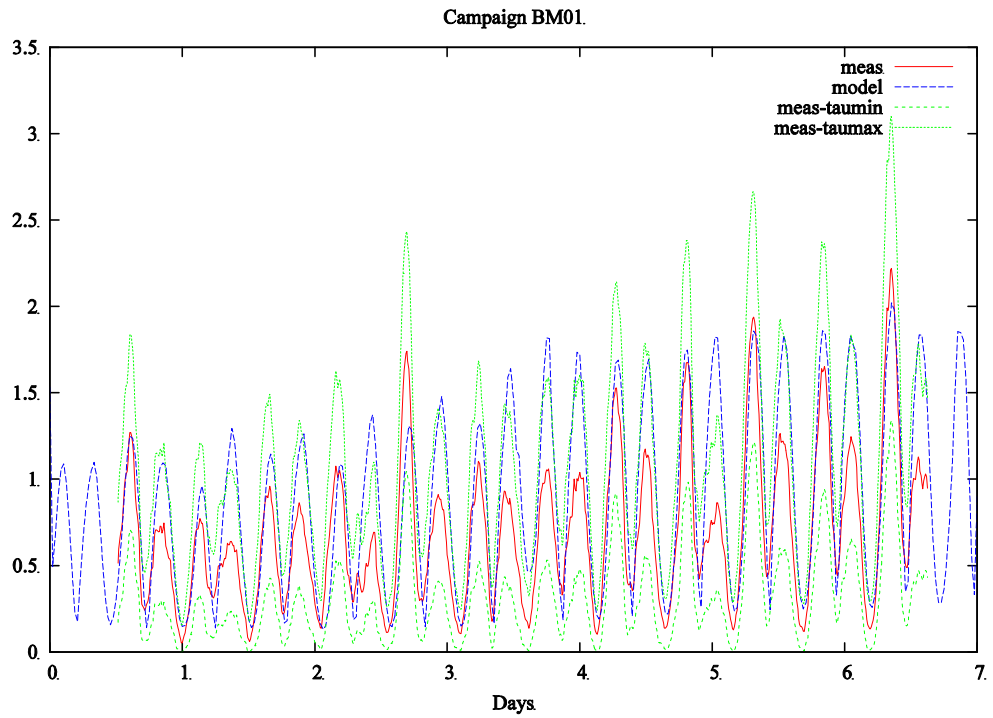


Figure 17: Time series of measured bottom shear stress (with confidence limits of 95%) and modelled bottom shear stress, with a bottom roughness length, predicted by the model, for campaign BM01.

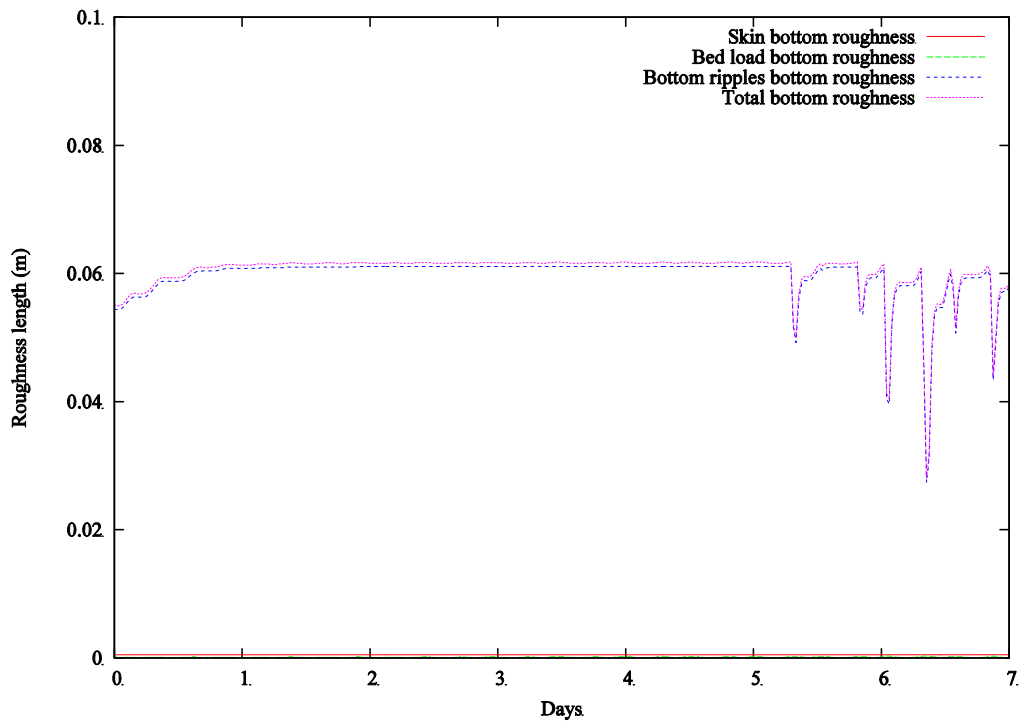


Figure 18: Time series of modelled skin bottom roughness length, bottom roughness length due to bed load, bottom roughness length, due to bottom ripples and total bottom roughness length, during campaign BM01.

The best results for the different campaigns, using the Grant-Madsen & Soulsby model for calculating the bottom roughness, due to bottom ripples, with a scaling factor of 0.10 is shown in Table 8.

Table 8: Bias, RMSE and Correlation and Percentage Good for the comparison between numerical model results and the bottom shear stress, calculated from the logarithmic current profile (lowest 5 m of the water column, moving averaged). Roughness length due to bed load: Roughness due to bottom ripples: Grant-Madsen & Soulsby model. Fac: scaling factor for roughness length.

Campaign	Model	Ripple	Fac	Bias (Pa)	RMSE (Pa)	Corr	PercGood (%)
BM01	Malarkey-Davies	GM&S	0.10	0.000	0.238	0.832	91.1
BM02	Malarkey-Davies	GM&S	0.10	-0.078	0.310	0.804	82.4
BM03	Soulsby-Clarke	GM&S	0.10	0.120	0.215	0.660	44.1
BM04	Soulsby-Clarke	GM&S	0.10	-0.282	0.427	0.790	80.5
BM06	Soulsby	GM&S	0.10	0.151	0.264	0.740	41.1

It can be seen that these model results are similar as the results obtained with a constant bottom roughness length. The modelling of the bottom roughness in the model itself does not give a clear advantage and better results. Therefore, it is recommended to use a constant bottom roughness length.

5.3. Influence of waves on bottom shear stress

In a last paragraph, the influence of the waves on the measured and modelled bottom shear stress is investigated in the Hinderbanks area. To see whether the waves have a large influence on the bottom shear stress in the two stations, the tidal averaged bottom shear stress is compared with the significant wave height. In Figure 19, the bottom shear stress, tidal averaged bottom shear stress and significant wave height are plotted for the campaigns BM01 and BM02. Although during periods, waves, exceeding 2 m are present, no clear influence on the bottom shear stress can be seen. For the two stations, east of the Oosthinder and along the southern part of the Oosthinder, the tidal averaged bottom shear stresses are plotted as a function of the significant wave height in Figure 20.

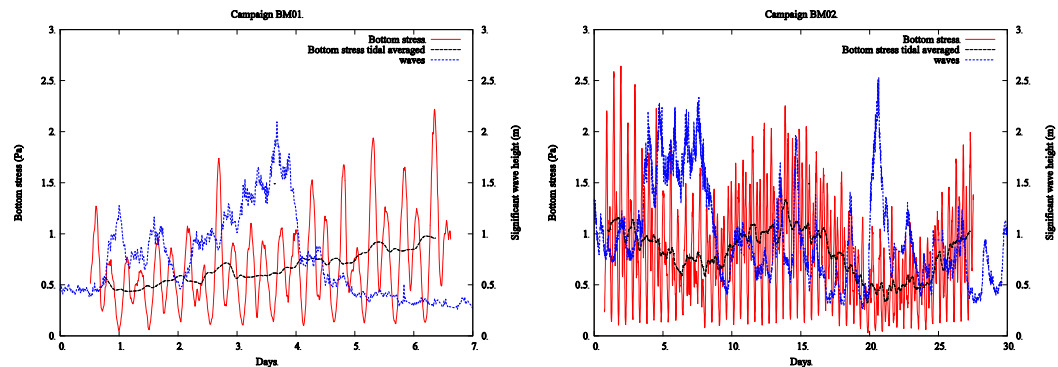


Figure 19: Time series of bottom shear stress and the tidal averaged bottom shear stress, and the significant wave height for campaign BM01 (left) and BM02 (right).

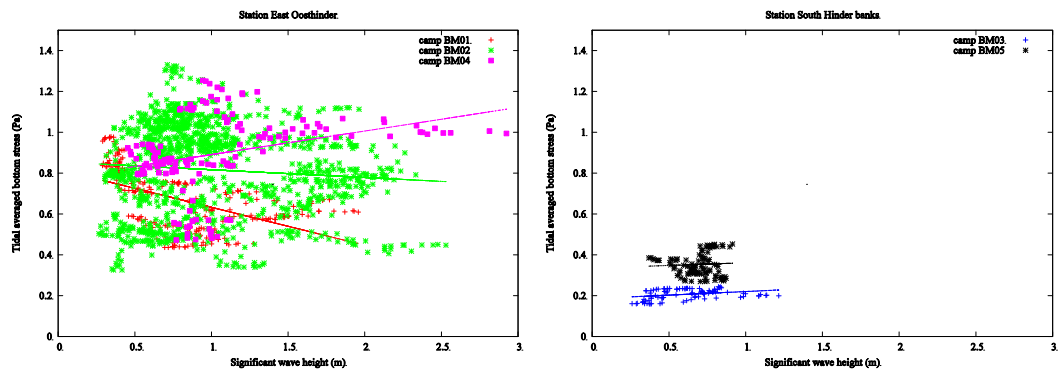


Figure 20: Tidal averaged bottom shear stress as a function of the significant wave height for the station east of the Oosthinder (left) and the station along the southern part of the Oosthinder sandbank (right).

For three campaigns, no clear relation between the bottom shear stress and the significant wave height is found. For campaign BM04, an influence of the significant wave height seems possible (slope: $+0.116$). The correlation coefficient is however very low. This mainly due to the coincidence that the high waves (significant wave height higher than 3 m) overlap with higher bottom shear stresses, due to spring tide. Overall, no clear influence of the waves on the bottom shear stress is found in the measurements. This is mainly due to the deeper waters.

Also in the model results, the effect of the waves on the bottom shear stress remains limited. Only during campaign BM02 and BM04, the waves influence the bottom shear stress (see Figure 21). However, it can be seen that the influence remains limited. For the station along the southern part of the Oosthinder sandbank the influence of the waves in the model results is even less, due to the low waves during these campaigns.

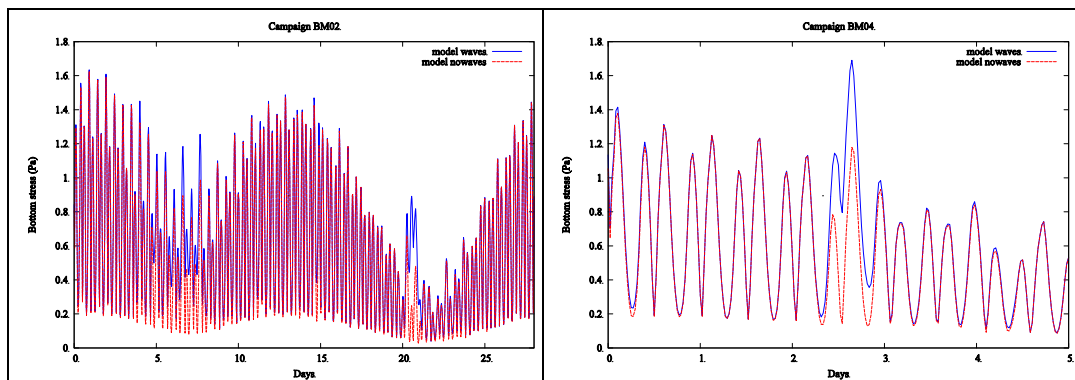


Figure 21: Bottom stress model results, with or without waves taken into account, for campaign BM02 (left) and BM04 (right).

5.4. Conclusions

In the present section, some analysis was executed on the bottom shear stress measurements first. It was shown that 5 m of the lowest part of the water column should be taken into account for the calculation of the bottom shear stress from the

current profile. Furthermore, it was recommended to apply a moving average filter, with a window of about 2 hours, to filter out the high frequency fluctuations in the measurements. The ratio between the minimum and maximum bottom shear stress with a confidence limit of 95%, and the calculated bottom shear stress varied between 0 and 0.5 for the minimum and 1.5 to 3.0 for the maximum bottom stress.

The validation showed that the bottom shear stress could be reasonably modelled by the numerical models. Using a constant bottom roughness, best results were obtained by the Soulsby model, using a constant bottom roughness length of 0.01 m. Similar results were obtained by the other models. The bias was around 0.20 Pa, with a RMSE of about 0.35 Pa, for campaign BM01. For more than 90% of the time, the modelled bottom shear stress was between the 95% confidence limits. Less good results were obtained for campaigns BM03 and BM06, at the station along the southern part of the Oosthinder sandbank. This is probably due to the poorer quality of the modelled currents and to the complex bathymetrical conditions at the site.

When the bottom roughness length was calculated by the model itself, the modelled bottom roughness length seemed to be too high, resulting in too high bottom shear stresses. When scaling the calculated bottom roughness length with a factor of 0.10, better results were obtained. However, also after scaling the bottom roughness length, the results were not significantly better than using the constant bottom roughness length. Therefore, for the time being, the use of a constant bottom roughness length is recommended.

Finally, it was shown that no clear influence of the significant wave height is found in the bottom shear stress measurements in the area of the Hinderbanks. This is mainly due to the deeper bathymetry at the stations.

6. Modelling the effect of extraction on bottom stress

6.1. *Introduction*

In the framework of the Marine Strategy Framework Directive (MSFD), Belgium prepared a report, in which different indicators were defined, that could be used to evaluate the impact of human activities at sea (Belgian State, 2012). By monitoring these indicators, the goal of the MSFD is to come to a Good Environmental Status of the sea.

Amongst these indicators, the indicator 7, on hydrographic conditions, uses the bottom shear stress. In the report it is stated that human impact asks consideration when the bottom shear stress, calculated by a validated mathematical model over a spring-neap tidal cycle, 1) increases by more than 10%, or 2) that the ratio of the period for erosion and the period for deposition is larger than -5% or +5%. Furthermore, it is stated that the impact, that needs consideration, should stay in a distance less than the square root of the area of the zone of activity, measured from the boundary of the area.

In the previous part of the report, some results were presented to develop a validated mathematical model of the bottom shear stress. In this section, some first results are presented to apply the method, as defined by the report, to evaluate the impact of extraction of marine aggregates in the Hinderbanks area.

6.2. *Simulations*

In Zone 4 for the extraction of marine aggregates, a maximum of 35 million m³ of marine aggregates is allowed to be extracted over a period of 10 years. In the present study, the effect of this maximum extraction on the bottom shear stress is evaluated. Three different scenarios are studied. In all scenarios, all material above a certain depth is extracted in the different sectors of extraction. This depth can however differ in the different sectors in the first scenario. In this scenario, in each sector the same maximum depth is extracted. To arrive at a total of 35 million m³, a maximum extraction of 6.93 m is applied. Almost 35% is in this case extracted in Sector 4a (north-east), which has the largest area. In the second scenario, extraction is executed in the four sectors, to the same critical depth as in the four sectors. In this case, extraction is executed up to a depth of 19.70 m. In this case, most of the material is extracted in Sector 4d, since this is the sector with the shallowest water depths. In this zone, an extraction of more than 10 m is executed, to extract almost 44% from this zone alone. In the last scenario, only material is extracted in Sector 4c, the sector, which is used most intensively at the moment and which is the closest to the coast (south-west). An extraction of almost 12 m is executed in this case, to a water depth of 26.05 m. An overview of the different simulations and the extraction depth and the amount of extracted marine aggregates is given in Table 9 and Table 10. The original bathymetry and the bathymetries after the extraction for the different scenarios are shown in Figure 22.

Table 9: Volume extracted (in Mm³) in the different sectors for the three simulations.

Simulation	4a	4b	4c	4d	Total
1	12,040	7,189	9,776	5,925	34,930
2	7,423	6,055	6,178	15,248	34,904
3	0	0	34,967	0	34,967

Table 10: Minimum depth after extraction and maximum extraction depth in the different sectors for the three simulations.

Simulation	Minimum depth after extraction (m)				Total thickness of extracted sediments (m)			
	4a	4b	4c	4d	4a	4b	4c	4d
1	20.81	19.98	21.06	16.35	6.93	6.93	6.93	6.93
2	19.70	19.70	19.70	19.70	5.82	6.65	5.57	10.28
3	-	-	26.05	-	0.0	0.0	11.92	0.0

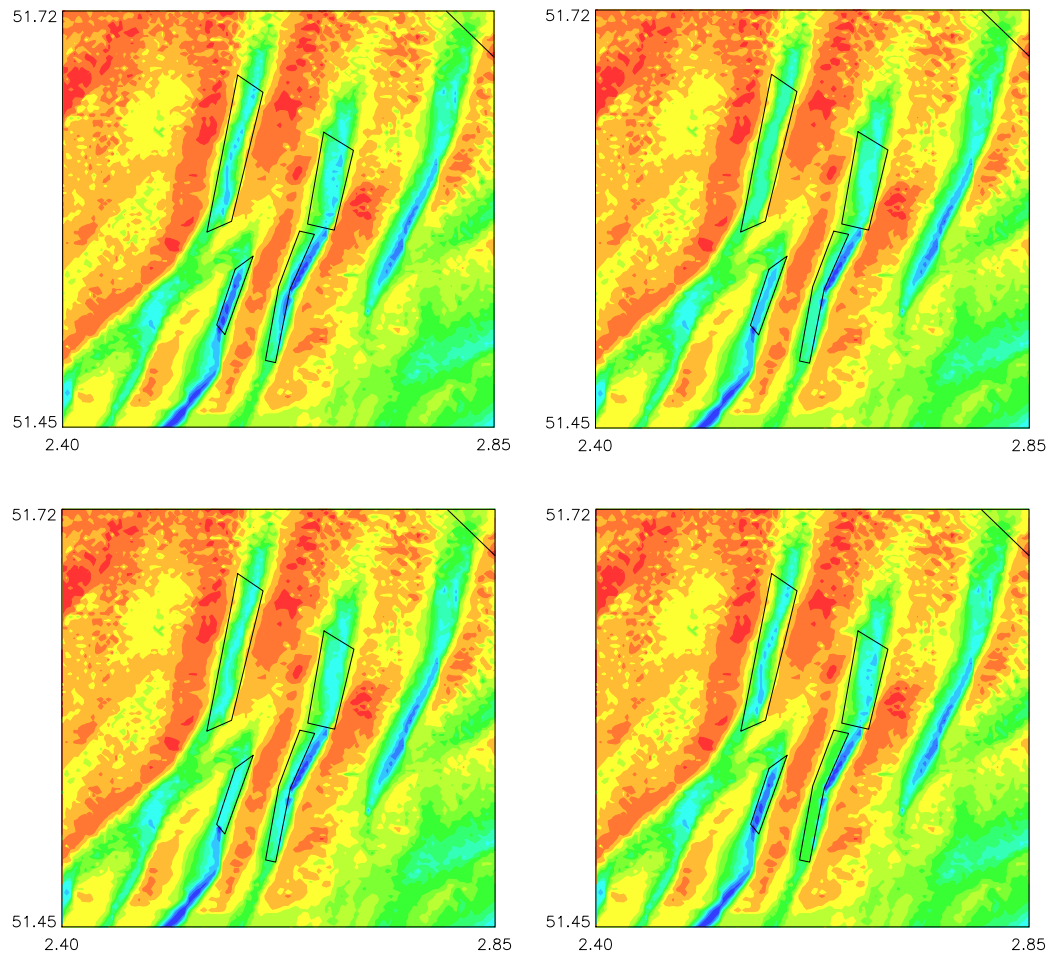


Figure 22: Bathymetries of the Hinderbanks area. Upper left: original bathymetry; upper right: bathymetry after extraction in scenario 1; lower left: bathymetry after extraction in scenario 2; lower right: bathymetry after extraction in scenario 3.

To evaluate whether the impact needs consideration, the effect should stay in a distance less than the square root of the area of the zone of activity, measured from the boundary of the area. Therefore the area of the extraction sectors 4a to 4d and the square root of these areas are given in Table 11. Note that not the entire area where extraction is permitted is effectively used. Therefore also the areas, used for extraction in the different sectors for the different scenarios are listed.

Table 11: Area of the different sectors and area of extraction for the different extraction sectors and for the simulations, together with the square root of the area. The latter is the distance along which changes are allowed following the requirements stipulated within the Belgian definition of MSFD.

	Area (km ²)					Distance (km)			
	4a	4b	4c	4d	Tot	4a	4b	4c	4d
Extraction	19.04	13.76	8.34	4.45	45.59	4.364	3.709	2.888	2.110
Sim 1	4.69	4.26	3.27	2.35	14.57	2.166	2.064	1.808	1.532
Sim 2	3.56	3.83	2.27	3.28	12.93	1.886	1.958	1.508	1.809
Sim 3	-	-	6.47	-	6.47	-	-	2.543	-

For the different bathymetries, the bottom shear stress is calculated using the three-dimensional hydrodynamic model COHERENS OPTOS-FIN, see above. In these first tests, the standard COHERENS bottom shear stress is used, which is based on a simple quadratic bottom shear stress. The influence of waves is not taken into account based on analyses showing that in deeper waters, waves do mostly not influence the bottom shear stress (see previous sections). Furthermore, in the report on the Belgian implementation of the MSFD (Belgian State, 2012), it is stated that the human impact needs consideration, when the bottom shear stress, calculated with a validated mathematical model, over a full spring-neap tidal cycle, meets certain conditions. Also in the MSFD, therefore, the influence of the waves on the bottom shear stress is not accounted for.

The simulations were executed for a full spring-neap tidal cycle, i.e., from March 29, 2013 00h00 till April 14, 2013, 12h00.

6.3. Results

6.3.1. Scenario I

In Figure 23, the differences are shown for the bottom shear stress, averaged over the full spring-neap tidal cycle for the first scenario, where in each sector the same thickness in sediment is extracted. One can see that the effect remains limited to the sector of extraction. To evaluate the results more in detail, three areas are defined: the sector of extraction, the area within a distance equal to the square root of the sector of extraction from the border (see Table 11), as defined in the MSFD report, and the area outside this distance. Following the recommendations of the MSFD report (Belgian State, 2012), the change in bottom shear stress should be limited to less than +10% or -10% outside the sector of extraction and the area within the specified distance. In Table 12 the minimum and maximum changes in bottom shear stress are listed. It can be seen that in the extraction sector itself, the difference can be up to -27%, while also in the region, within a distance, equal to

the square root of the area, the difference can be up to 15%. However, outside the region, the difference is limited to -2.16% to +3.52%.

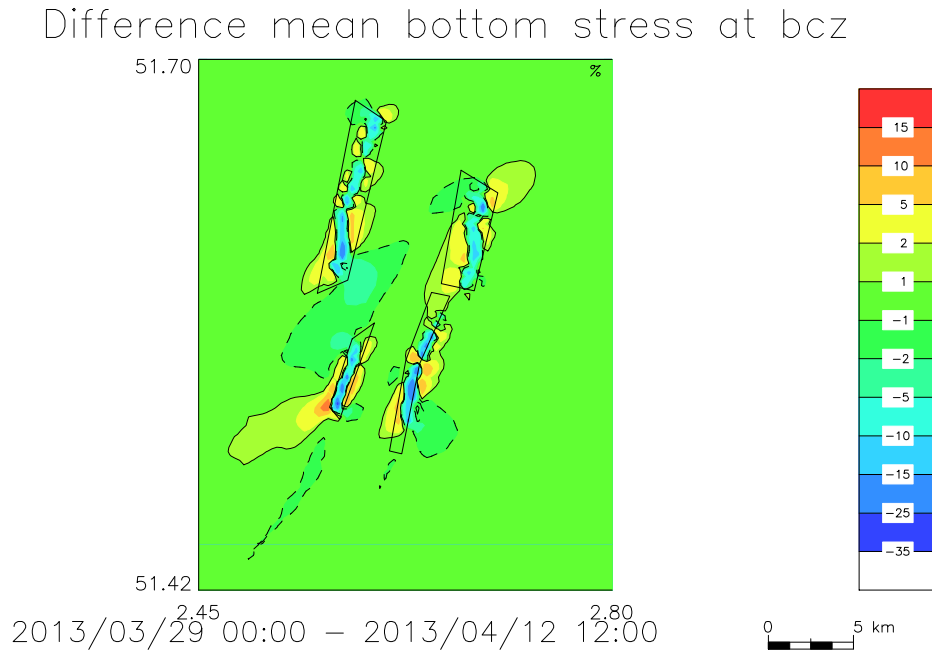


Figure 23: Differences of mean bottom shear stress over a spring-neap tidal cycle for scenario 1.

Table 12: For the three simulations, minimum and maximum change of bottom shear stress (in percentage) in the different areas (extraction sector, area within a distance from the border as defined in the MSFD implementation; area outside this distance).

	In the sector		Within distance		Outside distance	
	Min	Max	Min	Max	Min	Max
Sim 1	-27.33	9.71	-4.89	15.05	-2.16	3.52
Sim 2	-38.90	14.45	-6.48	26.80	-3.02	6.46
Sim 3	-35.59	12.62	-7.87	21.50	-3.46	2.58

In Figure 24 and Figure 25 the position of the points are given, for the three areas, with a higher change in bottom shear stress than 2% and 10% respectively. Almost over the entire zone of the extraction, the bottom shear stress changes over more than 2%. Outside the extraction zone, mainly southwest of zone 4a and around zone 4c and 4d, the bottom shear stress changes over more than 2%. Outside the zone, where impact is allowed, the bottom shear stress changes over more than 2% in a small area south east of Sector 4d. In only six points of the area, where impact is allowed, the difference is higher than 10%. These are located east of Sector 4d and west of Sector 4d.

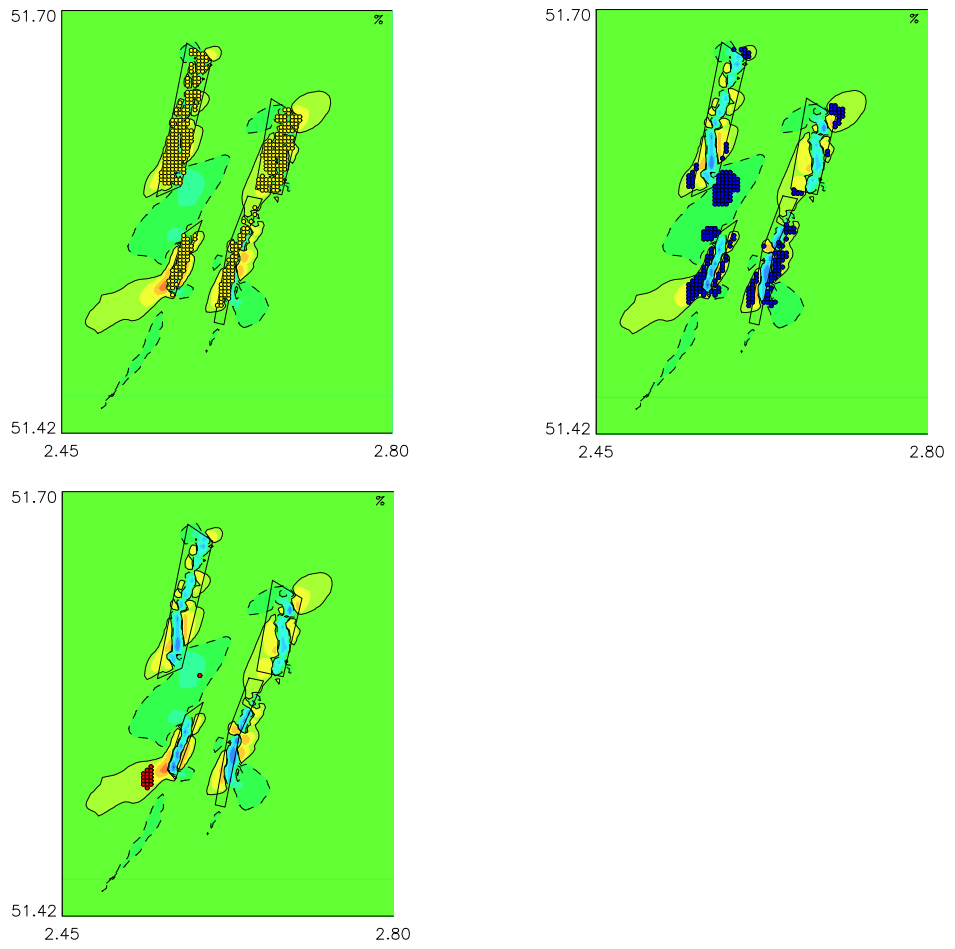


Figure 24: Position of the points with a difference higher than 2% for the extraction sector (upper left), area within a distance of the square root of the area of the sector from the border (upper right) and outside the distance (lower left) for scenario I.

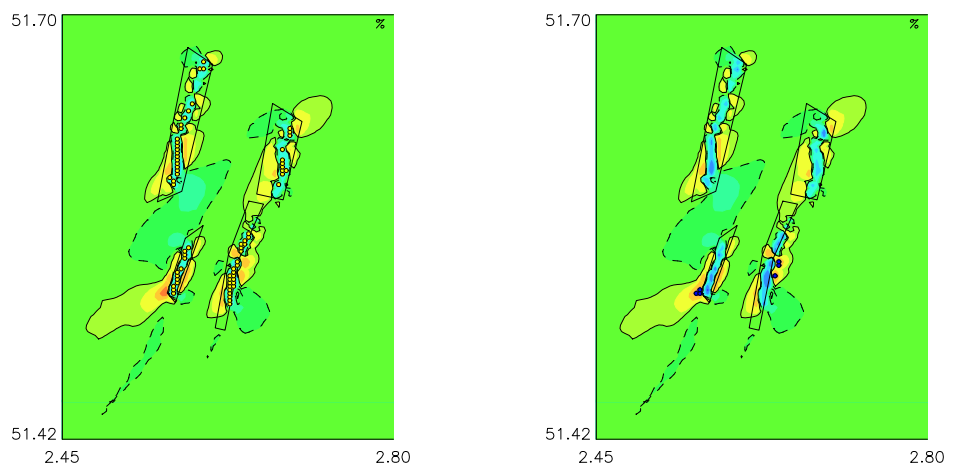


Figure 25: Position of the points with a difference higher than 10% for the extraction sector (left), zone within a distance of a square root of the area of the sector from the border (right) for scenario I.

Finally, in Figure 26, the number of points are plotted, where the change in bottom shear stress exceeds a certain percentage, for the different sectors. For the sectors, the number of points decrease from 496 points, with a change higher than 1% to 69 points, with a change higher than 10%. Remark that a grid points represents around 70,000 m² (or 0,07 km²). In the area, where impact is allowed, 770 points have a change higher than 1%, but only 6 points, a change higher than 10%. Finally, 322 points outside the area where impact is allowed, have a change higher than 1%, 17 points have a change higher than 2% and only 3 points a change higher than 3%.

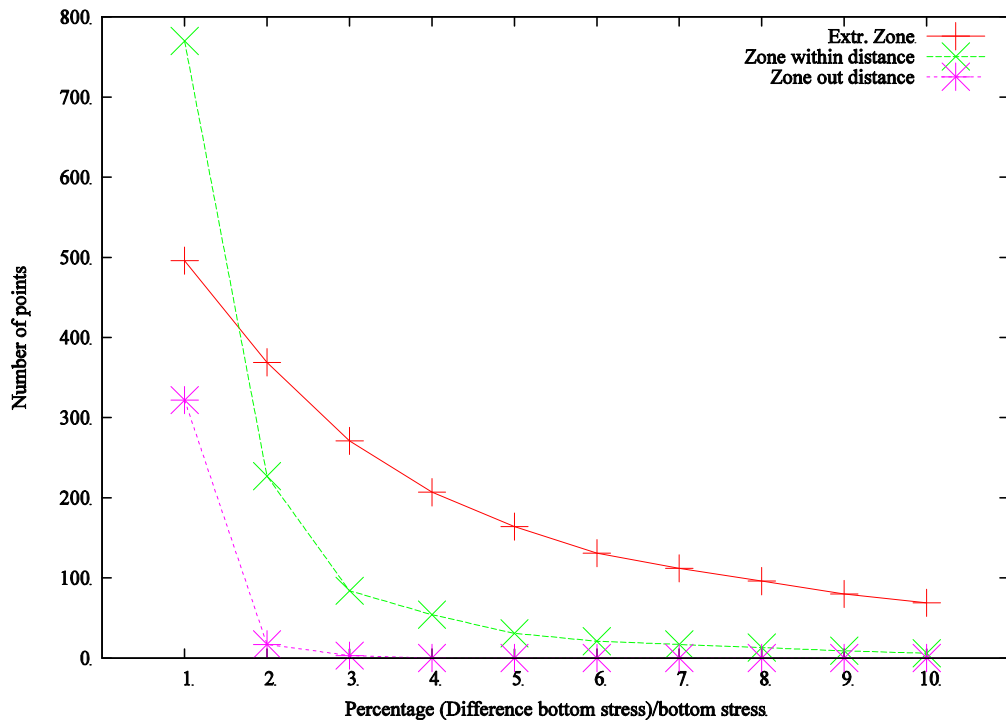


Figure 26: Number of points where the difference in bottom shear stress is exceeding a certain percentage, for the three defined areas for scenario 1.

6.3.2. Scenario 2

In Figure 27, the differences are shown for the bottom shear stress, averaged over the full spring-neap tidal cycle for the second scenario, where in each sector extraction was executed until the same water depth was reached. In this case, less extraction is executed in sectors 4a, 4b and 4c and much more extraction is executed in the shallow Sector 4d, where a maximum of more than 10 m is being extracted. This has influence on the changes in the bottom shear stress (see Table 11). In the sector itself, a maximum difference is found between +14% to almost -39%. Also in the zone where impact is allowed, the changes in bathymetry are higher up to more than 26%. However, also in this case, the change in bottom shear stress in the zone, where impact is not allowed, remains limited and is lower than 10%. In this case, the maximum changes are from -3% to +6.5%.

In Figure 28 and Figure 29 the position of the points is given, for the

three sectors, with a higher change in bottom shear stress than 2% and 10% respectively. Almost over the entire zone of the extraction, the bottom shear stress changes over more than 2%. Outside the extraction sectors, mainly southwest of Sector 4a and around Sector 4c and 4d, the bottom shear stress changes over more than 2%. Outside the sector, where impact is allowed, the bottom shear stress changes over a small zone south east of Sector 4d. In only 19 points of the zone, where impact is allowed, the difference is higher than 10%. These are located east of Sector 4d and west of Sector 4d.

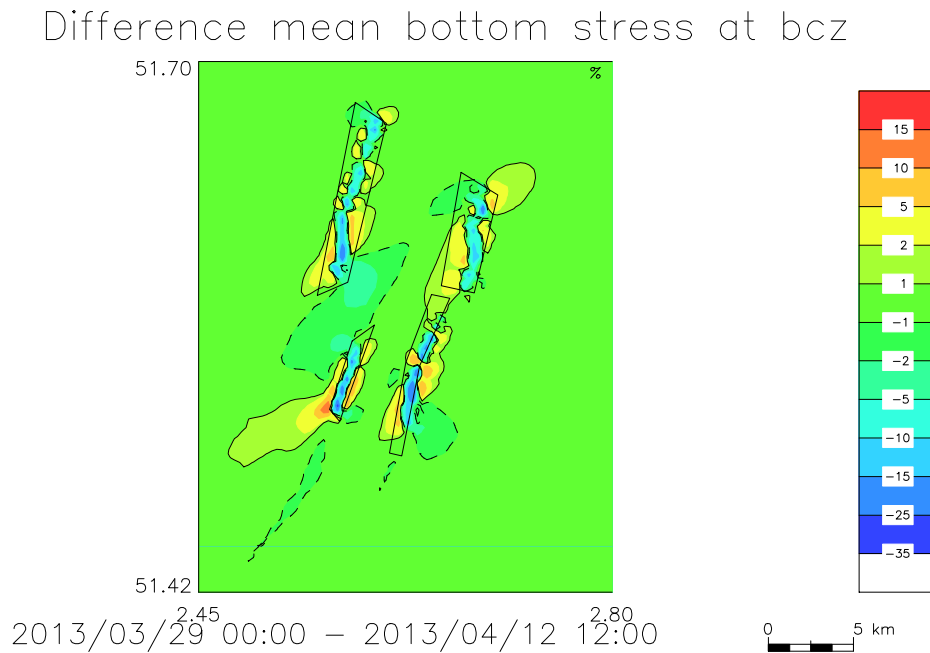


Figure 27: Differences of mean bottom shear stress over spring-neap tidal cycle for scenario 2.

In Figure 26, the number of points are again plotted, where the change in bottom stress exceeds a certain percentage for the different sectors and their surroundings. In the sectors themselves, 492 points have a change in bottom shear stress higher than 1%, which decreases to 67 points, with a change higher than 10%. In the area, where impact is allowed, 880 points have a change higher than 1%, which is clearly higher than in the case of scenario 1. In this area, 19 points have a change higher than 10%. In the area, where impact is not allowed, 545 points have a change higher than 1%, decreasing to 2 points, where the changes is higher than 6%.

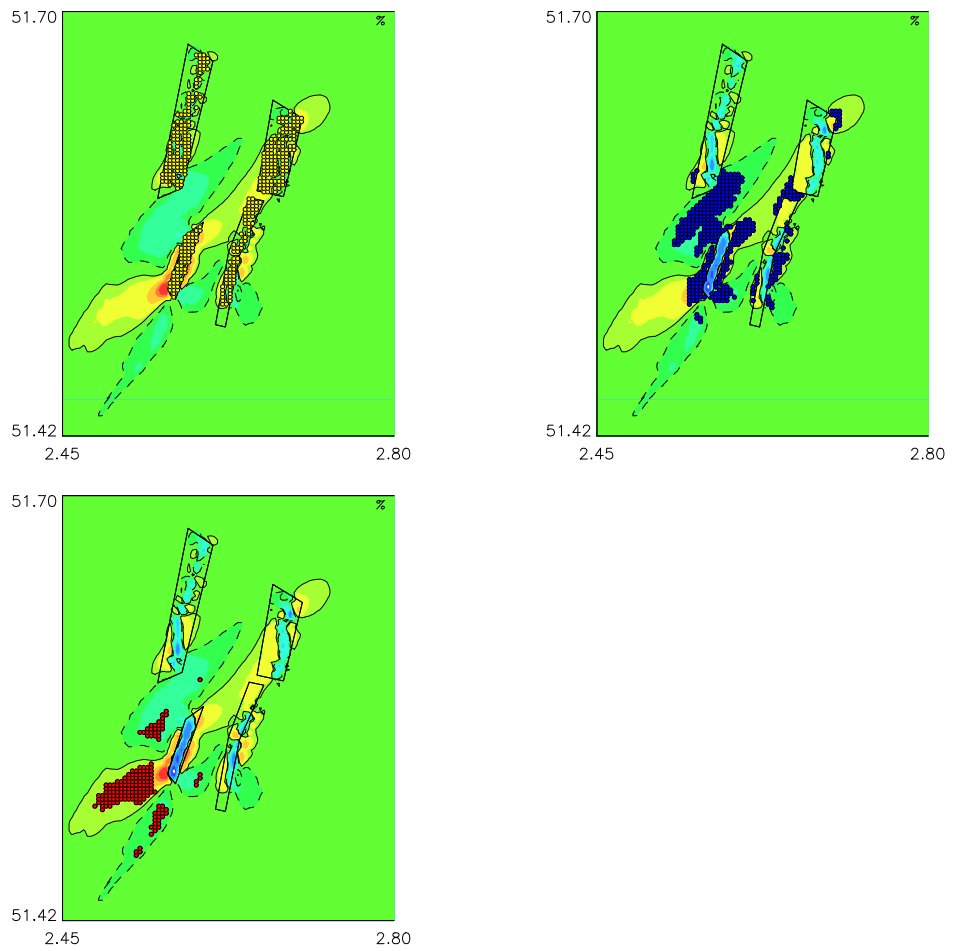


Figure 28: Position of the points with a difference higher than 2% for the extraction sector (upper left), area within a distance of a square root of the sector area from its border (upper right) and outside the distance (lower left) for scenario 2.

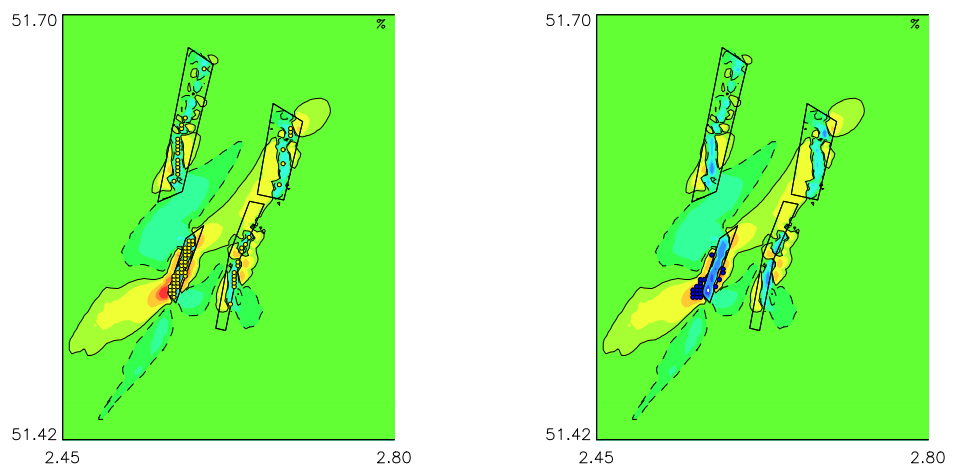


Figure 29: Position of the points with a difference higher than 10% for the extraction sector (left), area within a distance of a square root of the sector area from its border (right) for scenario 2.

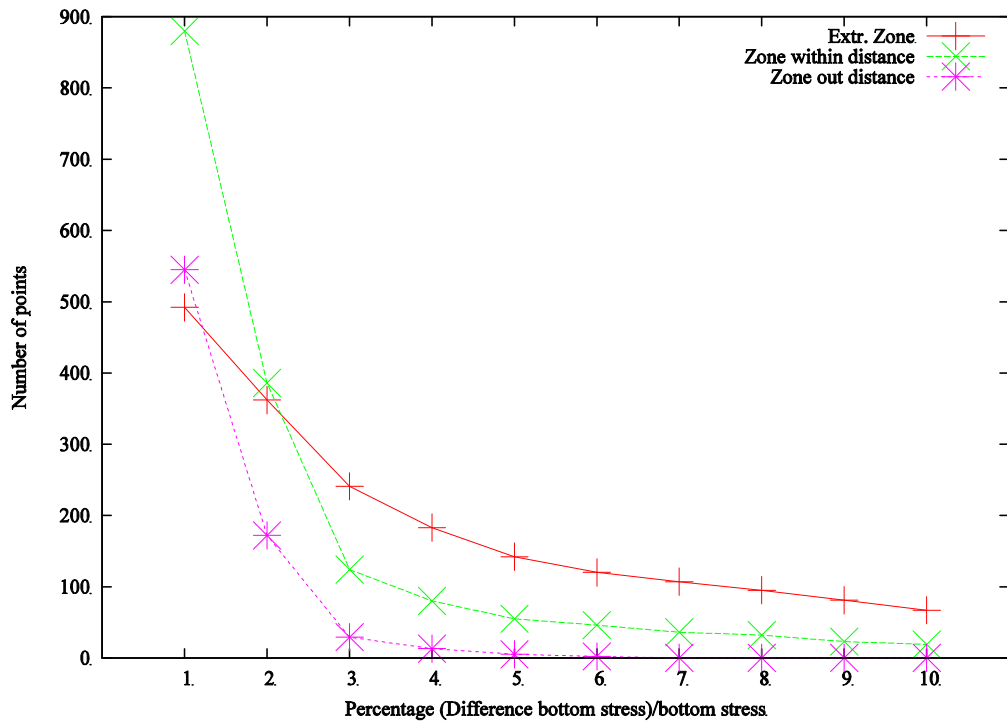


Figure 30: Number of points where the difference in bottom shear stress is exceeding a certain percentage, for the three defined areas for scenario 2.

It is clear that the impact of scenario 2 is higher than for scenario 1, but that the impact remains limited and that no changes of more than 10% are observed in the area where impact is not allowed.

6.3.3. Scenario 3

In Figure 23, the differences are shown for the bottom shear stress, averaged over the full spring-neap tidal cycle for the third scenario, where the extraction was executed only in Sector 4c. In this sector, a maximum of almost 12 m is being extracted. Although in this case, all extraction is executed in one sector only, the changes on the bottom shear stress remain limited. In the sector itself, the effect of an extraction of almost 12 m is of course considerable, with a maximum decrease of the bottom shear stress of -36% and a maximum increase of 13%. This is somewhat less than in scenario 2. Also in the area where impact is allowed, the changes in bottom shear stress are high, up to -8% to +22%. However, also for this scenario, bottom shear stress changes remain limited in the area where impact is not allowed and stay below 10%. The maximum and minimum in this case are -3.5% to +2.5%. Apparently, the effect of the extraction in Sector 4d is larger than that of the even larger extraction in Sector 4c. This is due to the fact that the bathymetry in Sector 4d is shallower.

In Figure 32 and Figure 33 the position of the points are again given, for the three areas, with a higher change in bottom shear stress than 2% and 10% respectively. Almost over the entire area of the extraction, Sector 4c in this case, the bottom shear stress changes over more than 2%. The bottom shear stress changes over more than 2% in a large area around Sector 4c. Outside the sector, where

impact is still allowed, the bottom shear stress changes over a small area west and south east of Sector 4c. In nine points of the zone, where impact is allowed, the difference is higher than 10%. These are located east of Sector 4c.

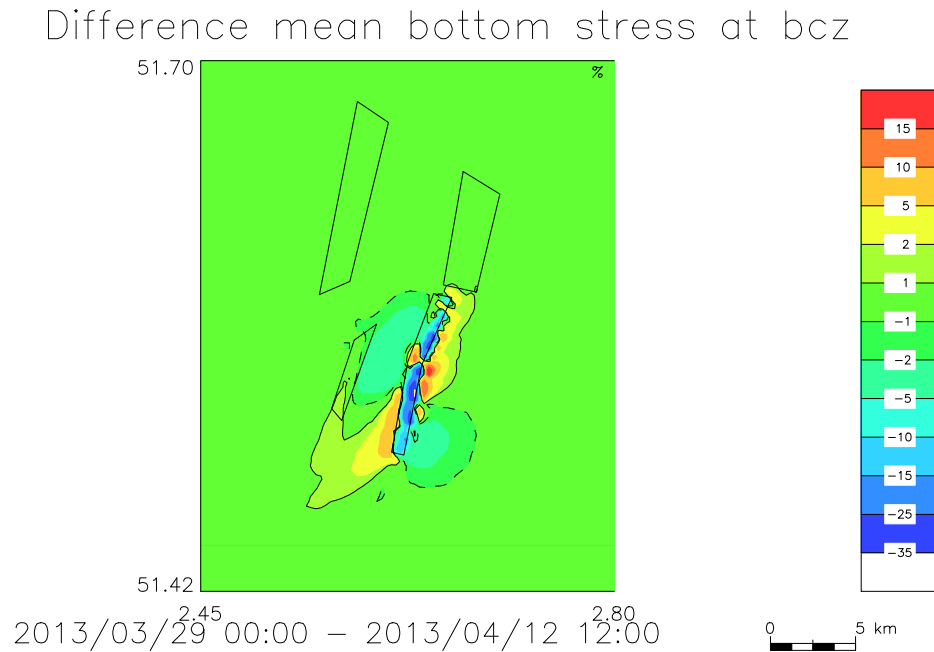


Figure 31: Differences of mean bottom shear stress over spring-neap tidal cycle for scenario 3.

Finally, one can observe in Figure 34, that in the extraction sector, a relative large amount of points have a change of bottom shear stresses higher than 10%. While 108 points have a change larger than 1%, still 53 points have a change larger than 10%. The effect of the intensive extraction in the zone itself is very important. In the area where impact is allowed, 509 points have a change higher than 1%, 9 points have a change in bottom shear stress higher than 10%. Finally, in the area where impact is not allowed, 407 points have a change higher than 1%, but only 14 a change in bottom shear stress of more than 3%.

In Figure 35, the number of points where the change in bottom shear stress is exceeding a certain percentage is plotted for the three scenarios and for the three different zones. One can see that in the area where impact is allowed, the most influence of the extraction is for scenario 3, while for the area, where impact is not allowed, the highest changes in bottom stress are generated during scenario 2. Overall however, the changes in bottom shear stress remain limited.

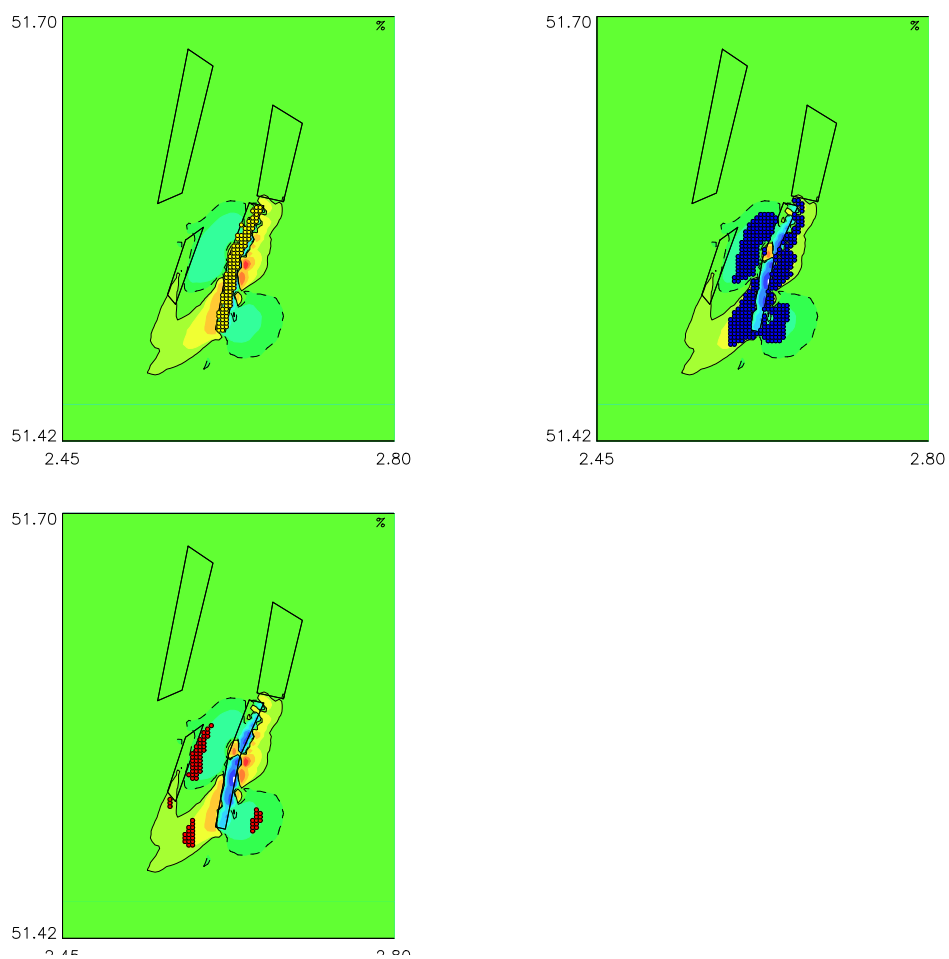


Figure 32: Position of the points with a difference higher than 2% for the extraction sector (upper left), area within a distance of a square root of the sector area from its border (upper right) and outside the distance (lower left) for scenario 3.

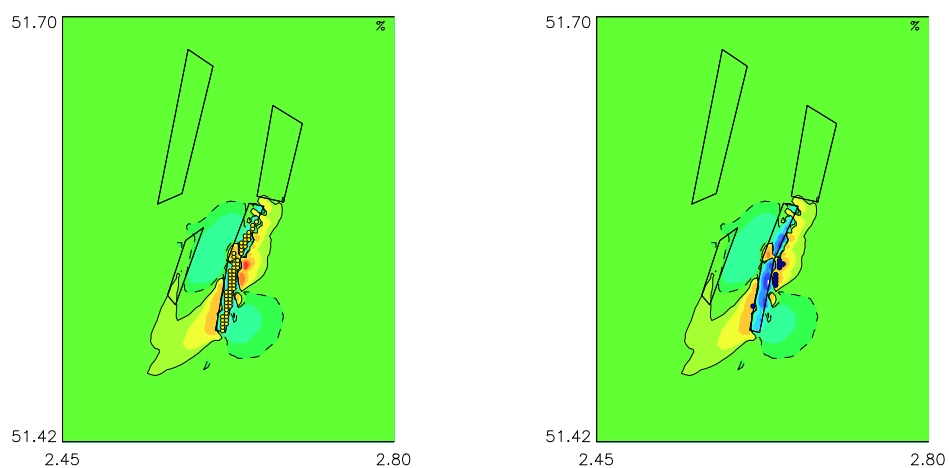


Figure 33: Position of the points with a difference higher than 10% for the extraction sector (left), area within a distance of a square root of the sector area from its border (right) for scenario 3.

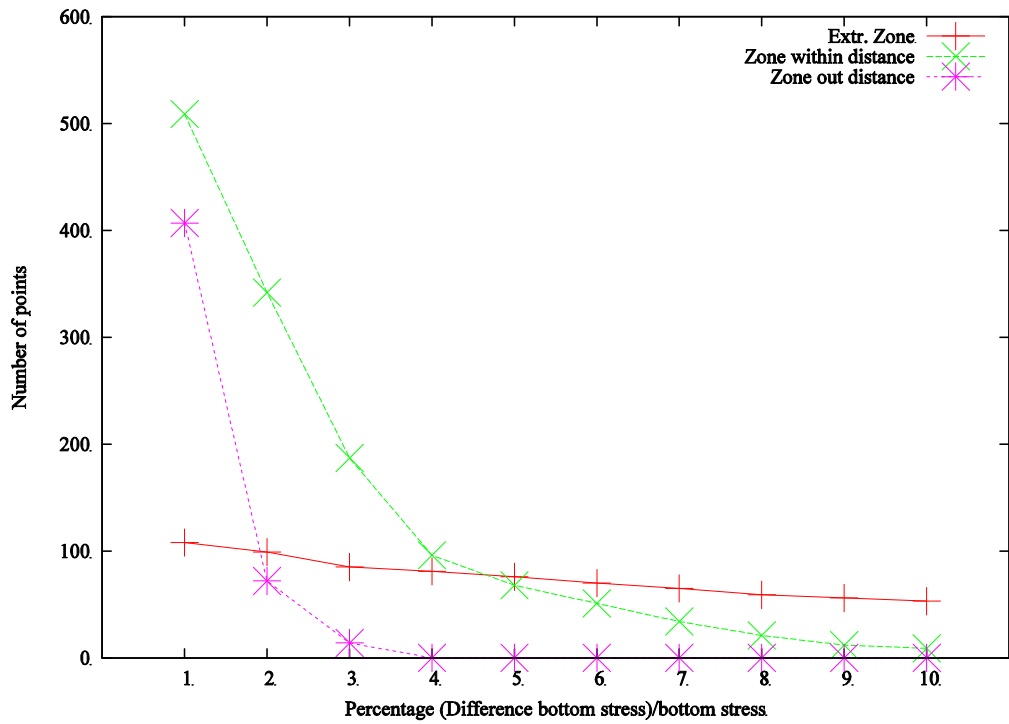


Figure 34: Number of points where the difference in bottom shear stress is exceeding a certain percentage, for the three defined areas for scenario 3.

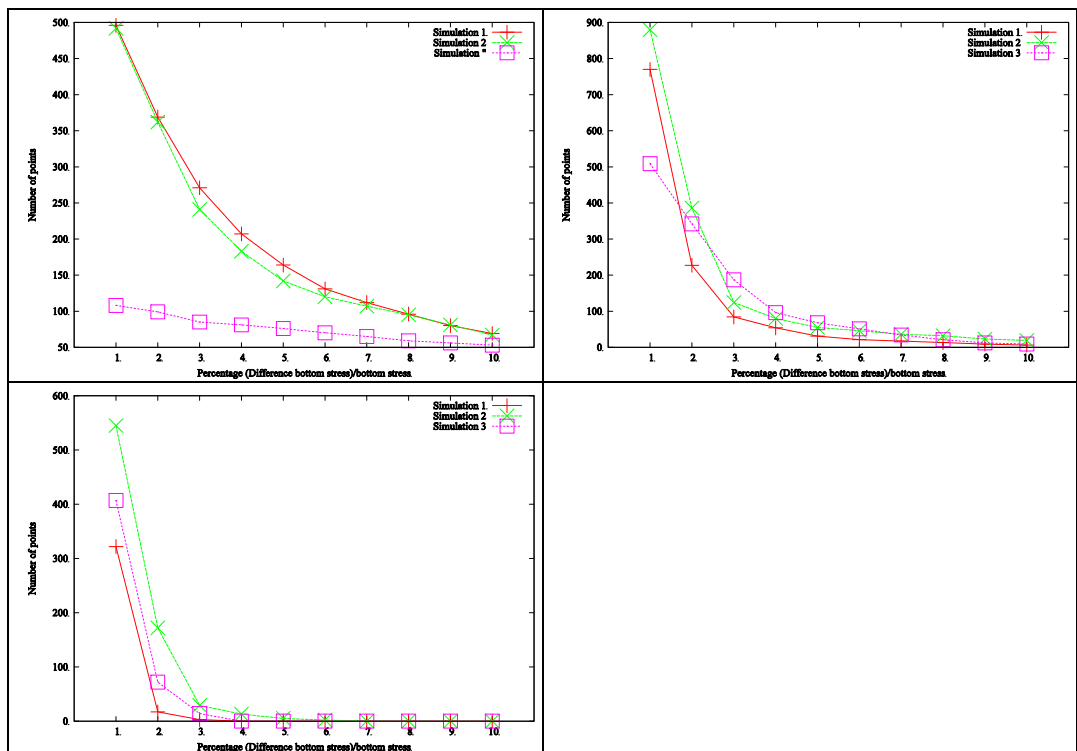


Figure 35: Number of points where the difference in bottom shear stress is exceeding a certain percentage, for the three scenarios and for the sector of extraction (upper left), area where impact is allowed (upper right) and area where impact is not allowed (lower left).

6.3.4. Conclusions

In the present section, three scenarios were modelled to investigate the influence of a large-scale extraction of marine aggregates (35 million m³) on the bottom shear stress in zone 4 of the Hinder Banks. In the framework of the MSFD, Belgium stated that an activity needs consideration when the bottom shear stress changes over more than 10%, at a place that is farther away from the border of the zone of impact than the square root of the area of the zone of impact. This was tested for the three scenarios. The first scenario used the same maximal extraction depth in the four extraction sectors, in the second scenario the four sectors were extracted until the same final water depth. In the third scenario, all the extraction was executed in Sector 4c. The simulations showed that for the three scenarios, the changes of the bottom stress in the area, where no impact was allowed remains limited to less than 6%. This is mainly due to the rather deep waters in the Hinder Banks area.

7. Conclusions

In the present report, the effect of extraction of marine aggregates on the bottom shear stress was evaluated in the framework of the MSFD. In the Belgian implementation of this directive, it was stated that a human impacts needs consideration when the bottom shear stress, calculated with a validated numerical model, changes with more than 10% at a specified distance of the activity. To test this for the extraction of marine aggregates in zone 4 of the Hinder Banks, first of all a validation is executed of some numerical models. Furthermore some scenarios were simulated to test the effect of the extraction on the changes of the bottom shear stress.

In a first part of the report the validation of the numerical model is executed. After presentation of the hydrodynamic, wave and bottom shear stress models, the validation of the hydrodynamic and wave model was discussed. The validation showed that the currents at the station along the eastern flank of the Oosthinder are well modelled. However, in the station along the southern part of the Oosthinder, the results are less good. This is probably due to the complex bathymetric situation, where the ADCP was placed in the trough of a barchan dune. Also the waves are modelled satisfactory.

Analysis of the bottom shear stress measurements showed that 5 m of the lowest part of the water column should be taken into account for the calculation of the bottom stress from the current profile. Furthermore, it was recommended to apply a moving average filter, with a window of about 2 hours, to filter out the high frequency fluctuations in the measurements. The ratio between the minimum and maximum bottom shear stress with a confidence limit of 95%, and the calculated bottom shear stress varied between 0 and 0.5 for the minimum and 1.5 to 3.0 for the maximum bottom shear stress.

The validation of the bottom shear stress model showed that the bottom shear stress could be reasonably modelled by the numerical models. Using a constant bottom roughness, best results were obtained by the Soulsby model, using a constant bottom roughness length of 0.01 m. Similar results were obtained by the other models. The bias was around 0.20 Pa, with a RMSE of about 0.35 Pa, for campaign BM01. In more than 90% of the time, the modelled bottom shear stress was between the 95% confidence limits. Less good results were obtained for measurements along the southern part of the Oosthinder sandbank. This is probably due to the less quality of the modelled currents and to the specific bathymetrical conditions at the site.

When the bottom roughness length was calculated by the model itself, the modelled bottom roughness length seemed to be too high, resulting in too high bottom shear stresses. When scaling the calculated bottom roughness length with a factor of 0.10, better results were obtained. However, also after scaling the bottom roughness length, the results were not significantly better than using the constant bottom roughness length. Therefore, using a constant bottom roughness length is recommended.

Finally, it was shown that no clear influence of the significant wave height is found in the bottom shear stress measurements in the area of the Hinderbanks. This is mainly due the deeper bathymetry at the stations.

In the second part of the report, three scenarios were simulated to investigate the influence of a large-scale extraction of marine aggregates (35 million m³) on the bottom shear stress in zone 4 of the Hinder Banks. The first scenario used the same maximal extraction depth in the four extraction sectors, in the second scenario the four sectors were extracted until the same final water depth. In the third scenario, all the extraction was executed in Sector 4c. The simulations showed that for the three scenarios, the changes of the bottom shear stress in the area, where no impact was allowed, remains limited to less than 6%. This is mainly due to the rather deep waters in the Hinder Banks area.

8. Acknowledgements

Wave buoy measurements were obtained from the Flemish Banks Monitoring Network, Flemish Government, Agentschap Maritieme Dienstverlening en Kust.

9. References

- Belgian State, 2012. Omschrijving van de Goede Milieutoestand en vaststelling van Milieudoelen, Kaderrichtlijn Marine Strategie, Art 9 & 10, 33 pp.
- Bijker, E.W., 1966. The increase of bed shear in a current due to wave motion. In: *Proceeding 10th Conference on Coastal Engineering*, Tokyo, 746-765.
- Dyer, K.R. and R.L. Soulsby, 1988. Sand transport on the continental shelf. *Annual Review of Fluid Mechanics*, 20, 295-324.
- Grant, W.D. and O.S. Madsen, 1982. Movable bed roughness in unsteady oscillatory flow. *Journal of Geophysical Research*, 87, C1, 469-481.
- Günther, H., S. Hasselmann and P.A.E.M. Janssen, 1992. Wamodel Cycle 4. DKRZ Technical Report No. 4, Hamburg, October 1992, 102 pp.
- Luyten, P. (editor), 2014. Coherens – A coupled hydrodynamic-ecological model for regional and shelf seas: user documentation. Version 2.6. RBINS Report, Operational Directorate Natural Environment, Royal Belgian Institute for Natural Sciences, Brussels, Belgium, 1554 pp.
- Malarkey, J. and A.G. Davies, 2012. A simple procedure for calculating the mean and maximum bed stress under wave and current conditions for rough turbulent flow based on Soulsby and Clarke's(2005) method. *Computers and Geosciences*, 43, 101-107.
- Mathys, P., J. De Rouck, L. Fernandez, J. Monbaliu, D. Van den Eynde, R. Delgado and A. Dujardin, 2012. Belgian Ocean Energy Assessment (BOREAS). Final Report. Belgian Science Policy Office, Brussels, 171 pp.
- Soulsby, 1995. Bed shear-stresses due to combined waves and currents. In: *Advances in Coastal Morphodynamics*. M.J.F. Stive, H.J. de Vriend, J. Fredsøe, L. Hamm, R.L. Soulsby, C. Teisson and J.C. Winterwerp (eds.), 4-20 to 4-23. Delft Hydraulics, The Netherlands.
- Soulsby, R., 1997. Dynamics of marine sands. A manual for practical applications. Telford, London, 249 pp.
- Soulsby, R.L. and S. Clarke, 2005. Bed shear-stresses under combined waves and currents on smooth and rough beds. Report TR 137. HR Wallingford, Wallingford, United Kingdom, 42 pp. (http://www.estproc.net/EstProc_library.htm).
- Soulsby, R.L. and R.J.S. Whitehouse, 2005. Prediction of ripple properties in shelf seas. Mark 2 Predictor for Time Evolution. Final Technical Report. Prepared for US Office of Naval Research, Contract No. N00014-04-C-0408. Report TR154, HR Wallingford, 41 pp + App.
- Van den Eynde, D., 2013. Comparison of the results of the operational HYPAS and WAM models. Report OPTOS/1/DVDE/201303/EN/TR1, Royal Belgian Institute for Natural Sciences, Operational Directorate Natural Environment, Brussels, Belgium, 39 pp.
- Van den Eynde, D., 2015. Measuring, using ADV and ADP sensors, and modelling bottom shear stresses in the Belgian coastal waters. Report ZAGRI-MOZ4/1/DVDE/201502/EN/TR02, Royal Belgian Institute for Natural Sciences, Operational Directorate Natural Environment, Brussels, Belgium, 49 pp.

- Van den Eynde, D. en J. Ozer, 1993. Sediment-Trend-Analyse: berekening van sedimenttransport met behulp van een mathematisch model. Studie uitgevoerd in opdracht van HAECON NV, betreffende de 'Sediment-Trend-Analyse' (STA) Activiteit 1. Beheerseenheid Mathematisch Model Noordzee, Brussel, 111 pp.
- Van den Eynde, D., A. Giardino, J. Portilla, M. Fettweis, F. Francken and J. Monbaliu, 2010. Modelling the effects of sand extraction, on the sediment transport due to tides, on the Kwinte Bank. *Journal of Coastal Research*, SI Eumarsand, 51, 101-116.
- Van den Eynde, D., M. Baeye and V. Van Lancker, 2014. Validation of the OPTOS-FIN model in the exploration 4 zone. Report ZAGRI-MOZ4/X/DVDE/201401/EN/TR/1, Royal Belgian Institute for Natural Sciences, Operational Directorate Natural Environment, Brussels, Belgium, 40 pp.
- Van Lancker, V., M. Baeye, M. Fettweis, F. Francken and D. Van den Eynde, 2014. Monitoring of the impact of the extraction of marine aggregates, in casu sand, in the zone of the Hinder Banks. Report MOZ4-ZAGRI/X/VVL/201401/EN/SR01, Royal Belgian Institute of Natural Sciences, Operational Directorate Natural Environment, 384 pp. (9 Annexes).
- Van Lancker, V., M. Baeye, D. Evangelinos & D. Van den Eynde, 2015. Monitoring of the impact of the extraction of marine aggregates, in casu sand, in the zone of the Hinder Banks. Period 1/1 – 31/12 2014. Brussels, RBINS-OD Nature. Report <MOZ4-ZAGRI/I/VVL/ 201502/EN/SR01>, 74 pp. (+5 Annexes, 109 pp).
- The WAMDI Group, 1988. The WAM Model – A Third Generation Ocean Wave Prediction Model. *Journal of Physical Oceanography*, 18, 1775-1810.
- Wilkinson, R.H., 1984. A Method for Evaluating Statistical Errors Associated with Logarithmic Velocity Profiles. *Geo-Marine Letters*, 3, 49-52.

10. Appendix I: Statistical parameters

For the validation, the statistical parameters bias, root mean square error (RMSE), the systematical and unsystematical RMSE and the correlation coefficient can be calculated.

Hereafter, the measurements series will be presented as x and the model results (that is subject to the test) as y .

The mean values of the time series are represented by \bar{x} (reference) and \bar{y} (subject to test):

$$\bar{x} = \frac{1}{N} \sum_{i=1}^N x_i$$

$$\bar{y} = \frac{1}{N} \sum_{i=1}^N y_i$$

where N is the length of the time series.

The bias is the difference between the mean of the modelled and the measured time series:

$$bias = \bar{y} - \bar{x}$$

The closer the bias is to zero, the better both time series correspond. A positive bias value means that the modelled time series are an overestimation of the observed time series. A negative bias value means that the modelled time series are an underestimation of the observed time series.

The root mean square error (RMSE) is a measure for the absolute error and is defined as:

$$RMSE = \sqrt{\frac{\sum_{i=1}^N (y_i - x_i)^2}{N}}$$

Corresponding time series will result in RMSE values close to zero.

Furthermore, a systematical RMSE ($RMSE_s$) and an unsystematical RMSE ($RMSE_u$) can be defined, that evaluate respectively, the (absolute) error, which is generated by the deviation from the linear regression of the modelled time series from the measurements, and the error that is generated by the deviation from the individual model results from the linear regression itself. While the systematical RMSE could be reduced by applying a correction, using the linear regression, the unsystematical RMSE is the error which is inherent from the variation from the results themselves. These parameters can be calculated as:

$$RMSE_s = \sqrt{\frac{\sum_{i=1}^N (\hat{y}_i - x_i)^2}{N}}$$

$$RMSE_u = \sqrt{\frac{\sum_{i=1}^N (y_i - \hat{y}_i)^2}{N}}$$

with \hat{y}_i is defined from the linear regression

$$\hat{y}_i = mx_i + b$$

with slope m and intercept b calculated from:

$$m = \frac{N \sum x_i y_i - \sum x_i \sum y_i}{N \sum x_i^2 - (\sum x_i)^2}$$

$$b = \bar{y} - m\bar{x}$$

The correlation between both signals is given by Pearson's correlation coefficient, defined as:

$$r = \frac{\sum_{i=1}^N (x_i - \bar{x})(y_i - \bar{y})}{\sqrt{\sum_{i=1}^N (x_i - \bar{x})^2} \sqrt{\sum_{i=1}^N (y_i - \bar{y})^2}}$$

The scatter index is a measure for the relative error and is defined by:

$$S.I. = \frac{RMSE}{\bar{x}}$$

○ COLOPHON

This report was issued by Operational Directorate Natural Environment in April 2016.

The reference code is ZAGRI-MOZ4-INDI67/1/DVDE/201604/EN/TR01.

- Status draft
 final version
 revised version of document
 confidential
- Available in English
 Dutch
 French

If you have any questions or wish to receive additional copies of this document, please send an e-mail to DVandenEynde@naturalsciences.be, quoting the reference, or write to:

Royal Belgian Institute of Natural Sciences
Operational Directorate Natural Environment
100 Gulledele
B-1200 Brussels
Belgium
Phone: +32 2 773 2111
Fax: +32 2 770 6972
<http://www.mumm.ac.be/>

Royal Belgian Institute of Natural Sciences
Operational Directorate Natural Environment
Suspended Matter and Seabed Monitoring and Modelling Group



The typefaces used in this document are Gudrun Zapf-von Hesse's *Carmina Medium* at 10/14 for body text, and Frederic Goudy's *Goudy Sans Medium* for headings and captions.

Annex D

This Annex forms part of the report:

Van Lancker, V., Baeye, M., Montereale-Gavazzi, G. & Van den Eynde, D. (2016). Monitoring of the impact of the extraction of marine aggregates, in casu sand, in the zone of the Hinder Banks. Period 1/1 - 31/12 2015 and Synthesis of results 2011-2015. Brussels, RBINS-OD Nature.



HBMC monitoring area

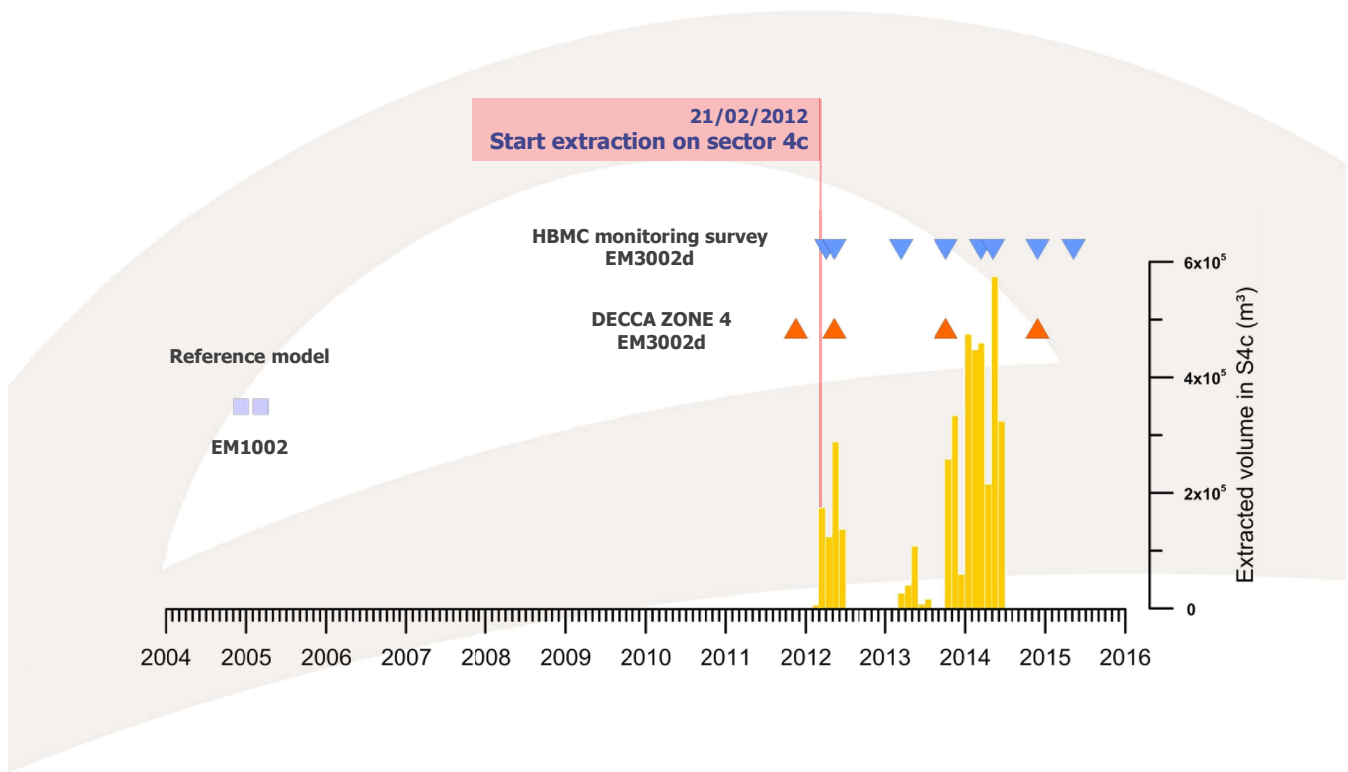
Results from 2012 to 2015

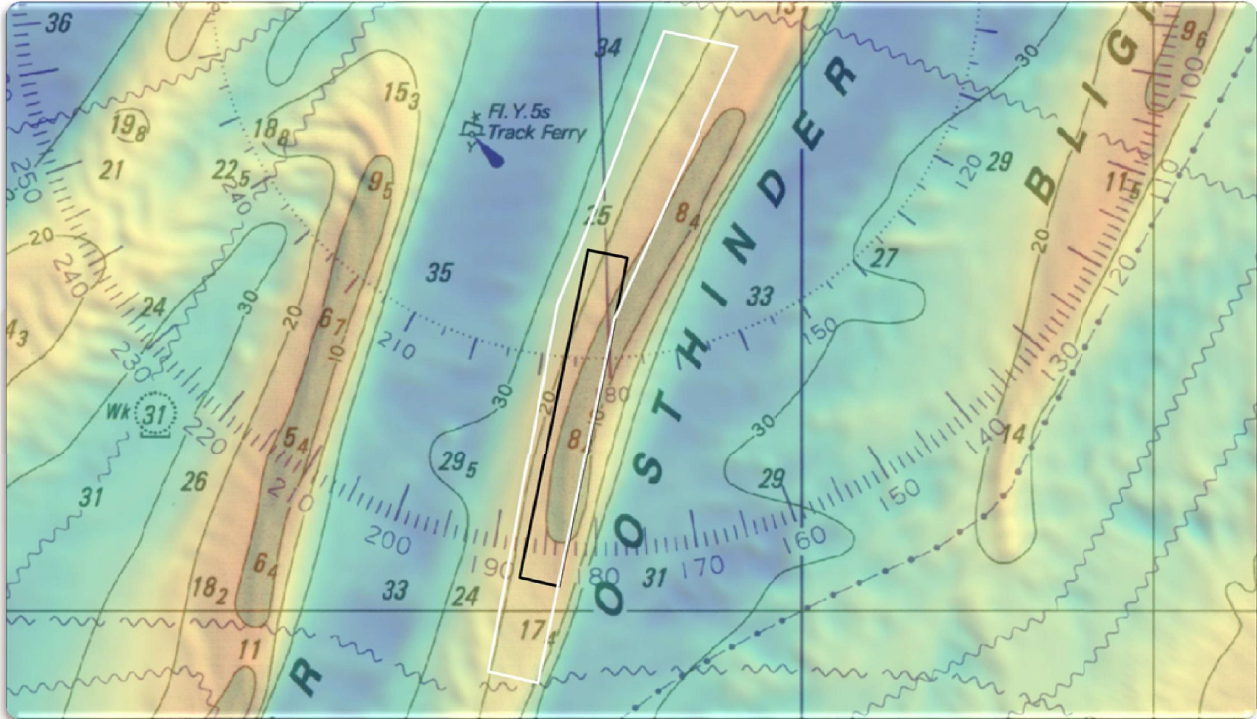
COPCO September 2015

<http://economie.fgov.be>

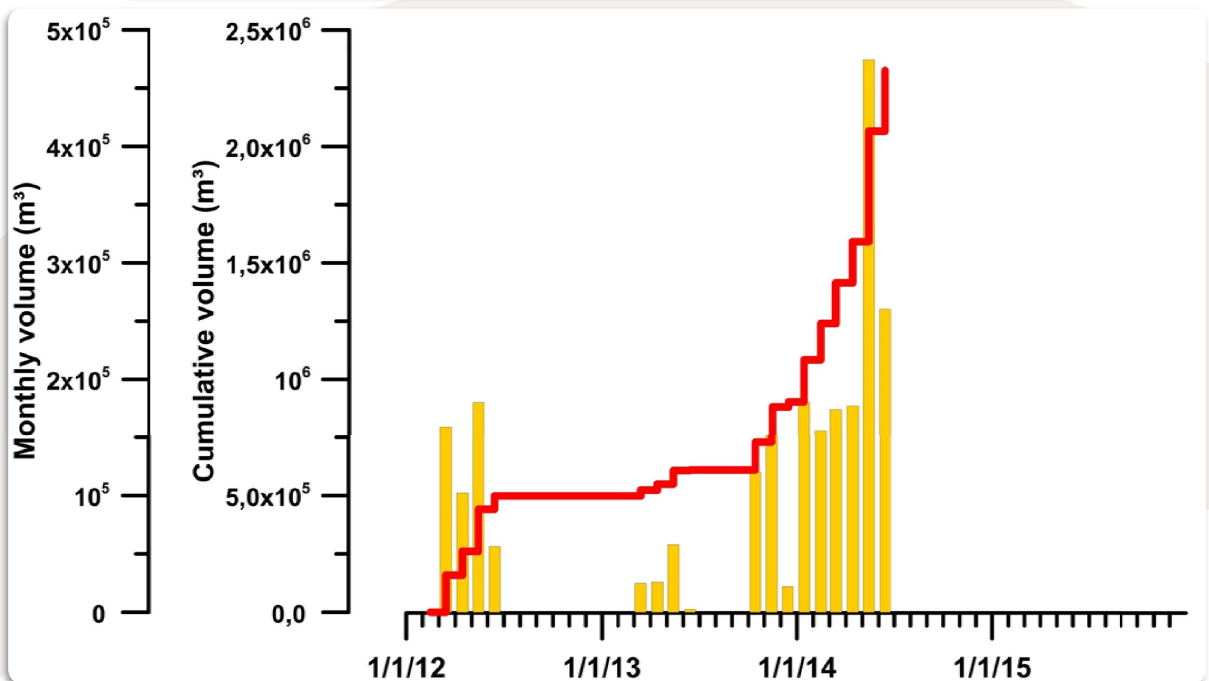
.be

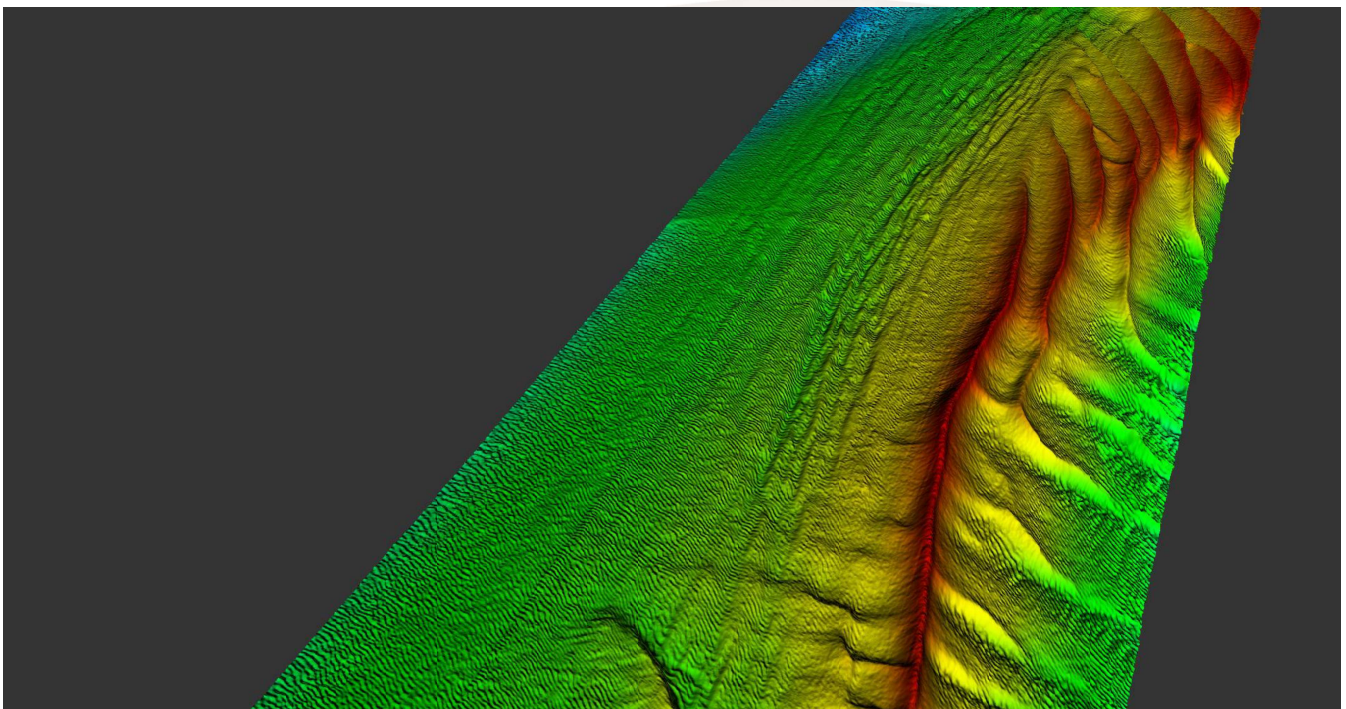
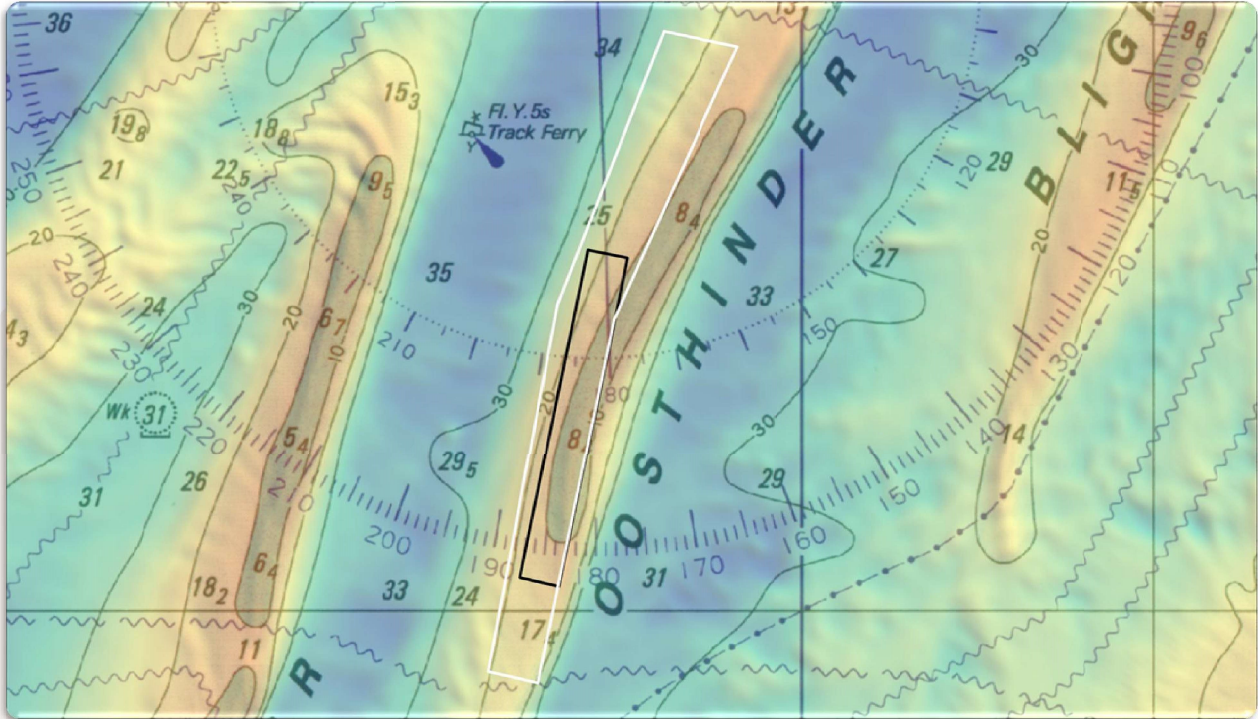
S4c dataset and history:



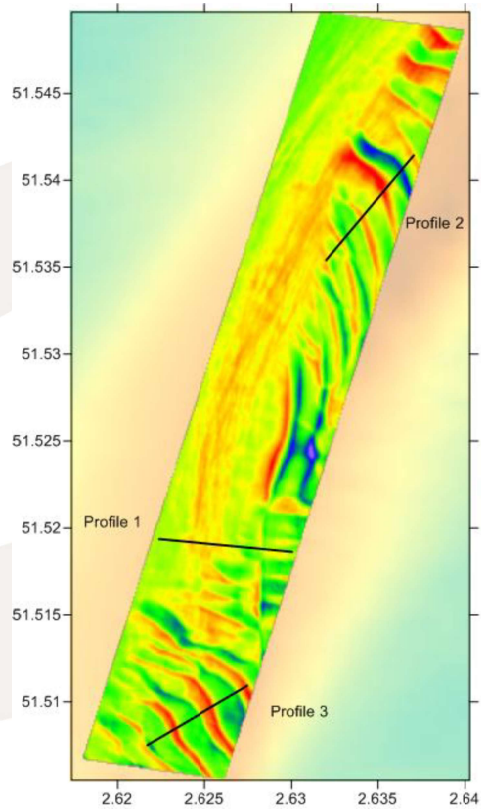
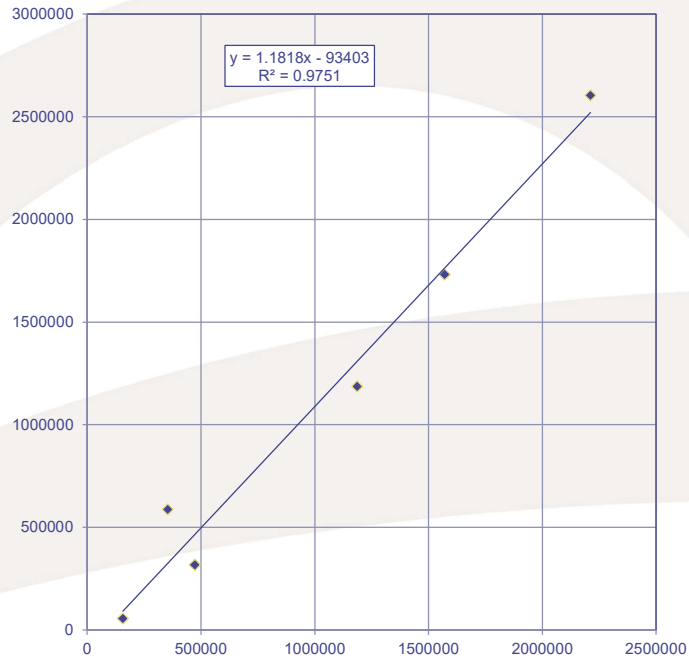


monthly volume
 cumulative volume

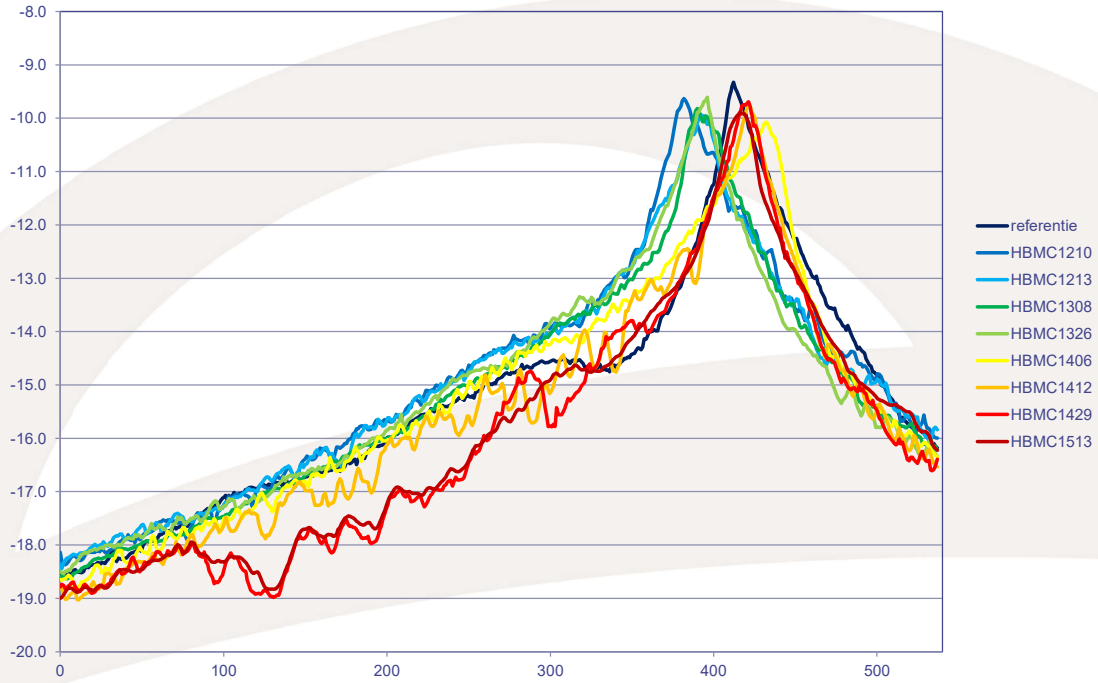




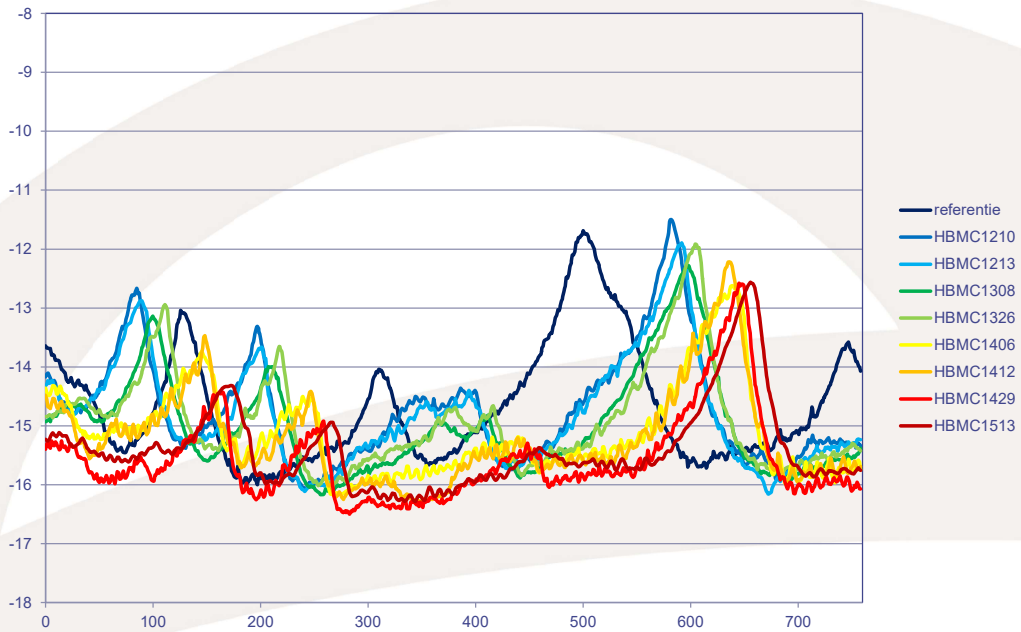
Extracted vs measured

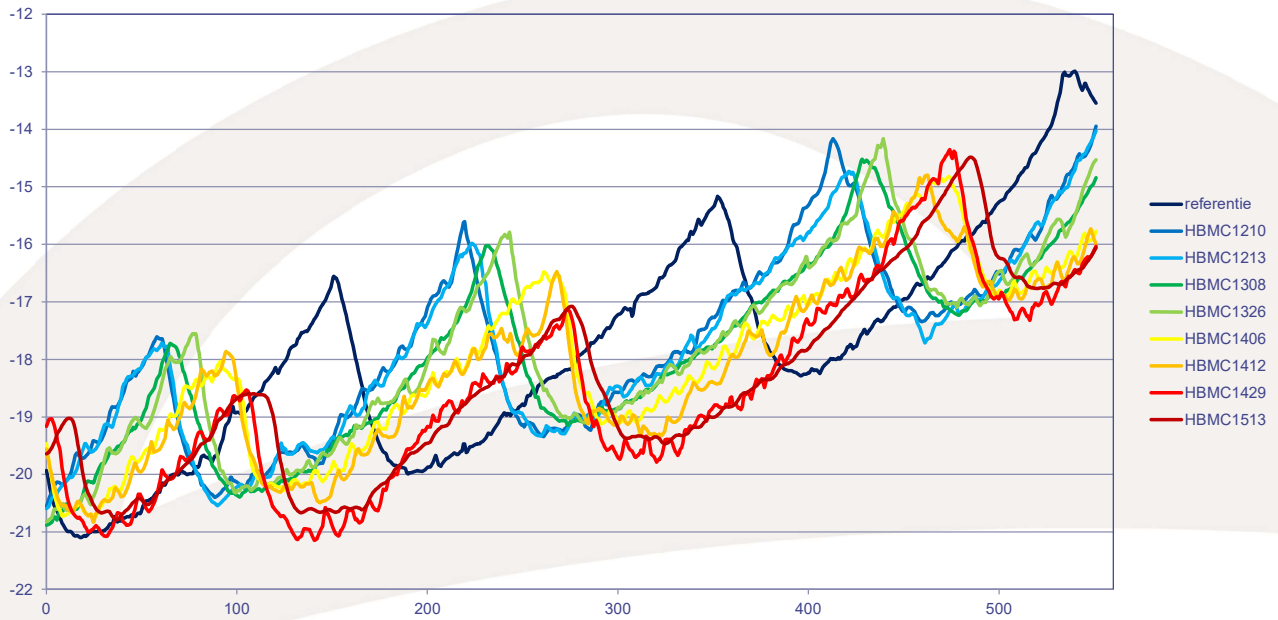


~ 10m/year → E

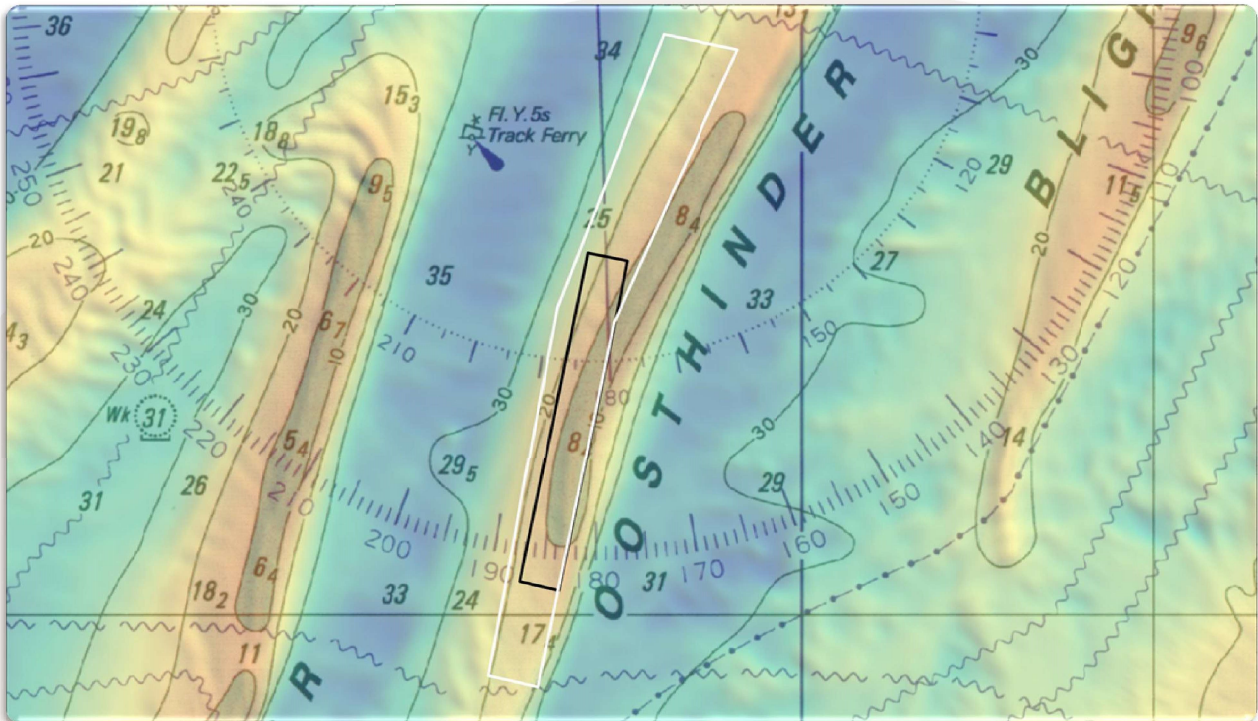


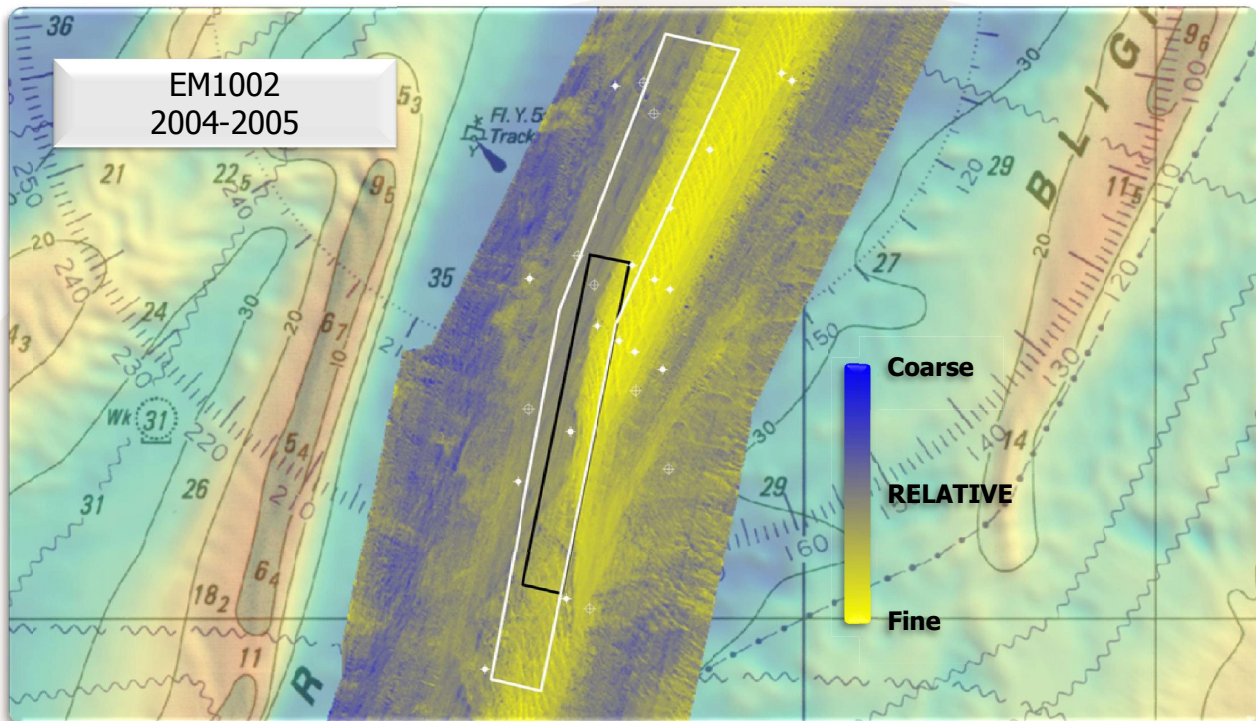
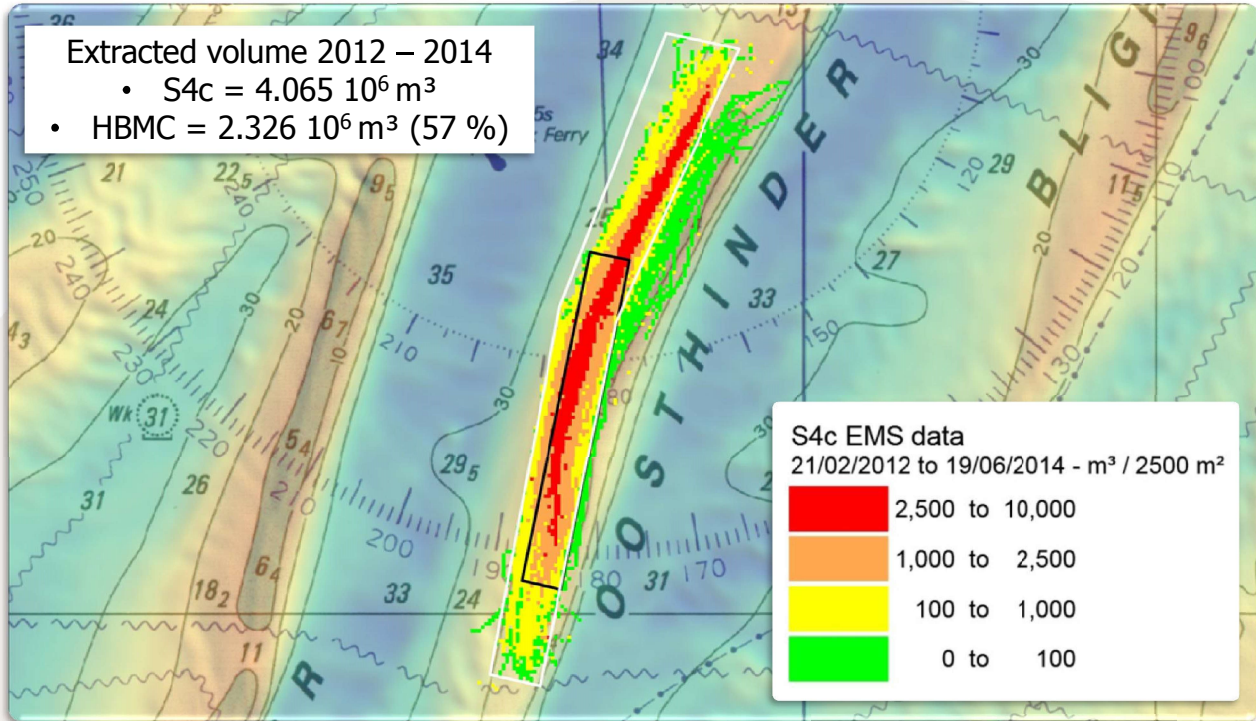
~ 30m/year → NE

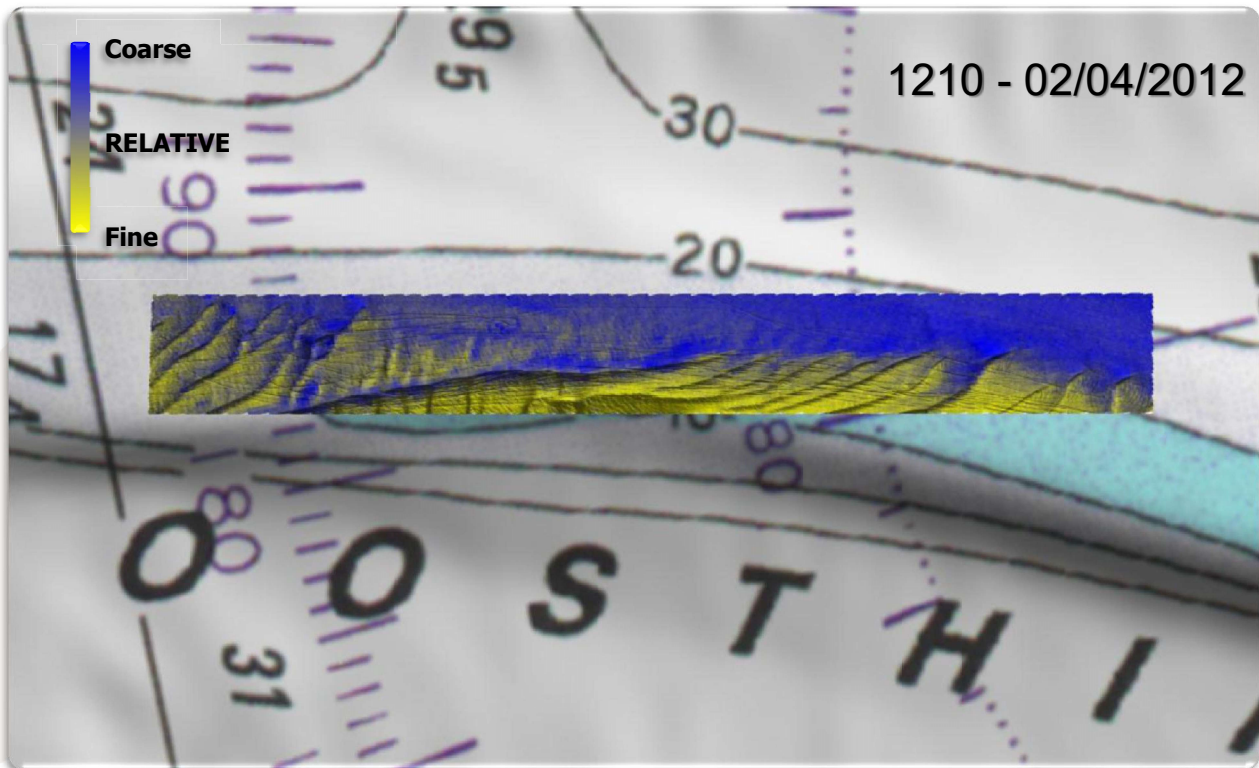
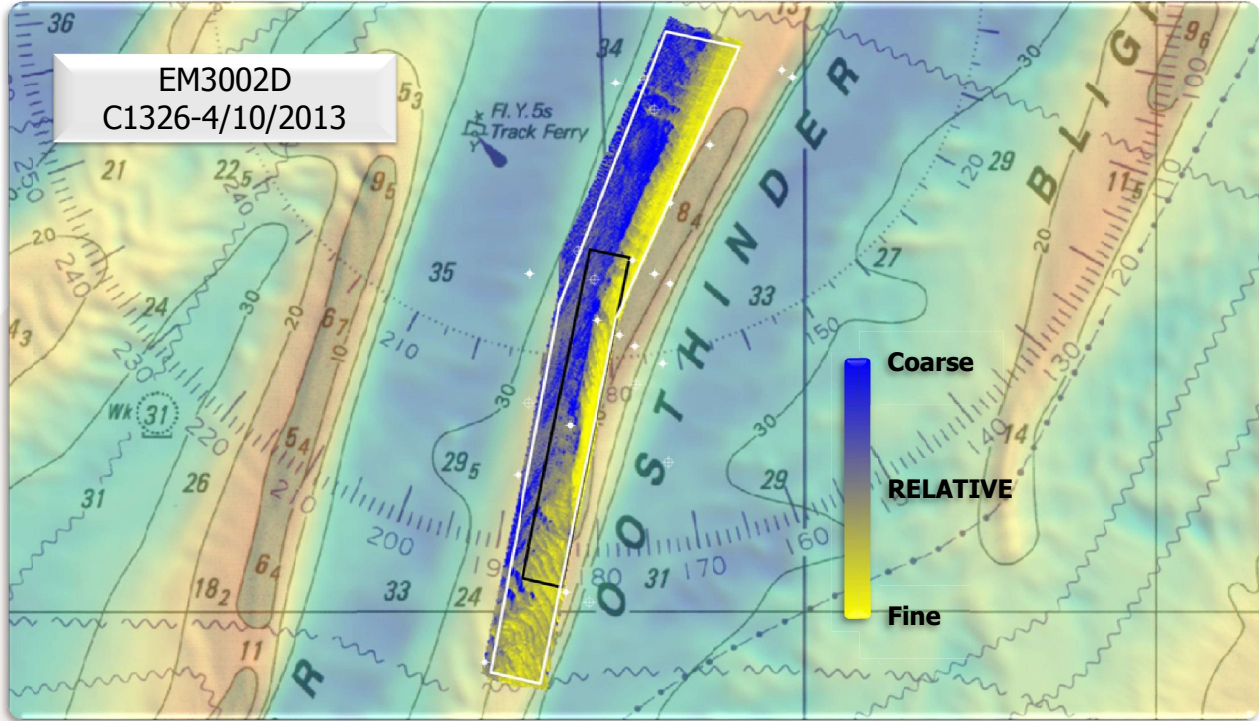


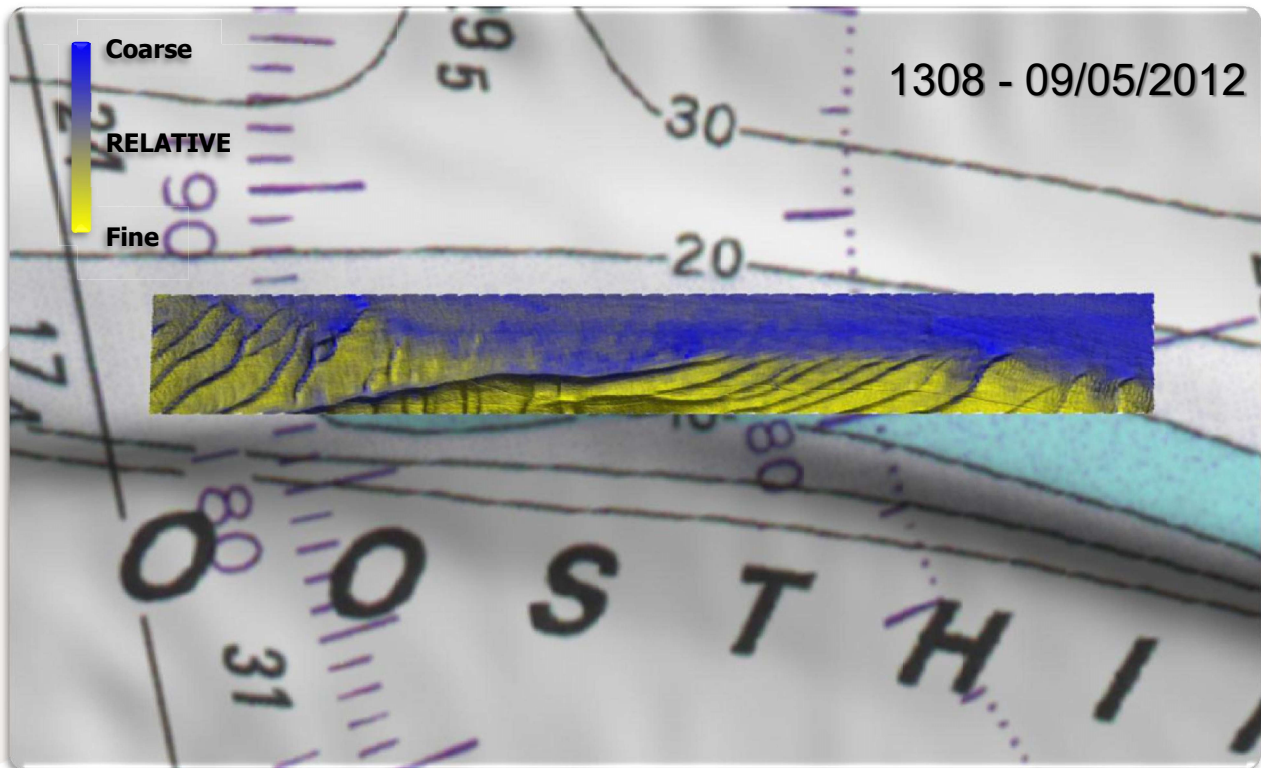
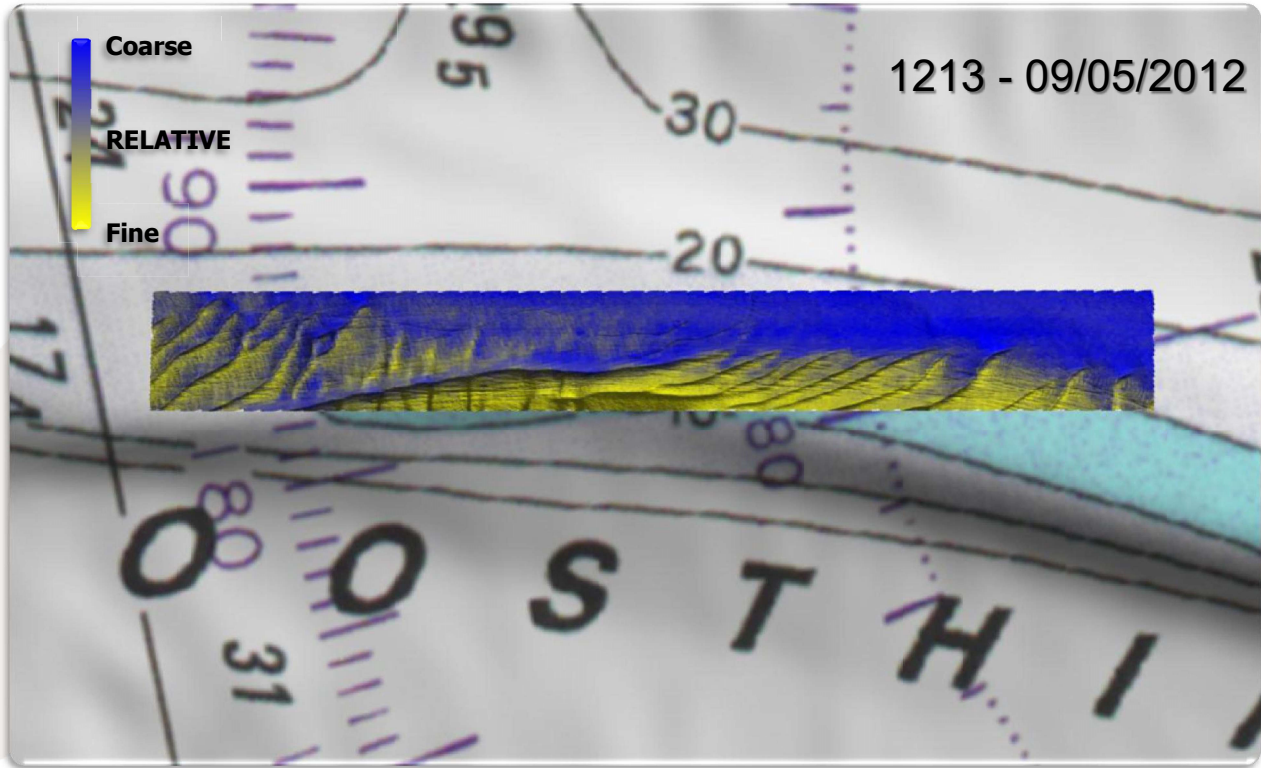


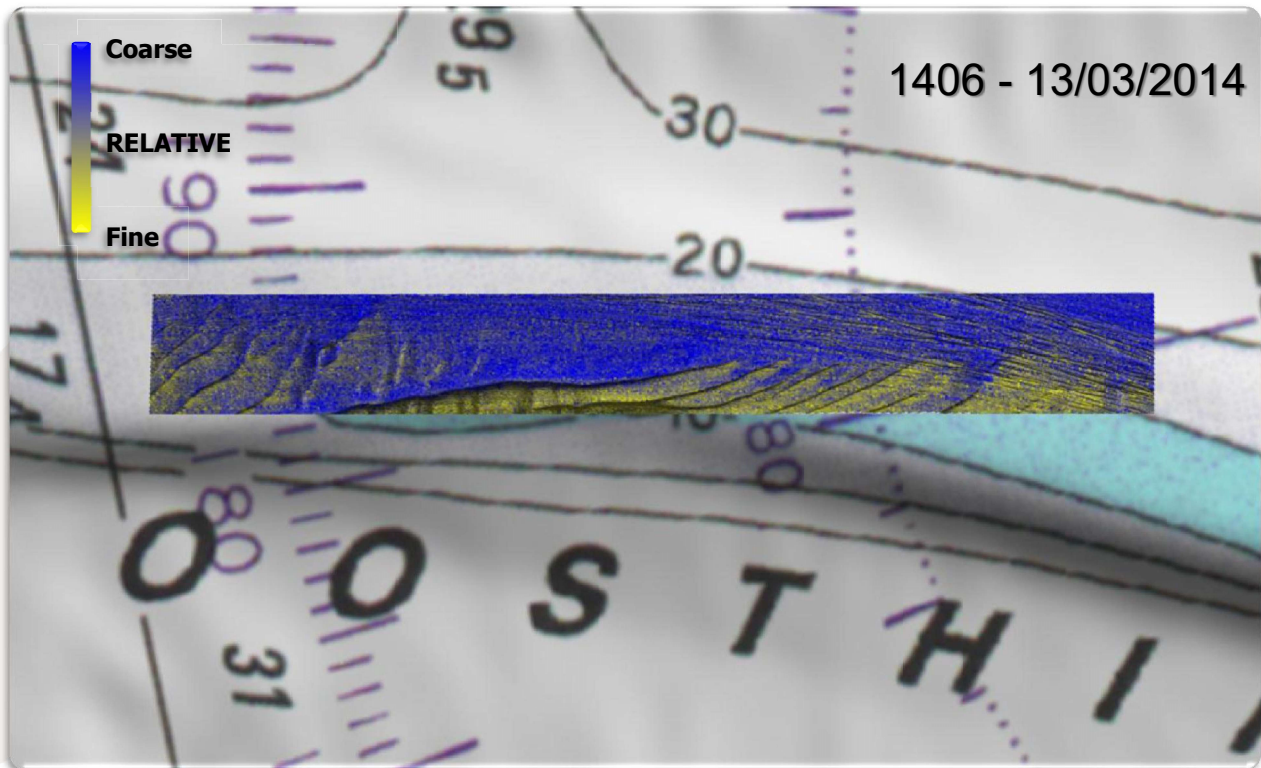
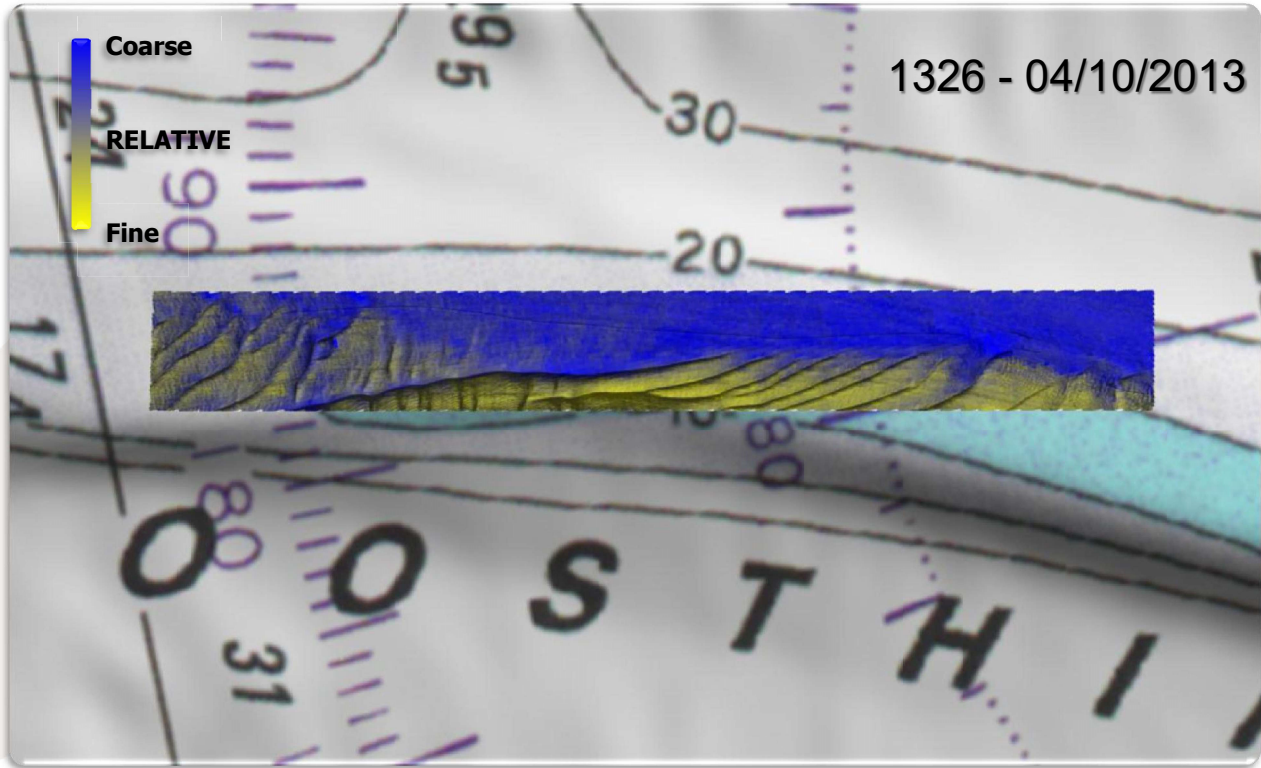
Relation Extraction and BS in HBMC

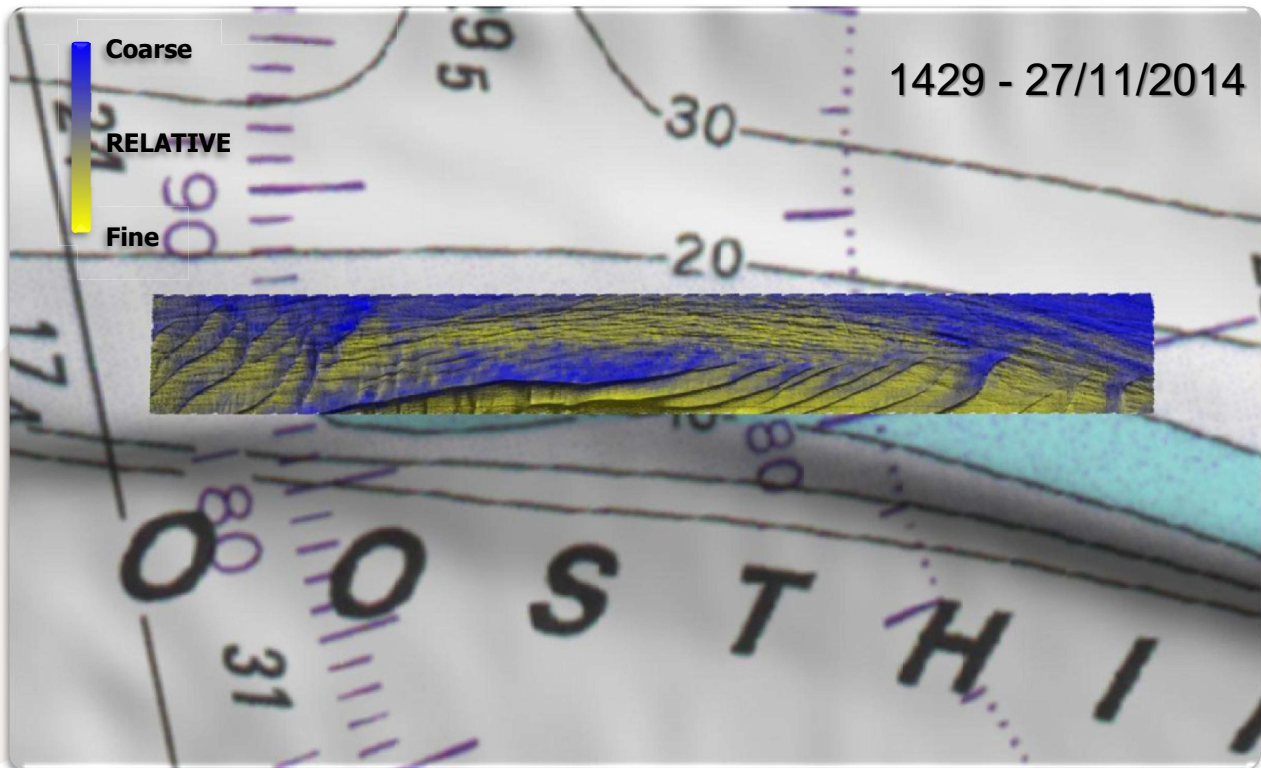
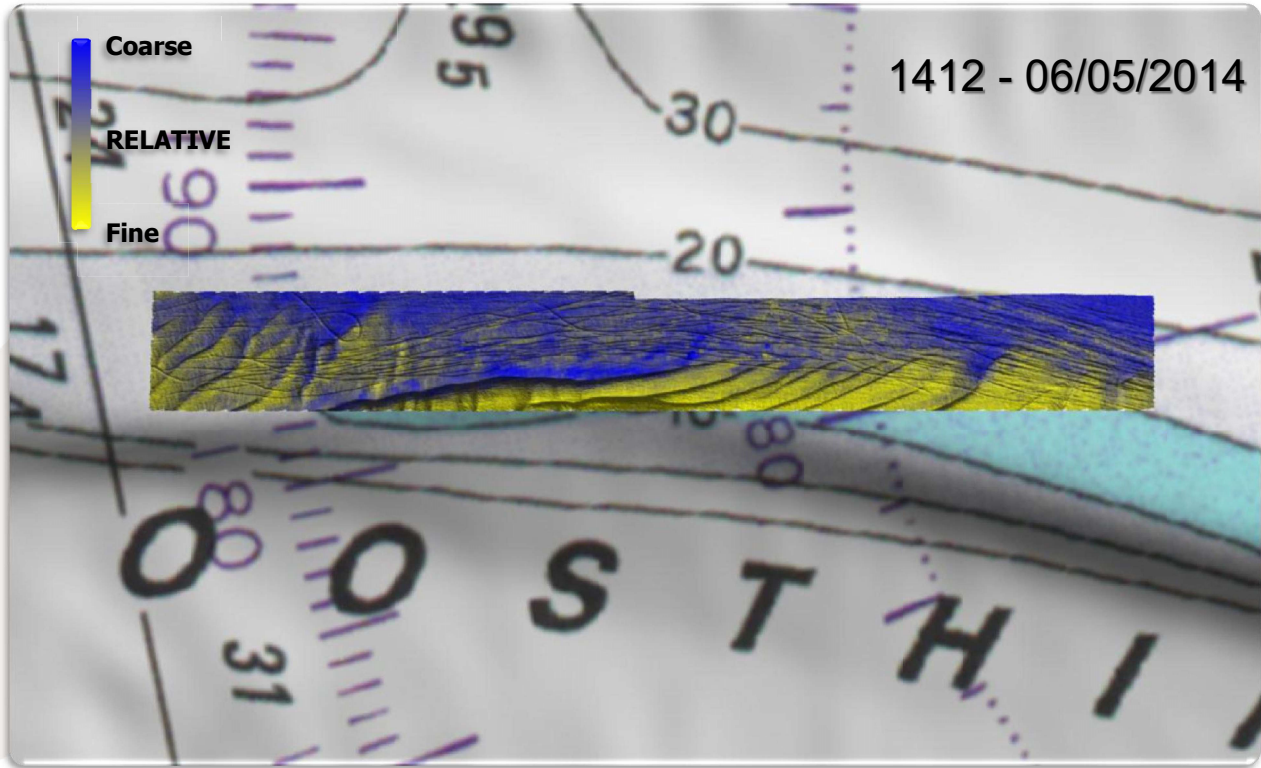


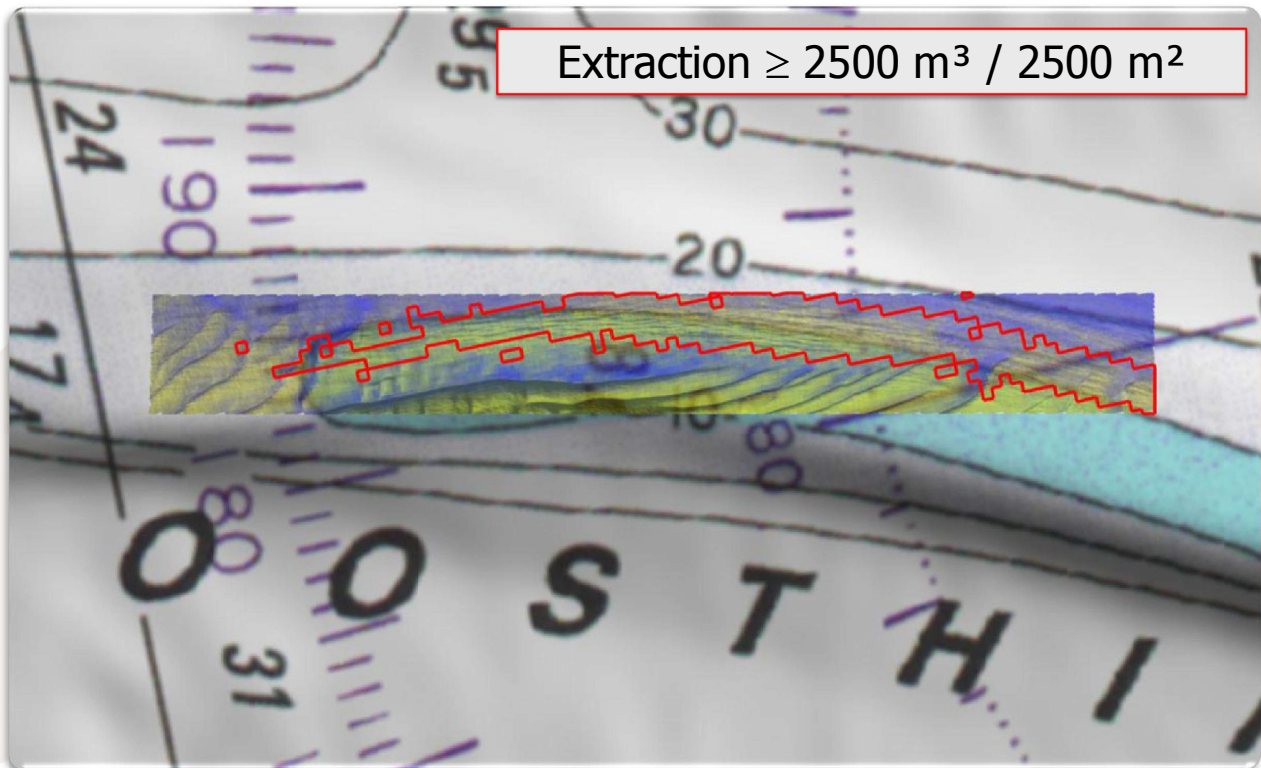
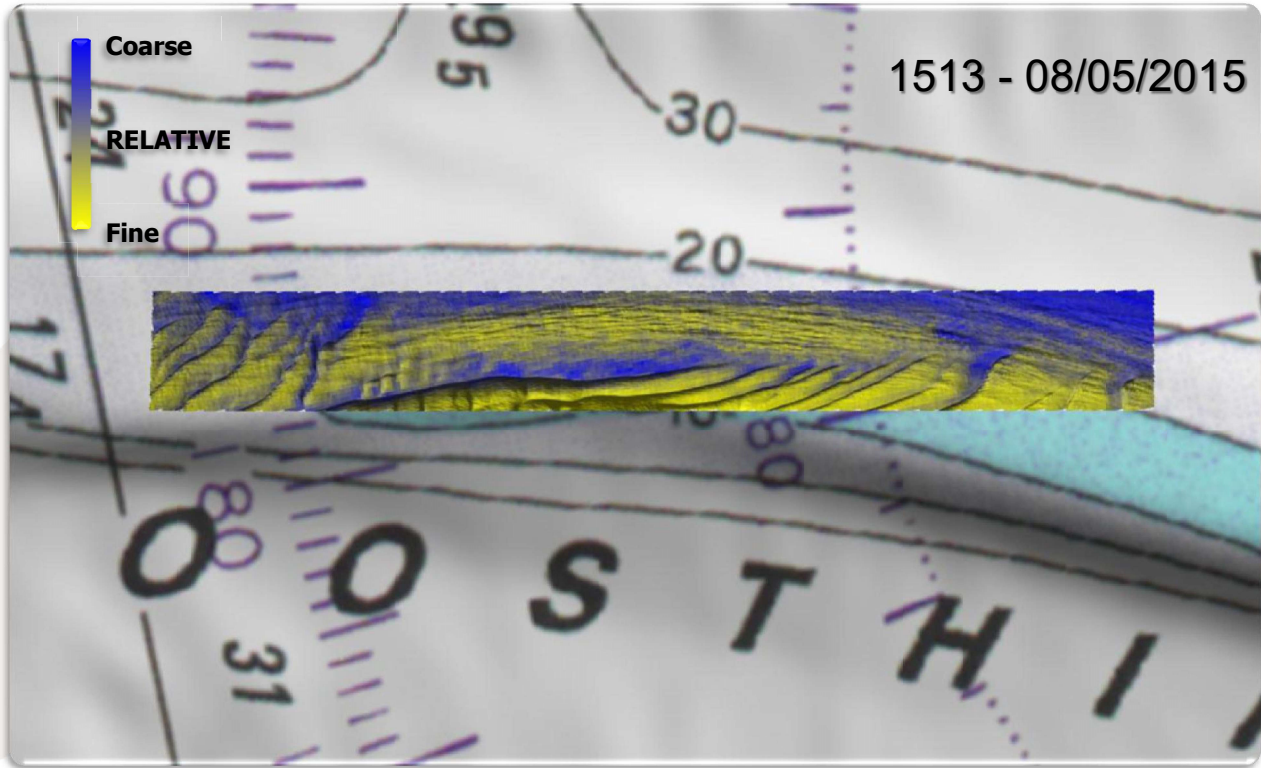












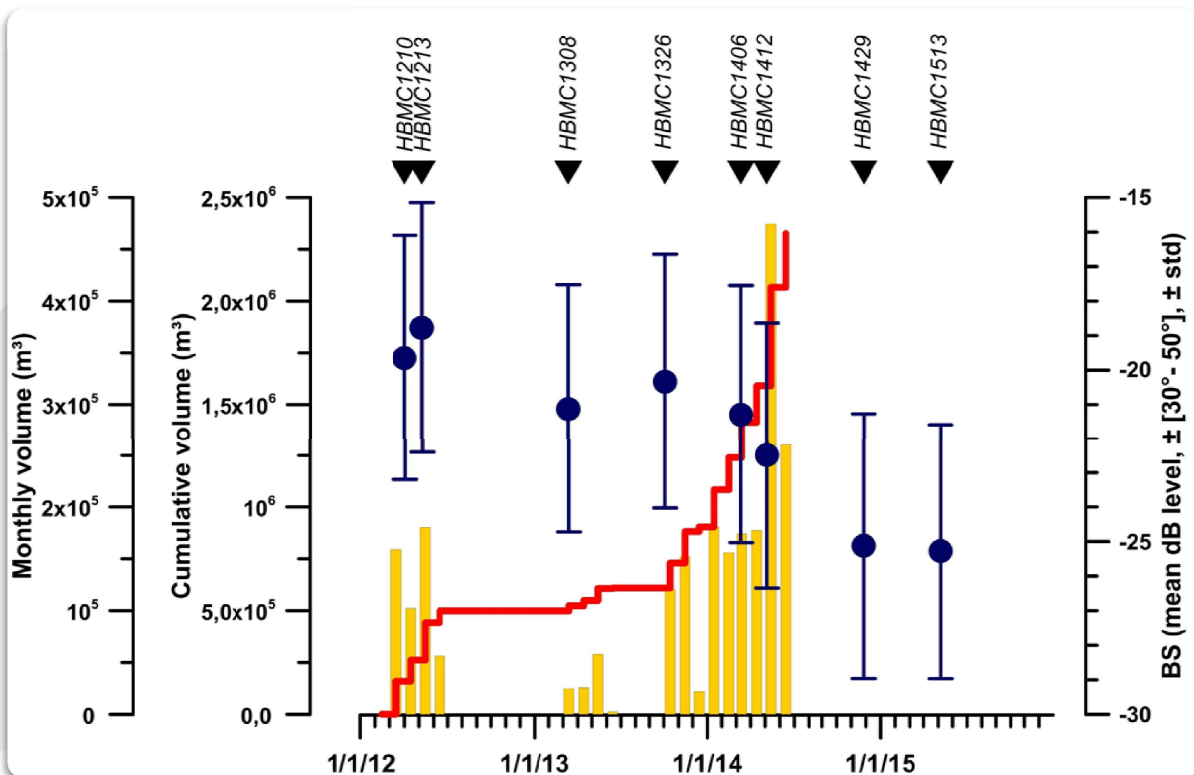
COPCO BS standardized processing for monitoring data:

1. Remove KS correction
2. By line: 1x1m mosaic
 - a) Tx compensation = flattening using the data itself, no a priori model!
 - b) Extraction of $\pm [30^\circ-50^\circ]$ = only oblique incident BS!
3. Merging the lines:

→ mosaic of $\pm [30^\circ-50^\circ]$ compensated dB values per survey
4. GIS dB comparative statistics inside masks (geo areas)

For this study, mask =
HBMC geo area where extraction $\geq 2500 \text{ m}^3 / 2500 \text{ m}^2$

HBMC extraction and BS evolution:



Annex E

Publications

This Annex forms part of the report:

Van Lancker, V., Baeye, M., Montereale-Gavazzi, G. & Van den Eynde, D. (2016). Monitoring of the impact of the extraction of marine aggregates, in casu sand, in the zone of the Hinder Banks. Period 1/1 – 31/12 2015 and Synthesis of results 2011-2015. Brussels, RBINS-OD Nature.

Annex E. Publications 2015

A1 publication

Van Lancker, V. & Baeye, M. (2015). Wave glider monitoring of sediment transport and dredge plumes in a shallow marine sandbank environment. *PloS one*, 10(6), e0128948.

Book chapter

Van Lancker, V., Lauwaert, B., De Mol, L., Vandenreyken, H., De Backer, A., Pirlet, H. (2015). Zand- en grindwinning, in: Pirlet, H. et al. (Ed.) Compendium voor Kust en Zee 2015: Een geïntegreerd kennisdocument over de socio-economische, ecologische en institutionele aspecten van de kust en zee in Vlaanderen en België. pp. 109-118.

Abstracts and Proceedings (poster/oral presentations)

Evangelinos, D., Baeye, M., Bertrand S., Van den Eynde, D., & Van Lancker, V. (2015). Dispersion and deposition of sediment plumes, resulting from intensive marine aggregate extraction, pp. 1-4. Proceedings 11th Panhellenic Symposium on Oceanography and Fisheries, Mytilene, Lesbos island, Greece, 13-17/5/2015.

Papili, S, Jenkins, C, Roche, M, Wever, T, Lopera, O, and Van Lancker, V. (2015). Influence of shells and shell debris on backscatter strength: investigation using modeling, sonar measurements and sampling on the Belgian Continental Shelf. In: Seabed and Sediment Acoustics: Measurements and Modelling, ed. by Blondel et al., vol. 37(1), pp. 304-310, University of Bath, Bath, Institute of Acoustics. Proceedings of the Institute of Acoustics.

Van den Eynde, D.; Baeye, M.; Fettweis, M.; Francken, F.; Van Lancker, V. (2015). Validation of modelled bottom shear stress under the influence of currents and waves, using long-term measurements, in: Toorman, E.A. et al. (Ed.) (2015). INTERCOH2015: 13th International Conference on Cohesive Sediment Transport Processes. Leuven, Belgium, 7-11 September 2015. VLIZ Special Publication, 74: pp. 116-117. (oral)

Van Lancker, V. (2015). Habitat change assessment in dynamic shallow water systems - Lessons learned and way forward, pp. 77. GeoHab Conference (Marine Geological and Biological Habitat Mapping). Salvador de Bahia (Brazil), 3-8/5/2015. (oral)

Van Lancker, V. (2015). TILES project on Transnational and Integrated Long-term Marine Exploitation Strategies) and the estimation of far field effects of marine aggregate extraction in an offshore sandbank environment, pp. 75-76. In: ICES (2015). Interim Report of the Working Group on the Effects of Extraction of Marine Sediments on the Marine Ecosystem (WGEXT), 20-23 April 2015. Ostend, Belgium. ICES CM 2015/SSGEPI:06, 102 pp. (oral, invited)

RESEARCH ARTICLE

Wave Glider Monitoring of Sediment Transport and Dredge Plumes in a Shallow Marine Sandbank Environment

Vera Van Lancker*, Matthias Baeye

Operational Directorate Natural Environment, Royal Belgian Institute of Natural Sciences, Brussels, Belgium

* vera.vanlancker@naturalsciences.be



OPEN ACCESS

Citation: Van Lancker V, Baeye M (2015) Wave Glider Monitoring of Sediment Transport and Dredge Plumes in a Shallow Marine Sandbank Environment. PLoS ONE 10(6): e0128948. doi:10.1371/journal.pone.0128948

Academic Editor: Vanesa Magar, Centro de Investigacion Cientifica y Educacion Superior de Ensenada, MEXICO

Received: January 12, 2015

Accepted: May 1, 2015

Published: June 12, 2015

Copyright: © 2015 Van Lancker, Baeye. This is an open access article distributed under the terms of the [Creative Commons Attribution License](http://creativecommons.org/licenses/by/4.0/), which permits unrestricted use, distribution, and reproduction in any medium, provided the original author and source are credited.

Data Availability Statement: Raw and processed ADCP-derived current and turbidity data, as well as raw and processed surface turbidity data are available through the VLIZ Marine Data Archive open data repository (<http://www.vliz.be/en/imis?module=dataset&david=4886>; <http://dx.doi.org/10.14284/2>). Hydro-meteorological data are publicly available from Flanders Hydrography (<http://www.meetnet/vlaamsebanken.be>). Third party vessel monitoring data are available upon request from "Schelderadarketen" (<http://www.agentschapmdk.be/vts.htm>).

Abstract

As human pressure on the marine environment increases, safeguarding healthy and productive seas increasingly necessitates integrated, time- and cost-effective environmental monitoring. Employment of a Wave Glider proved very useful for the study of sediment transport in a shallow sandbank area in the Belgian part of the North Sea. During 22 days, data on surface and water-column currents and turbidity were recorded along 39 loops around an aggregate-extraction site. Correlation with wave and tidal-amplitude data allowed the quantification of current- and wave-induced advection and resuspension, important background information to assess dredging impacts. Important anomalies in suspended particulate matter concentrations in the water column suggested dredging-induced overflow of sediments in the near field (i.e., dynamic plume), and settling of finer-grained material in the far field (i.e., passive plume). Capturing the latter is a successful outcome to this experiment, since the location of dispersion and settling of a passive plume is highly dependent on the ruling hydro-meteorological conditions and thus difficult to predict. Deposition of the observed sediment plumes may cause habitat changes in the long-term.

Introduction

To ensure sustainable development of the marine environment, international agreements and environmental legislation call for the monitoring of a range of biotic and abiotic parameters [1,2]. In Europe, the Marine Strategy Framework Directive (MSFD, 2008/56/EC) requires Member States to demonstrate good environmental status of their marine environments by 2020. All elements that make up the ecosystem (physical, chemical and biological variables) and all human activities need consideration, calling for inclusion of functional and ecosystem-based approaches in monitoring programmes [3,4,5]. As such, there is a necessary move from 'station-oriented monitoring' to 'basin or system-oriented monitoring', in combination with specific 'cause—effect' studies [6].

Traditionally, the status of the marine environment is monitored using ships, allowing for synchronous measurements of air, water column and seabed properties [7]. Both station and transect monitoring can be performed, with increasing possibilities when also ships of

Funding: Liquid Robotics (www.liquidr.com) provided the platform and sensors to conduct the experiment. This involvement does not alter our adherence to PLOS ONE policies on sharing data and materials. The study design relates to the project MOZ4 (Flemish Authorities, Agency Maritime Services and Coast, Coast, contract 211.177). Data collection and analysis were supported by the ZAGRI contract, a continuous monitoring programme, paid from the revenues of marine aggregate extraction activities. The paper contributes also to the Brain-be project TILES (Transnational and Integrated Long-term marine Exploitation Strategies), subsidised by Belgian Science Policy under contract BR/121/A2/TILES (grant VVL).

Competing Interests: The authors have declared that no competing interests exist.

opportunity, such as ferries, are equipped with instrumentation [8]. Additionally, ships allow, in a most practical way, repetitive mapping of the water column and the seabed, providing unprecedented spatial detail of physical and biological features over vast areas [9,10,11,12]. To obtain long time series and/or higher temporal resolutions of some parameters, the use of moorings and/or multi-sensor benthic landers are required [13,14,15,16]. Expanding on these possibilities, coastal and seafloor observatories most often guarantee a long-term commitment to acquire continuous time series [17,18,19]. However, natural and man-made changes to the marine environment need measurements at different time- and space scales of which the magnitude and extent is often unpredictable [20]. This complicates survey planning, as also the choice of the optimal location of moorings and landers.

Therefore, we assessed the use of an unmanned surface vehicle (USV) as an alternative approach to monitoring. Since their development in the '90s [21], USVs have been increasingly deployed, though mostly for surveying along long distances (e.g., crossing the Pacific [22]; southern North Sea [23]). Together with gliders [24,25], as well as autonomous underwater vehicles (AUV) [26,27,28], these new technologies widely increase the potential of environmental monitoring, and of impact assessments in particular.

The USV used in this study is a Liquid Robotics 'Wave Glider' [29]. From April 15th to May 6th 2013 (Day of Year (DoY) 105–126), this USV was deployed, for the first time, in a shallow sandbank environment of 8 to 40 m deep water with surface currents of more than 1 ms⁻¹. The Belgian part of the North Sea, one of world's busiest sea areas, proved to be highly challenging for the Wave Glider and its pilots. The USV was fitted with current and turbidity sensors suitable for assessing the effects of marine aggregate extraction, needed ultimately to recommend more sustainable exploitation practices [30]. Scientific aims were (1) collection of a continuous time series on the natural variability of advection and resuspension ('background conditions') during a neap-spring cycle, and (2) detection of turbidity plumes created by the dredging activity.

In relation to marine aggregate extraction, one can expect three types of dredge plumes, each having a typical behaviour [31]: (1) a surface plume dispersing away from the vessel (i.e., trailer suction hopper dredger); (2) a dynamic plume, representing the coarser part of the initial plume, and descending in the near field; and (3) a passive plume, bringing together the finest fractions from the surface and dynamic plumes, and from a near-bed plume caused by the draghead. The passive plume can easily extend several km from the vessel [31,32,33]. Research on the transport and fate of the released fine sediments requires a suite of techniques and instruments that can be used to generate long time series over extended areas, and thus increase the chance to measure local effects at locations that are difficult to predict [34,35].

This paper provides the complete framework of the Wave Glider deployment, including the mission plan and sensors used, and interprets the data in a marine aggregate-extraction and sandbank morphodynamics' context. On the basis of this analytical work, recommendations are given on survey designs optimising future environmental monitoring of human impacts in the shallow-marine environment. Applications are wide-spread, especially when extensive and long spatio-temporal time series are needed (i.e., plumes in river mouths and estuaries), or where the use of small surface vessels are considered too dangerous: e.g., for measuring hydrothermal discharges in shallow water or for assessing water turbidity effects over lava flows entering the ocean.

Study Area

The monitoring of advection and resuspension and the dynamics of dredge plumes was investigated in the Hinder Banks area, a sandbank complex located 40 km offshore in the Belgian part

of the North Sea (BPNS). Depths of the sandbank crests range from -8 m to -30 m mean lowest low water at Spring (MLLWS); they are superimposed with a hierarchy of dune forms, commonly more than 6 m in height. The lows in between the sandbanks reach depths up to -40 m. At present, extraction of aggregates takes place mainly on the Oosthinder sandbank (Fig 1). Here, medium- to coarse sands dominate with less than 1% of silt-clay, however, locally higher percentages have been measured [36]. Near-bottom tidal currents reach up to 1 ms^{-1} ; for 2011–2013, significant wave heights exceeded 1 m for approximately 44% of the time.

Over a 10-yr period, intensive extraction of marine aggregates (up to 2.9 million m^3 over 3 months) is allowed in this area, with a maximum of 35 million m^3 over a period of 10 years. The largest vessels can extract 12500 m^3 per run. For the entire BPNS, yearly volumes recently surpassed 3 million m^3 , the majority of which has been extracted using vessels with an individual capacity of 1500 m^3 . The intensive extraction is new practice in the BPNS and the environmental impact is yet to be determined. South of the Hinder Banks concession, a Habitat

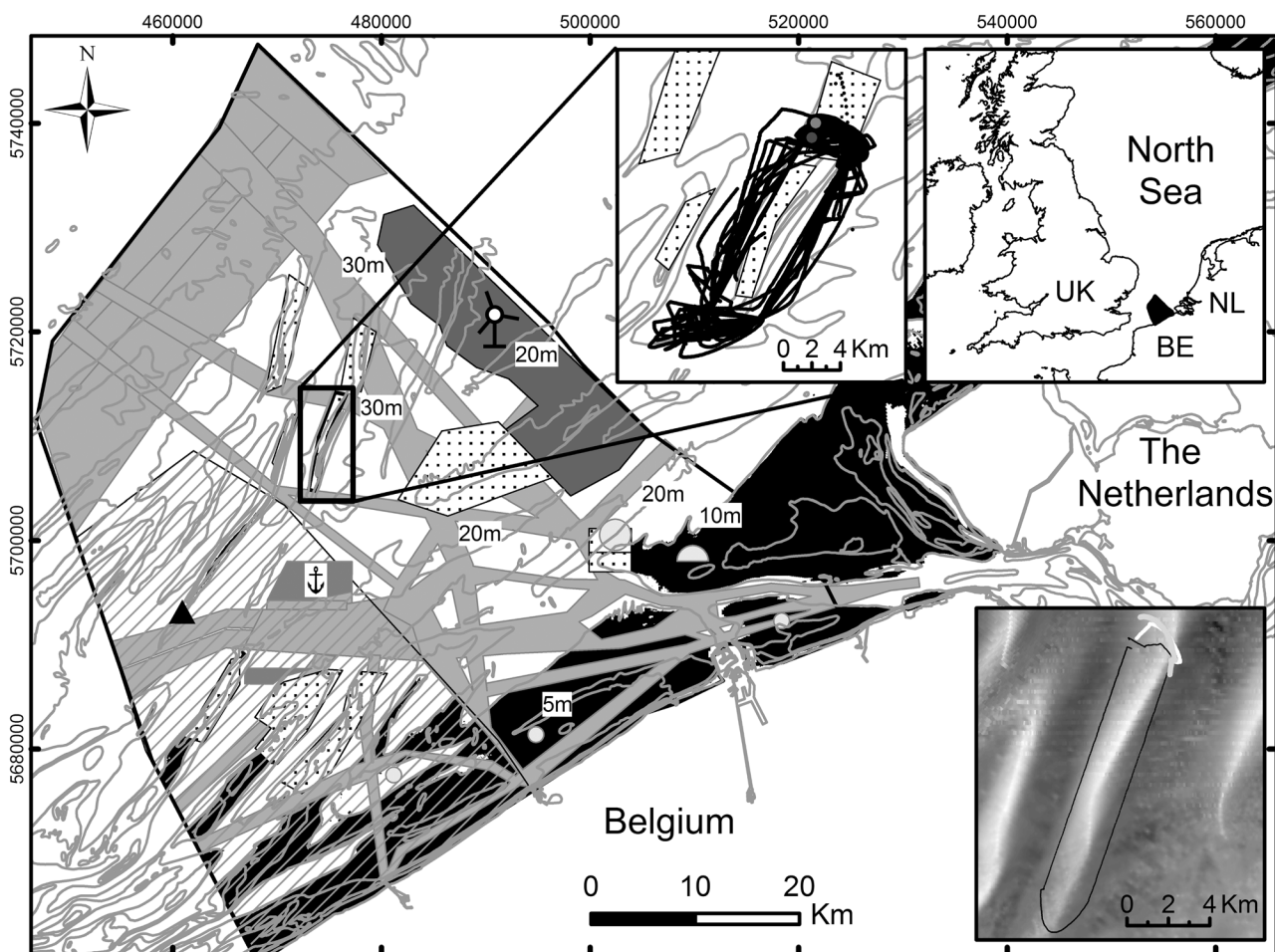


Fig 1. Belgian part of the North Sea with the location of the Wave Glider experiment. Left inset shows the detailed trajectory of 39 laps (22 days) around a marine aggregate concession zone (dotted area). A Habitat Directive area (hatched) is present as close as 2.5 km from the southernmost extraction sector. The Wave Glider could only operate outside of navigation routes (light grey), in areas deeper than -10 m (non-black), and outside a safety buffer of 1 km around major human activities (e.g., wind-farm area, darkest grey; anchor zone, dark grey). Also shown is the location of Flanders Hydrography's hydro-meteo pole MOW7 (triangle) at the Westhinder sandbank, close to which a Wavec buoy measures wave parameters. Lower right inset is a digital terrain model of the area of the experiment. Superimposed is a typical Wave Glider trajectory, as also profile locations. Main bathymetric contours (Mean Lowest Low Water, Spring) have been labelled.

doi:10.1371/journal.pone.0128948.g001

Directive area is present, hosting ecologically valuable gravel beds [37]. To prevent degradation of these beds, it is critical to assess the effect of multiple and frequent deposition events related to dredge plumes.

Materials and Methods

Ethics statement

The Wave Glider's mission plan accounted for a safety buffer of 1 km around the delineation of the marine aggregate sector (Ministerial Decree 2010-12-24/03). Flemish Authorities, Agency Maritime Services and Coast (MDK), Maritime Rescue and Coordination Centre (MRCC) and the Coast Guard granted permissions for the experiment. MDK's Coast department, commissioner of the marine aggregate extraction activities was notified of the experiment. The field studies had no impact on endangered or protected species.

Wave Glider

Platform. The Wave Glider of Liquid Robotics is a commercially available USV, measuring simultaneously in air and water. Its propulsion is based on the conversion of wave motion into thrust and the vehicle utilises solar power to feed its instruments (e.g., for navigation and measurements). This technology is highly favourable where employment endurance is of paramount importance [38]. Long-term integrated data series can thus be captured at the same or reduced cost as from ships and using buoys.

The Wave Glider is composed of two parts: a float which is roughly the size and shape of a surfboard and stays at the surface; and a sub having wings and hanging 4 m below the float on an umbilical tether (Fig 2). Because of the separation, the float experiences more wave motion than does the sub. This difference allows wave energy to be harvested to produce forward thrust (www.liquidrobotics.com). Iridium Satellite communication is used for command, control and data exfiltration, and GPS satellite transmissions for positioning. The USV was deployed and recovered with the oceanographic vessel RV Belgica, respectively on April 15th and May 6th. Pilots controlled the Wave Glider from shore during the whole period (7 days a week, 24 hours a day).

Payload. Apart from navigation- and payload-control computers and satellite-communication systems, the Wave Glider was equipped with a fluorometer (Turner Designs, C3 submersible fluorometer), with sensors for measuring colour dissolved organic matter (CDOM) and crude and refined (poly- and mono-aromatic hydrocarbons) oil fluorescence, and for turbidity and water temperature just below the float of the Wave Glider. The fluorometer featured three optical sensors covering the spectrum from the deep ultraviolet to the infrared. The light-emitting diode for measuring turbidity from the scattering of light operated at a wavelength of 850 nm. Measured values were expressed in relative fluorescence units (RFU) (www.liquidrobotics.com).

Additionally, the float of the Wave Glider housed a broadband Acoustic Doppler Current Profiler (ADCP) (Teledyne/RD Instruments, 307.2 kHz). Current and acoustic backscatter data were acquired in three parts: part 1 with a vertical bin or cell size of 1 m, and glider motion removed, part 2 with a cell size of 2 m, because of an additional bottom track, and part 3 with similar settings as part 1. The Wave Glider had an average speed of 0.59 ms^{-1} , with a maximum of 0.87 ms^{-1} . ADCPs detect the echoes returned from suspended material (i.e. 'sound scatterers') from discrete depths of the water column. Echo intensities, per transmitted pulse, were recorded in counts (also termed the Received Signal Strength Indicator (RSSI), providing indirect information on the currents and density of suspended matter ('backscatter') within each ensonified bin.

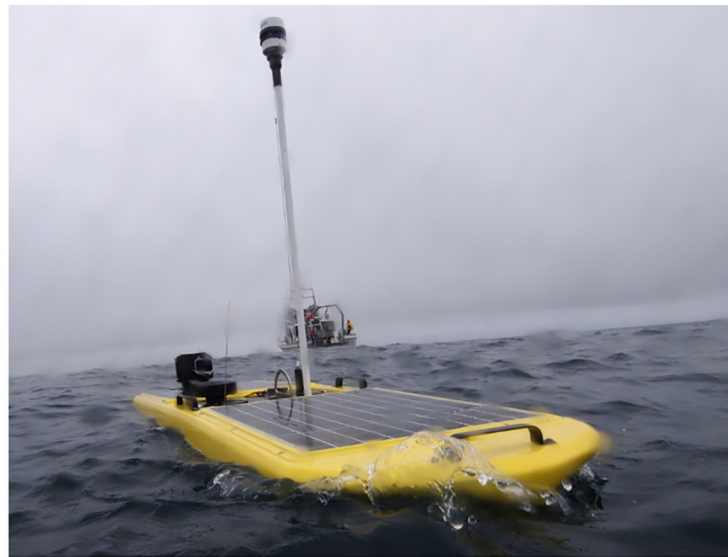


Fig 2. Wave Glider SV2. (Top) Blow-out showing the near-surface float housing the payload (including an ADCP (blue) and fluorometer), and connected to a sub ('glider part'). The wave-induced friction between the two parts, connected through an umbilical, provides thrust. (Below) The Wave Glider in operation showing the antenna and solar panels. (Pictures courtesy of Liquid Robotics Inc.).

doi:10.1371/journal.pone.0128948.g002

Mission plan. The scientific goal of the mission was to characterise a shallow-water sand-bank environment where intensive aggregate extraction takes place. On the one hand, background information was needed on the variability of natural advection and resuspension events. On the other hand, aggregate extraction is known to create dredge plumes; the challenge was to detect these plumes, as also their dispersal, and likely place of deposition. For this reason, the Wave Glider's path was chosen to optimize the chance of characterizing both the

natural and anthropogenic suspended sediment. In preparation of the mission, information was gathered on water depths, navigation hazards, vessel traffic, weather conditions and typical sea states. After accounting for technical exclusion zones (e.g., water depths shallower than -10 m, intensive shipping routes), a box was defined contouring the extraction site at a safety distance of at least 1 km (Fig 1). From a navigation-technical point of view, the Wave Glider was programmed with waypoints and headings to sail along the western (-37 m shallowest) and eastern (-39 m shallowest) lows during the ebbing (SW) and flooding (NE) phase of the tide, respectively. The southern (-16 m shallowest) and northern (-12 m shallowest) profiles crossed the sandbank. Pilots lengthened or shortened the Wave gliders' path to sail those profiles under the most favourable tidal conditions, i.e., around slack water when currents were weakest, and never during spring ebb and flood. For these reasons, the Wave Glider undersampled the sandbank, providing little information on the hydrodynamics and sediment transport in the shallowest waters during high-energy conditions. The Wave Glider sailed for 22 days, completing 39 laps around the extraction site. Each lap took approximately 12.5 hours to complete, the length of the principal lunar semi-diurnal cycle. During this period, 28 extraction events took place.

Data processing

Fluorescence data. The C3 turbidity RFU data were converted into Nepheloid Turbidity Units (NTU) after laboratory calibration ($NTU = (RFU - 6.9) / 16.6$) (pers. comm. Liquid Robotics Inc.). To obtain SPM mass concentration data in gl^{-1} , NTU was further multiplied with a factor 1.6, which is a typical value derived from near-shore and offshore calibrations of optical turbidity sensors in Belgian waters [39].

Acoustic Doppler Current Profiler (ADCP). For recalculation of bin depth to actual depth values, a draught of 0.25 m was applied for the distance of the ADCP below the water surface. The first bin that could be used was around -10 m only, because of contamination of the data in the upper water layers by the submerged part of the Wave Glider. Pulses were averaged into ensembles at a time interval of 60 seconds per sample. Together with an average platform speed of $0.59 ms^{-1}$, this resulted in an average horizontal resolution of 40 m.

The ADCP echo intensities, in dB, were corrected for beam spreading and water attenuation [40]. As with the ADCP current direction and magnitude data, the first bin started at -10 m water depth. To obtain rough estimates of mass concentration values, the dBs at -10 m were plotted against the C3 turbidity data (RFU). The assumption here is that the upper water column (first 10 m) has a uniform sediment concentration, so that the ADCP backscatter corresponds with the C3 turbidity data. For this conversion only RFU and dB data from calm periods (significant wave heights less than 1.4 m) were retained, and running-averages (20-min) were used in the linear regression analysis (resulting R^2 of 0.89). A second conversion, similar to that of the C3 data, was applied to transform the turbidity RFU into NTU ($NTU = (RFU - 6.9) / 16.6$) (pers. comm. Liquid Robotics Inc.), based on laboratory calibrations. The latter units were then also multiplied with a factor 1.6 to generate SPM concentration values in gl^{-1} . The values were within an order of magnitude of those obtained from ship-borne measurements in the same period of the year and in the same area [41]. For further quantitative analyses, time series of currents and SPM were extracted at appropriate levels (e.g., representative for the upper and lower water layers, and depth-averaged). A running average was applied over a 20-min window.

External data

MODIS Satellite data. The temporal variation of the C3 turbidity sensor, mounted in the Wave Glider float, was validated using imagery from the Moderate Resolution Imaging

Spectroradiometer (MODIS) (via MUMM/GRIMAS extraction tool (<http://www2.mumm.ac.be/remsem/timeseries/>) [42]). The main motivation for this analysis was to have an independent dataset to verify and provide context for the variations in the field dataset. For each Wave Glider record, a nearest window of 25 pixels (1 km x 1 km) was defined. In the case of no clouds, an SPM concentration value was calculated at each of these pixels. For the correlation with the C3 data, a median MODIS-derived SPM value was retained when measurements were available for 13 of the 25 pixels, and when the measurement time difference between the Wave Glider and MODIS data was less than 2 hours. A median value was chosen to reduce bias from an ephemeral cloud cover and/or water glint. During the period of Wave Glider employment, the frequency of the daily image provision by MODIS was between 12h and 13h45.

Hydro-meteorological data. Wave information (e.g., significant wave height (H_s in m); and direction of low- and high-frequency waves ($^\circ$), with a period less (H_z) and more than 10 s, respectively) were obtained, at 30-min intervals, from a Wave buoy (Flanders Hydrography) at 18 km southwest of the study area (MOW7 measuring pole; location see Fig 1). Wind climate, at 10-min intervals, was derived from the same pole. Water levels, current velocity and direction (10-min intervals) were extracted from an operational 3D hydrodynamic model [43]. On the basis of these data, the timing of high and low waters was extracted and transferred to the Wave Glider dataset.

Vessel monitoring data. To distinguish natural from human-induced variability in SPM concentration (e.g., caused by dredging, but also induced by wakes of nearby ships), ship-navigation data were analysed (Schelderadarketen, [44] and, where relevant, coupled to the time series (e.g., shortest distance to the Wave Glider). To detect dredging-induced sediment plumes, the timing of dredging activities was marked in the Wave Glider time series. During the Wave Glider experiment, 28 extractions took place using a trailer hopper dredger with a capacity of approximately 2500 m³. To enable discharge on the upper beach during the flood tide, all extractions were made during the ebbing phase of the tide.

All data were time-stamped to Universal Time Coordinates (UTC) allowing more easy correlation of various observations. Position coordinates were in UTM31 WGS84.

Results

The Wave Glider's time series provided a unique record of current and turbidity events over a period of 22 days. Analyses on current variability, and on external wave and wind data are summarised in the section on hydro-meteorological conditions. Next, turbidity events are described, first those that are thought to be naturally induced, and secondly those that could be related to the dredging activity. Quantification of hydro-meteorological conditions was particularly important in evaluating the sediment resuspension potential, and in constraining the magnitude and dispersal direction of the dredge plumes. In case of dominant SW dispersal of fines, the ecologically important gravel fields in the adjacent Habitat Directive area could be affected.

Hydro-meteorological conditions

During the Wave Glider experiment, hydro-meteorological conditions were rather calm, with waves exceeding 1 m only 28% of the time (H_s max = 2.60 m) (Fig 3). Mean tidal range increased from 3.67 m during neap to 4.73 m during spring conditions. Currents measured with the Wave Glider showed a 17° offset with the sandbank axis. The NE-directed flood and SW-directed ebb currents were more or less equal in strength, with the flood lasting somewhat longer (around 8%), and the ebb keeping its directionality for a longer period. Current velocities increased clearly from neap- to spring-tidal levels with surface values of up to 1.2 ms⁻¹. In the

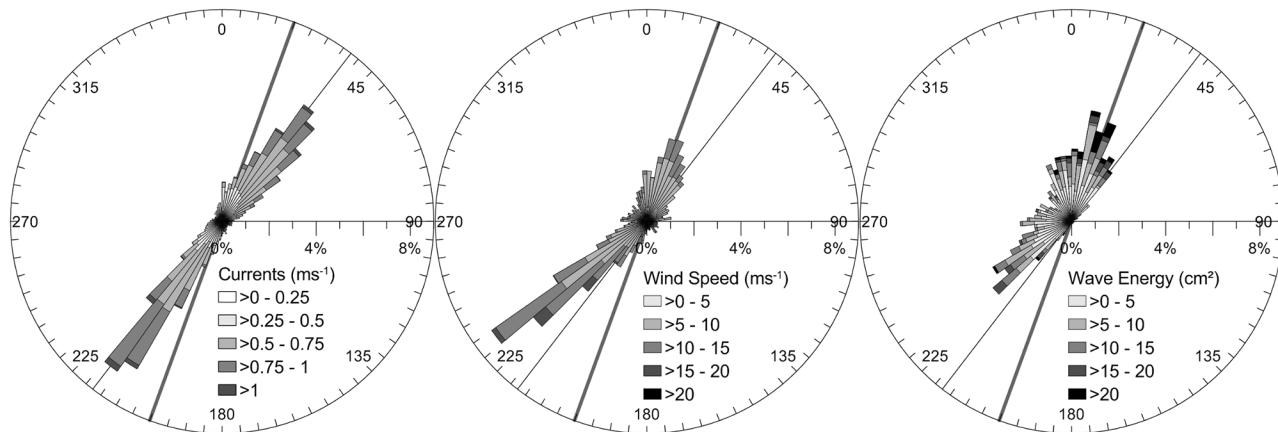


Fig 3. Hydro-meteorological conditions during the experiment. From left to right: Current velocity and direction (Wave Glider ADCP), wind velocity and direction, and low-frequency energy (frequency band of 0.03 H_z to 0.1 H_z) and direction of low-frequency waves ($H_z < 10$ s) (MOW7 location, Fig 1). Bold line represents the axis of the sandbank; thin line is the axis of maximum currents.

doi:10.1371/journal.pone.0128948.g003

deeper waters of the troughs, the surficial currents were approximately 21% stronger than those above the shallower sandbank slopes and crests. Winds blew mostly from a SW direction; winds of more than 20 ms^{-1} gave rise to high-frequency waves ($H_z > 10$ s) with an amplitude of more than 2 m (H_s). This wave direction prevails in the BPNS. During employment, SW waves were present around 55% of the 22 days, whilst N to NE waves were active only 29% of the time. For low-frequency waves ($H_z < 10$ s), SW and NE conditions equalled. Significant wave heights were higher under SW conditions, though the low-frequency energy (0.03 H_z to 0.1 H_z) of the northerly waves was significantly higher. This latter wave direction aligned with the sandbank's axis (Fig 3).

Natural variation of SPM concentration

Tidally-induced variation. Peaks in SPM concentrations were linked mostly to peaks in current strength, both along the lows, parallel to the sandbank, and across its crest. Most obvious was the neap-to-spring variation (Fig 4). During spring tide, the ADCP-derived SPM concentrations were high throughout the water column, with highest values near the seabed. The time series of the surficial C3 fluorometer sensor, proxy for turbidity, showed a similar trend from neap to spring tide (Fig 4).

SPM concentrations were similar under NE- and SW-directed currents (Fig 5), though slightly higher concentrations were measured under flood (NE) conditions. In the upper water layers, at -10 m, median values of SPM concentration reached about 0.010 gl^{-1} ; concentrations in the surface waters were around 0.001 to 0.002 gl^{-1} (Fig 4), for neap and spring tide respectively. SPM median concentrations in the lower waters were 0.011 to 0.015 gl^{-1} in the deepest areas and up to 0.019 gl^{-1} over the sandbank crests. However, peak concentrations were consistently missed, since the Wave Glider crossed the sandbanks under the most favourable conditions, with the weakest currents.

At the few occasions that the sandbank was crossed at higher current velocities, tide-topography effects were observed resulting in resuspension (Fig 6), also in the lee sides of the superimposed bedforms.

Wave-induced variation. With increasing wave heights, higher SPM concentration values were derived, especially over topographic highs (Fig 6). Most obvious was a good

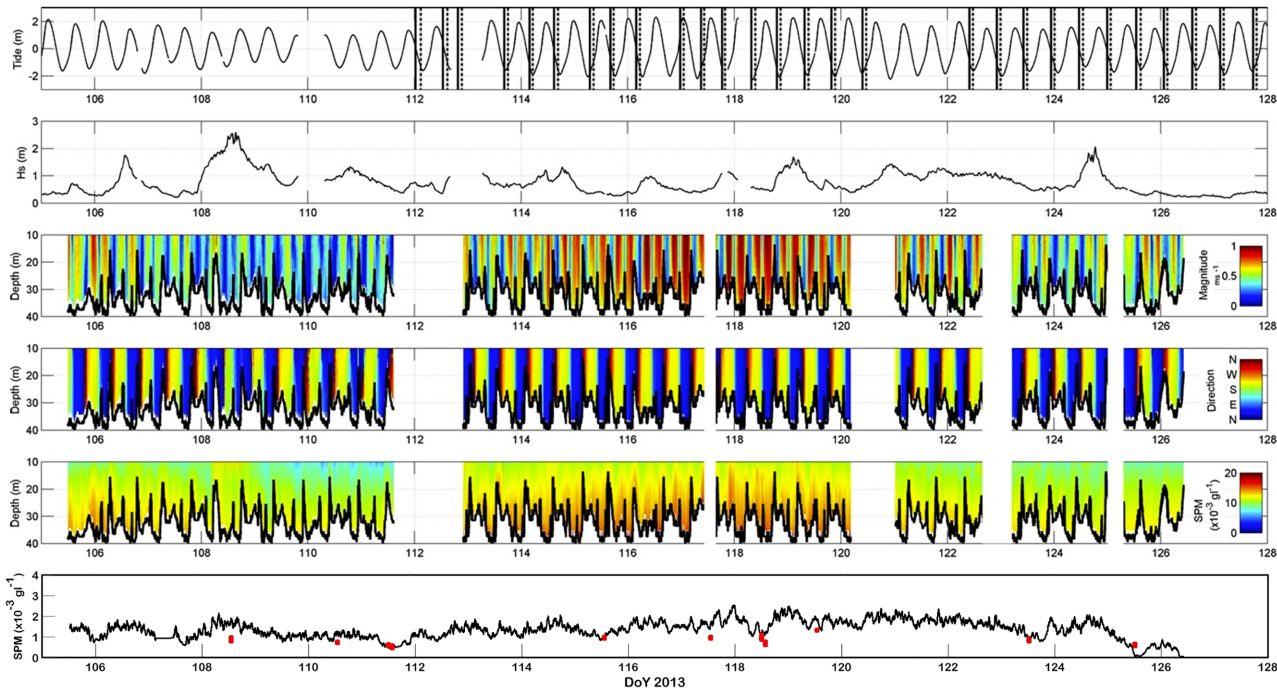


Fig 4. Composite of the Wave Glider measurements, together with the main hydro-meteorological conditions. From top to bottom, the figure shows: (1) water level, with the extraction events (28) superimposed; (2) significant wave height; (3) and (4) ADCP-derived current strength and direction; (5) ADCP-derived SPM concentrations; (6) surface SPM concentrations from the C3 sensor, superimposed with turbidity estimates derived from cloud-free MODIS satellite imagery data (red dots).

doi:10.1371/journal.pone.0128948.g004

correspondence between the values of the surface C3 turbidity sensor and the wave heights (Fig 4). Evaluating the whole time series of the C3, it was striking that, contrary to ADCP SPM values, the C3 values remained high after spring tide (DoY 120–123; Fig 4). During this period of 2.5 days wave heights were between 1 and 1.4 m, and originated consistently from the ENE direction. A mild storm occurred around DoY 108–109 (mid tide) (Fig 4). Waves originating from the SW reached a significant height of 2.6 m. The Wave Glider’s ADCP data showed a corresponding overall increase in current strengths, especially over the sandbank. Equally

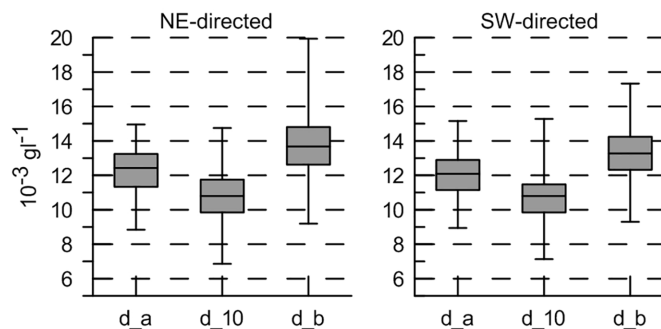


Fig 5. Boxplot of ADCP-derived SPM concentrations under NE- and SW-directed currents. Results are shown for currents stronger than 0.4 ms^{-1} , being the sediment resuspension threshold. From left to right, values are depth-averaged (d_a); around -10 m (d_10); and near bottom (d_b). Values are most representative for SPM concentrations in the troughs fringing the sandbank.

doi:10.1371/journal.pone.0128948.g005

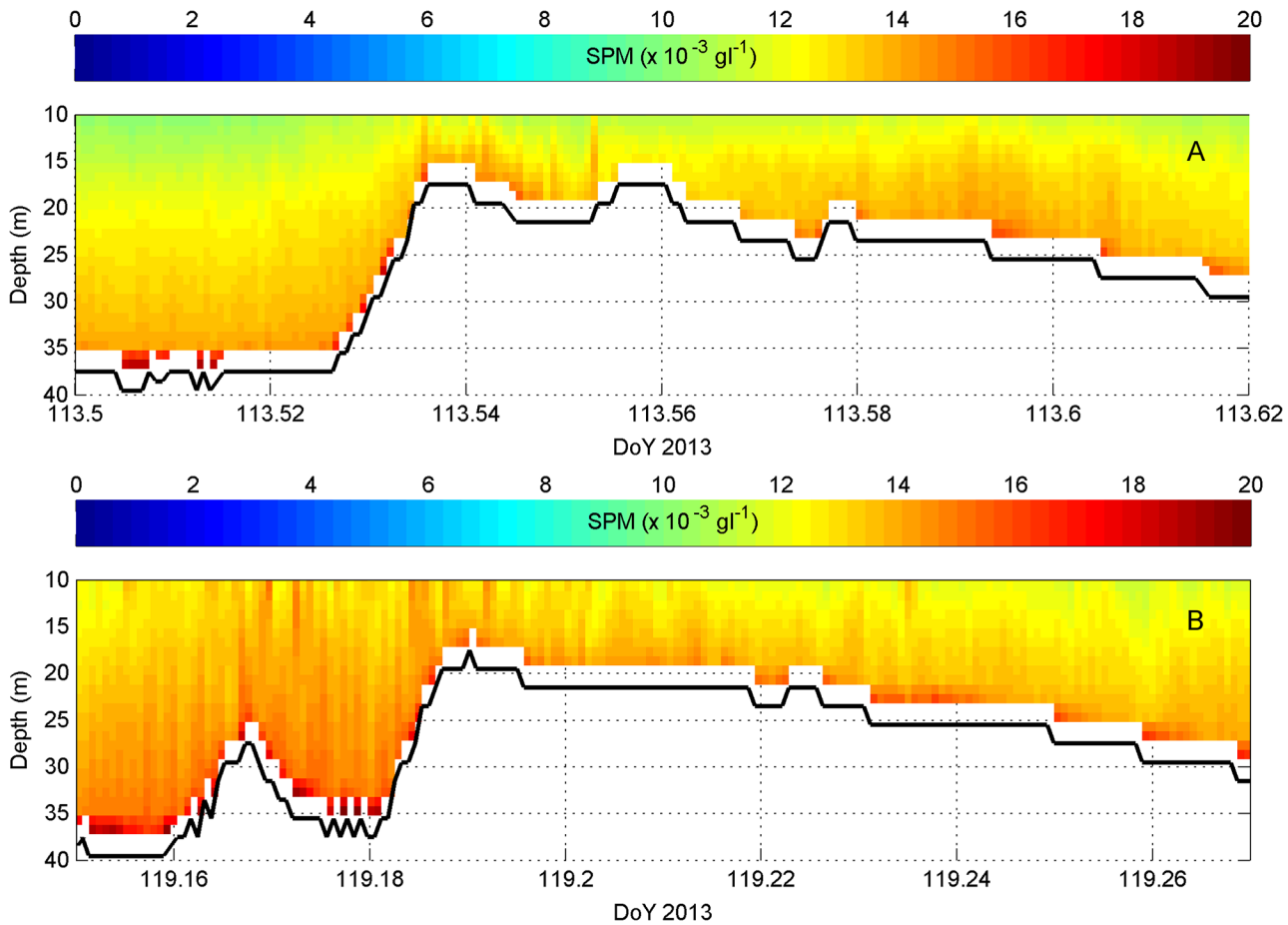


Fig 6. Examples of tide-topography interaction. (A): under low wave heights ($H_s < 1$ m; DoY 113.54); (B): with wave interaction (H_s : 1–2 m; DoY 119.18). In both cases, the Wave Glider passed the top of the sandbank approximately 2.4 h after High Water. Location Oosthinder sandbank; northern cross-bank profiles in lower right inset of Fig 1.

doi:10.1371/journal.pone.0128948.g006

strong upper- and lower-water currents indicated strong mixing. SPM concentrations were raised not just over the sandbank, but also more regionally, suggesting that fine sediments advected away from the sandbank.

Human-induced variation. During the Wave Glider monitoring period, 28 extractions were made using a small dredging vessel of approximately 2500 m^3 . Generally, the Wave Glider was 0.5 to 1 km away from the vessel. This distance was too far to detect larger scale differences in SPM concentrations before, during and after the dredging. Important anomalies in SPM concentration values did suggest the detection of individual dredging-induced surface, dynamic and passive plumes, and unambiguously showed the descent of such plumes from the upper waters to the seabed. Fig 7 shows where these anomalies were depicted, whilst Fig 8 visualizes them. SPM concentrations in the surface plumes, containing released fines, were difficult to quantify, due to dispersal and to uncertainty in the nature of the increases compared to other influences, such as air bubbles. However, dynamic plumes were visualised clearly when the Wave Glider was close to the dredging vessel (i.e., less than 600 m away) and when currents were directed towards the Wave Glider. These dynamic plumes suggest deposition of the main overflow from the dredging vessel. Increases in SPM concentrations were measured over a

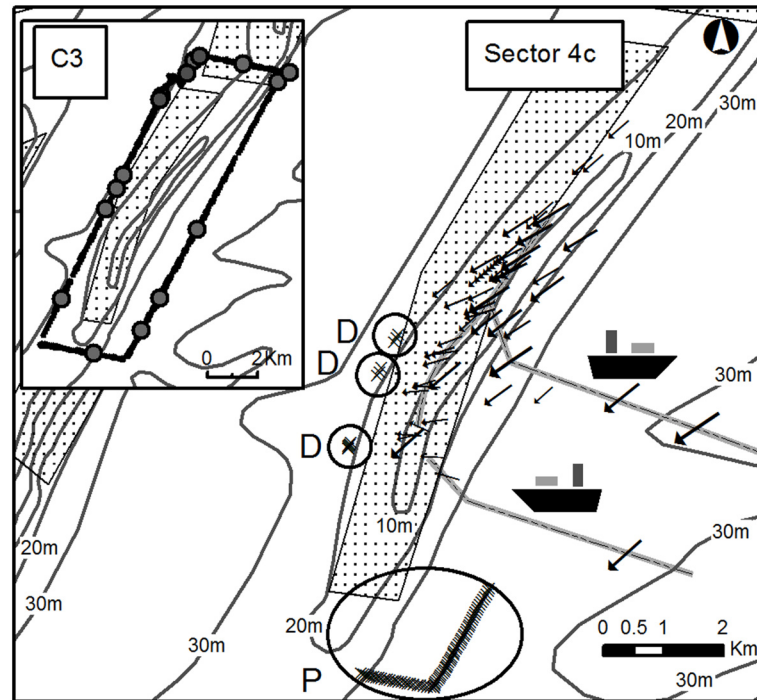


Fig 7. The concession area (dotted) with ADCP-derived locations of dredging-induced sediment plumes. Important SPM concentration anomalies were observed along the western edge of the sandbank: in the circles 'D', these suggest the occurrence of dynamic plumes (x); in circle 'P', a passive plume (x). Modelled surface current vectors (arrows; 10-min averaged) during the extraction events were all SW-directed. One typical aggregate extraction pathway is shown in grey. In the inset, C3-derived surface turbidity values are shown for the tour in which the ADCP detected the passive plume (circle P). The largest dots represent higher SPM concentration amounts. Note, that no consistently high surface concentrations were recorded, pointing to a mid-water position of the passive plume. For location of the C3 inset, note the position of the data in respect to the delineation of Sector 4c (dotted) in the main figure.

doi:10.1371/journal.pone.0128948.g007

distance of around 120 m and were a factor of 1.25 greater than the natural background values. Most intriguingly, a passive plume was observed also, around 3 hours after the preceding extraction event, 7.8 km away. The position of this plume corresponded well with modelled predictions of deposition that took into account the measured current velocities and directions in the area. During and after the dredging event, currents (around 0.7 ms^{-1}) were directed to the SW and were reinforced by the waves; winds blew in the same direction. No other ships were nearby.

Discussion

Wave Glider as monitoring platform

Overall, the Wave Glider proved to be a stable platform for monitoring both naturally and human-induced variability in hydrodynamic and sediment processes. Natural resuspension and advection were successfully observed under tidally and wave-induced currents. Most importantly, the instruments on the Wave Glider allowed identification of well-delineated sediment plumes resulting from marine aggregate extraction. Advantages as well as disadvantages are summarised in more detail in [Table 1](#).

The most important strengths and added value of the Wave Glider were its endurance and its versatile platform, allowing for the integrated operation of *ad hoc* sensors. The combined

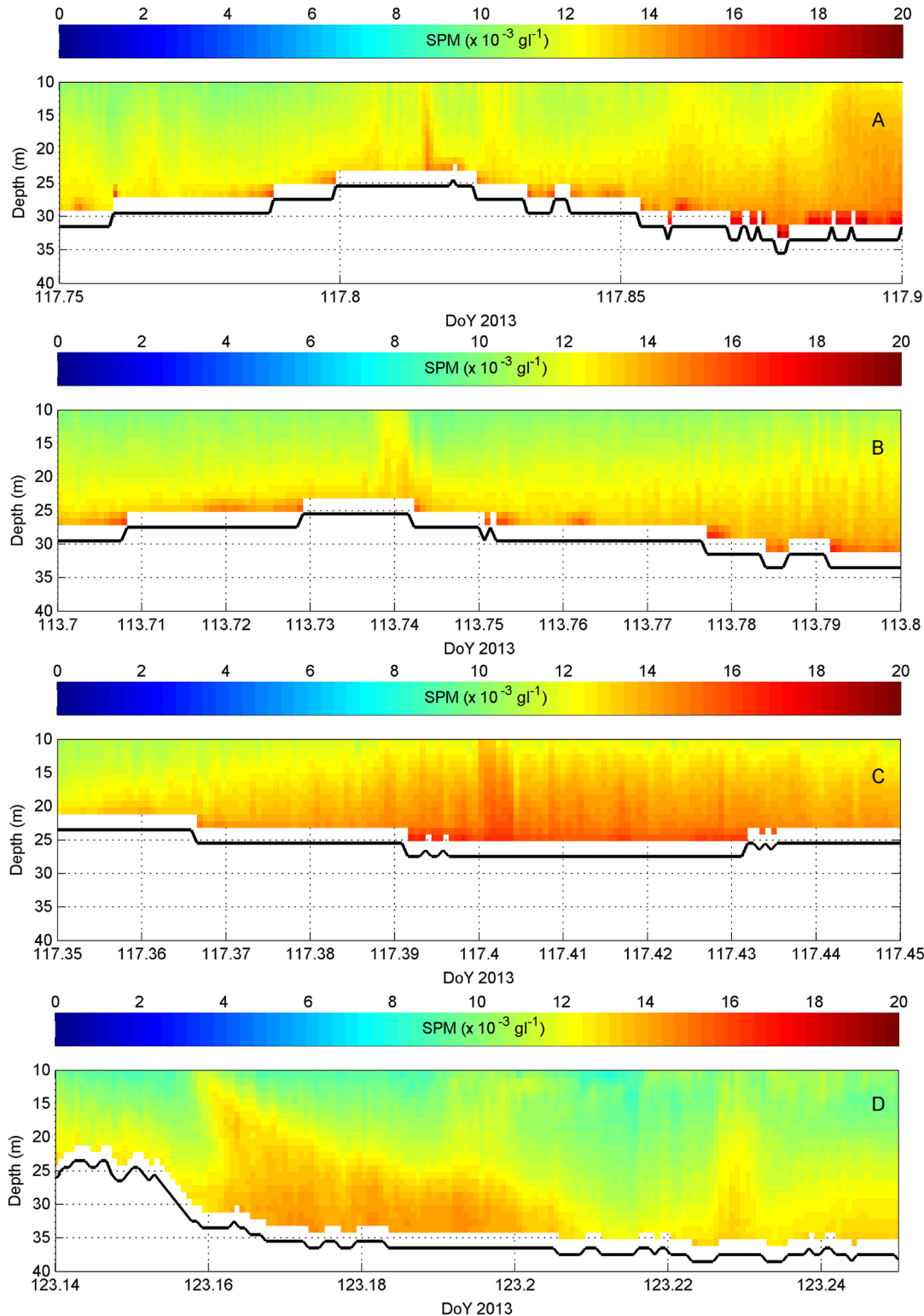


Fig 8. Examples of dredging-induced sediment plumes (from ADCP backscatter data) (A-B-C-D). Locations are from North to South in Fig 7, and correspond to (1) Dynamic plumes ‘D’ (DoY 117.815 (A), 113.74 (B), 117.4 (C)), as observed close to the dredging vessel (< 600 m). Dimension of the plumes was less than 140 m; and (2) Passive plume ‘P’ (DoY 123.16 (D)), observed in the far field, and transported by the SW-directed ebb tidal current. Note that DoY 123.14–123.177 (minimum 780 m wide) was cross-sandbank oriented; afterwards the Wave Glider sailed parallel to the sandbank, for approximately 1.8 km (see Fig 7). Relating to this passive plume, the last extraction event was 7.8 km away from the Wave Glider.

doi:10.1371/journal.pone.0128948.g008

Table 1. Pros and cons determined from our Wave Glider monitoring experiment.

Pros
Stable platform in a tidally and wave-influenced energetic environment
Simultaneous operation of <i>ad hoc</i> sensors for an integrated spatio-temporal dataset
Long-term quasi continuous data series, covering natural variability and human-induced effects
High-frequency measurements for high spatial resolution
Opportunity for event detection, by measuring effects from any phase of the event, including lag effects
Effective remote control by pilots, avoiding collisions in busy traffic and optimising the Wave Glider's performance by taking account of the tides
Cost-effectiveness
Cons
Limitations related to survey design: Unequal representation of conditions, with more data obtained in the troughs than over the sandbank ridges, which were crossed around slack water, missing out on the highest-turbidity events
Low temporal resolution per sublocation, because of the lap time of the trajectory compared to the tidal oscillation
Detection of events, but no quantification of their dilution rate
Lack of calibration and validation, critical for quality assurance
Additional datasets needed for balanced evaluations of environmental conditions
Need for continuous piloting

doi:10.1371/journal.pone.0128948.t001

use of a C3 optical sensor for surficial turbidity and an ADCP that acoustically measured turbidity throughout the water column showed high promise, and enabled comparisons with satellite-derived turbidity data. However, as in earlier studies in the area [45,46]), results showed that the surface-turbidity values were not reliable indicators of sediment advection and resuspension in the water column as shown by the ADCP (Fig 4). This limitation is an important consideration when using satellite data for the monitoring of turbidity [47].

Data quality (i.e., internal consistency) was overall very good, but deteriorated under higher wave events. Values of the surface C3 sensor followed a similar trend as the wave height. Although, it is plausible that more sediments are advected away from the sandbanks under highly than under lowly energetic wave conditions [48,49,50], it cannot be excluded that wave-induced pitch-and-roll movements led to trapping of air bubbles on the optical face of the sensor, and therefore to overestimations of sediment load. Next-generation fluorometers (www.turnerdesigns.com) with air purge slots in shade caps should be used in future surveys. The ADCP data may also have been biased by air bubbles [51]. At higher wave heights (mostly > 2 m), ADCP data increasingly showed bands of anomalous backscatter values in the upper part of the water column, though values normalised farther down the water column.

Most of the disadvantages listed in Table 1 were inherent to the survey design, and difficult to account for in the analyses. Since nearby extractions were on-going during the experiment, the Wave Glider had to sail in rectangular laps around the extraction sector on the sandbank, resulting in bank-parallel sections of around 12 km in the troughs, separated by much shorter cross-bank transects of around 3 km. It needs reiteration that the Wave Glider sailed with the tides: the western part of the lap was always sailed during ebb, and the eastern part always during flood. Since the sandbank was crossed mostly during slack water, important peak SPM concentrations over the sandbanks were missed; hence, the final dataset is marked by an unequal representation of different-strength forces acting on the sandbank area.

The spatial extent of the aggregate-extraction sector was such that one lap by the Wave Glider took 10–15 hrs, meaning that each location was sampled only once during a tidal cycle

(12.25 hrs) on average. The measured changes in sediment concentrations were biased by the spatial position of the Wave Glider with the tidal phase. For a regional characterisation of natural background conditions, such limited temporal resolution is acceptable. If sandbank dynamics or detailed impacts need quantification, however, short laps or transects and higher sampling frequencies for each location are favourable.

The Wave Glider captured a few dynamic plumes when it was close enough to a dredging vessel in operation. However, when quantification of the behaviour (e.g., particle size and nature), dispersal and dilution of sediment plumes is targeted, monitoring from ships is more informative because these can be equipped with a more complete set of instruments and more easily manoeuvred to stay within a plume [31,33,34,35,52]. Uniquely, the Wave Glider's ADCP detected the descent of a passive plume. Such plumes combine fines released from the surface as well as from dynamic plumes, and travel in the middle part of the water column [31]. A passive plume was detected only once over the entire time series during which 28 extraction events (day and night) took place. Owing to the large space and time lag with respect to the time and location of the corresponding dredging activities, this plume would most probably have been difficult to detect using a ship with typically shorter monitoring periods. Even a Wave Glider, which can be operational for much longer monitoring periods, will only depict human-induced SPM increases when the platform crosses the sediment plume, which lies downstream of its originating dredging event. The migration and dispersal of plumes are governed by highly variable hydro-meteorological conditions and therefore difficult to predict. Measurements at fixed locations (e.g., with multi-sensor benthic landers) also provide little chance to detect dredging-induced sediment plumes, despite providing long time series at very high temporal resolution. In trying to capture and understand sediment plumes, Wave Gliders can play an important role, but there will always be a trade-off between the desired temporal versus spatial resolution and simple versus a more complete set of instrumentation. If possible, a flexible, long-term monitoring strategy is followed, taking full advantage of the complementarity of autonomous vehicles, landers and ship-based observations.

At least for the time being, ships remain important for *in situ* calibration of all sensor data (e.g., water sampling and other instrumentation to determine nature, size and concentration of SPM) and for more complete synchronous measurements (e.g., multibeam bathymetry and backscatter) than are currently possible with Wave Gliders. However, with increasing use of autonomous platforms, development and optimisation of sensors and other equipment suitable for use on Wave Gliders are on-going. Promising examples are the incorporation of small-sized water samplers for calibration of sensor data [53], and experiments in towing light-weight hydro-acoustic instruments for high-resolution depth and sonar registrations [54].

Time-series analyses

Wave Glider monitoring generates time series from multiple instruments that offer new possibilities for process-response analysis. In our study, important SPM events could be visualised, especially when the colour scale of images was fine-tuned to show the highest contrast within the range of values that mattered most. It proved difficult, however, to find significant quantitative correlations between the long time series and the main processes driving SPM concentrations and transport. Overall patterns were obvious, but quantitative links were mostly biased by interference of multiple processes, including noise.

An important source of bias is the overestimation of ADCP-derived SPM-concentration values. Variations in echo-intensity data are not an exclusive function of suspended sediments, but relate to a mixture of sources with individual contributions that are hard to disentangle [55,56]. Correlations with tides, currents and waves, which are easiest to hindcast, are

overprinted by much more unpredictable or even random effects of debris, phyto- and zooplankton [57,58], mammals, air bubbles [51] and noise of ships [59]. Ideally, every effort should be made to constrain the uncertainties associated with these effects. In our study, all SPM events that were interpreted as dredge plumes were verified first against current- and wave influence and against ship passages. The Wave Glider's pitch-and-roll information was used additionally, to evaluate the chance of encountering spikes. Biological influence was also observed in the dataset, be it indirectly. Around the timing of the phytoplankton bloom, as reported around DoY 123.5 (Fig 4) from MODIS-derived Chlorophyll-a values, our ADCP SPM data showed wisps of high backscatter in the upper water layers (up to a water depth of -20 m; 10 m above seabed). Other possible causes for this shallow backscatter anomaly were excluded: wave heights were around 0.5 m only, and the nearest ships were more than 4 km away; values for colour dissolved organic matter, as measured by the Wave Glider, and a useful proxy for debris from dead organic matter [60] were low too.

To discriminate human forcing in the time series, it is important to note that extraction-induced dynamic sediment plumes may have a limited spatial extent, no more than 2*60-second ensembles in our Wave Glider SPM data, and are ephemeral in nature. During the experiment, the human-induced increases in SPM values fell within their natural range (for a relative small dredging vessel of 2500 m³). Thus, these events are missed easily in autonomously (USV, AUV) recorded time series, especially if automated routines would be used for their identification. Due to its much larger dimension, the detection of the passive plume was straightforward. For such plumes, though, correlation with a source and with processes governing its advection is complicated by the large space and time lag with respect to the preceding dredging event.

Hydro-meteorological forcing drives the dispersal of all plumes [31] and needs to be accounted for when evaluating plume events. In the present case, extraction occurred consistently during ebb, limiting the transport of plumes to SW directions. Using this knowledge, some SPM events, as measured by the Wave Glider, could not be due to the dredging.

The identification of the overall SW-directed transport of the sediment plumes was very important as it showed that the probability of deposition of fines in the Habitat Directive area, only 2.5 km southwards of the extraction site, was high. The potential impact of these fines on the ecologically valuable gravel habitats is now under investigation. In this light, future plume research will focus on more advanced modelling of their spatial dimensions, dispersal pathways and depositional patterns. The Wave Glider data series, supplemented by other sensor observations and by ground-truthing, will be pivotal in the validation of these plume-dispersal models. The present dataset was already used to select and sample seabed areas where human-induced changes in habitat characteristics would be most likely, given the on-going extraction activities. Should consistent deposition patterns be found, fining of surface sediments or even smothering of habitats is of considerable concern. Any significant net deposition within the down-drift Habitat Directive area, hosting sensitive and unique habitats, will necessitate adaptation of the dredging practices (e.g., alternating between extraction locations or no persistent dredging during ebb).

Conclusions

Through careful planning and 24-hr piloting, a Wave Glider was employed successfully in one of Worlds' most heavily navigated and exploited sea areas, recording long time series of natural and human-induced spatio-temporal variability in various parameters. Using the Wave Glider data, it was possible to identify and evaluate human-induced sediment plumes in light of

natural, tidally and wave-induced forcing on SPM concentrations and on sediment-transport directions.

During the Wave Glider experiment, 28 extractions took place. The effect of only a few was observed in the dataset, mostly due to an overall distance of 0.5 to 1 km to the dredging vessel. After careful evaluation of all potential sources, instruments did depict dredging-induced increases in turbidity, but overall the concentrations fell within the limits of natural variation. Dimensions of well-delineated dredging-induced dynamic and passive sediment plumes were assessed, as also was their deposition area. In the near field, quasi-immediate deposition is suggested of the main overflow, whilst finer-grained material, segregated from the main plume and the erosion around the draghead, ended up in the far field. The latter formed the passive plume, resided temporarily below the middle of the water column, and was deposited three hours after the last extraction activity. The spatio-temporal pattern of far-field spreading was in agreement with the prevailing hydro-meteorological forcing.

For the monitoring of sediment processes and dredge plumes, a flexible monitoring strategy is recommended that combines short- and long-term measurements from mobile platforms and at fixed locations in carefully considered survey designs. Such an approach ensures that predictable events and processes are quantified, including spatio-temporal background conditions and the dilution of observed SPM increases. Long-term measurements are needed to increase the likelihood that unpredictable or random events and processes are captured. From a time and cost perspective, the Wave Glider proved valuable in environmental monitoring of sediment processes, and aided in the optimisation of follow-on monitoring and research of processes of which the knowledge base is still too fragmented. For the time being, ship-borne measurements remain essential for calibration and validation of the sensor data, but on-going technological developments in Wave Glider construction and instrumentation will increase the stand-alone value of its measurements.

Acknowledgments

Francois Leroy and Ryan Carlon at Liquid Robotics Inc. provided the opportunity to deploy the Wave Glider Hermes in the Belgian offshore waters. The RV Belgica, with ship time granted by Belspo and by the Royal Belgian Institute of Natural Sciences, was used for deployment and recovery. The Liquid Robotics team, Lieven Naudts (and team) and Dries Van den Eynde gave logistical support. Sébastien Legrand supplied modelled data on currents and water levels derived from OPTOS-BCZ; Quinten Van Hellemont derived turbidity values from MODIS satellite imagery; and Reinhilde Van den Branden, Gregory De Schepper, and Gerrie Eikenhout (Schelderadarketen) offered vessel monitoring data. Hydro-meteorological data were derived from 'Meetnet Vlaamse Banken', Flanders Hydrography, through Flanders Marine Institute (VLIZ). Sytze van Heteren and Neil Mitchell are thanked warmly for improving the manuscript.

Author Contributions

Conceived and designed the experiments: VVL. Performed the experiments: VVL MB. Analyzed the data: MB VVL. Contributed reagents/materials/analysis tools: MB VVL. Wrote the paper: VVL MB.

References

1. Borja A, Bricker SB, Dauer DM, Demetriades NT, Ferreira JG, Forbes AT, et al. Overview of integrative tools and methods in assessing ecological integrity in estuarine and coastal systems worldwide. *Marine Pollution Bulletin*. 2008; 56: 1519–1537. doi: [10.1016/j.marpolbul.2008.07.005](https://doi.org/10.1016/j.marpolbul.2008.07.005) PMID: [18715596](https://pubmed.ncbi.nlm.nih.gov/18715596/)

2. Morris D, O'Brien C, Larcombe P. Actually achieving marine sustainability demands a radical re-think in approach, not "more of the same". *Marine Pollution Bulletin*. 2011; 62: 1053–1057. doi: [10.1016/j.marpolbul.2011.02.027](https://doi.org/10.1016/j.marpolbul.2011.02.027) PMID: [21397916](https://pubmed.ncbi.nlm.nih.gov/21397916/)
3. Borja Á, Elliott M, Carstensen J, Heiskanen A-S, van de Bund W. Marine management—Towards an integrated implementation of the European Marine Strategy Framework and the Water Framework Directives. *Marine Pollution Bulletin*. 2010; 60: 2175–2186. doi: [10.1016/j.marpolbul.2010.09.026](https://doi.org/10.1016/j.marpolbul.2010.09.026) PMID: [20965524](https://pubmed.ncbi.nlm.nih.gov/20965524/)
4. Tallis H, Levin PS, Ruckelshaus M, Lester SE, McLeod KL, Fluharty DL, et al. The many faces of ecosystem-based management: Making the process work today in real places. *Marine Policy*. 2010; 34: 340–348. doi: [10.1016/j.marpol.2009.08.003](https://doi.org/10.1016/j.marpol.2009.08.003)
5. Rice J, Arvanitidis C, Borja A, Frid C, Hiddink JG, Krause J, et al. Indicators for Sea-floor Integrity under the European Marine Strategy Framework Directive. *Ecological Indicators*. 2012; 12: 174–184. doi: [10.1016/j.ecolind.2011.03.021](https://doi.org/10.1016/j.ecolind.2011.03.021)
6. De Jonge VN, Elliott M, Brauer VS. Marine monitoring: Its shortcomings and mismatch with the EU Water Framework Directive's objectives. *Marine Pollution Bulletin*. 2006; 53: 5–19. doi: [10.1016/j.marpolbul.2005.11.026](https://doi.org/10.1016/j.marpolbul.2005.11.026) PMID: [16426645](https://pubmed.ncbi.nlm.nih.gov/16426645/)
7. Binot J, Da obeita J, Muller T, Nieuwejaar PW, Rietveld MJ, Stone P. European Ocean Research Fleets—Towards a Common Strategy and Enhanced Use. Strasbourg, France: Marine Board-ESF; 2007 p. 62. Marine Board Position Paper 10.
8. Petersen W. FerryBox systems: State-of-the-art in Europe and future development. *Journal of Marine Systems*. 2014; 140, Part A: 4–12. doi: [10.1016/j.jmarsys.2014.07.003](https://doi.org/10.1016/j.jmarsys.2014.07.003)
9. Degrendele K, Roche M, Schotte P, Lancker VRMV, Bellec VK, Bonne WMI. Morphological Evolution of the Kwinte Bank Central Depression Before and After the Cessation of Aggregate Extraction. *Journal of Coastal Research*. 2010; 77–86.
10. Van Lancker V, Moerkerke G, Du Four I, Verfaillie E, Rabaut M, Degraer S. 14—Fine-Scale Geomorphological Mapping of Sandbank Environments for the Prediction of Macrobenthic Occurrences, Belgian Part of the North Sea. In: Baker PTHK, editor. *Seafloor Geomorphology as Benthic Habitat*. London: Elsevier; 2012. pp. 251–260. Available: <http://www.sciencedirect.com/science/article/pii/B9780123851406000141>
11. Brown CJ, Blondel P. Developments in the application of multibeam sonar backscatter for seafloor habitat mapping. *Applied Acoustics*. 2009; 70: 1242–1247. doi: [10.1016/j.apacoust.2008.08.004](https://doi.org/10.1016/j.apacoust.2008.08.004)
12. Harris PT, Baker EK, editors. *GEOHAB Atlas of Seafloor Geomorphic Features and Benthic Habitats* [Internet]. London: Elsevier; 2012. Available: <http://www.sciencedirect.com/science/article/pii/B9780123851406000670>
13. Cacchione DA, Sternberg RW, Ogston AS. Bottom instrumented tripods: History, applications, and impacts. *Continental Shelf Research*. 2006; 26: 2319–2334. doi: [10.1016/j.csr.2006.07.027](https://doi.org/10.1016/j.csr.2006.07.027)
14. Palinkas CM, Ogston AS, Nittrouer CA. Observations of event-scale sedimentary dynamics with an instrumented bottom-boundary-layer tripod. *Marine Geology*. 2010; 274: 151–164. doi: [10.1016/j.margeo.2010.03.012](https://doi.org/10.1016/j.margeo.2010.03.012)
15. Sternberg RW, Aagaard K, Cacchione D, Wheatcroft RA, Beach RA, Roach AT, et al. Long-term near-bed observations of velocity and hydrographic properties in the northwest Barents Sea with implications for sediment transport. *Continental Shelf Research*. 2001; 21: 509–529. doi: [10.1016/S0278-4343\(00\)00103-5](https://doi.org/10.1016/S0278-4343(00)00103-5)
16. Black KS, Fones GR, Peppe OC, Kennedy HA, Bentaleb I. An autonomous benthic lander: preliminary observations from the UK BENBO thematic programme. *Continental Shelf Research*. 2001; 21: 859–877. doi: [10.1016/S0278-4343\(00\)00116-3](https://doi.org/10.1016/S0278-4343(00)00116-3)
17. Favali P, Beranzoli L. Seafloor Observatory Science: a Review. *Ann Geophys*. 2006; 49. doi: [10.4401/ag-3125](https://doi.org/10.4401/ag-3125)
18. Goff JA, Mayer LA, Traykovski P, Buynevich I, Wilkens R, Raymond R, et al. Detailed investigation of sorted bedforms, or "rippled scour depressions," within the Martha's Vineyard Coastal Observatory, Massachusetts. *Continental Shelf Research*. 2005; 25: 461–484. doi: [10.1016/j.csr.2004.09.019](https://doi.org/10.1016/j.csr.2004.09.019)
19. Monna S, Falcone G, Beranzoli L, Chierici F, Cianchini G, De Caro M, et al. Underwater geophysical monitoring for European Multidisciplinary Seafloor and water column Observatories. *Journal of Marine Systems*. 2014; 130: 12–30. doi: [10.1016/j.jmarsys.2013.09.010](https://doi.org/10.1016/j.jmarsys.2013.09.010)
20. Sternberg RW, Nowell ARM. Continental shelf sedimentology: scales of investigation define future research opportunities. *Journal of Sea Research*. 1999; 41: 55–71. doi: [10.1016/S1385-1101\(98\)00037-9](https://doi.org/10.1016/S1385-1101(98)00037-9)
21. Manley JE. Unmanned surface vehicles, 15 years of development. *OCEANS 2008. IEEE*; 2008. pp. 1–4. Available: http://ieeexplore.ieee.org/xpls/abs_all.jsp?arnumber=5152052

22. Villareal TA, Wilson C. A Comparison of the Pac-X Trans-Pacific Wave Glider Data and Satellite Data (MODIS, Aquarius, TRMM and VIIRS). *PLoS ONE*. 2014; 9: e92280. doi: [10.1371/journal.pone.0092280](https://doi.org/10.1371/journal.pone.0092280) PMID: [24658053](https://pubmed.ncbi.nlm.nih.gov/24658053/)
23. Hull, T., Sivyer, D. Wave Glider trial, final report. September 2013 [Internet]. 2013 p. 18. Available: http://www.cefas.defra.gov.uk/publications/files/WaveGliderReport_Cefas_11Sept2013.pdf
24. Miles T, Glenn SM, Schofield O. Temporal and spatial variability in fall storm induced sediment resuspension on the Mid-Atlantic Bight. *Continental Shelf Research*. 2013; 63, Supplement: S36–S49. doi: [10.1016/j.csr.2012.08.006](https://doi.org/10.1016/j.csr.2012.08.006)
25. Piterbarg L, Taillandier V, Griffa A. Investigating frontal variability from repeated glider transects in the Ligurian Current (North West Mediterranean Sea). *Journal of Marine Systems*. 2014; 129: 381–395. doi: [10.1016/j.jmarsys.2013.08.003](https://doi.org/10.1016/j.jmarsys.2013.08.003)
26. Fong DA, Jones NL. Evaluation of AUV-based ADCP measurements. *Limnology and Oceanography: Methods*. 2006; 4: 58–67.
27. Foster SD, Hosack GR, Hill NA, Barrett NS, Lucieer VL. Choosing between strategies for designing surveys: autonomous underwater vehicles. *Methods Ecol Evol*. 2014; 5: 287–297. doi: [10.1111/2041-210X.12156](https://doi.org/10.1111/2041-210X.12156)
28. Wynn RB, Huvenne VAI, Le Bas TP, Murton BJ, Connelly DP, Bett BJ, et al. Autonomous Underwater Vehicles (AUVs): Their past, present and future contributions to the advancement of marine geoscience. *Marine Geology*. 2014; 352: 451–468. doi: [10.1016/j.margeo.2014.03.012](https://doi.org/10.1016/j.margeo.2014.03.012)
29. Daniel T, Manley J, Trenaman N. The Wave Glider: enabling a new approach to persistent ocean observation and research. *Ocean Dynamics*. 2011; 61: 1509–1520. doi: [10.1007/s10236-011-0408-5](https://doi.org/10.1007/s10236-011-0408-5)
30. Van Lancker V, Bonne WMI, Garel E, Degrendele K, Roche M, DV den Eynde, et al. Recommendations for the sustainable exploitation of tidal sandbanks. *Journal of Coastal Research*. 2010; 151–164.
31. Spearman JR, De Heer A, Aarninkhof SGJ, Van Koningsveld M. Validation of the TASS system for predicting the environmental effects of trailing suction hopper dredgers. *Terra et Aqua*. 2011; 125: 14–22.
32. Newell RC, Hitchcock DR, Seiderer LJ. Organic Enrichment Associated with Outwash from Marine Aggregates Dredging: A Probable Explanation for Surface Sheens and Enhanced Benthic Production in the Vicinity of Dredging Operations. *Marine Pollution Bulletin*. 1999; 38: 809–818. doi: [10.1016/S0025-326X\(99\)00045-4](https://doi.org/10.1016/S0025-326X(99)00045-4)
33. Hitchcock DR, Bell S. Physical Impacts of Marine Aggregate Dredging on Seabed Resources in Coastal Deposits. *Journal of Coastal Research*. 2004; 101–114. doi: [10.2112/1551-5036\(2004\)20\[101:PIOMAD\]2.0.CO;2](https://doi.org/10.2112/JCOASTRES-D-12-00148.1)
34. Smith SJ, Friedrichs CT. Size and settling velocities of cohesive floes and suspended sediment aggregates in a trailing suction hopper dredge plume. *Continental Shelf Research*. 2011; 31: S50–S63. doi: [10.1016/j.csr.2010.04.002](https://doi.org/10.1016/j.csr.2010.04.002)
35. Duclos P-A, Lafite R, Le Bot S, Rivoalen E, Cuvilliez A. Dynamics of Turbid Plumes Generated by Marine Aggregate Dredging: An Example of a Macrotidal Environment (the Bay of Seine, France). *Journal of Coastal Research*. 2013; 25–37. doi: [10.2112/JCOASTRES-D-12-00148.1](https://doi.org/10.2112/JCOASTRES-D-12-00148.1)
36. Van Lancker V, Baeye M, Dimitris Evangelinos, Van den Eynde D. Monitoring of the impact of the extraction of marine aggregates, in casu sand, in the zone of the Hinder Banks. *Scientific Report 2—January—December 2014*. Brussels: Royal Belgian Institute of Natural Sciences, OD Nature; 2015 p. 74 pp. +5 Annexes.
37. Haelters J, Kerckhof F, Houziaux JS. The designation of marine protected areas in the Belgian part of the North Sea: a possible implementation of OSPAR Recommendation 2003/3 in Belgium. Brussels: Royal Belgian Institute of Natural Sciences, OD Nature; 2007 p. 46.
38. Liquid Robotics, Inc. Wave Glider (Model 08) User Manual. Version 2.41. 2010 p. 190.
39. Fettweis M. Uncertainty of excess density and settling velocity of mud floes derived from in situ measurements. *Estuarine, Coastal and Shelf Science*. 2008; 78: 426–436. doi: [10.1016/j.ecss.2008.01.007](https://doi.org/10.1016/j.ecss.2008.01.007)
40. Deines KL. Backscatter estimation using Broadband acoustic Doppler current profilers. *Proceedings of the IEEE Sixth Working Conference on Current Measurement, 1999*. 1999. pp. 249–253. doi: [10.1109/CCM.1999.755249](https://doi.org/10.1109/CCM.1999.755249)
41. Van Lancker V, Baeye M, Fettweis M, Francken F, Van den Eynde D. Monitoring of the impact of the extraction of marine aggregates, in casu sand, in the zone of the Hinder Banks. Brussels: Royal Belgian Institute of Natural Sciences, OD Nature; 2014 p. 46 pp. + 9 Annexes.
42. Vanhellemont Q, Nechad B, Ruddick K. GRIMAS: gridding and archiving of satellite-derived ocean colour data for any region on earth. *Proceedings of the CoastGIS 2011 conference held in Ostend*. 2011. pp. 5–8.

43. Luyten PJ, Jones JE, Proctor R, MUMM. A coupled hydrodynamical-ecological model for regional and shelf seas: User Documentation. Brussels: Royal Belgian Institute of Natural Sciences, OD Nature; 2011 p. 1177.
44. Van den Branden R, De Schepper G, Naudts L. Automatische registreersystemen geïnstalleerd aan boord van de zandwinningschepen: overzicht van de verwerkte data van het jaar 2012. Brussels: Royal Belgian Institute of Natural Sciences, OD Nature; 2013.
45. Fettweis M, Nechad B, Van den Eynde D. An estimate of the suspended particulate matter (SPM) transport in the southern North Sea using SeaWiFS images, in situ measurements and numerical model results. *Continental Shelf Research*. 2007; 27: 1568–1583. doi: [10.1016/j.csr.2007.01.017](https://doi.org/10.1016/j.csr.2007.01.017)
46. Fettweis MP, Nechad B. Evaluation of in situ and remote sensing sampling methods for SPM concentrations, Belgian continental shelf (southern North Sea). *Ocean Dynamics*. 2011; 61: 157–171. doi: [10.1007/s10236-010-0310-6](https://doi.org/10.1007/s10236-010-0310-6)
47. Chen Z, Hu C, Muller-Karger F. Monitoring turbidity in Tampa Bay using MODIS/Aqua 250-m imagery. *Remote Sensing of Environment*. 2007; 109: 207–220. doi: [10.1016/j.rse.2006.12.019](https://doi.org/10.1016/j.rse.2006.12.019)
48. Williams J.J., Humphery JD, Hardcastle PJ, Wilson DJ. Field observations of hydrodynamic conditions and suspended particulate matter in the southern North Sea. *Continental Shelf Research*. 1998; 18: 1215–1233. doi: [10.1016/S0278-4343\(98\)00041-7](https://doi.org/10.1016/S0278-4343(98)00041-7)
49. Vincent CE, Stolk A, Porter CFC. Sand suspension and transport on the Middelkerke Bank (southern North Sea) by storms and tidal currents. *Marine Geology*. 1998; 150: 113–129. doi: [10.1016/S0025-3227\(98\)00048-6](https://doi.org/10.1016/S0025-3227(98)00048-6)
50. Giardino A, Van den Eynde D, Monbaliu J. Wave effects on the morphodynamic evolution of an offshore sand bank. *Journal of Coastal Research*. 2010; 51: 127–140.
51. Guerrero M, Rüther N, Szupiany RN. Laboratory validation of acoustic Doppler current profiler (ADCP) techniques for suspended sediment investigations. *Flow Measurement and Instrumentation*. 2012; 23: 40–48. doi: [10.1016/j.flowmeasinst.2011.10.003](https://doi.org/10.1016/j.flowmeasinst.2011.10.003)
52. Wood JD, Boye D. Monitoring Suspended Sediment Plumes Using an Acoustic Doppler Current Profiler. *OCEANS 2007*. 2007. pp. 1–7. doi: [10.1109/OCEANS.2007.4449165](https://doi.org/10.1109/OCEANS.2007.4449165)
53. Ferri G, Manzi A, Fornai F, Ciuchi F, Laschi C. The HydroNet ASV, a Small-Sized Autonomous Catamaran for Real-Time Monitoring of Water Quality: From Design to Missions at Sea. *IEEE Journal of Oceanic Engineering*. 2014; PP: 1–17. doi: [10.1109/JOE.2014.2359361](https://doi.org/10.1109/JOE.2014.2359361)
54. Munday E, Acker T, Dawson J. Specialized Tools for Biological Assessment Using Split Beam Hydroacoustics. 144th Annual Meeting of the American Fisheries Society. Afs; 2014. Available: [ftp://dns.soest.hawaii.edu/bhowe/outgoing/IEEEOES_2013/papers/130503-136.pdf](http://dns.soest.hawaii.edu/bhowe/outgoing/IEEEOES_2013/papers/130503-136.pdf)
55. Thorne PD, Hanes DM. A review of acoustic measurement of small-scale sediment processes. *Continental Shelf Research*. 2002; 22: 603–632. doi: [10.1016/S0278-4343\(01\)00101-7](https://doi.org/10.1016/S0278-4343(01)00101-7)
56. Gartner JW. Estimating suspended solids concentrations from backscatter intensity measured by acoustic Doppler current profiler in San Francisco Bay, California. *Marine Geology*. 2004; 211: 169–187. doi: [10.1016/j.margeo.2004.07.001](https://doi.org/10.1016/j.margeo.2004.07.001)
57. Lorke A, McGinnis DF, Spaak P, Wüest A. Acoustic observations of zooplankton in lakes using a Doppler current profiler. *Freshwater Biology*. 2004; 49: 1280–1292. doi: [10.1111/j.1365-2427.2004.01267.x](https://doi.org/10.1111/j.1365-2427.2004.01267.x)
58. Jiang S, Dickey TD, Steinberg DK, Madin LP. Temporal variability of zooplankton biomass from ADCP backscatter time series data at the Bermuda Testbed Mooring site. *Deep Sea Research Part I: Oceanographic Research Papers*. 2007; 54: 608–636. doi: [10.1016/j.dsr.2006.12.011](https://doi.org/10.1016/j.dsr.2006.12.011)
59. H van Haren. Ship-induced effects on bottom-mounted acoustic current meters in shallow seas. *Continental Shelf Research*. 2009; 29: 1809–1814. doi: [10.1016/j.csr.2009.06.002](https://doi.org/10.1016/j.csr.2009.06.002)
60. Rochelle-Newall E, Hulot FD, Janeau JL, Merroune A. CDOM fluorescence as a proxy of DOC concentration in natural waters: a comparison of four contrasting tropical systems. *Environ Monit Assess*. 2014; 186: 589–596. doi: [10.1007/s10661-013-3401-2](https://doi.org/10.1007/s10661-013-3401-2) PMID: 24072524